SEDIMENTOLOGY AND PALAEOGEOGRAPHY OF CENOMANIAN NIMAR SANDSTONE, CENTRAL INDIA

Ph.D. THESIS

by

SUPARNA JHA

DEPARTMENT OF EARTH SCIENCES
Indian Institute of Technology, Roorkee
Roorkee- 247667 (INDIA)
May, 2018

SEDIMENTOLOGY AND PALAEOGEOGRAPHY OF CENOMANIAN NIMAR SANDSTONE, CENTRAL INDIA

A Thesis

Submitted in partial fulfilment of the requirements for the award of the degree

of

DOCTOR IN PHILOSOPHY

in

EARTH SCIENCES

by

SUPARNA JHA

DEPARTMENT OF EARTH SCIENCES
Indian Institute of Technology, Roorkee
Roorkee- 247667 (INDIA)
May, 2018

INDIAN INSTITUE OF TECHNOLOGY ROORKEE
ROORKEE

CANDIDATE'S DECLARATION

I hereby certify that the work which is being presented in the thesis entitled **"SEDIMENTOLOGY AND PALAEOGEOGRAPHY OF CENOMANIAN NIMAR SANDSTONE, CENTRAL INDIA"** in partial fulfilment of the requirements for the award of the Degree of Doctor of Philosophy and submitted in the Department of Earth Sciences of the Indian Institute of Technology Roorkee, Roorkee is an authentic record of my own work carried out during a period from July, 2013 to May, 2018 under the supervision of Dr. Biplab Bhattacharya, Assistant Professor, Department of Earth Sciences, Indian Institute of Technology Roorkee, Roorkee and co supervision of Dr. Suparna Hazra, Senior Geologist, Geological Survey of India, Jabalpur.

The matter presented in this thesis has not been submitted by me for the award of any other degree of this or any other Institution.

Suparna Jha

(SUPARNA JHA)

This is to certify that the above statement made by the candidate is correct to the best of my knowledge.

Suparna Hazra

(Suparna Hazra)

Bhattacharya 09/05/2018

(Biplab Bhattacharya)

Dr. Biplab Bhattacharya
Assistant Professor
Department of Earth Sciences
Indian Institute of Technology Roorkee
Roorkee-247 667, Uttarakhand, INDIA

Date: 09 May, 2018

This thesis is dedicated to

My Mentor Dr. Biplab Bhattacharya

&

My Family

ABSTRACT

Cretaceous global sea level rise affected almost all the continents including India, resulting in inundations of huge landmasses. Evidences of late Cretaceous marine transgression is chronicled in different basins (namely, Kutch, Bengal-Assam, Shillong, Cauvery, few parts of Himalaya, and Son-Narmada rift valley, etc.,) in the western, north-eastern, southern and central part of the Indian subcontinent. Sedimentological study of those sedimentary basins reveals important clues to understand the late Cretaceous palaeoclimatic and palaeotectonic changes in the Indian subcontinent. The Son-Narmada rift valley in central India is a repository of such deposit in the Bagh Group, which bears the evidences of late Cretaceous inundation of the Indian subcontinent. The present thesis is an attempt to assess the Nimar Sandstone, the lower most lithounit within the Bagh Group, which chronicles the evidences of first marine incursion in the area. The research work aims to delineate the palaeogeographic changes in Central India during late Cretaceous time based on detailed facies architecture, sediment-organism interaction pattern, geochemical analysis and sequence stratigraphic study of the Nimar Sandstone.

Detailed sedimentological study of the Nimar Sandstone from excellently preserved and exposed sections reveals total seventeen facies types, which are clubbed under five distinct facies associations. Channel-fill facies association (FA-1) consists of clast supported conglomerate facies (1A), matrix supported conglomerate facies (1B), pebbly sandstone facies (1C) and trough cross stratified sandstone facies (1D). Overall lenticular shaped geometry of this facies association, presence of both matrix and clast supported conglomerates, dominance of immature sediments and alternate pebble-rich and pebble-poor sandstones indicate fluctuation in energy within fluvial channel filling system. Overbank facies association (FA-2) consisting of sandstone-mudstone interbedded facies (2A) and plane bedded sandstone facies (2B) with dominance of fine clastics in a fining-upward succession suggests deposition in overbank/ flood plains of the channels. The fluvial-dominated fluvio-tidal facies association (FA-3) consists of (i) large-scale trough cross stratified sandstone facies (3A) and (ii) planar cross-stratified sandstone facies (3B), both characterized by tidaly-reworked features like mud draped foresets (tidal bundles) with reactivation surfaces. Such sand-dominated facies with influence of tidal current indicates a fluvial-dominated tide–influenced channel bar depositional

setting. Tide-dominated fluvio-tidal facies association (FA-4) is more tide dominated within a fluvio-tidal interactive system, consists of sandstone mudstone heterolithic facies (4A), mud clast conglomerate facies (4B), plane laminated fine-grained sandstone-mudstone facies (4C), bioturbated sandstone facies (4D) and green sandstone facies (4E). This facies association is enriched with various tidal features, changing into wave reworked tidal features towards upsection. Dominance of lenticular bedding and wavy bedding with bi-directional cross-strata, sigmoidal strata bundles and laterally accreted tidal bundles confirm an inter-tidal to sub-tidal flat setting for deposition of FA-4. Predominance of tidal features along with very low wave reworking indicates a relatively sheltered situation, where waves were not strong enough for reworking the tidal sediments. Shore facies association (FA-5) consists of coarsening up to fining up sandstone sequence of fossil bearing sandstone facies (5A), *Thalassinoides–Ophiomorpha* bearing thinly laminated sandstone/mudstone facies (5B), wave ripples bearing sandstone facies (5C) and massive mudstone facies (5D). Presence of marine body fossils, round crested ripples, interference ripples and ladder back ripples indicates deposition in wave dominated beach condition. Gradual increase in mud content and decreasing bioturbation intensity towards the up section indicates increasing water depth resulting in more suspension deposition.

Overall facies architectural pattern of the Nimar Sandstone and fining upward succession indicates a tide-dominated wave led sheltered estuarine setting. Based on the lateral and vertical distribution of the facies association, three major palaeodepositional conditions are envisaged - (i) a river dominated (FA-1) inner estuary with an fluvial channel and overbank setting (FA-2), changing into localized bay-head delta zones when influenced by tidal current (FA-3), (ii) tide dominated central estuary zone, forming dominantly inter-tidal to sub-tidal setting in the middle part of the succession, and (iii) an outer estuary zone where wave-reworked open shore condition prevailed with sub-tidal flat environment.

Predominance of tidal features in FA-3 and FA-4, and wave reworked tidal features in upper part of FA-4 and FA-5 helps to understand precisely the palaeodepositional environment. The major tide-generated primary structures in the study area are laterally accreted strata bundle with reactivation surface, bi-directional cross strata set with development of herringbone cross strata, vertically accreted strata bundles, sigmoidal strata, and cyclical tidal rhythmites. From the eastern to western part and towards the up section of the studied area, increasing dominance

of wave generated structures and sequential gradation of tide-to wave-generated structures signify gradual shift in depositional condition from intertidal to subtidal to open marine setting within an estuarine condition.

Appearances of SSDS are restricted in particular beds and they are delimited by undeformed bed. The major SSDS from Nimar Sandstone includes convolute laminae, load and flame structures, pseudonodules, slump structures, contorted beds, syn-sedimentary faults and sand dykes. SSDS are mainly associated with the sandstone and mudstone beds of FA-3 and FA-4. The SSDS-bearing beds are identified as seismites. Association of the seismites with fluvio-tidal facies association indicates a correlation between marine incursion and reactivation of faults, which triggered basinal subsidence and shift in depositional condition from fluvial to fluvio-tidal interactive.

The studied estuarine sediments are characterized by abundant trace fossils. Altogether fourteen ichnoforms, grouped in four ichnofacies are identified from the study area namely, mixed Skolithos-Glossifungites ichnofacies, mixed Cruziana-Glossifungites ichnofacies, Glossifungites ichnofacies and mixed Skolithos-Glossifungites ichnofacies. Overall ichnodiversity is low and bioturbation intensity gradually increases towards western part of the study area with presence of both suspension- and deposit-feeding burrows. Distribution of trace fossils signifies pattern of sediment-organism interaction in response to changes in energy condition, fluctuating salinity and oxygen availability during sedimentation under fluvio-marine interactive system.

Geochemically the rocks show wide range of major oxide concentrations. Major oxide ratios decipher a transition from non-marine to marine depositional environment, with prevalent humid climatic condition in a passive margin setting. Various discrimination diagrams of the major elements oxides decipher a quatzosedimentary to granodioritic provenance. The geochemical interpretations related with depositional setting validate the proposed estuarine depositional model for the Nimar Sandstone.

Integration and interpretation of facies architecture, ichnofabric and geochemical character point to an west to eastward marine encroachment during the Nimar sedimentation. Overall fining up succession of the Nimar Sandstone constitutes part of a 2nd order transgressive system tract (TST) within the Bagh Group of rocks, delimited by unconformity at the base and a

flooding zone at the top (the overlying Nodular Limestone). This 2nd order TST is further subdivided into two stacked transgressive cycles - a lower transgressive cycle (TL), and upper transgressive cycle (TU), representing the 3rd order transgressive systems tracts (3rd order TSTs). TL incorporating fluvial sediments of FA-1 and FA-2 mostly, with some fluvio-tidal sediment of FA-3 whereas, TU includes fluvio-tidal and shore sediments of FA-3, FA-4 and FA-5. Each 3rd order TST is further divided into higher frequency (lower rank) regressive-transgressive cycles (T-R cycles), and are identified as the parasequences of 4th order. Overall stratal architecture and multiproxy evidences of marine transgression events in central India during late Cretaceous time suggest creation of accommodation space by global eustatic sea level rise in association with tectonic subsidence (reactivation of Son-Narmada South fault).

ACKNOWLEDGEMENT

One of the most beautiful journey of my life is at its final feet. Throughout this journey so many people made their contributions of time, care, patient, inspiration and the most important they kept their faith in me. A simple thank you is not just enough to express my gratitude towards them. I must say that during this journey I have not only collected technical knowledge and the degree but also packed my bag with love and care of so many well-wishers, who really cares for me. During this journey, Roorkee has become a home away from home for me.

First and foremost I want to express my gratitude and respect towards the person who made my Ph.D. journey so comfortable, my mentor ***Dr. Biplab Bhattachaya****. He always said "first be honest with your work". I was privileged to work under his guidance. I am forever grateful to him for his optimist nature; he taught me how to extract the positivity from any constrained situation of life. He introduced me to the domain of sedimentology and then gradually and steadily assisted me to construct a firm base on sedimentology. He has always made himself obtainable to clear my doubts and quarry from his hectic timetable. I would like to express a deep sense of gratitude to you 'sir' for your profound guidance.*

I acknowledge my co-supervisor Dr. Suparna Hazra for her support and encouragement. I am thankful to Prof. Pradipta Banerji, the former Director of IIT Roorkee and Prof. Ajit Kumar Chaturvedi, the present Director of IIT Roorkee for providing me with the infrastructure to carry out my research work in this institute. I also thankful to the organization Geological Survey of India to provide me with the no objection to pursuing my research work further, after joining the organization. My thankfulness goes out to Prof. Arun K. Saraf, Prof. Deepak C. Srivastava, and Prof. Sunil Bajpai former and present Head of the Department of Earth Sciences, respectively, for their aid and support in providing a research environment in the department. I am also thankful to the members of my research committee, Prof. Mohammad Israil (former DRC Chairman), Prof. R. Krishnamurthy (present DRC Chairman), Prof. Dilip K. Mukhopadhyay (SRC Chairman), Prof. Amit K. Sen (internal SRC member) and Prof. R. K. Dutta (external SRC member) for their constructive scientific advice. I want to thank Mrs. Shiba Ramola Ma'am, former Assistant Register for her constant support during the time of my Ph.D. status conversion from full-time to part-time.

I am also grateful to the Director, and Dr. A.K.Singh, Scientist of Wadia Institute of Himalayan Geology (WIHG), Dehradun, for providing me with the facility of XRF.

I want to thank the office shafts of Department of Earth Sciences, IIT Roorkee especially Nair Ji, Surinder Ji, and Bhim Singh Ji for their constant non-technical help.

I want to thank Sharma uncle ji (field driver). He is such a nice and kind hearted person. During our field days in Bagh area his constant support is remarkable.

I want to express my love and warmth towards my all lab mates Joyeeta di, Sarita, Sunil, Harshul, Abhirup, Anirudhha, Ekta, Pawan, Tarun, Subham, Rohini, Tamanya, Akash, Ravi, Saswata, Arpita, Tanmay, Sounak, Malini, Nupur, Harshit, Lovely, and Sapna. All of them are very supportive and kind, they create a familiar environment in the laboratory which helps me a lot to work happily. Among all of them, Sarita deserves a special thank for her help in my research work and for her endless encouragement.

I want to acknowledge the institute where I was introduced to the world of geology, Durgapur Government College, West Bengal. I express my gratitude and respect towards all the teachers of Geology Department for their endless effort and motivation towards making our future bright in the field of geology. I want to thank Dr. Tapas Kumar Gangopadhyay, IIEST Shibpur, my dissertation guide for introducing me to the Bagh Group of Rocks and its palaeontological aspects. Thanks are due for all the teachers back at my school; they helped me to strengthen my root in each and every step of life by their valuable suggestions and blessings. I would like to thank all the authors/ researchers whose work helped me to enhance my sedimentological knowledge.

I want to express my love towards Shreya and Piu, they became a part of my life. I am privileged to have such awesome friends in Roorkee, their valuable suggestions, encouragement helped me a lot to become a more mature being.

Titli, my niece, bundle of happiness. The most precise gift of my life, the one who loves me unconditionally is deserves a special mention for her sparkling, lively and bubbly nature. I express my gratitude toward Boudi (Mrs. Supriya Bhattacharya); her affection, love and constant care never make me realize that I had stayed away from my home in Roorkee. I want to express my respect to Jethima (Mrs. Tapati Bhattacharya) for her affection and valuable advice in the course of my Ph.D. journey.

*Hearty thanks go to my family, who always kept their hope and faith high in me. They constantly support me in each and every step of my life. I consider myself the fortunate in the world to have such a supportive family, standing behind me with their love and support. My Mother (**Ma**) is the only reason for whatever I am today. I want to thank my father Dr. Ashis*

Jha (Baba) for always being with me. I extend my respect towards my paternal (Thamma) and maternal (Dida) grandma and all elders in the family. I don't imagine a life without their love and blessings. I would like to thank my grandfather (Dadu) Late Satyendra Nath Jha for all the love he gave in my childhood days. A warm thanks to my sister Rimpa, for being my blind supporter in every situation of my life, lots of love for you dear. A thank for my cousins Mampi and Rony for all their love and support. Thank you Ma, Baba, Kaku (uncle), Kakima (aunty), Chotomama and Boromama (maternal uncles) for keeping your faith in me and giving me the liberty to choose what I desired.

My special thanks are owed to Mr. Sayan Sinha, my best friend, my love for life, for his understanding, concern, inspiration, and loving support during this journey. I want to express my gratitude for all his criticisms, which though initially was painful but deep inside it helped me a lot to become a stronger and mature one. Thank you Sayan for always being with me.

Finally, I thank to the Almighty for everything in my life. ***Thank you!***

SUPARNA JHA

Research scholar
Department of Earth Sciences
IIT, ROORKEE

CONTENT

List of publications

1. Bhattacharya, B., Jha, S., 2014. Late Cretaceous diurnal tidal system: a study from Nimar Sandstone, Bagh Group, Narmada Valley, Central India. Current Science 107(6), 1032-1037.
2. Jha, S., Bhattachraya, B., Nandwani, S., 2017. Significance of seismites in the Late Cretaceous transgressive Nimar Sandstone succession, Son-Narmada rift valley, Central India. Geological Journal 52, 768-783.

List of Tables

1 Introduction

2 Geological Background

3 Facies Analysis

5 Ichnology

7 *Geochemistry*

List of Figures

1 Introduction

2 Geological Background

3 Facies Analysis

4 Tide and wave generated structures

5 Ichnology

6 Soft sediment deformation structures

7 Geochemistry of Nimar Sandstone

8 Discussion

CHAPTER- 1

Introduction

1.1. Foreword

Sea level fluctuation is one of the most common and significant geological phenomenon on the Earth surface. The fluctuation in relative sea level is a combined effect of change in ocean volume or in the volume of water in the ocean due to eustatic causes (Wagreich et al., 2014) or local tectonic subsidence and climatic changes (Miller et al., 2005). Globally, sea level was raised and fallen several times in the geological past. Several major and minor fluctuations have been recorded based on various sedimentological and geochemical parameters as well as different macro and micro flora-fauna indices. However, from various global fluctuations of sea level in geological time, late Cretaceous experienced the maximum rise of sea-level (Miller et al., 2005) i.e., 100-170 m. higher than today's sea level (Muller et al., 2008). Mostly, all the subcontinents of the supercontinent Gondwanaland were fully or partially submerged under water at different time phases during the Cretaceous time, which causes the formation of various shallow epicontinental seas in North America, South America, Russia, Australia and Africa. During early Cretaceous, parts of the Arctic, Canada, Russia and western Australia were submerged, while east-central Australia experienced major inundation during the middle Cretaceous period. At this time, Indian subcontinent confronted the major palaeogeographic changes due to the fragmentation of the Indian plate from the Africa and Madagascar, followed by its north-east ward movement (Acharya, 1991). The effect of Cretaceous global sea level rise is also reflected in Indian subcontinent in terms of changes in sedimentation pattern, sediment-organism interaction pattern and climatic condition. Evidence of Cretaceous sea level rise in Indian subcontinent is recorded within thick sediment successions of the Cauvery basin (Nagendra et al., 2011; Nagndra et al., 2013; Bansal et al., 2018), the Shillong basin (Singh and Mishra, 2000), the Kutch basin (Desai et al., 2013), the Bengal-Assam basin, few portion of the Himalayan belt and the Son-Narmada rift valley basin (Acharya and Lahiri, 1991).

Cauvery basin, Shillong basin and other Cretaceous Indian basins are well studied in terms of sedimentological attributes. Based on sedimentological parameters from Cauvery basin four eustatic cycles were documented by Sundaram et al. (2001). In comparisons, the Bagh Group

of rocks in the Son-Narmada rift valley basin has remained neglected. The depositional time of the Bagh Group sediments (late Cretaceous), preservation of marine evidence both in terms of primary structures, trace fossils, rich invertebrate body fossils and its depositional setting within an active rift system (Son-Narmada rift valley area) increased its geological significance. Combination of all these parameters demands a detailed sedimentological study of the Bagh Group of rocks.

Late Cretaceous Bagh Group sedimentation was started within the Son-Narmada rift valley system during the Cenomanian time, directly over the Proterozoic Bijawar rocks. Bagh Group of rocks comprises of three formations-the lowermost siliciclastic Nimar Sandstone of Cenomanian age, followed by Turonian Nodular Limestone in middle and Coniancian Coralline Limestone at the top. Presence of various sedimentary facies, ichnofabrics and varied palaeontological attributes within the Bagh Group manifest distinct changes in the depositional environment. The Nimar Sandstone records evidences of distinct changes from fluvial to marine depositional setting. The fluvial to marine transition zone is one of the most complex zone on the Earth where both fluvial and marine processes interact side by side and produced typical facies architecture. So a thoughtful integrated study on the sedimentary facies variation, primary sedimentary structure, trace fossils, geochemical and systematic sequence stratigraphic study will be helpful to interpret a correct palaeoenvironmental and palaeogeographic condition for the Nimar Sandstone.

The absence of detailed sedimentological work, its stratigraphic position (both in time and space) and well preservation of sedimentary structure stimulated the present research work for detailed sedimentological analysis. The present thesis is a combination of various attributes: detailed sedimentological facies analysis, ichnological aspects, geochemical analysis and systematic sequence stratigraphic study. All these parameters together aid to reconstruct the palaeogeographic conditions of the basin as an effect of the late Cretaceous sea level rise in Indian subcontinent. With this purpose, intense literature studies were done, a wide range of data is generated during the field studies and laboratory analysis and their systematic representation have been carried out in the following chapters.

1.2. Previous Work

1.2.1. International status

The late Cretaceous period has long been recognized as a time of intense tectonic activities, volcanism, changes in climatic and greenhouse condition (Miller et al., 2005; Sames et al., 2016). These were accompanied by a prolonged sea level rise with the warm anoxic oceanic condition. Worldwide inundation of landmasses due to high sea level rise during Cretaceous time has been reported by various workers (Hancock and Kauffman, 1979; Forster et al., 1983; Hilbrecht et al., 1986; Haq et al., 1988; Hallam, 1992; Roper and Rothgaenger 1995; Shiraishi and Kano 2004; Miller et al., 2005, Shiraishi and Yoshitomi, 2005). The extreme greenhouse climatic condition due to high CO_2 concentration along with tectonic subsidence are the causes behind the Cretaceous sea level fluctuation (DeConto and Pollard, 2003; Robson et al., 2014; Sames et al., 2016). Analyzed data of δO^{18} and δC^{13} from benthic foraminifera at Deep Sea Drilling Project (DSDP) Site 511 and 327 (Falkland Plateau ~58°S - 62°S palaeolatitude) in the southern part of the South Atlantic ocean and Cenomanian, Coniacian, Santonian foraminifera from DSDP Site 258 (Naturaliste Plateau ~58°S palaeolatitude) in southern part of the Indian Ocean reveal a gradual warming of surface water (Huber et al., 1995). δO^{18} curve shows a gradual increase in sea surface temperature from Turonian to early Campanian where cooling trend began in the late Campanian to Maastrichtian (Stoll and Schrag, 2000; Price and Hart, 2002; Friedrich et al., 2008, 2012; Wang 2013). Zakharov et al. (2011) reported that during the Cretaceous time atmospheric as well as sea surface temperature was changed frequently. Continuous change in sea surface temperature supported that sea level fluctuation was very frequent. To estimate the Cretaceous oceanic temperature from pole to equator, ratio of stable isotope $^{18}O/^{16}O$ in foraminifera calcite from sediment cores has been used (Sellwood et al., 1994; Huber et al., 1995; Noris and Wilson, 1998). Based on the carbon isotope data from northern Tunisia three major 3rd order eustatic cycles were marked which are associated with Campanian transgression. A major sea level transgression of late Cenomanian time was recorded by Kauffman (1993) from the western interior basin of North America, he stated that trigger of this transgression is a combined effect of subsidence and the tectono-eustatic highstand. Kellar et al. (2004) supported this event by a study of rapid positive $\delta^{13}C$ shift value in foraminifera. The rapid positive $\delta^{13}C$ shift that marks the onset of Oceanic Anoxic Event 2

(OAE 2) at Pueblo section occurred over a period of about 100 ky (93.90-94.00 Ma), and coincided with the major sea level transgression event. Lake Pueblo section is the Global Stratotype for Cenomanian/Turonian boundary (Kennedy et al., 2000).

The evidence of early Cenomanian marine transgression was also recorded in Libya from Kurfa basin (Barr, 1972). According to Sebastian et al. (2000), presence of shale and evaporites overlain by the carbonate within Kurfa basin are results of marine incursion; this deposit was interpreted as a coastal mudflat deposit near the Tethys shoreline. Naidin (1983) also reported evidence of late Cretaceous transgression (Cenomanian) event from Russian platform. Hilbercht et al. (1996) interpreted a long term sea level rise during late Cenomanian time based on the increased value of $\delta^{13}C$ throughout carbonate sequence from Regensburg area, southern Germany. Based on the correlation of basinal to outer platform sections of south-east France, constrained by both micropalaeontological and isotope data, Grosheny et al. (2017) identified a transgressive event. This transgression is related to a short lived compressive tectonic pulse probably connected with the early compressive movement of African and European plate. Late Cretaceous palaeodepositional condition of Songliao Basin in north-east China is still in controversy. Based on the presence of nanofossils, brackish water algea and foraminifera, Xi et al. (2016) stated that Songliao basin is affected by several phases of marine water encroachment during Cretaceous time, whereas Wang et al. (2017) interpreted more marginal to non-marine condition based on the appearance of non-marine ostracod fauna for Songliao basin.

Several parts of the different continents confronted transgression during Cretaceous time, for examples parts of Arctic Canada, Russia, and western Australia were submerged under water during the early Cretaceous time, whereas east-central Australia was inundated during the middle Cretaceous time. In various time-span of the Cretaceous, most of western Europe, eastern Australia, parts of Africa, South America, India, Madagascar and Borneo were inundated. In the book "Cretaceous World" Skelton (2002) described the sea level fluctuation history in a diagram, showing that during the Cenomanian-Turonian time southern part of the Indian subcontinent (Cauvery basin) was submerged under water. Sundram et al. (2001) revised the palaeoclimatic condition of the Cauvery basin from southern India and interpreted onshore depositional settings. In few parts of the Central India, depositions of contemporaneous marine sedimentations (Bagh Group) are also reported.

1.2.2. National status

In India, sediments of late Cretaceous Bagh Group deposited directly over the Proterozoic Bijawar rocks. Geologically, the Bagh Group of sediment was first accounted by Capt. Dangerfield (1818). Subsequently, Captain J. Stewart (1821) published a note on the geology of the Bagh area. Abundance of vertebrate and invertebrate body fossils within the Bagh sediments fascinated researcher since long. Palaeontologically Bagh Group is well documented; various invertebrate body fossils like ammonites, bivalve, brachiopods, echinoids are reported from the Bagh Group. First fossil from the Bagh Group was discovered by Capt. Keating (1856), followed by its report by Oldham (1856) from Chirakhan area. Based on the presence of invertebrate body fossils and their community Oldham (1856) suggested the Neocomian age for the Bagh Group. Keatinage and Blackwell (1857) also specified that Bagh Group was enriched with fossils. Based on systematic studies of echinoids and ammonites from Bagh Group Duncan (1887), Vredenburg (1907, 1908) and Fourtau (1918) concluded that those fossils have Mediterranean affinities and gave late Albian to Cenomanian age for the host sediments (mainly Nodular and Coralline Limestone). Chiplonkar (1939) was the first to systematically describe the Bryozoans from the Bagh Group, although their presence was mentioned earlier by Bose (1884). After that there was a series of publication on bryozoans from the Bagh Group, where Chiplonkar and Ghare (1975, 1976) documented new species of bryozoans and Guha and Ghosh (1975) described those species in details. The palaeoecological aspect of Bagh Group was well described based on bryozoans by Badve and Ghare (1978). Similarly, the palaeogeography of Bagh Group was described by using the occurrence of algae *Halimeda* and absence of belemnites by Barron (1987) and Funnel (1990). In a series of publications Gangopadhyay and Bardhan (1993, 1998 and 2002) described the bivalves and ammonites from Bagh sediments in a systematic way and interpreted as marine depositional environment. By using the cells of echinoids, Smith (2010) dated the Bagh Group of rocks to be of Late Turonian age. Jaitly and Ajane (2013) commented on morphologically variable ammonoid taxon *Placenticeras mintoi vredenburg* from Nodular Limestone and modified the stratigraphic succession of the Bagh Group.

Records of micropalaeontological and palaeobotanical aspects of the Bagh sediments were also plenty; Murty et al. (1963) documented the first plant fossil from this area. Jafar (1982)

reported nanoplanktons from the Bagh Group and concluded about the Turonian transgression in Central India. Investigation of microorganism started by Nayak (1987), who documented foraminifera from the Nimar Sandstone for the first time. Kundal and Sanganwar (1998) recognized calcareous algae from the contact between Nodular Limestone and Nimar Sandstone, involving 72 species of 26 genera, identifying *Cyanophyta*, *Rhodophyta* and *Chlorophyta*. These calcareous algae are genetically similar with Indo-Mediterranean Tethyan realm algae. Based on the algal assemblages the same workers predicted a tropical climatic condition during the deposition of the Nimar Sandstone.

Chiplonkar and Badve (1969, 1970, 1972 and 1973) and Chiplonkar and Ghare (1975) documented trace fossil from the Bagh Group and identified various ichnogenus. Badve and Ghare (1980) proposed a 3D bathymetric model of the Son-Narmada rift valley during the Nimar sedimentation based on trace fossil study. Sanganwar and Kundal (1997) identified 16 ichnospecies and classified them into eleven ichnogenera from the middle part of the Nimar Sandstone. Based on these ichnospecies they considered all ichnofossils of the middle part of the Nimar Sandstone under Cruziana ichnofacies and inferred a slow and continuous sedimentation pattern for Nimar sandstone.

Another special attraction of Bagh Group sediments is the preservation of bones and eggshells of dinosaurs. Huene and Matley (1933) first time reported imprints of dinosaur fossils. Based on the properties of those fossils they identified *Saurischia* and *Ornithischia* genus. Para-taxonomic classification of dinosaur eggshells from Bagh Group was given by Khosla and Sahani (1995). Khosla (2001) reported diagenetic alteration of dinosaur eggshells from the Bagh Group. Though dinosaurs body fossils are not reported commonly from Nimar Sandstone, Khosla et al. (2003) first time reported dinosaur bones from the Nimar Sandstone.

However, even after so many studies, the stratigraphic division and the age of individual units of the Bagh Group is still controversial and is not properly age constrained. Several researchers proposed different stratigraphic succession for the Bagh Group. First generalized stratigraphic succession was given by Blanford (1869) from Chirakhan area (Table 1.1).

Bose (1884) resurveyed the area and gave a more detailed stratigraphic succession for the Bagh Group (Table 1.2). With time, several modifications were made in the stratigraphic succession by various workers.

Table: 1.1. Stratigraphic succession of the Bagh Group by Blanford (1869).

Deccan Trap	
Bagh Group (Late Cretaceous)	Coralline limestone
	Fossiliferous argillaceous limestone Abounding in Echinoderms (Hemiaster)
	Unfossiliferous Nodular Limestone
	Sandstone and Conglomerate
Archean Metamorphic	

Chiplonkar was the first to give a detailed comprehensive stratigraphy of the Bagh Group. Road and Chiplonkar (1935) made some changes in the detailed stratigraphic succession proposed by Bose (1884) and added two new horizons within the Coralline Limestone instead of one (Table 1.3). Roychowdhury and Sastri (1962) mapped the area and gave a general description for each stratigraphic unit. They considered that Deola-Chirakhan marl was weathered part of Nodular Limestone; and do not bear status of a separate stratigraphic unit in Bagh Group, as mentioned by Bose (1884). Till date, the controversy about the position of Deola-Chirakhan Marl bed exists.

Table: 1.2. Detailed stratigraphic succession of the Bagh Group by Bose (1884).

Deccan Trap	
Upper Cretaceous	Lameta (Lacustrine)
	Coralline Limestone
	Deola-Chirkhan Marl
	Nodular Limestone
Lower Cretaceous (Neocomian)	Nimar Sandstone
Jurassic	Mahadeva
Proterozoic	Vindhyans
Archean	Bijawars, Metamorphic

Table: 1.3. Stratigraphic details of the Bagh Group of rock after Road and Chiplonkar (1935).

Upper Cretaceous	Deccan Trap- Fossil wood and Breccia zone	
Lower Cretaceous	Bagh Group	Upper Coralline Limestone
		Deola-Chirakhan Marl
		Lower Coralline Limestone
		Nodular Limestone
		Nimar Sandstone
Proterozoic	Basement	

Enrichment of body fossils, as well as trace fossils, always amplified the palaeontological significance of the Bagh Group of rocks. Based on the palaeontological study a broad shallow marine depositional setting was predicted for the Bagh Group. Pascoe (1959) first time interpreted the depositional setting of the Nimar Sandstone (lowermost formation of the Bagh Group) as fluvial, based on primary sedimentary structure and lithology. Robinson (1967) supported the opinion of Pascoe (1959) and considered that the lower part of the Nimar Sandstone is a product of fluvial sedimentation based on the dominant lithology of the area, whereas upper part is the product of marine sedimentation. Sarkar (1973) studied all the formations of the Bagh Group including Lameta Formation in and around Alwaldaman and Bagh area and considered a 'tidal deltaic' depositional setup. Raiverman (1975) considered marine depositional background for the Bagh Group. Singh and Ghosh (1977) and Singh and Srivastava (1981) exhibited that the bottom part of the Nimar Sandstone is fresh water sediment whereas the top part is marine in nature. Singh and Srivastava (1981) reported Nimar sedimentation as a freshwater to shallow marine intertidal to subtidal depositional setting. Bose and Das (1986) deliberated and marked five major facies variations in Nimar Sandstone from the Alwaldaman section, and described a transgressive marine shelf sequence.

However, Bhattacharya et al. (1997) based on carbon isotope dating of 18 samples of the Nimar Sandstone predicted a freshwater depositional setting.

In terms of sedimentological point of view, the entire late Cretaceous sedimentary basin share the same depositional setting due to global sea level rises. Other Cretaceous Indian sedimentary basins bears the evidence of several transgressive-regressive phases which are already documented and correlated with late Cretaceous global sea level rises. Nagendra et al. (2017) stated that late Aptian to the mid Albian sea level cycle of Cauvery basin shows some correspondence with the northern Gulf of Mexico sea level fluctuations. Organic rich sediment of late Aptian, early Albian (OAE-1b), late Albian (OAE-1d), late Cenomanian and early Turonian (OAE-2) times in Cauvery basin indicates an anoxic condition due to major transgression episodes and are correlated in a global scale (Govidan, 1993 ; Reddy and Rao, 2011). For Shillong shelf sediments, Acharya and Lahiri (1991) stated that the rich marine shelf sediments of Mahadek Formation of the Campanian-Maastrichtian age is closely similar to those recorded from the Ariyalur Group in the Cauvery Basin. So, in terms of various sedimentological parameters, Indian Cretaceous basins are well documented and they are globally co-related except the Bagh Group sediments in Son-Narmada rift valley. So detailing of the Bagh Group of sediments is required to know the exact palaedepositional setting.

1.3. Gaps to be addressed- Defining the research problem

The Bagh Group of sediment is a window to the late Cretaceous world in the Indian subcontinent. The Bagh Group of sediment is key to reveal the late Cretaceous history in terms of palaeoclimatic condition, basinal morphology and depositional environment, and will be significant in understanding the effect of global sea level rises in the Indian subcontinent. From the detailed literature study, it seems obvious that the Bagh Group of rocks required a detailed sedimentological attention. Still, there has been a considerable confusion in the understanding of the depositional model of the Bagh Group sediments. The detailed sedimentological analysis in terms of provenance study, facies architecture and interpretation of individual primary structures, trace fossils, sequence stratigraphy and reconstruction of the palaeogeography is not done yet. According to literature survey, the overall depositional condition of the Bagh Group is controversial, as per some researcher it is purely fluvial and other researcher stated that depositional condition was gradually changed from fluvial to marine setting (discussed earlier).

Present research work focus on the sedimentological attributes of the Cenomanian Nimar Sandstone which is the lowermost lithounit of the Bagh Group. It is expected that the first imprint of Cenomanian global sea level rise possibly chronicled within this lowermost lithounit. Thus, detailed sedimentary facies analysis, interpretation of various facies architectural pattern, analysis of various ichnoassociation, sequence stratigraphy in terms of sea level fluctuation and palaeogeographic reconstruction of the Nimar Sandstone are the main aspects of this research work. The main aim of this research work is to find out the relationship between the fluvial and marine processes during sedimentation and correlate them with major transgressive-regressive cycles in terms of tectono-eustatic changes in Son-Narmada rift valley in the light of global late Cretaceous sea level fluctuation. Such detailed sedimentological-ichnological and integrated sequence stratigraphic study from the Nimar Sandstone has not been attempted yet.

1.4. Objectives

To fulfill the aforementioned research gaps, current research work has been outlined with the following objectives:

- Characterization of the Nimar Sandstone in terms of physical, chemical and biological properties under the fluvio-marine interactive depositional system.
- Interpretation of major palaeoclimatic and palaeoenvironmental changes based on sediment-organism interaction pattern in response to changing palaeoecological controls.
- Reconstruction of temporal and spatial evolution in basinal palaeogeography in relation to tectono-eustatic changes.

1.5. Methodology

This research work is mainly field oriented. The overall methodology includes field study, sampling, logging, ichnological study, petrographic study under polarized microscope, major and trace element study using X-ray fluorescence (XRF) (Figure 1.1). All these methods are divided into four categories.

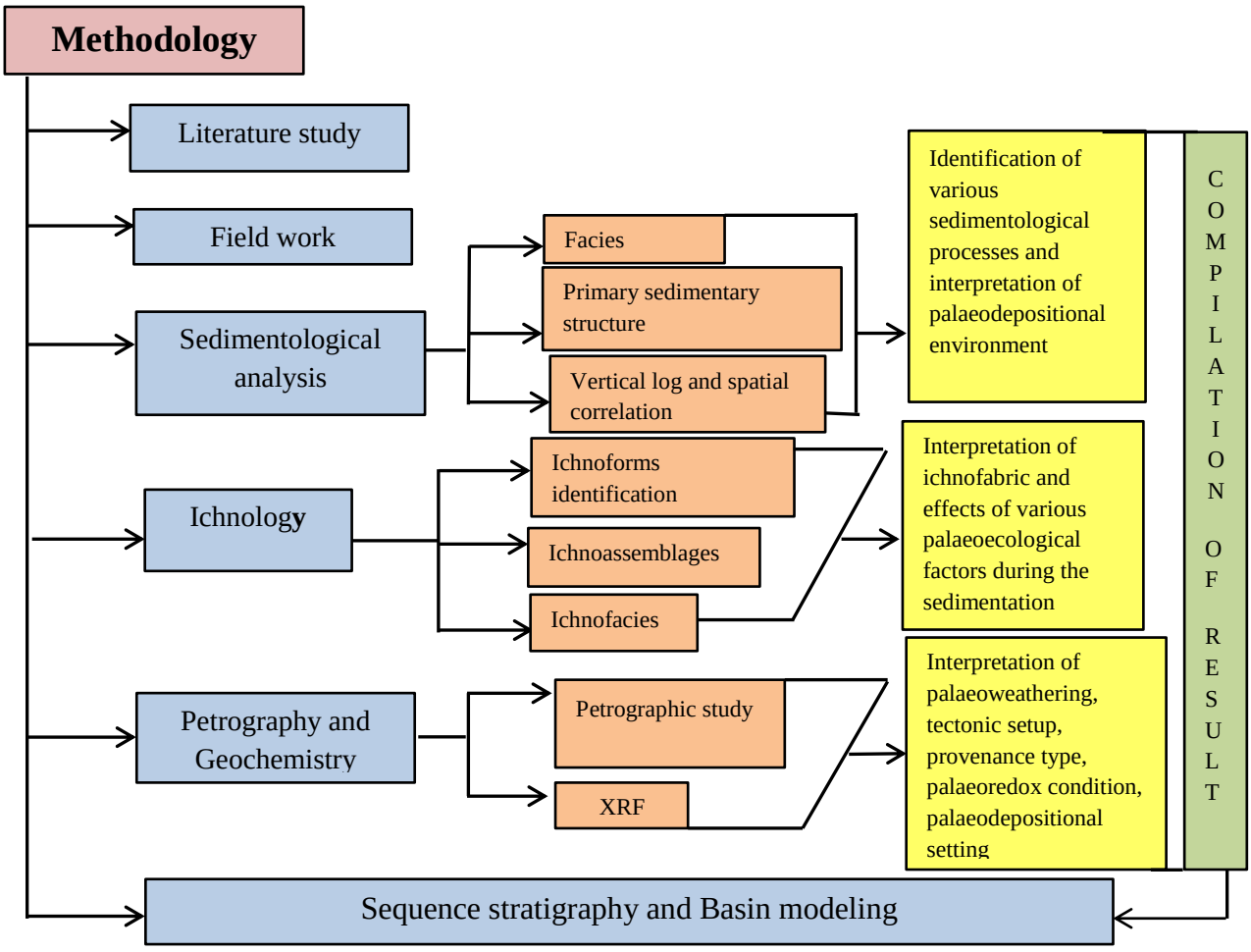

Figure: 1.1. Flowchart showing the various methodologies used during the present research work and their inter relationship.

1.5.1. Sedimentological analysis

- Identification of different facies types and interpretation of their depositional condition based on their transportation process, agents and mechanisms of deposition and bathymetric configurations.
- Preparation of lithologs from different parts of the Nimar Sandstone and incorporating the sedimentological and ichnological data.
- Correlation of the lateral and vertical distribution of different facies types to understand their spatio-temporal distribution in the study area and to identify the various sedimentary events.

- Study of different primary sedimentary structures to interpreted their origin, flow pattern and processes, which helps to predict the tectono-sedimentary relation and palaeodepositional condition of the study area.
- Detailed petrographic studies of different rocks types and interpret their textural pattern, compositional variation to know about the provenance type and transportation history of the sediments.

1.5.2. Ichnology

- Identification and systematic description of various ichnoforms and their associations.
- Ichnofabric and ichnoassemblages study to know the various palaeoecological controls and their intensity on the sediment-organism interaction pattern during the time of sedimentation.
- Interpretation of palaeodepositional condition in terms of various ichnoassociations.

1.5.3. Geochemical analysis

- Inorganic geochemistry was done for samples of different facies types for high-precision petrological and geochemical analyses by using XRF quantify the elemental concentration of the rocks.
- Interpretation of geochemical data to know the tectonic setting, provenance type, degree of weathering and palaeodepositional condition.

1.5.4. Sequence stratigraphy and Palaeogeographic reconstruction

- Preparation of palaeodepositional model to determine the role of non-marine marine influence on the sedimentation pattern and preparing the overall high resolution sequence stratigraphic architecture of the basin during the time of Nimar Sandstone sedimentation.
- Identification of various stages of transgression-regression event and major sequence boundaries to deciphering the nature and cause of change over from the fluvial to the fluvio-marine interactive sedimentary setup.
- Interpretation of tectono-sedimentation interrelationship during the time of Nimar sedimentation from various degrees of cyclicities in the vertical succession.
- Interpretation of palaeogeographic and palaeoenvironmental condition in relation with late Cretaceous sea level rise for the Nimar Sandstone.

Sequence stratigraphy and palaeogeographic reconstruction is basically a product of aforementioned all three categories. Detailed sedimentological, ichnological and geochemical analysis helps to identify the sequence boundaries, to make a palaeodepositional model and to reconstruct the palaeogeographic setting of the Nimar Sandstone.

1.6. The significance of the present research work

Organized sedimentological study of Nimar Sandstone in Son-Narmada rift valley still remains to be documented. This research work addresses all the sedimentological gaps from the study area and interprets them in term of spatio-temporal variation in depositional environments and tries to correlate them with global late Cretaceous sea level fluctuations. Sedimentological interpretation of the Nimar Sandstone will decipher new insights into the understanding of the pattern of tectono-sedimentary evolution of the Bagh Group sediments in the Son-Narmada rift valley in relation to regional tectono-eustatic changes during the late Cretaceous time in peninsular India. The study will also reveal the relation between late Cretaceous global sea level rises and the local tectono-eustatic changes in Central India.

1.7. Organization

The present research work and their various methodologies with the outcomes in this thesis have been organized as follows:

CHAPTER 1 includes general introduction along with a foreword, broad literature survey in terms of both international and national aspects to create a strong base for the present work, research problem, objectives, methodologies and the significance of the research work and the arrangement of the thesis.

CHAPTER 2 comprises of a general introduction along with general geology of the Son-Narmada Rift valley followed by general geology of the Bagh group and geological setting of the study area.

CHAPTER 3 identifies the various facies types based on their characteristic, appearance and classified them into various facies association. Interpretation of the various facies types and

their associations in terms of processes and depositional environment also included in this chapter. At the end overall depositional condition of the Nimar Sandstone is discussed.

CHAPTER 4 deals with the description of various tide-and wave-generated primary structures and their interpretation. Presence of these structures in the study area helps to interpret the palaeodepositional condition precisely.

CHAPTER 5 comprises of identification of various ichnoforms up to genus level and their systematic description. Description of various ichnoassociations and ichnofacies of the study area are also discussed in this chapter in terms of various palaeoecological factors. Impacts of palaeodepositional and palaeoecological factors during the sedimentation of the Nimar Sandstone in the study area based on the sediment-organism interaction pattern also discussed.

CHAPTER 6 describes various soft sediment deformation structures (SSDS) and interprets them based on their deformation processes and finds their trigger mechanism. Studied SSDS are marked as seismites and presence of the seismites in the study area helps to identify the magnitude of the palaeoearthquake and the origin of seismic shock. Restriction of the seismites in distinct beds in Nimar Sandstone indicates tectono-sedimentary controls during deposition of the Nimar Sandstone.

CHAPTER 7 represents geochemical data and their interpretation in terms of palaeoredox, palaeoclimatic condition, palaeotectonic setting, provenance type and palaeodepositional setting.

CHAPTER 8 comprises of general discussion with compilation of the main findings of this research work. This chapter deals with the major aspect of this research work the T-R cycles, sequence boundaries, reconstruction of palaeogeographic condition of the Nimar Sandstone during the late Cretaceous time in relation with global Cretaceous sea-level rise and the final conclusions.

CHAPTER- 2

Geological Background

2.1. Introduction

The Cretaceous time period is one of the significant times for Indian subcontinent. During this time-span breakup of Gondwanaland created several linear intracratonic basin belts in the Indian subcontinent. Major palaeogeographic changes accompanied the creation of Indian Ocean and Neo-Tethyan Ocean during this time period. New sedimentary basins with numerous small epicontinental seas were also formed. Son-Narmada basin (Figure 2.1A) is one of such Cretaceous intra-cratonic basin, which formed during the late Cretaceous time and bears the evidence of marine sedimentation.

2.2. General Geology of the Son-Narmada rift valley

Geologically, Central India is highly diversified. Thick stratigraphic successions from various ages with evidence of multiple phase deformations are common in Central India. Central Indian Tectonic Zone (CITZ) is one of the prevailing structural components after Himalaya. During the Palaeoproterozoic time, due to suturing between the Bastar craton and the Bundelkhand craton CITZ was evolved (Yedekar et al., 1990; Yoshida et al., 2001; Roy and Prasad, 2003; Abdul Azeez et al., 2013). Along the CITZ differential crustal movement has been reported several times, as evident from reactivations of numerous fault systems (Acharya and Roy, 2000). Deformation along the CITZ continues to present day as demonstrated by the manifestation of earthquake at both upper and lower crustal depth, which indicate the ongoing reactivation of crustal faults related to the palaeo-rift setting (Rao et al., 2002; Mall et al., 2005). CITZ have two sub-parallel elements, which demarcate the boundaries among stratigraphic units, one is Sausur mobile belt in the south and the other is Son Narmada Tapti (SONATA) lineament zone in the north. A major portion of the SONATA lineament falls in Madhya Pradesh (Figure 2.1A), where a wide variety of rock types ranging from age Archean to recent are present (Jain et al., 1995). According to Crawford (1978), Son-Narmada lineament having an extension across the northern Madagascar appeared as narrow seismic rift and acted as a deep-seated fault. Correlation of structural and geophysical data indicates that the Narmada and Tapti lineament together represent an intraplate rift setting with a central (Satpura

Mountains) horst. Satpura Mountains is bounded on each side by grabens in the northern side Narmada graben and the Tapti graben in the southern side. The Son-Narmada rift valley is affected by two dominant deep-seated fault systems (Figure 2.1B) the east-west-trending-Son-Narmada North Fault and the Son-Narmada South Fault (Biswas, 1987; Tewari et al., 2001). Major lineaments within this area are the Barwani-Sukta Fault, Dhar lineament, Rakhabdev lineament and Jaoalaier lineament.

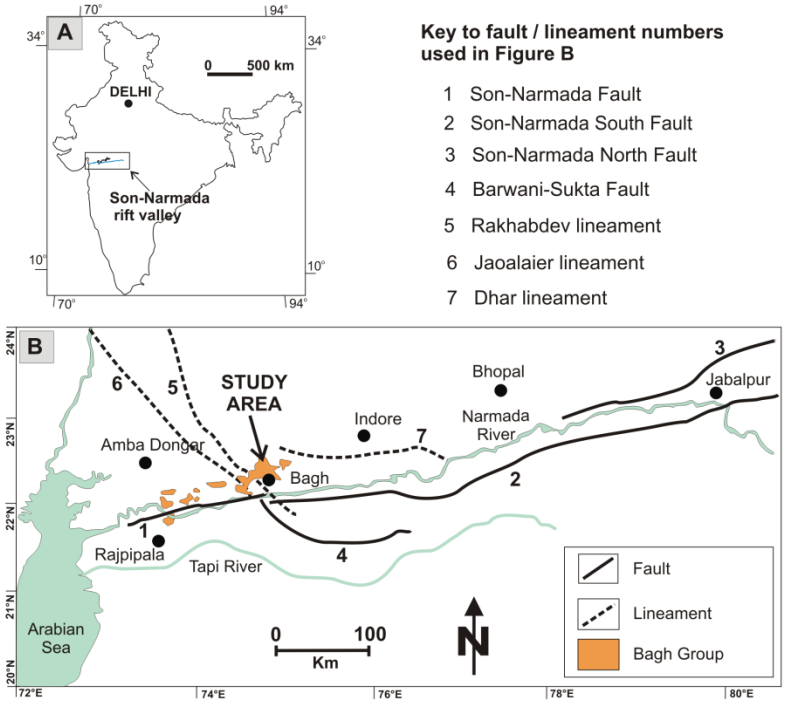

Figure: 2.1. (A) Map of India showing location of the Son-Narmada rift valley. (B) Generalized geological map of the Son-Narmada rift valley (modified after Abdul Azeez et al., 2013) showing the distribution of major faults and lineaments and the occurrence of the Bagh Group of rocks (also see, Jha et al., 2017). The study area is marked on the map.

2.3. General Geology of the Bagh Group

Reactivation of the rift systems along with basinal subsidence created accommodation space for Cretaceous sedimentation in Indian subcontinent. Son-Narmada South fault and Son-Narmada North fault are two major continental discontinuities in this area along with several lineaments. According to the published literature, there was no reactivation history of the Son-Narmada North fault whereas the Son-Narmada South fault was reactivated in several times from the Precambrian to Phanerozoic time (Acharya and Roy, 2000). Reactivation histories of

the other major lineaments were not recorded after their formation. Son-Narmada fault system was reactivated mainly in three phases (Tewari et al., 2001). The first phase of reactivation was started during the Palaeoproterozoic time when only the Son-Narmada North Fault was activated. Reactivation of this fault is designated by presence of trachytic intrusive and associated lamprophyres and syenite plutons along the fault of around 1600–1800 million years ages (Jain et al., 1995). This fault has remained non-active since the Neo-Proterozoic time (Acharya and Roy, 2000). The second phase of reactivation was recorded during the Jurassic-early Cretaceous time when the Son-Narmada South Fault was reactivated. As evidence of this reactivation presence of mafic intrusives is found south of Narmada graben and east of Barwani-Sukta lineament (Tewari et al., 2001). During the late Cretaceous time again the Son-Narmada South Fault was reactivated (third phase). This phase of reactivation is coincided with the passage of India over Reunion plume and caused subsequent emplacement of Deccan volcanics from the plume head along the western coast and covered a huge area. In Mesozoic time along the western margin of the Indian subcontinent three different rift basins were formed, Kutch-Saurashtra basin, Cambay basin and Son-Narmada basin. Son-Narmada basin was rifted along the Satpura trend during the early Cretaceous time (Biswas, 1987). Among these three basins only the Son-Narmada basin bears the evidence of late Cretaceous marine sedimentation (Bagh Group sediment).

Bagh Group of sediments is mainly confined to the western segment of the Son-Narmada rift valley. Extension of Bagh Group sediments are not continuous, they are patchy in nature. The eastern boundary of the Bagh Group sediment is marked by Barwaha town (N22°15′30″ E76°02′00″) in Madhya Pradesh (Jain et al., 1995). The western extension of the Bagh Group within the Son-Narmada rift valley is marked up to near Amba Dongar (N22°30′00″ E74°04′00″) and Rajpipala (N21°47′00 E73°30′30″) in Gujarat (Kumar, 2014). The maximum thickness of the Bagh Group sediments is exposed in the Bagh area in Madhya Pradesh (Figure 2.2).

Bagh Group of rock comprises of three formations, where the lowermost formation is siliciclastic Nimar Sandstone of Cenomanian age followed by Turonian Nodular Limestone and Coniancian Coralline Limestone. Nodular Limestone and Coralline Limestone are enriched with marine body fossils, trace fossils, microfauna and dinosaur bones-eggshells. This

sequence is overlain by Lameta Formation and both the Bagh Group of sediments and Lameta Formation is covered by Deccan flood basalt (Table 2.1).

Table: 2.1 Generalized stratigraphic table of the study area (modified after Singh and Srivastava, 1981; Jaitly and Ajane, 2013).

Age		Group	Formation	Member
		Deccan Trap		
Late Cretaceous	Maastrichtian	Lameta Group		
	Coniacian	Bagh	Coralline Limestone	
	Turonian		Nodular Limestone	Chirakhan
				Karondia
	Cenomanian		Nimar Sandstone	
---------- Unconformity /fault ----------				
Precambrian		Gneisses, granodiorites and crystalline rocks of Bijawar		

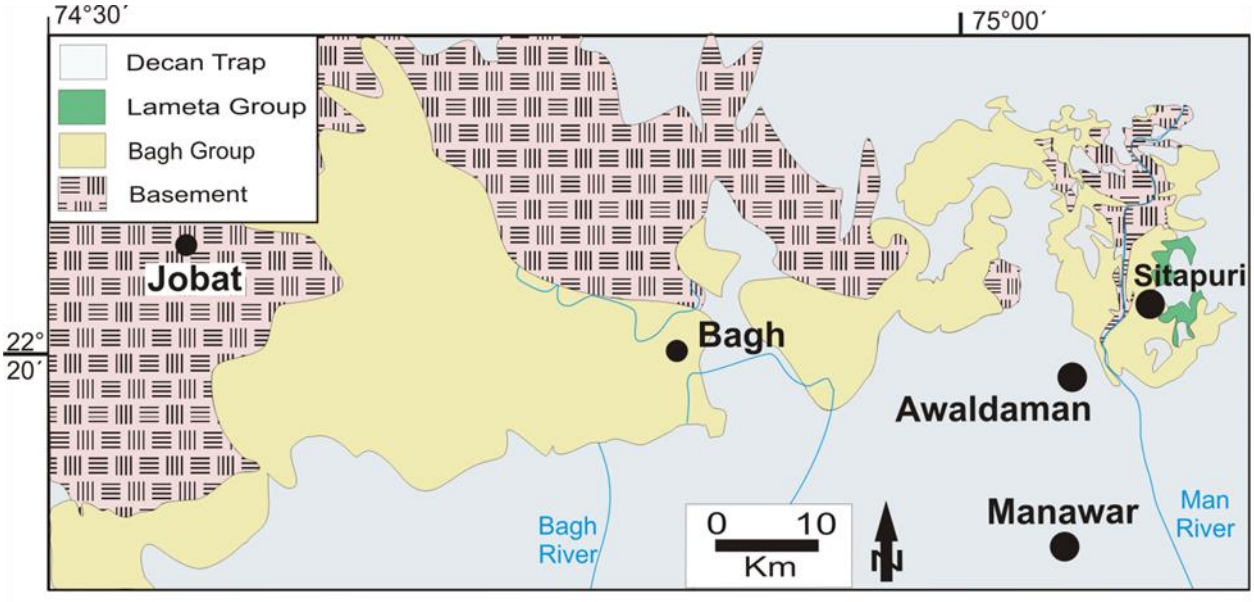

Figure: 2.2. Generalized geological map of the study area showing distribution of major lithounits (modified after Singh and Srivastava, 1981).

2.3.1. Nimar Sandstone

Nimar Sandstone is the only siliciclastic component of the Bagh Group that overlies the Precambrian gneiss of Bijawar Group. Nimar Sandstone shows a non-conformable relationship with the Bijawar genesis. Near Awaldaman along the Man river section it shows faulted contact with the underlying basement rocks. The thickness of this formation gradually increases towards the western side. Overall this is a medium to coarse-grained sandstone with ferruginous nature. In previous literature lower part of the Nimar Sandstone was considered as a gritty sandstone unit whereas upper part calcareous in nature (Bose, 1884). The overall depositional setting of the Nimar Sandstone is controversial. Sarkar (1973) considered Nimar sediment as a "tide-deltaic" product. Akhtar et al. (1994) interpreted that the Nimar Sandstone was deposited under a humid tropical palaeoclimatic condition based on the highly quartzose nature of sandstone. Bhattacharya et al. (1997) concluded Nimar Sandstone as a product of fresh water condition.

2.3.2. Nodular Limestone

Fossiliferous Nodular Limestone Formation conformably overlies the Nimar Sandstone, characterized by buff yellow colored, nodular, loosely packed calcareous unit. In Nodular Limestone two distinct stacks of carbonate unit have been defined, separated by an extensive and well-marked hardground (synsedimentarily cemented carbonate layers) surface. The lower part of the Nodular Limestone is known as Karondia member and upper part Deola-Chirakhan marl (Chiplonkar and Badve, 1979). Akhtar and Khan (1997) classified four litho-facies type within the Nodular Limestone -lime mudstone, bioclastic wackestone, whole fossil gastropod wackestone and calc spheroidal bioclastic wackestone. According to them a below wave base condition is preferable depositional setting for this formation. Nodular Limestone is a storehouse of marine invertebrate body fossils- bivalve, ammonite, gastropod, and echinoids are reported from this formation. Rajsekhar (1995) studied the foraminifera from this horizon and said 90% are benthic and 10% are planktonic. Based on the distribution pattern of the foraminifera Rajsekhar (1995) interpreted that the overall sequence shows a transgressive phase. Based on the restricted occurrences of nautiloids Gangopadhyay and Halder (1996) established a limited deep inland setting which differs from open marine setting for deposition of Nodular Limestone.

2.3.3. Coralline Limestone

Coralline Limestone is conformably overlain on Nodular Limestone. The contact between Nodular and Coralline Limestone has been marked by a bryozoan rich layer. In between the Nodular Limestone and Coralline Limestone, many workers defined an independent stratigraphic unit, Deola-Chirakhan marl. Deola-Chirakhan marl is a calcareous unit which characterized by buff to cream colored, and argillaceous in nature (Bose, 1884). The stratigraphic position of Deola-Chirakhan marl is controversial. There are two schools of thought; according to Bose (1884), Deola-Chirakhan Marl is an individual stratigraphic unit in between Nodular and Coralline Limestone, whereas Roy and Chowdhury (1962), Sahni and Jain (1966) considered Deola-Chrikhan marl as a weathered part of lower Coralline Limestone. Lower Coralline Limestone is characterized by cross-bedded calcarenite unit up to 120 cm thick, forms a more resistant bed of dark red colored, heavily bioturbated and rich in bryozoan. The top surface of this unit is highly fossiliferous with abundant *Thalassinoides* burrows, which indicates a hiatus in sedimentation (Smith, 2010). Upper Coralline Limestone is a calcarenitic unit; top of this unit is marked by hematite coated hardground surface. Large scale planar- and trough cross-stratification with flaser bedding are dominant primary sedimentary structure (Akhtar and Ahamed, 1997).The overall character of this limestone is argillaceous and flaggy type (Bose, 1884; Tripathi, 2006), which indicates relatively deeper water depositional settings in comparison to Nodular Limestone.

2.3.4. Lameta Formation

After the deposition of the Bagh Group sediments, a fluvial unit was deposited during the late Cretaceous time known as Lameta Formation. Lameta Formation unconformably overlies the Coralline Limestone and is overlain by the Deccan flood basalt. Sedimentation of Lameta Formation was started by deposition of conglomerate followed by gritty sandstone, purple Lameta sandstone, and cherty Lameta sandstone. It is characterized by bioturbated, mottled, brecciated calcareous sandstone. Presence of dinosaur fossils and wood fossils within this formation enhanced its chronostratigraphic importance. Deposition of Lameta over Coralline Limestone indicates a fall in sea level, resulting in regression of the shoreline (Roy and Chowdhury, 1962).

2.3.5. Deccan Trap

One of the most extensive continental flood basalt in the world is Deccan Trap Basalt. This is a large igneous province that covered all the sediments in western, central and southern part of the Indian peninsula during the late Cretaceous time. Mainly the basalt is a tholeiitic type but other varieties like nephelinite, lamprophyre, alkalinite and carbonatites are also present. A deep-seated mantle plume is associated with Deccan volcanism (Auden, 1949). Reunion hotspot is suspected to cause the Deccan eruption. Different plume models show a close link-up between the Indian plate motion and eruptive history of the Deccan volcanism. Based on data from marine magnetic profiles, a pulse of unusually rapid plate motion begins at the equivalent period as the first pulse of Deccan flood basalts, which is dated at 67 million years ago. According to Cande and Stegman (2011), the spreading rate of the Indian plate rapidly improved and reached a maximum value, at the same time as the peak of basaltic eruptions. The spreading rate then released, with the decrease occurring around 63 million years ago, by which time the main phase of Deccan volcanism ended.

2.4. Geological setting of the study area

The Bagh Group of rocks is exposed along the western flank of the Son-Narmada rift basin. The study area is bounded by latitude 22º15´00"N to 22º35´00" N longitude 74º30´00" E to 75º15´00"E. Bagh Group of sediments are mainly patchy and discontinuous in nature. All the three formations i.e., Nimar Sandstone, Nodular Limestone and Coralline Limestone are exposed at different localities. The rocks of the Nimar Sandstone are well developed and exposed along the Man River section near Awaldaman area, Sitapuri, Bagh River, Rampura, Bagh Cave section and Jobat area (Figure 2.3). Nimar Sandstone is characterized by conglomerate, arenaceous to arkosic sandstone, sandstone-mudstone heterolith and mudstone. In the study area general orientation of beds are strike N15ºE-S15ºW to N-S with near sub-horizontal dip (8º-10º). The study area falls under parts of Survey of India toposheet nos. 46N/03, 46J/15, 46J/16 and 46J/11. Geological map of the study area is given below.

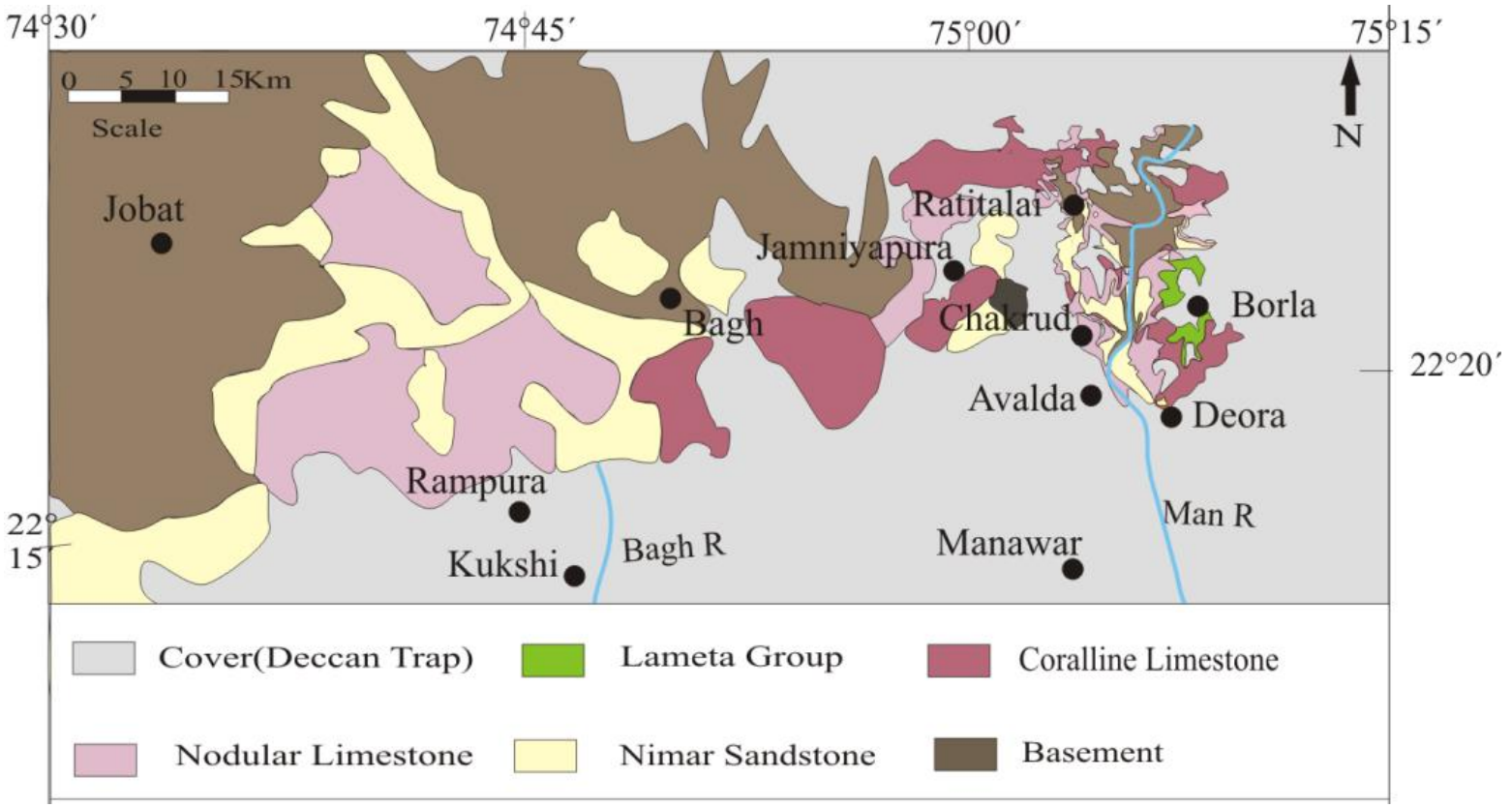

Figure: 2.3. Generalized geological map of the study area showing distribution of different lithounits of the Bagh Group (modified after Jaitly and Ajane, 2013).

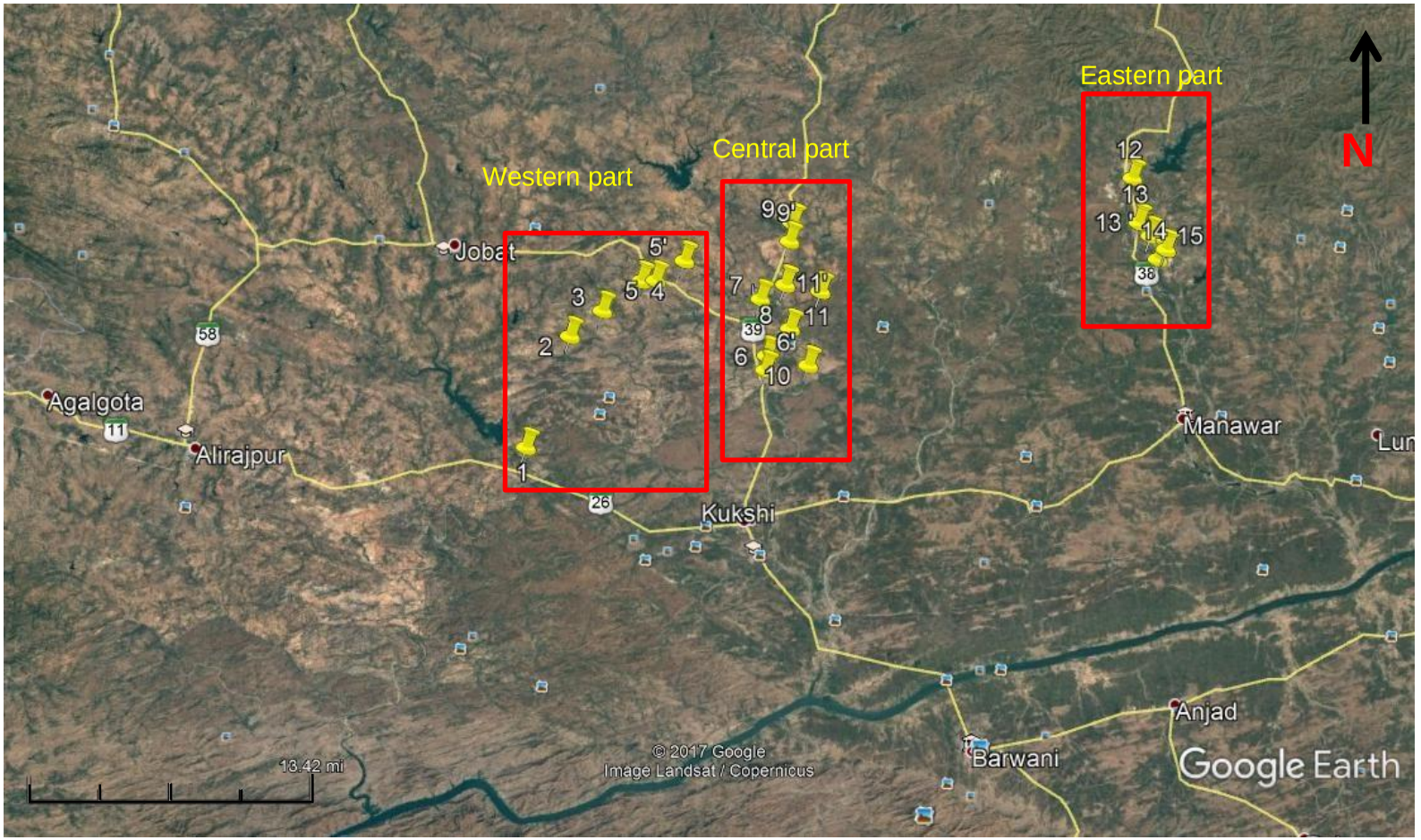

Figure: 2.4. Google Earth map shows locations (marked with nos.) of well-exposed sections of the Nimar Sandstone in the field. The locations are grouped into western, central and eastern parts.

Based on the field location points and well-exposed successions of the Nimar Sandstone the study area has been divided into three sectors i.e., eastern part, central part and western part (Figure 2.4). Western part of the studied area comprises Phata (Loc: 1), Ghoda section (Loc: 2), Chitapoti (Loc: 3), Dhursal (Loc: 4) and Akhara (Loc: 5). In the central part, major localities are Rampura section (Loc: 6), Baghini temple section (Loc: 7), Bagh cave and river section (Loc: 8), Neemkheda (Loc: 9), Dam section (Loc: 10) and Raisinghpura, Mahakalpura section (Loc: 11 and 11′). In eastern part Ratitalai area (Loc: 12), Baria (Loc: 13), and along the Man river section near Awaldaman (Loc: 14) and Sitapuri (Loc: 15) are the main localities. In all these sections Nimar Sandstone is well developed and shows well preservation of various sedimentary rocks with characteristic primary structures. The average sediment thickness of Nimar sandstone in the study area varies from 25m to 30m. The maximum thickness of Nimar Sandstone is observed in the central part.

.

CHAPTER-3

Facies Analysis

3.1. Introduction

According to Reading (1986), the most common definition of a facies is "a body of rock with specified characteristic". Characteristic of a sedimentary rock is determined by both the intensity of the formative process working on it and the time through which such action is continued (Pettijohn, 1957). Generally, sedimentary facies is described as an areally restricted, three-dimensional body of rock or sediments that is characteristically distinguished from another rock unit by its geometry, lithology, sedimentary structures and fossil content. According to Andreton (1985), a facies can be descriptive or interpretive (genetic). There should be no objection to using the definition of interpretative facies, so long the description of interpretative and descriptive facies is distinct and indicates individual depositional processes. A facies can be defined in a many ways depending upon the purpose of the study, the time available to make the measurements and the abundances of descriptive features in the studied strata (Walker, 2006).

In this research work, the term facies is used both in a descriptive and interpretative sense. Firstly in the descriptive sense where all the litho-units are classified based on their geometry, lithotypes, primary structures and grain size and then interpret their process under which they are formed and they are grouped in few associations based on their genetic processes.

Within the studied Nimar Sandstone succession total seventeen facies types are identified. Facies have a limited value when they considered as individuals. According to Reading (1986), an association of facies is more significant for environmental interpretation. In the present research work the seventeen facies types of Nimar Sandstone are grouped under five facies associations based on their genetic appearances, lateral and vertical extension and similarity in their lithotypes, primary structures etc. These five facies associations are namely, channel-fill facies association (FA-1), overbank facies association (FA-2), fluvial-dominated fluvio-tidal facies association (FA-3), tide-dominated fluvio-tidal facies association (FA-4) and shore facies association (FA-5). Distribution of different facies types in each facies association is given in Table 3.1.

3.2. Facies Associations

Channel-fill facies association (FA-1) mainly occurs at basal portion of the Nimar Sandstone. The maximum thickness of this facies association is ~ 5m, laterally discontinuous, lenticular shaped in nature. This facies association is well developed in the eastern portion (Figures 3.1, 3.2 and 3.3A) and few parts of the central portion of the studied area (Neemkheda, Baghini mandir section, Rampura section) (Figures 3.4, 3.5, 3.6B and 3.7). This facies association consists of four facies types, namely, (i) clast supported conglomerate facies (1A) (ii) matrix supported conglomerate facies (1B), (iii) pebbly sandstone facies (1C) and (iv) trough cross-stratified sandstone facies (1D).

Lithologically, overbank facies association (FA-2) is composed of red colored fine to medium-grained sandstone and mudstone bed. FA-2 appeared as an extensive sheet over the FA-1. The maximum thickness of FA-2 is ~6m. Sandstone-mudstone interbedded facies (2A) and plane bedded sandstone facies (2B) are the two dominant unit of this association. At the central part of the studied area near Baghini mandir section and towards the western part in Dhursal section this facies association is well developed (Figures 3.6B and 3.8).

Fluvial dominated fluvio-tidal facies association (FA-3) consists of two facies types namely, Large scale trough cross-stratified sandstone facies (3A) and planar cross-stratified sandstone facies (3B). In terms of primary sedimentary structures large scale trough cross-strata, planar tabular cross-strata and soft sediment deformation structures like load and flames are common in this facies association. At places (Rampura section) poorly developed bi-directional cross-strata are also observed. FA-3 is well developed in the central part near Bagh section, and Rampura section (Figures 3.5 and 3.7). In the Bagh section, the maximum thickness of FA-3 is ~7m.

Tide-dominated fluvio-tidal facies association (FA-4) is well developed throughout the study area. Sandstone-mudstone heterolithic facies (4A), mud clast bearing conglomerate facies (4B), plane laminated sandstone facies (4C), bioturbated sandstone facies (4D) and green sandstone facies (4E) are the major components of this facies association. Various soft sediment deformation structures i.e., convolute lamination, slump structures, synsedimentary fault and pseudonodules are common in this association. Presences of bi-directional cross- strata, sigmoidal cross-strata, lenticular bedding, wavy bedding, inclined heterolithic strata and mud drapes are significant within the sandstone-mudstone heterolithic facies (4A). FA-4 is well developed throughout the study area (Figures 3.1-3.11). Bioturbated sandstone facies (4D) and

green sandstone facies (4E) are mainly developed in the central and western part of the studied area (Figures 3.4, 3.5, 3.7, 3.8, 3.9, 3.10 and 3.11)

Shore facies association (FA-5) appeared as a widespread sheet throughout the study area. Fossils bearing sandstone facies (5A), *Thalassinoides-Ophiomorpha* bearing thinly laminated sandstone-mudstone facies (5B), wave ripples bearing sandstone facies (5C) and massive mudstone facies (5D) are the main lithofacies of this association. Evidence of wave reworking is common within the FA-5; maximum thickness of this association is ~10m with lateral continuation throughout the basin.

Table: 3.1. Different facies associations and their facies types from the Nimar Sandstone.

Facies Association	Facies types	Environment
FA-1 Channel-fill facies association	**1A** Clast supported conglomerate facies	**Fluvial**
	1B Matrix supported conglomerate facies	
	1C Pebbly sandstone facies	
	1D Trough cross-stratified sandstone facies	
FA-2 Overbank facies association	**2A** Sandstone-mudstone interbedded facies	
	2B Plane bedded sandstone facies	**Fluvio-tidal interactive condition**
FA-3 Fluvial-dominated fluvio-tidal facies association	**3A** Large-scale trough cross-stratified sandstone facies	
	3B Planar cross-stratified sandstone facies	
FA-4 Tide-dominated fluvio-tidal facies association	**4A** Sandstone-mudstone heterolithic facies	
	4B Mud clast bearing conglomerate facies	
	4C Plane laminated sandstone facies	
	4D Bioturbated sandstone facies	
	4E Green sandstone facies	
FA-5 Shore facies association	**5A** Fossil-bearing sandstone facies	**Wave-influenced condition**
	5B *Thalassinoides–Ophiomorpha* bearing thinly laminated sandstone-mudstone facies	
	5C Wave ripples bearing sandstone facies	
	5D Massive mudstone facies	

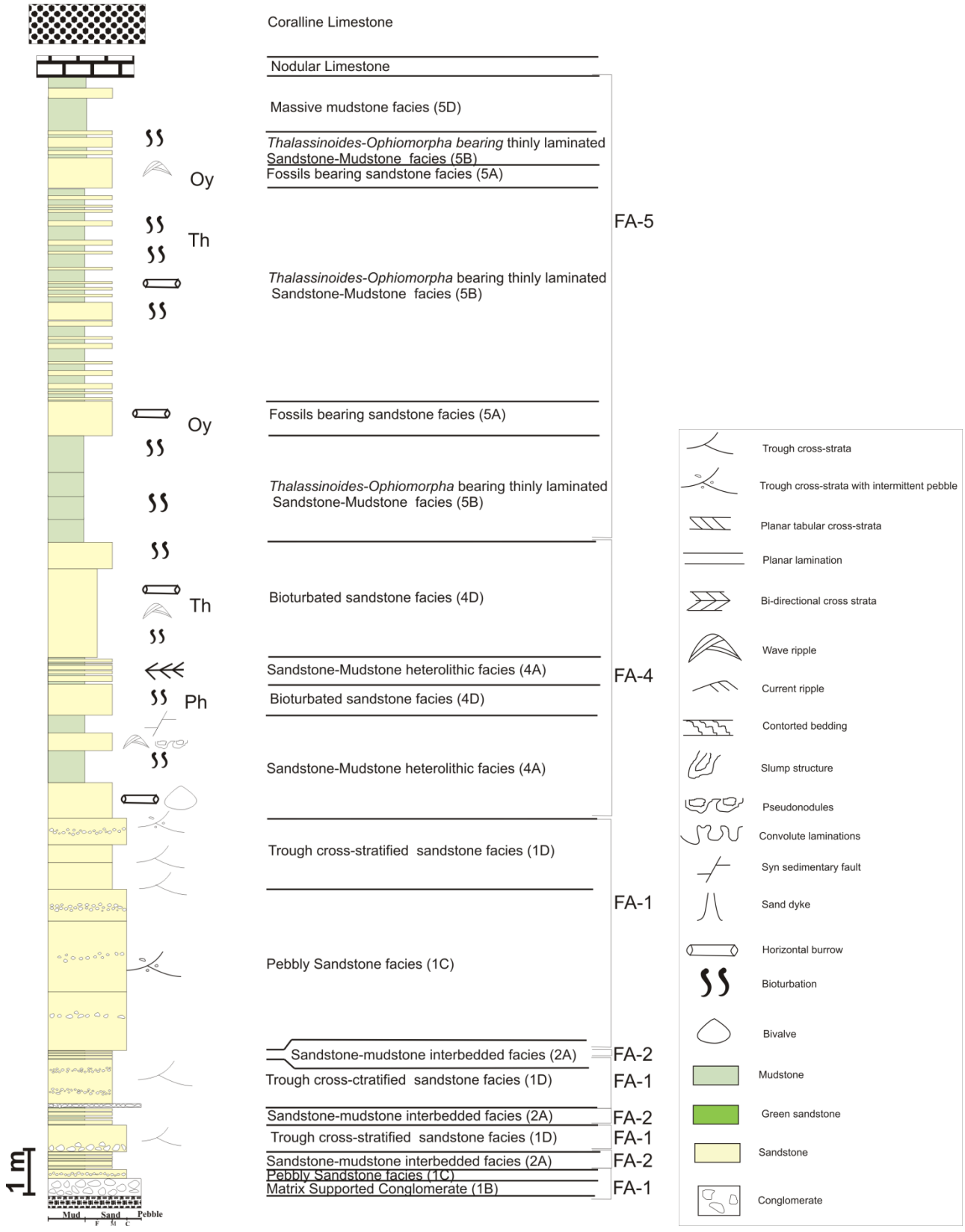

Figure: 3.1. Litholog from the Sitapuri area (Location 15 in Figure 2.4) along the eastern bank of the Man River section, showing distribution of various facies types and their associations. The legend is same for figures 3.1-3.11.

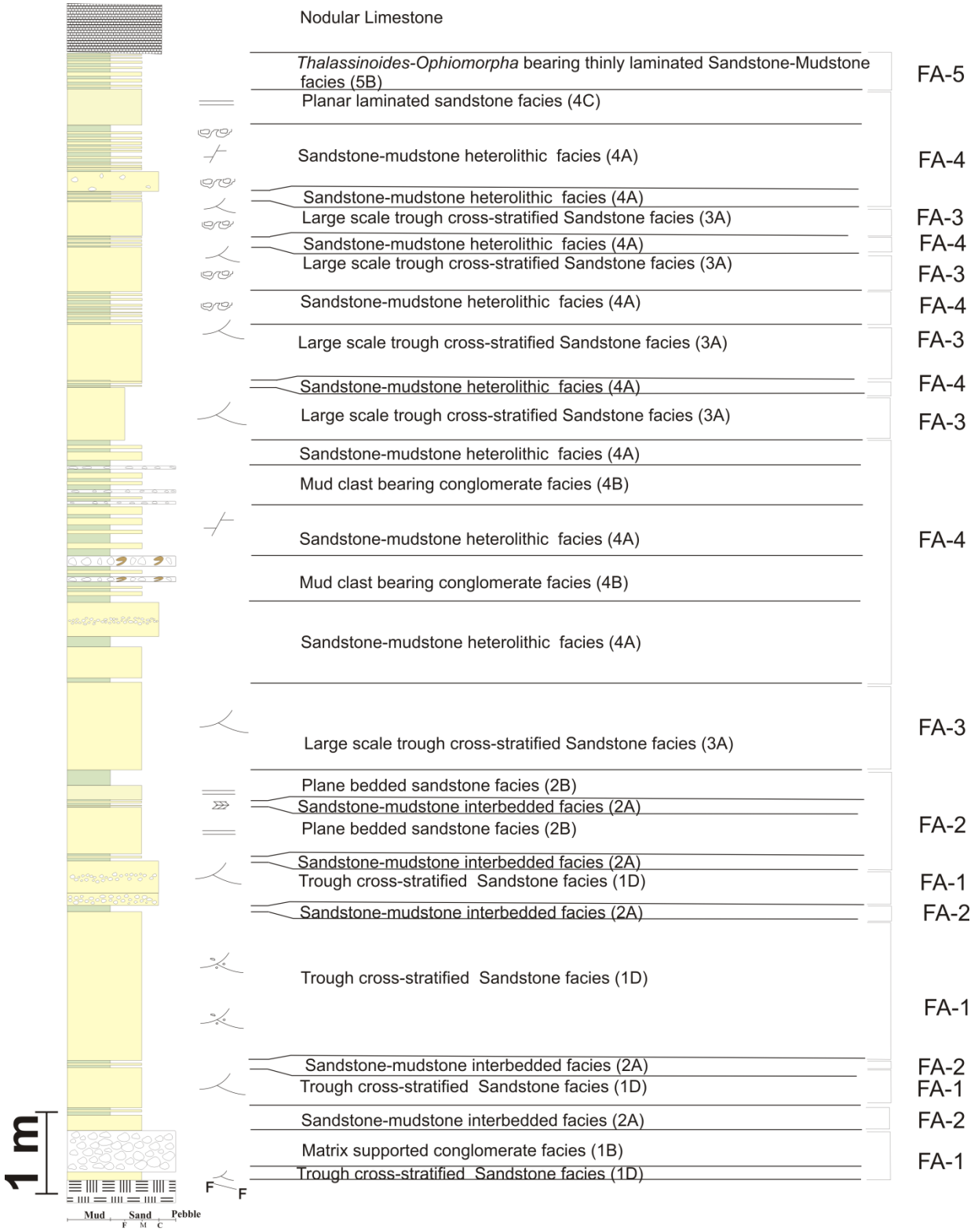

Figure: 3.2. Litholog from the Awaldaman section in the eastern part of the study area showing distribution of various facies types and their associations (Location 14 in Figure 2.4).

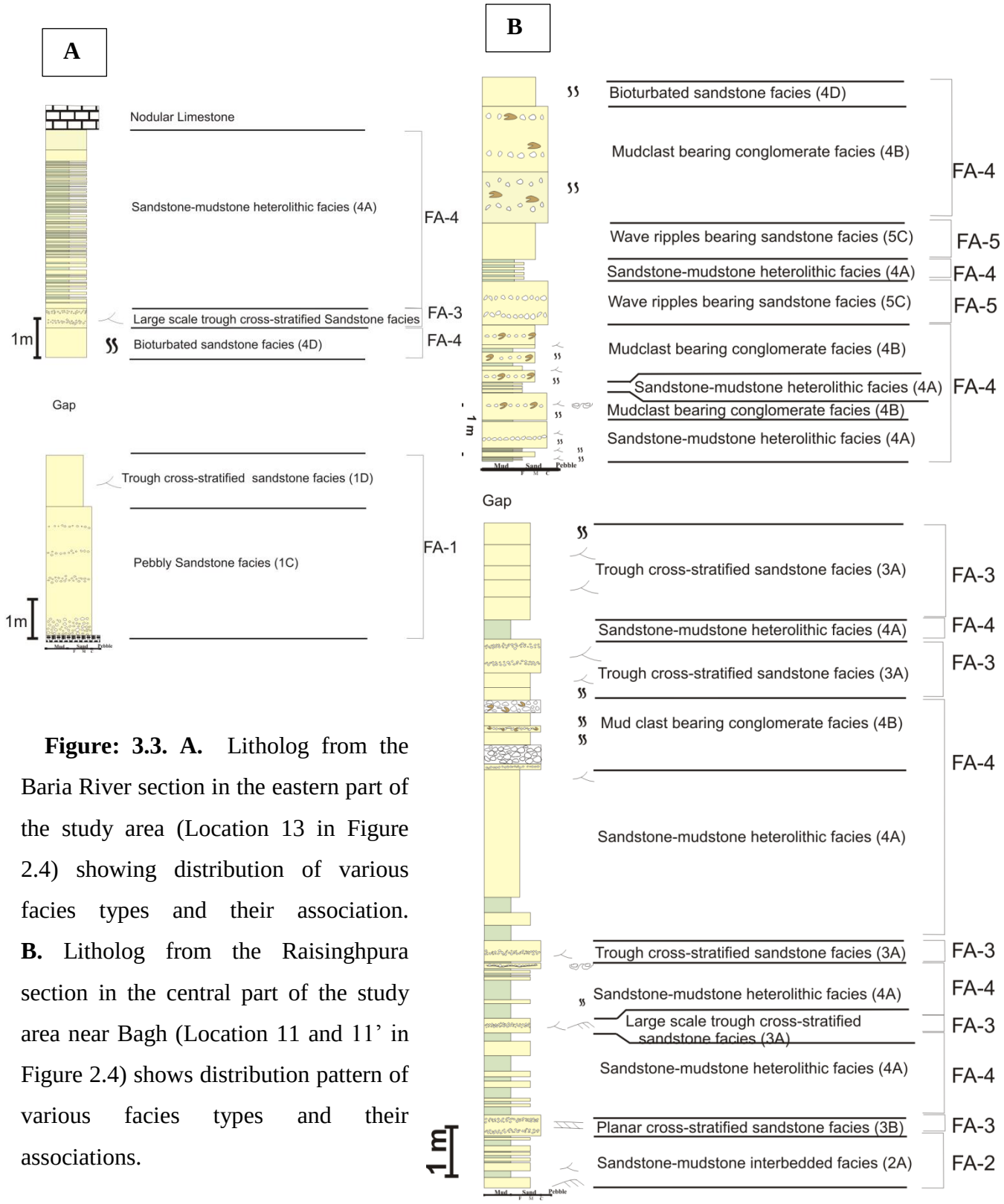

Figure: 3.3. A. Litholog from the Baria River section in the eastern part of the study area (Location 13 in Figure 2.4) showing distribution of various facies types and their association. **B.** Litholog from the Raisinghpura section in the central part of the study area near Bagh (Location 11 and 11' in Figure 2.4) shows distribution pattern of various facies types and their associations.

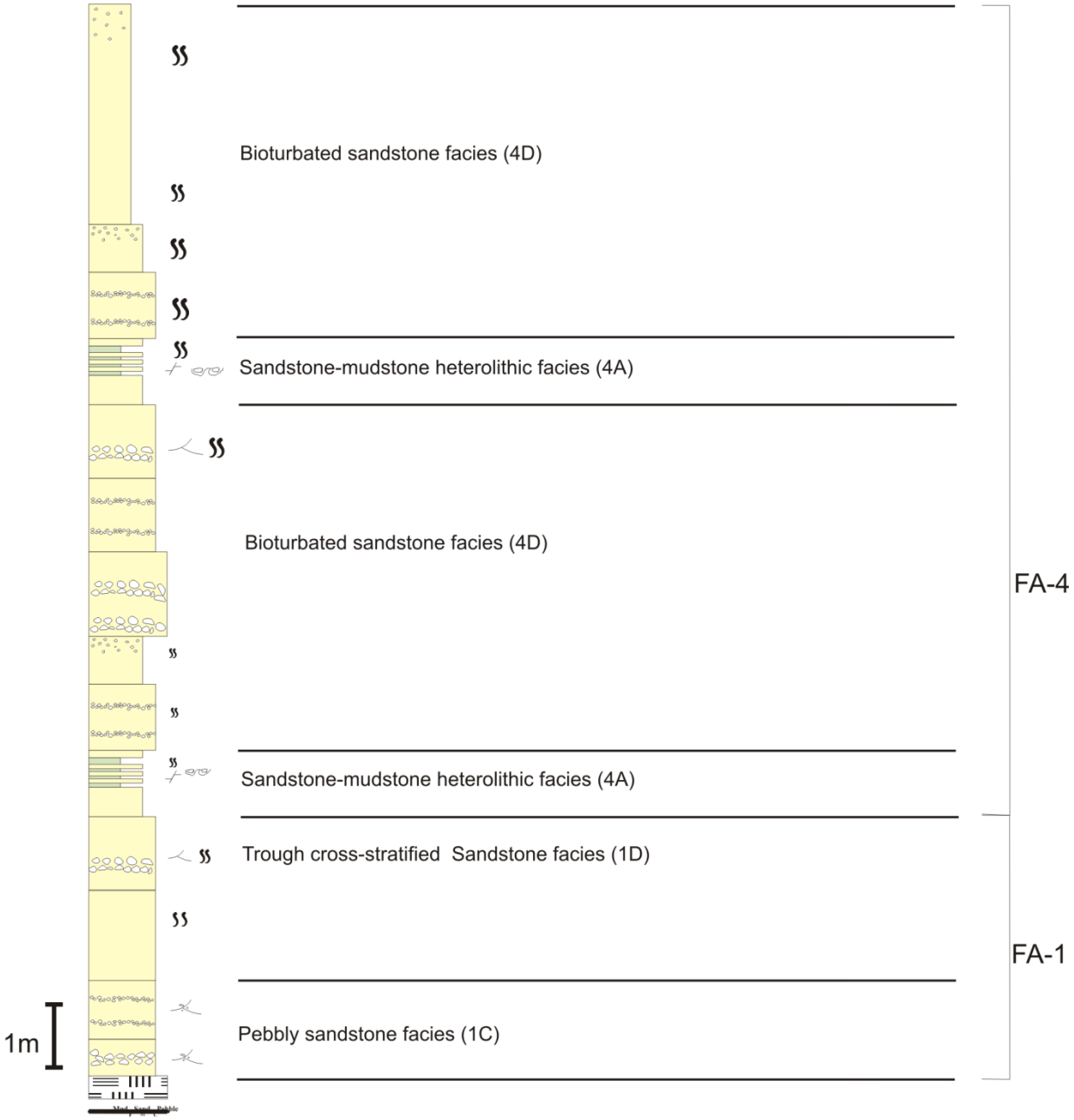

Figure: 3.4. Litholog from the Neemkheda section (Location 9 in Figure 2.4) in the central part of the study area showing distribution of various facies types and their associations.

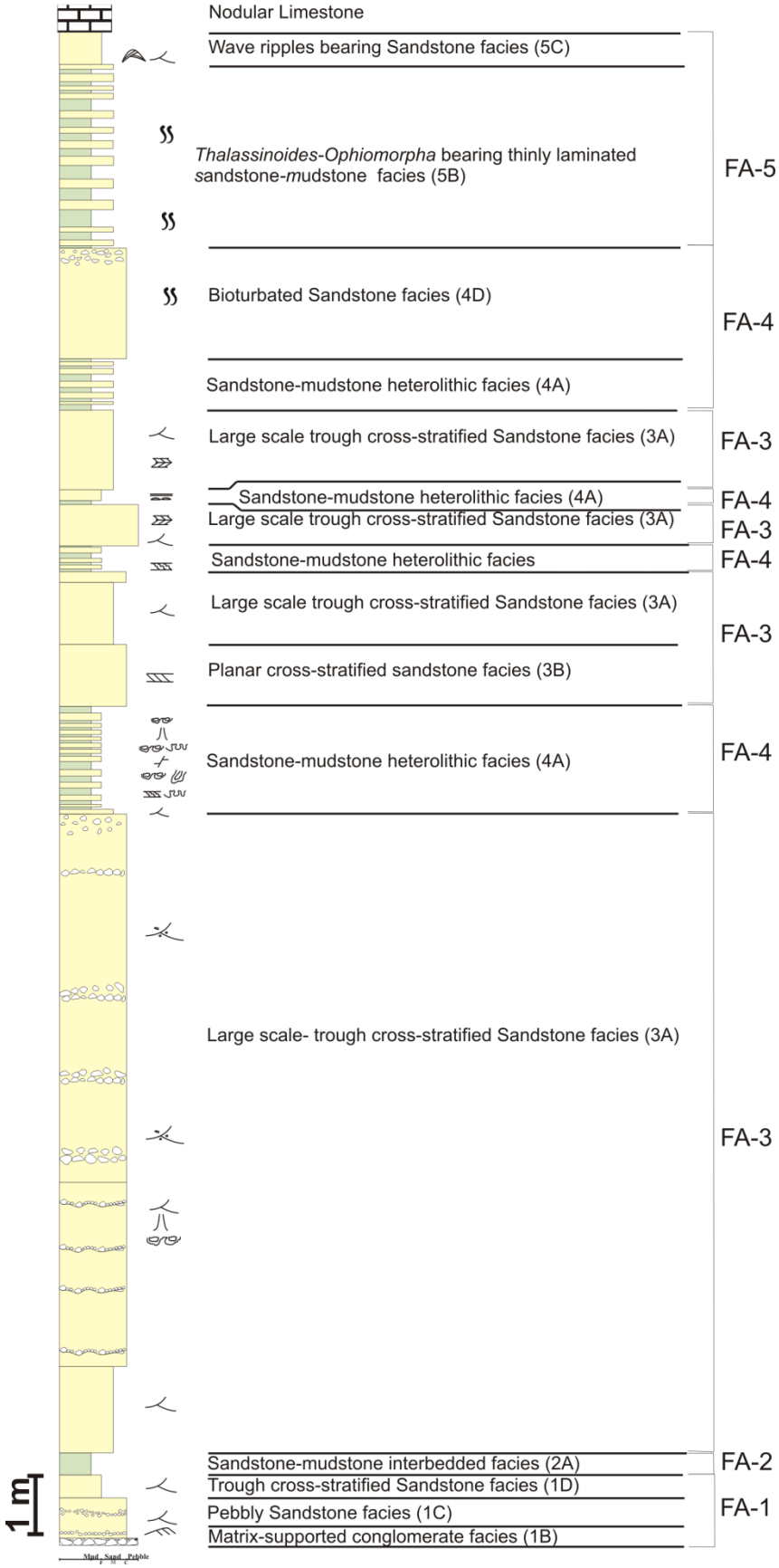

Figure: 3.5. Litholog from the Bagh section (Location 8 in Figure 2.4) in the central part of the study area showing distribution of various facies types and their associations.

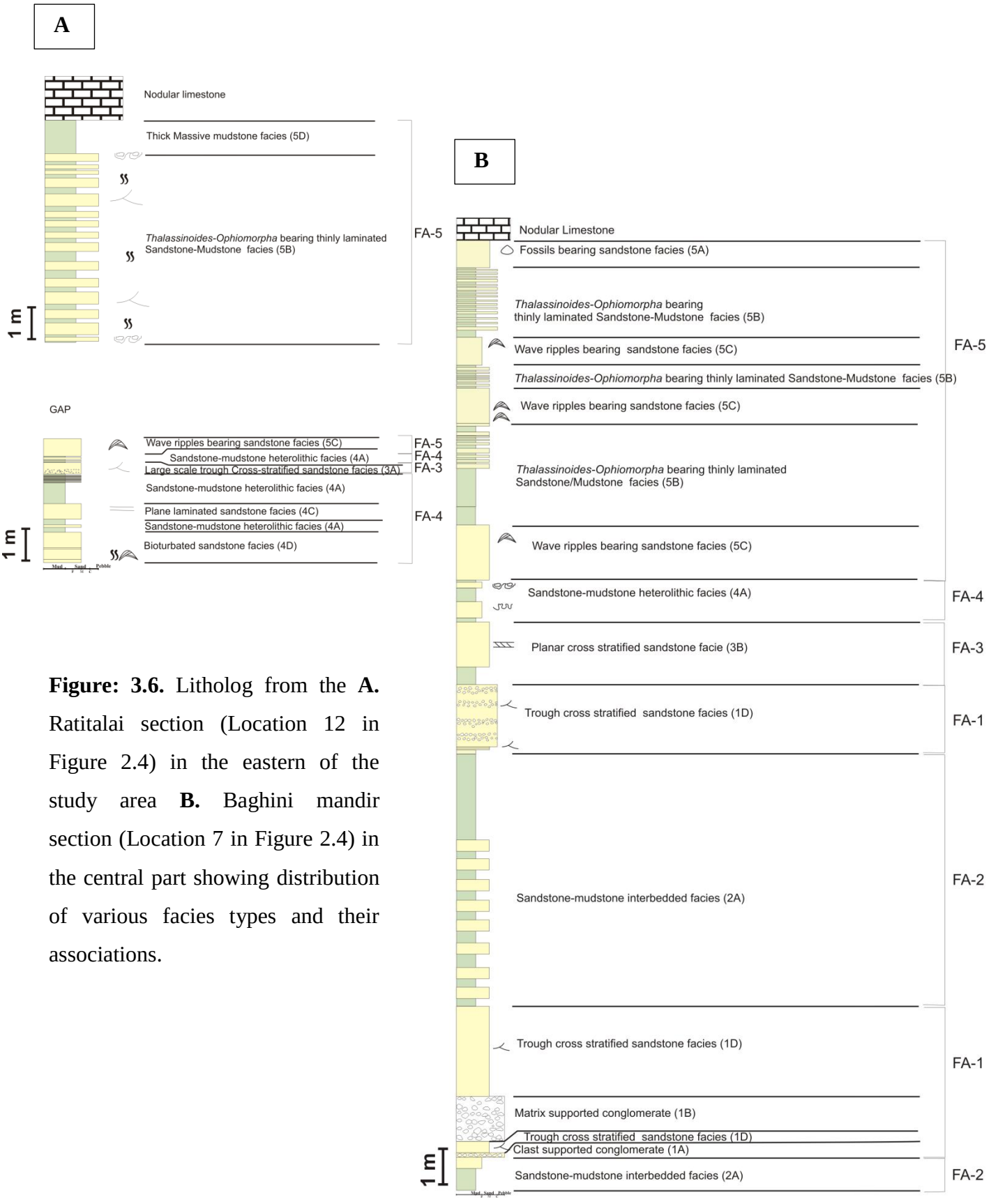

Figure: 3.6. Litholog from the **A.** Ratitalai section (Location 12 in Figure 2.4) in the eastern of the study area **B.** Baghini mandir section (Location 7 in Figure 2.4) in the central part showing distribution of various facies types and their associations.

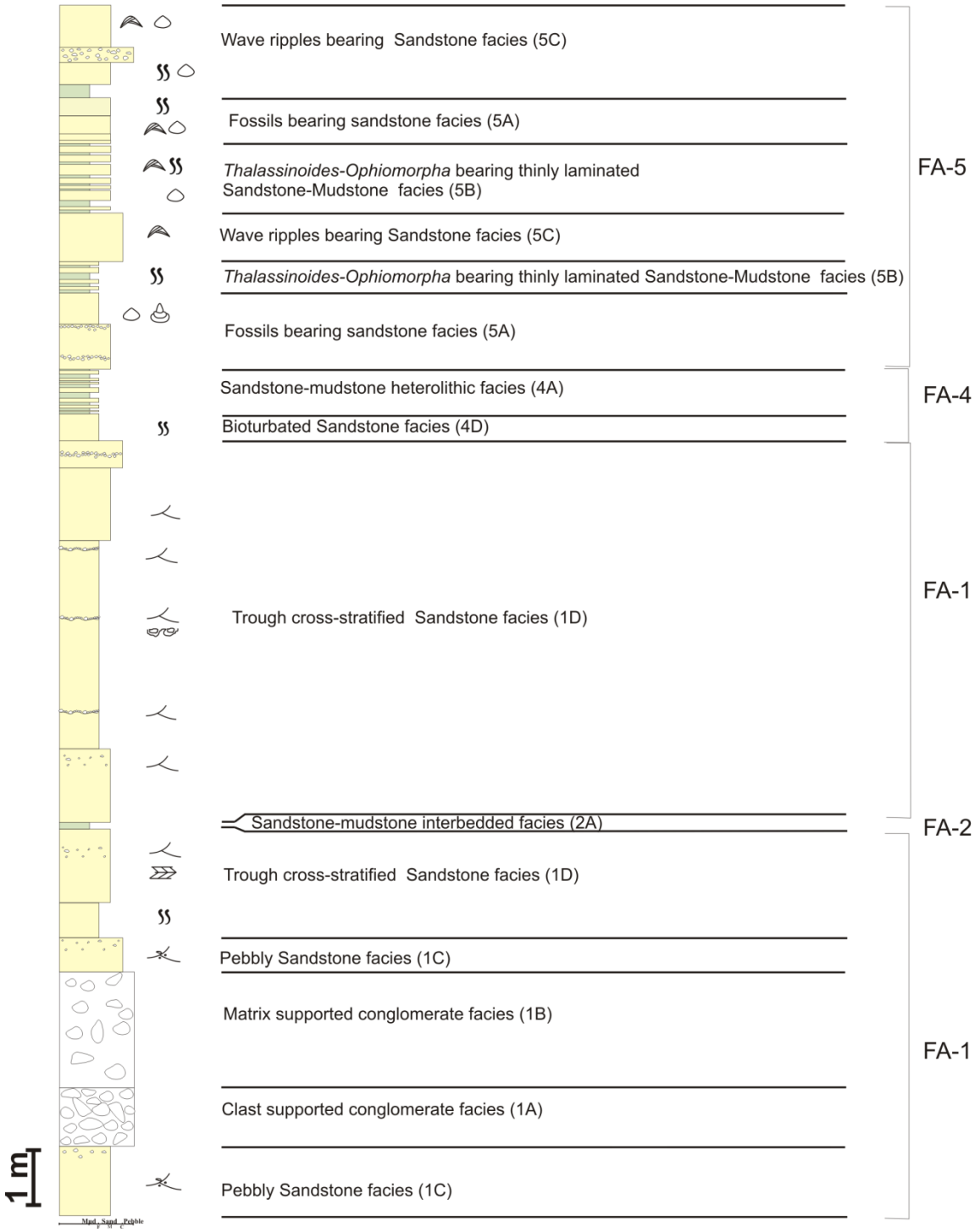

Figure: 3.7. Litholog from the Rampura section (Location 6 in Figure 2.4) in the central part of the study area showing distribution of various facies types and their associations.

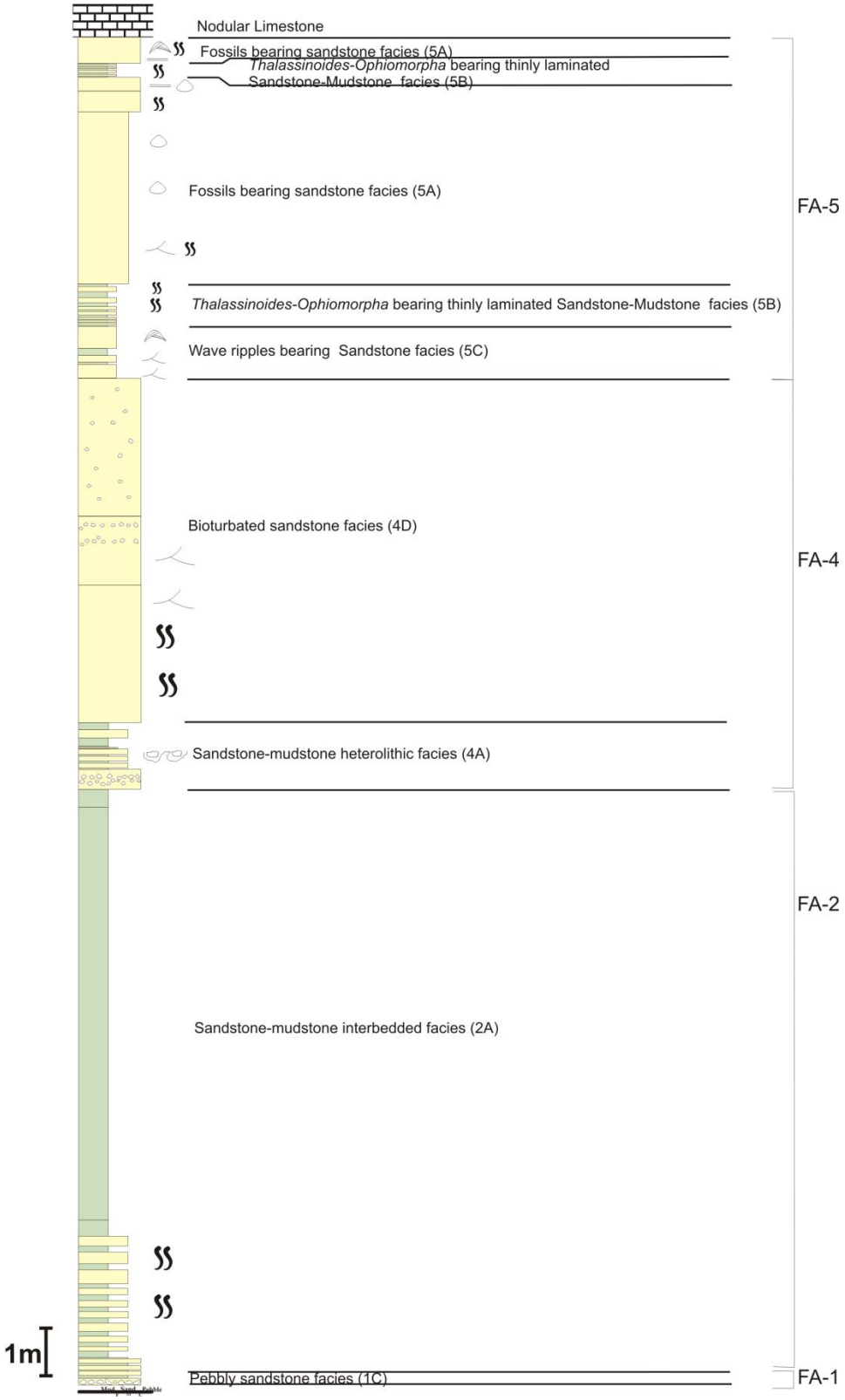

Figure: 3.8. Litholog from the Dhursal section (Location 4 in Figure 2.4) in the western part of the study area showing distribution of various facies types and their associations.

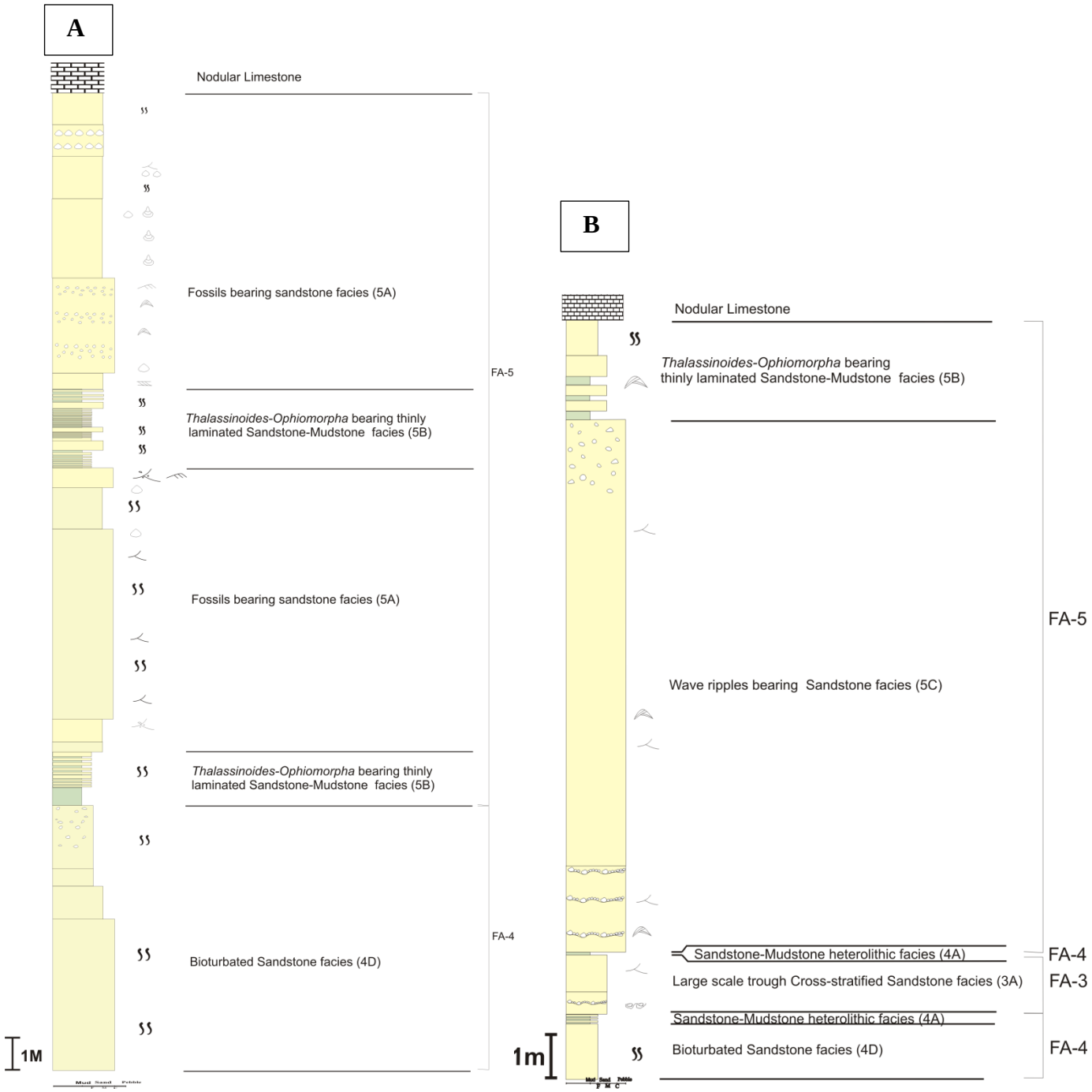

Figure: 3.9. A. Litholog from the Akhara section (Location 5 in Figure 2.4) in the western part of the study area showing distribution of various facies types and their association**. B.** Litholog from the Dam section (Location 10 in Figure 2.4) in the central part of the study area showing distribution of various facies types and their association**.**

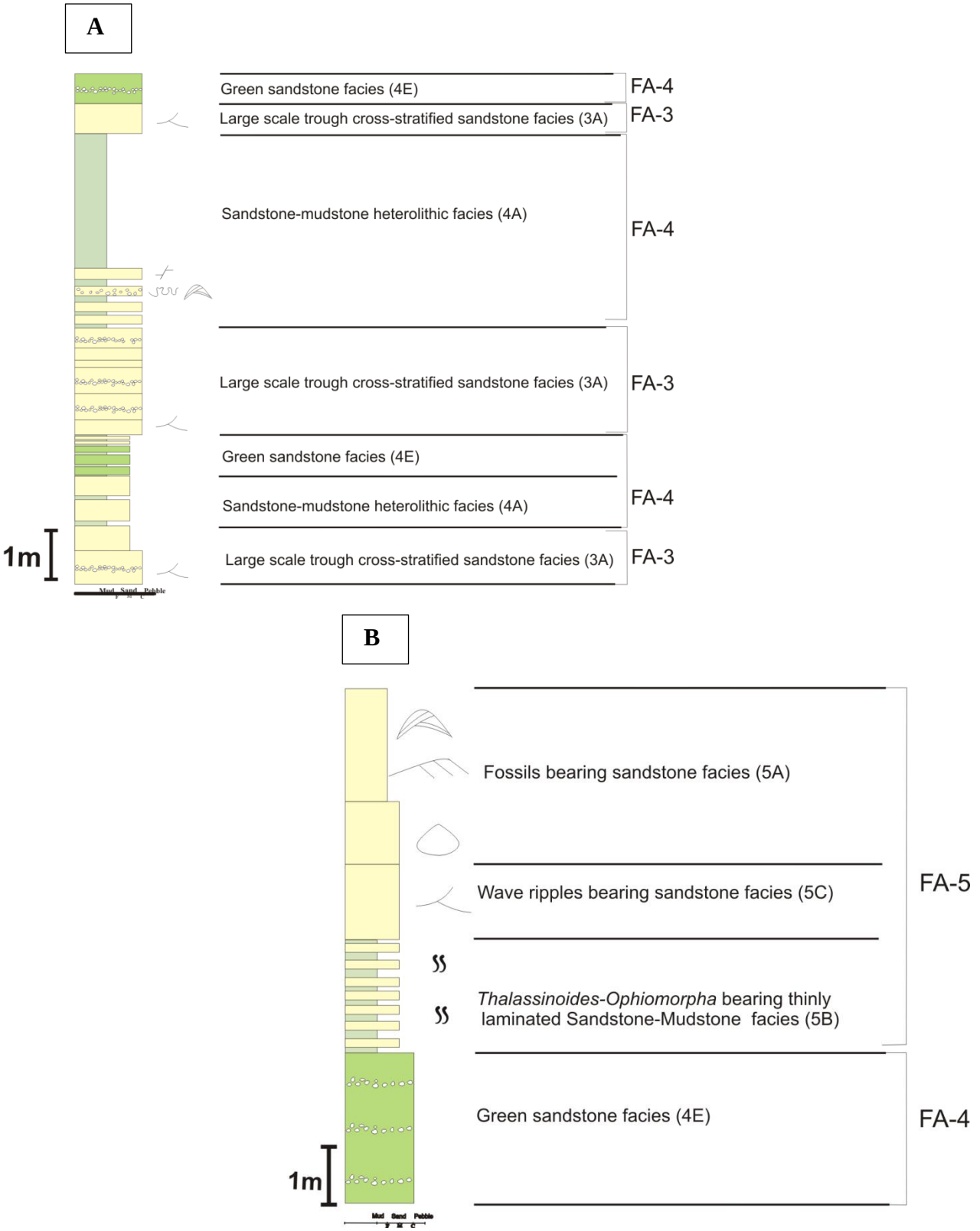

Figure: 3.10. A. Litholog from the Ghoda section (Location 2 in Figure 2.4) in the western part of the study area showing distribution of various facies types and their associations. **B.** Litholog from the Chikapoti section (Location 3 in Figure 2.4) in the western part of the study area showing distribution of various facies types and their associations.

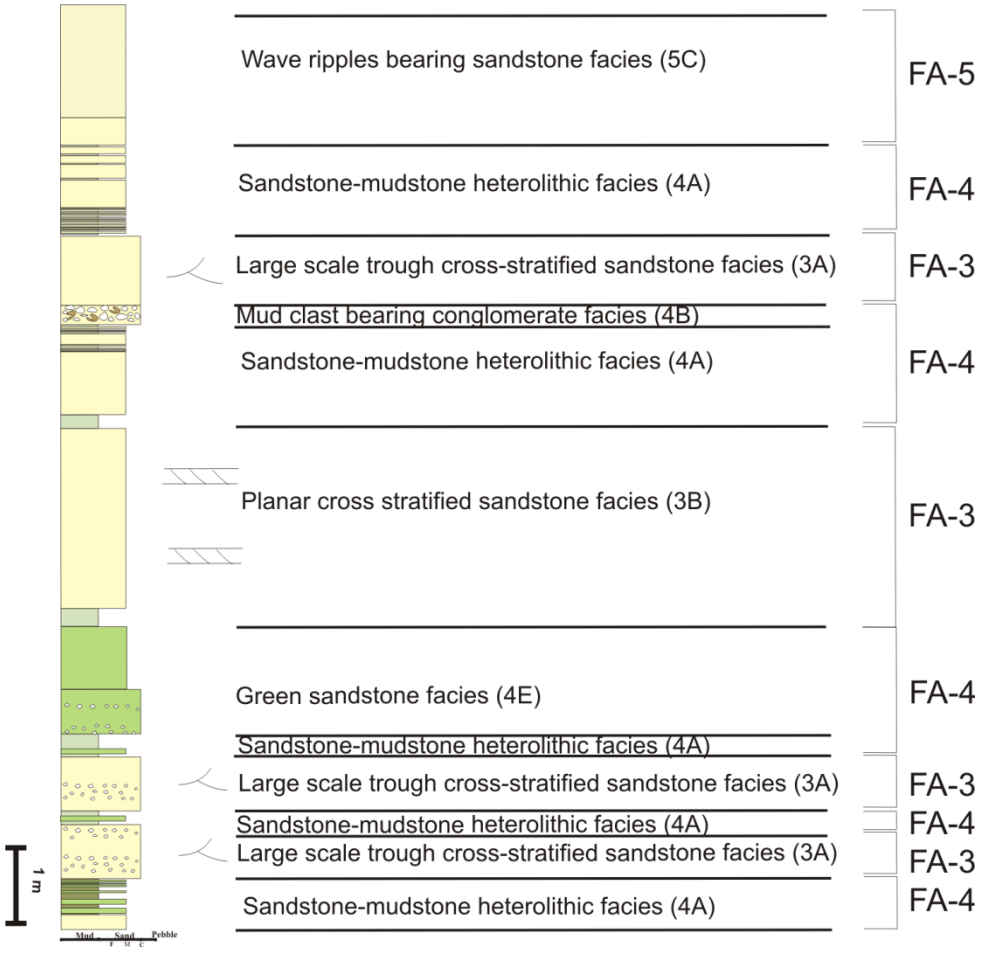

Figure: 3.11. Litholog from the Phata section (Location 1 in Figure 2.4) in the western part of the study area showing distribution of various facies types and their associations.

Detailed description of individual facies types are given below-

3.3. Facies Association 1- Channel-fill facies association

Clast supported conglomerate facies (1A), matrix supported conglomerate facies, pebbly sandstone facies (1C) and trough cross-stratified sandstone facies (1D) are the four component of this facies association.

3.3.1. Facies 1A: Clast supported conglomerate facies

Lenticular shaped, clast supported polymictic conglomerate is exposed at the basal portion of Nimar Sandstone. This conglomerate shows a non-conformable relation with the basement rock (Figure 3.12A). The maximum thickness of this facies is 90 cm. Clasts are variable in composition but mainly dominated by fragments of the Precambrian gneissic basement. Clasts are angular to sub-angular in nature and randomly oriented without any imbrication (Figure 3.8B). At places, crudely developed grading is observed.

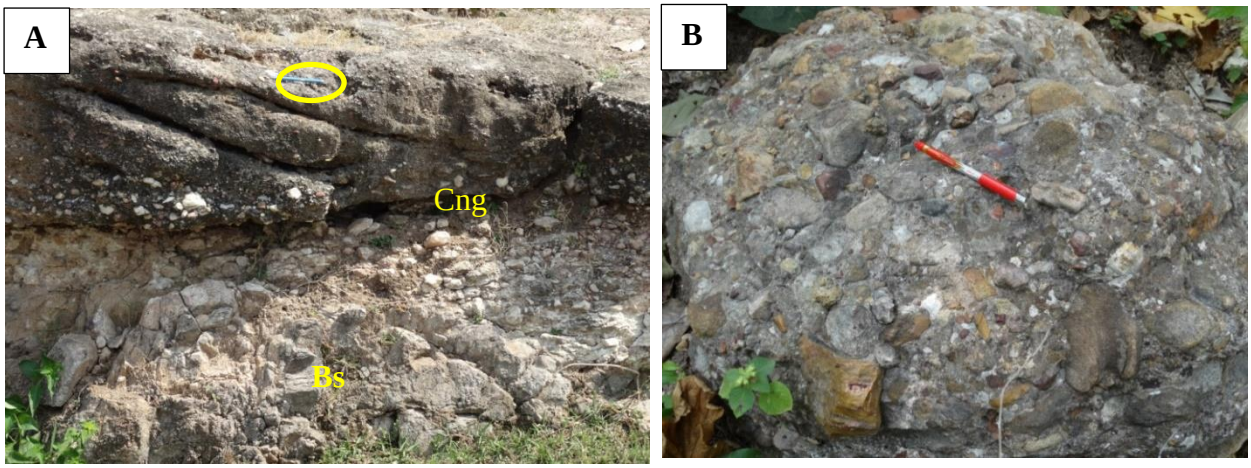

Figure: 3.12. A. Field photograph of clast supported conglomerate facies (1A) (marked as Cng) overlies the basement rock (Bs) showing non-conformable contact. The pen is encircled. Length of the pen is 14.4 cm. **B.** Field photograph of clast supported conglomerate facies (1A) showing angular to subangular clasts of basement gneissic rock. Length of the pen is 14.5 cm.

Interpretation

Miall (2006) stated that, clast supported conglomerates are the product of traction current deposit mainly. The absence of imbrication and angular to sub-angular nature of the clasts indicate very low transportation. Crudely developed grading indicates rapid sedimentation (Lowe 1976; Pandita et al., 2014). Lenticular shaped geometry with scoured contact specifies

channel deposit. Malaza et al. (2013) interpreted that clast-supported, polymictic, lenticular shaped and texturally immature conglomerates are most probably deposited as small bodies of channel lag or longitudinal braided bars of low sinuous streams.

In the studied area lenticular shape of the conglomerate unit with large clast of basement fragments, scoured base and absence of any primary sedimentary structures indicate an intrabasinal channel lag deposit.

3.3.2. Facies 1B: Matrix supported conglomerate facies

Matrix rich, texturally immature conglomerate comprises clasts of quartz, jasper and basement rock fragments. In few places, clast of mud is also present (Figure 3.13). Matrix is arenaceous in nature. Clasts are sub-rounded, sizes vary from 2-10 cm in diameter and randomly oriented. At places, sandstone is interbedded with the conglomerate. The overall geometry of this facies is lenticular shaped in nature.

Figure: 3.13. Field Photograph of the matrix supported conglomerate facies (1B). Arrows indicate presences of mud clasts. The diameter of the coin is 2.5 cm.

Interpretation

Presence of more matrix component than clasts indicates a debris flow condition (Miall, 1982). Matrix rich with sub-rounded clasts within conglomerates is evidence of textural inversion, indicating multiple provenances and varied transportation history. Presence of mud clast

indicates very high energy condition where underlying mud layer is scooped out and deposited as cohesive mud clast.

3.3.3. Facies 1C: Pebbly sandstone facies

At the basal portion of the Nimar Sandstone, a pebbly sandstone facies is well developed in all the sections.The maximum thickness of this facies is ~2.5 m. It is characterized by coarse to medium-grained sandstone with small scales trough cross-strata (set thickness 20-30 cm); at places, large scale trough cross-strata (set thickness 50-55 cm) are also developed. Trough sizes are decreasing towards up-section (Figure 3.14). Individually sandstone layers are separated by pebble rich layers which grade finer up-section. The distribution pattern of pebble layers, within trough cross-strata is random, at some places they are concentrated at the bottom part (e.g., Sitapuri section) whereas at some places (e.g., Baria, Rampura sections) towards the top part. Pebbles are angular to sub-angular, poorly sorted in nature whereas sand grains are moderately sorted and sub-rounded. Overall geometry is lenticular shaped but laterally extended and traceable.

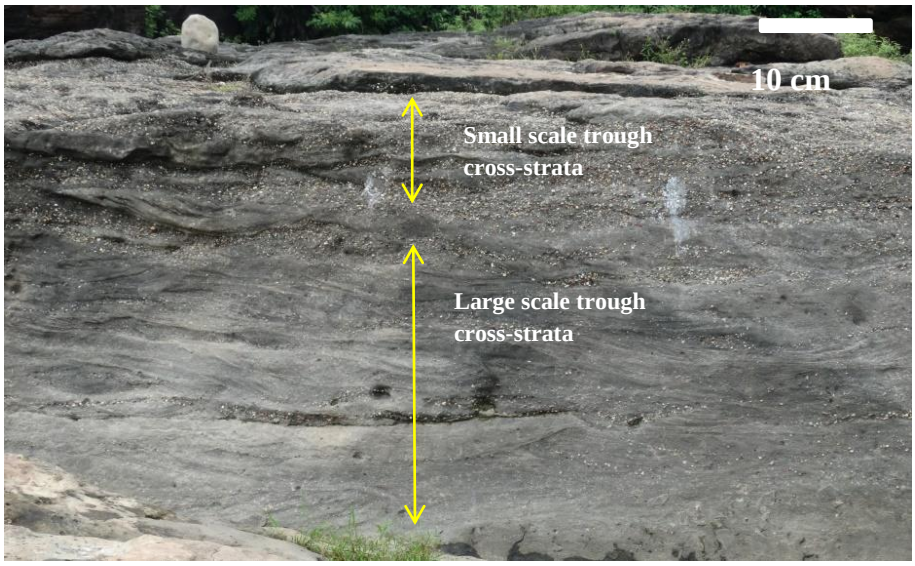

Figure: 3.14. Field photograph of pebbly sandstone facies (1C) showing development of different trough cross-strata with decreasing size of the troughs from bottom to top.

Interpretation

In the study area alternate pebble rich and pebble poor layer forming local finning up successions indicates a rhythmic fluctuation of energy condition. Each pebble layers indicate a high energy condition whereas pebble free sandstone layers indicate relatively low energy condition. Small scale trough cross-strata and foreset is generally product of lower point-bar

setting (Reineck and Singh, 1973). A low sinuous high gradient meandering stream can transport coarse sand along with pebble to cobble-sized gravel in bed load (McGowen and Garner, 1970). The lenticular-shaped sheet-like pebbly sandstone facies with small troughs in the study area indicates product of channel bar migration (Miall, 1977).

3.3.4. Facies 1D: Trough cross-stratified sandstone facies

This sandstone facies is characterized by medium to coarse-grained, moderately sorted, and angular to subrounded grains of sand. Foresets of trough cross-strata show tangential contact at the bottom and truncated top (Figure 3.15A). The local concentration of pebbles is observed at places, which formed load and flame structure locally (Figure 3.15B).

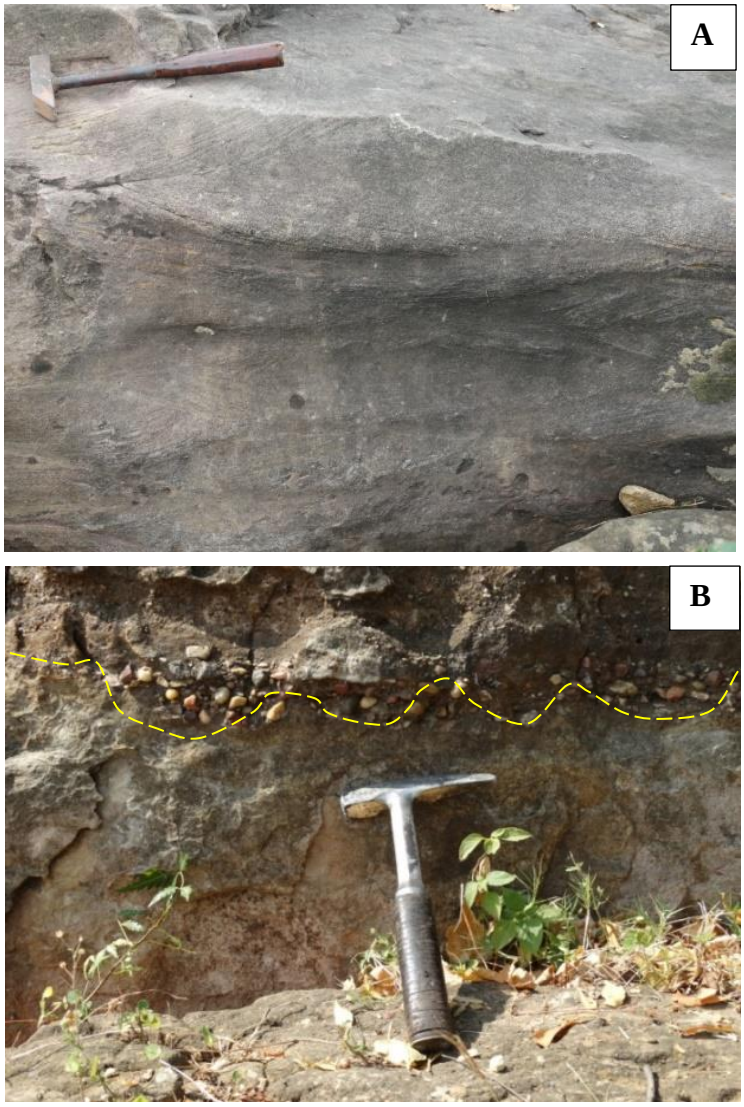

Figure: 3.15 A. Field photograph of trough cross-stratified sandstone facies (1D). **B.** Load structures (marked with dotted line) in the trough cross-stratified sandstone facies (1D). Length of the hammer in both photographs is 30 cm.

Small scale asymmetrical ripples are preserved on the top surface of this facies. This facies is predominant in almost all the studied section. Facies thicknesses vary from 5cm to 50 cm. Maximum thickness (up to 1m) of this facies is observed near Bagh River section.

Interpretation

Migration of bar or 3D ripple form creates trough cross-stratification. Best and Kostaschuk (2002) stated that in vertical section bars and their cross-stratification may be tabular, sigmoidal or tangential, depending on the shape of the lee side profile and bounding surfaces between sets of cross-stratification may be planar tabular, planar wedge-shaped or trough-shaped, depending on the 3D form of the associated bedforms and the orientation of the cross-section relative to the flow direction. In the studied trough cross-stratified sandstone facies local concentration of pebbles indicates fluctuation in energy conditions. Due to density contrast between the pebble layers and sandstone load structures are developed at places. Absence of large scale 3D ripples rules out the process of ripple migration for the formation of this facies. Therefore, down current migration of bars is the reason for the formation this trough cross-stratified sandstone facies.

3.3.5. Interpretation of Facies association 1

The overall lenticular shaped geometry of both the conglomerates facies indicates (1A, 1B) a channel-fill deposit. Presence of clast supported and matrix supported conglomerate bears evidence of both traction and debris flow condition with the fluctuation of energy. Scoured contact with the basement indicates flow turbulence during the time of deposition. Texturally and compositionally immature clasts signify less transported lag deposit. Small or large scale trough cross-strata is the result of migration of bar. Alternate layers of pebble rich and pebble poor strata indicate fluctuation in energy condition during the time of deposition. Presence of sandstone along with pebbles indicates low sinuous high gradient meandering channel system where small-scale trough represents lower point bar migration setting. Absence of any marine signature designates that FA-1 is typically a product of the fluvial processes.

3.4. Facies Association 2- Overbank facies association

This facies association is mainly composed of fine grained sandstone and mudstone. The two dominant facies are-sandstone-mudstone interbedded facies (2A) and plane bedded sandstone facies (2B).

3.4.1. Facies 2A: Sandstone-mudstone interbedded facies

This facies is characterized by laterally persistent alternate thick-thin sandstone-mudstone beds with sheet-like geometry. Red color mudstone bed appeared as a blanket over the sandstone bed and is devoid of any primary structures. Within the sandstone bed very crude plane laminations are developed at places. Overall both the sandstone and mudstone beds are equally dominated (Figure 3.16A) but at places thick and massive beds of mudstone with very thin sandstone interbeds (Figure 3.16B) are also developed. In general within this facies interbedded unit starts with sandstone which gradually becomes muddy upward. In this facies, sandstone beds are characterized by fine to medium grain size, moderately sorted, subrounded in nature. Under microscope, sandstone shows bimodal distribution pattern of grain size with <15 % matrix. Among the framework grains, ~ 90 % is quartz (Figure 3.16C) and rest is constituted of plagioclase feldspar and microcline. Quartz grains are mainly monocrystalline in nature but polycrystalline grains are also common. Quartz grains shows both straight and undulose extinction. Grains are subrounded in nature.

Interpretation

Presence of fine grain sandstone-mudstone beds indicates a relatively low energy depositional condition. Deposition of mudstone alternate with thinly laminated sandstone indicates deposition from suspension along with some bed load, respectively (Reincek and Singh, 1980). Overall sheet-like geometry (blanket type) of this facies pattern with thin lamination and dominance of suspension settling indicates that the deposition was took place under still water condition. Interbedded of medium to fine-grained sandstone indicates bed load transportation under relatively higher energy condition.

Presence of both the low and high energy condition with crudely developed lamination and the sheet-like geometry indicates an overbank setting; where mud is deposited from suspension and sandstone are product of bed load when flow velocity change. Presence of both sandstone and mudstone within an overbank setting indicates rapid changes in channel flow velocity during the time of flooding (Leopold and Wolman, 1957).

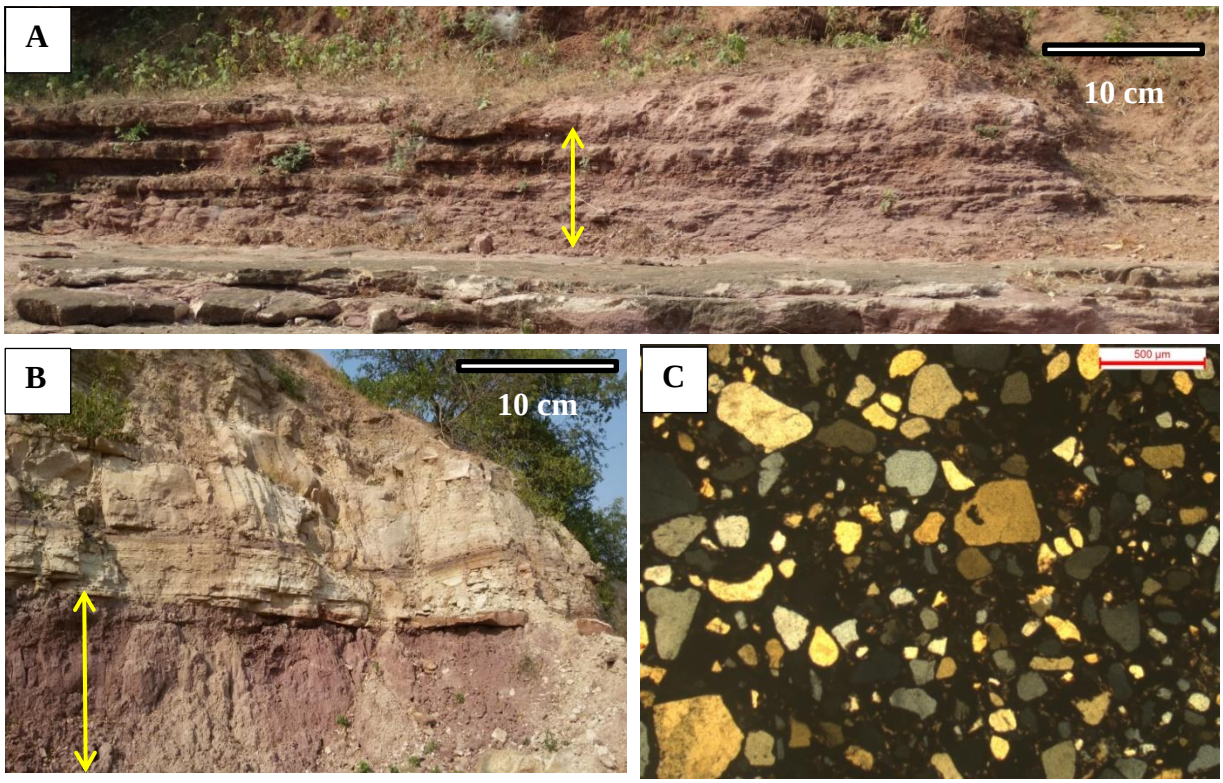

Figure: 3.16.A. Field photograph of sandstone-mudstone interbedded facies (2A) (marked with arrow). **B.** Sandstone-mudstone interbedded facies (marked by arrow) with thick mudstone and very thin sandstone beds overlain by facies association 3. **C.** Photomicrograph of sandstone of the sandstone-mudstone interbedded facies (2A) showing predominance of quartz grains.

3.4.2. Facies 2B: Plane bedded sandstone facies

This facies is comprises of fine to medium grained sandstone. Individual bed thickness varies from few cm to more than 10 cm. Grains are moderately sorted in nature. Planar bedding in association with current parting lineation (Figure 3.17A) is a common feature in this facies. Well sorted, subrounded to rounded grains of quartz, plagioclase feldspar and lithic fragments are dominant framework components within this facies (Figure 3.17B). This sandstone is represented by arenites having less than 10 % matrix. The modal concentration of feldspar is ~8 %, which makes the rock sub-arkosic in nature. Quartz grains of this facies are dominated by monocrystalline in nature with straight extinction. At places top surface of this sandstone unit shows the presence of small-scale 2D ripple marks. Mainly bioturbation by *Skolithos* isp. is common within this facies.

Interpretation

Paola et al. (1989) stated that planar bedding with current parting lineations results from transportation of sand under supercritical upper flow regime. This type of condition is possible during the peak flood time (Miall, 1977). In the upper part where plane lamination or slightly inclined laminations are associated with ripples indicate a shallow channel under subcritical flow rather than super-critical flow condition (Paola et al., 1989).

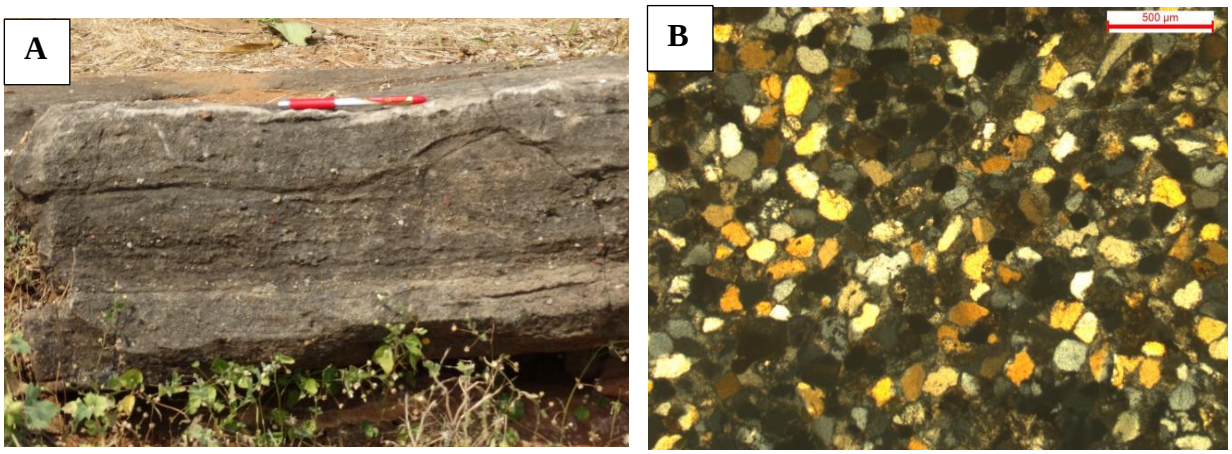

Figure.3.17. A. Field photograph of the plane bedded sandstone facies (2B). Length of the pen is 14.5 cm. **B.** Photomicrograph of plane bedded sandstone facies showing quartz rich mineralogy.

3.4.3. Interpretation of Facies association 2

Sandstone-mudstone interbedded facies and plane bedded sandstone facies suggested two processes are responsible for the formation of this facies association. Fine-grained mudstone unit was deposited under low energy suspension condition along with relatively higher energy sandstone deposit. FA-2 is intimately associated with FA-1 and appeared as a blanket over it and laterally continuous throughout the study area. Overall geometry, distribution pattern, fluctuation in energy condition and presence of planar-lamination with current parting lineation and small-scale 2-D ripples marks suggested an overbank depositional setting.

3.5. Facies Association 3- Fluvial dominated fluvio-tidal facies association

This facies association mainly consists of cross-stratified sandstone namely, large scale trough cross-stratified sandstone facies (3A) and planar cross-stratified sandstone facies (3B).

3.5.1. Facies 3A: Large-scale trough cross-stratified sandstone facies

Medium-grained, moderately sorted and subrounded sand grains along with trough cross-strata is characteristic of this facies. Thickness of the individual bed varies from 20 cm to 50 cm. Trough cross-strata are developed in large scale (in meter scale) showing lateral accretion of foresets (Figure 3.18). The thickness of the individual sets is more than 30 cm. The individual cross-strata set shows normal grading. Draping of mud within the foreset is also a common phenomenon in this unit. Soft-sediment deformation structures (convolute laminations) are also observed in this facies type. Due to the presence of convolute lamination foresets are disturbed at places.

Interpretation

Large scale trough cross-stratification with the lateral accretion of the foresets indicates that deposition took place mainly by migration of the bar or large scale ripples (Bose and Das, 1986) like lunate/linguoid ripples. Lateral variations in bed thickness indicate fluctuation in sediments supply. According to Nichols (2009), during high or low tide condition when the current is changing direction at the time of no flow situation mud deposited as a drape on the foresets from suspension. During the high energy conditions sand are deposited and each of the mud drapes indicates a low energy condition or a slack phase. Presence of soft-sedimentary deformation structures is the result of contemporaneous liquefaction and fluidization with lithification due to sudden impulsive tremors during or just after the deposition of sediments (Sarkar et al., 2014).

.

Figure: 3.18. Field photograph shows large scale trough cross-stratified sandstone facies (3A) along the western bank of the Man river section, arrows showing lateral accretion surfaces.

3.5.2. Facies 3B: Planar cross-stratified sandstone facies

This facies comprises of medium to coarse-grained sand with local pebble content. Pebbles are not continuous; they dispersed along the bedding planes and foresets. The overall geometry of the facies is lenticular shaped. The thicknesses of cross-bed set ranges from 10-35 cm, set boundaries are sub-horizontal in nature (Figure 3.19A). The upper bounding surfaces of cross-bed sets may exhibit uneven reactivation surfaces. Each set is showing a fining up succession where base starts with coarse to medium grain sandstone and grades up to a fine grain sandstone. Characteristically, in some places, thin mud veneers are present within the foresets. Mineralogically this cross-stratified sandstone facies is dominated by quartz grains with minor amount of k-feldspar and lithic fragments. Quartz grains are subrounded in nature. At places well-rounded grains are also observed (marked by red circles in figure 3.19B). The modal concentration of the quartz grains within framework component is ~95 % and matrix is less than 15 %; classifying this sandstone as quartz arenites in composition.

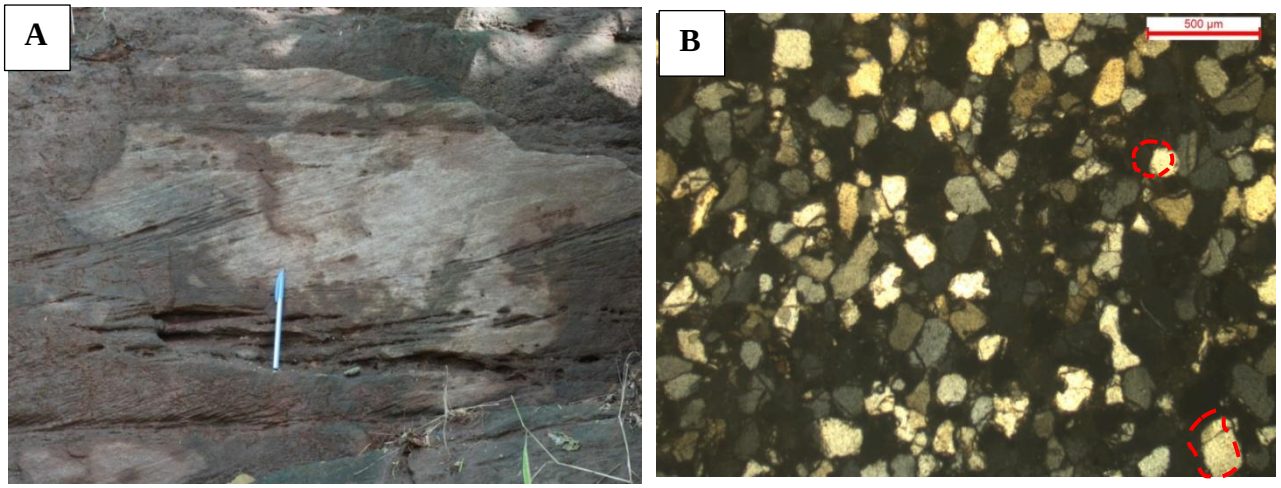

Figure: 3.19. A. Field photograph of planar cross-stratified sandstone facies (3B). Length of the pen is 14.5 cm. **B.** Photomicrograph showing planar cross-stratified sandstone facies enriched with quartz grains.

Interpretation

Downstream migrations of 2-D ripples are the reason for the formation planar tabular cross-strata (Harms et al., 1982). It forms under lower flow regime conditions. The overall geometry of the facies, unidirectional flow pattern and finning up sequences indicates a channel

bar deposits within the channel. Presence of thin mud veneers along the foresets indicates fluctuation in energy condition due to the occasional tidal influences.

3.5.3. Interpretation of Facies association 3

Cross-stratified sandstone beds with internal mudstone drapes on foresets indicate high energy currents interrupted by slack-water phase. The large width, tabular to convex upward lenticular shape and lack of a basal erosion surface indicate that these facies were deposited as unconfined sheets or bars. Presence of mud drape and reactivation surfaces indicates the influence of tidal activity. These facies association 3 indicates a fluvial dominated tide influenced channel bar depositional setting.

3.6. Facies Association 4- Tide dominated fluvio tidal facies association

This facies association mainly consists of fine-grained sandstone and mudstone unit. This association comprises of five facies types namely; sandstone mudstone heterolithic facies (4A), mud clast conglomerate facies (4B) plane laminated fine-grained sandstone facies (4C), bioturbated sandstone facies (4D) and green sandstone facies (4E).

3.6.1. Facies 4A: Sandstone-mudstone heterolithic facies

This facies type is characterized by three sub facies unit- ripple cross-stratified sandstone subfacies (4A1), wavy-lenticular bedded sandstone-mudstone subfacies (4A2), and inclined sandstone-mudstone heterolithic facies (4A3).Various soft-sediment deformation structures (SSDS) are well preserved within this facies (detailed description of SSDS are given in Chapter 6).

3.6.1.1. 4A1 Ripple cross-stratified sandstone sub facies

This subfacies is represented by 2-10 cm thick sandstone beds. Fine to medium-grained sand with moderate sorting is the characteristic of this sandstone unit. Mineralogically, this sandstone is comprised of quartz grains, plagioclase feldspar, and muscovite. Grains are subangular to angular in nature but well-rounded grains are also present (Figure 3.20A). Grain shows line contact dominantly. Presence of both well rounded and angular grains indicates a textural inversion pattern. Thick (2- 10 cm) sandstone beds are characterized by ripple cross-laminated trough cross- strata (Figure 3.20B). Nature of the foresets is changed from straight to truncating with asymptotic toe. Foresets are laterally accreted and change the inclination across

reactivation surfaces with the draping of muds. Sigmoidal cross-strata are also presented. In places thickness of the mud drapes vary. Local preservation of ripple form with mutually opposite flow direction has led to the development of herringbone cross-strata. Apparent bi-directional strata bundles in vertically adjacent sets are common. Climbing ripples are also characteristic of this sandstone unit.

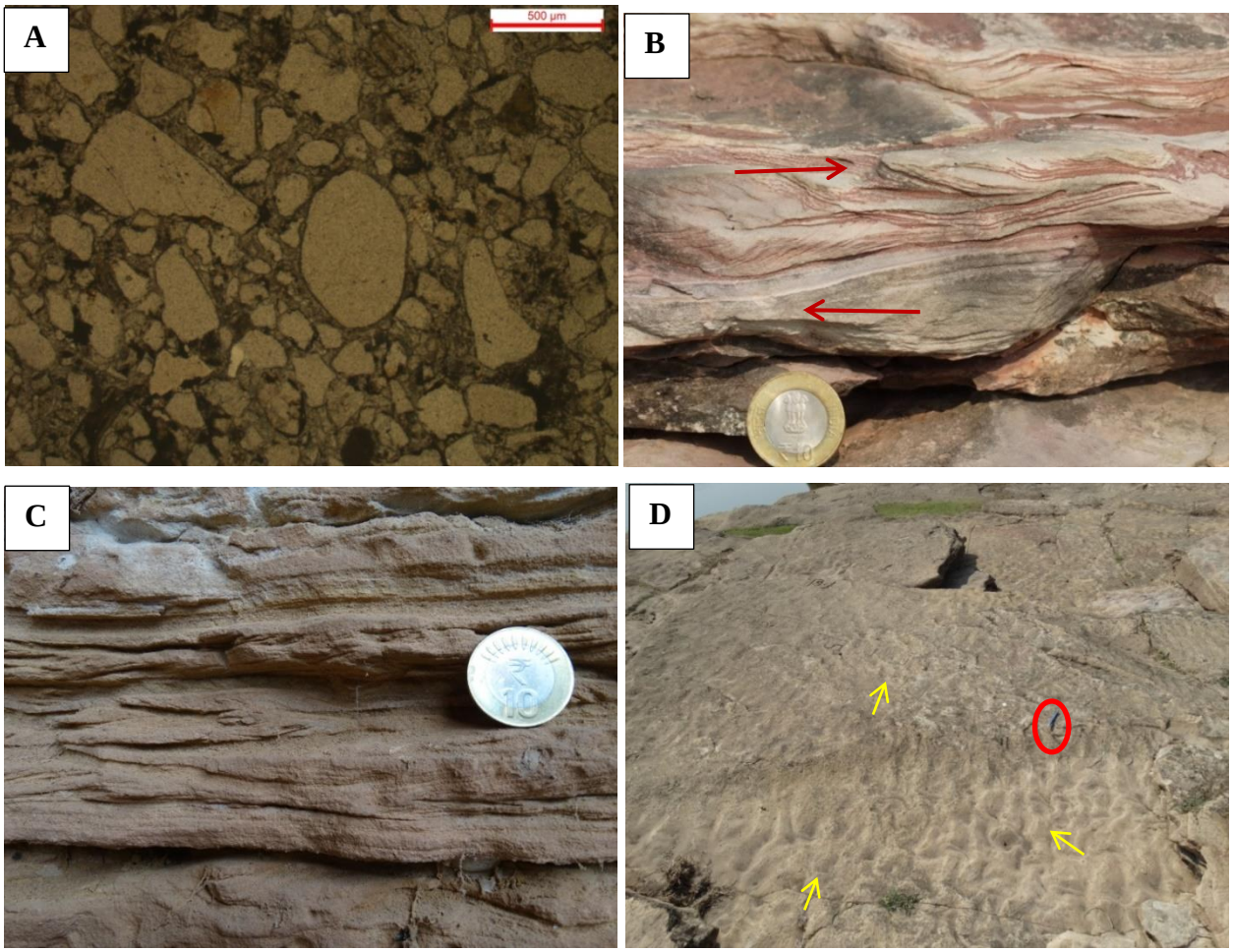

Figure: 3.20. A. Photomicrograph of ripple cross-laminated sandstone subfacies (4A1) showing both well rounded and angular grains indicates textural inversion. **B.** Field photograph of ripple cross-stratified sandstone subfacies showing presence of mud drapes and poorly developed bi-directional cross-strata. **C.** Ripple cross-stratified subfacies along with broad crested ripple with reactivation surface. Coin diameter both in B and C photograph is 2.5 cm. **D.** Interference ripples with bifurcation of crest line (arrow marks) exposed on the sandstone bedding surface in Man river section. Length of the pen (encircled) is 14.5 cm.

Broad crested symmetrical wave ripples with mud drapes (Figure 3.20C) are common primary sedimentary structures within this sub facies. Majority of the ripples are low amplitude symmetrical wave ripples with broad crest and trough. In few places, asymmetrical current ripples are also observed. Asymmetrical ripples are characterized by a straight/sinuous crest with the bifurcation of crest line. Linguoid ripple is also observed on the exposed bed surface of sandstone. Interference of both wave and tidal current within the ripples is observed which formed interference ripples. Bifurcation of the ripple crest lines is preserved in the Man river section (Figure 3.20D). Wave reworked interference ripples and combined flow ripples are more dominated towards the western part of the study area.

Interpretation

Ripple cross-stratification is considered as a result of a rapid deposition in areas of high sediment input (McKee, 1965). As stated by Jopling and Walker (1968) and Allen (1970) this structure allows estimating the ratio between the sediment deposition from suspension and the bedload transportation rate. Presence of mutually opposite cross-strata indicates reversal of depositional current (Elliot, 1986). The presence of mud drapes along the foresets of ripple cross-strata designates tidal activities (Kelin, 1971; Boersma and Terwindt, 1981). Symmetrical ripples along with interference ripples show that a mixed tide-wave led situation was present during the deposition of this sandstone subfacies.

3.6.1.2. 4A2 Wavy-lenticular bedded sandstone-mudstone subfacies

This subfacies comprises of interlaminated fine-grained sandstone and mudstone. The sandstone is yellowish in color and mudstone is red colored. Wavy mudstone beds are alternating with discontinuous ripple bedded sandstone (Figure 3.21). The thickness of the beds varies from 5 to 20 cm.

In lenticular bedding discontinues sand lenses are preserved within the mudstone layers both in vertical and horizontal direction. Sand lenses are 2-4 cm in thickness and asymmetrical and discontinuous in nature. Gradually in up section sand lenses become continuous and symmetrical (Figure 3.21). In few lenses, internal laminae are preserved which are draped by mud. Contact between the sand lenses and mudstone layers are sharp.

Interpretation

Wavy-bedding requires a condition where the deposition and preservation of both sand and mud are possible along with traction current and termination of traction current followed by

suspension (Reineck and Singh, 1980). This unit is basically an intermediate phase of flaser and lenticular bedding. The surface of the mud layer follows the concavity and convexity of the underlying ripples surface and formed wavy bedding (Reineck and Wunderlich, 1968).

Reineck and Singh (1980) stated that, lenticular bedding is produced when incomplete sand ripples formed on muddy substratum and preserved as a result of deposition of next mud layer. For the formation of lenticular bedding deposition and preservation of mud is more needed than sand. Preservation of mud along slightly current flow for the formation of incomplete ripple forms is the perfect setting for lenticular bedding. Towards the upsection sand lenses become thicker and continuous which indicates supply of sand increased with respect to mud.

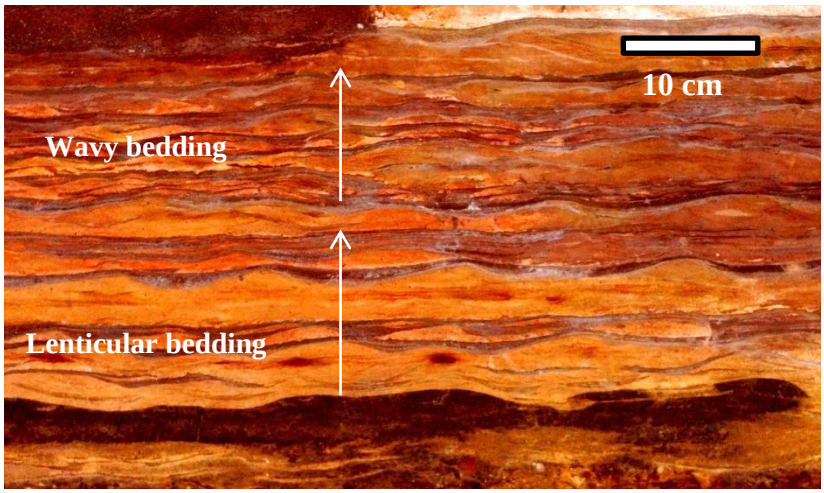

Figure: 3.21. Field photograph of lenticular and wavy bedding developed within the sandstone-mudstone subfacies (4A2).

3.6.1.3. 4A3 Inclined heterolithic sandstone-mudstone subfacies

Millimeter thick-thin interlamination of mudstone and fine grain sandstone is the characteristic of this subfacies. The thickness of the sandstone laminae ranges between 1 and 8 mm and mudstone laminae are 0.5 and 2 mm thin. Inclination of the strata varies from 4º to 6º. At places, mudstone laminae are discontinuous in nature (Figure 3.22A). Microscopic study of the sandstone-mudstone heteroliths shows alternate sand-rich and mud-rich layers (Figure 3.22B). Grains are commonly aligned along the bedding plane. The sand-rich units comprise of about 20% matrix whereas the mudstone units have about 75% matrix. Quartz is the major framework component along with k-feldspar, the modal concentration of the quartz grain varies from 60-65 % rest are mainly k-feldspar (Figure 3.22C).

Interpretation

Reineck and Singh (1980) stated that, alternate rhythmic repetition in lithology required regular changes in the transport or production of the material. These changes can be of short duration (tidal changes) or long-term changes. According to Reineck and Wunderlich (1967a, b; 1969), sand layers are deposited during the periods of current activity, both flood and ebb currents. The mud is deposited during stand-still phases of high-water or low-water tide (Choi, 2010). Repeated changes in grain size due to tidal current fluctuations are resulting in inclined heterolithic strata (IHS) (Thomas et al., 1987; Choi et al., 2004; Fagherazzi et al., 2004).

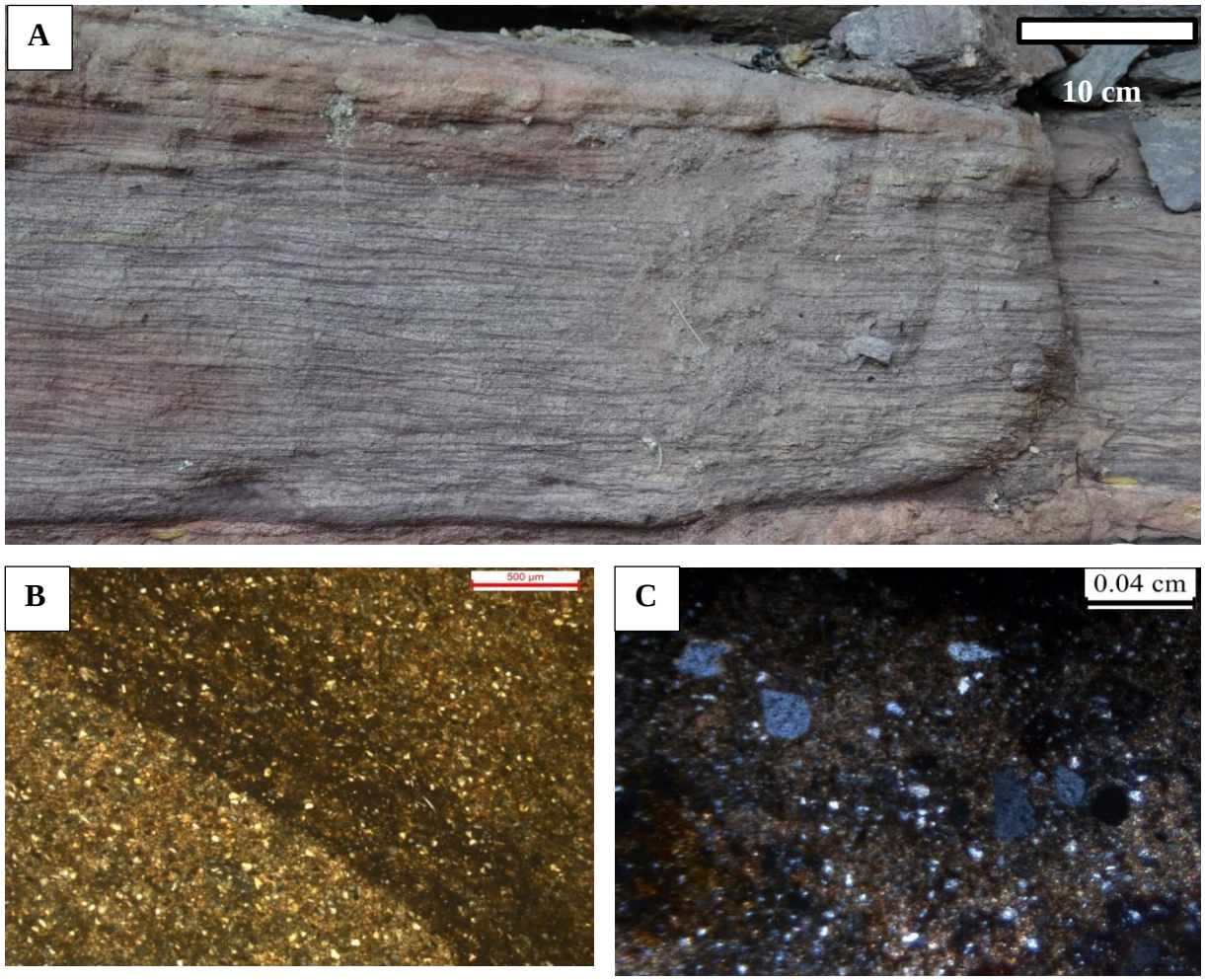

Figure: 3.22.A. Field photograph of inclined heterolithic sandstone-mudstone subfacies (4A3). **B.** Photomicrograph of inclined heterolithic subfacies showing alternate layers of sandstone and mudstone. **C.** Photomicrograph showing the dominance of quartz grains within the framework component.

3.6.2. Facies 4B: Mud clast conglomerate facies

This facies is small lenticular shaped conglomerate body with the dominance of mud clasts (Figure 3.23). The thickness of the beds varying from 5-10 cm and is comprised of bent clasts of mud. Size of the mud clast varies from 0.2-3 cm. Mud clasts are angular to subangular in nature and the matrix is arenaceous in composition. Subangular clasts of mud with low sphericity are dominant and show three colors: yellow to brown, faded violet and white. The base of this conglomerate unit is sharp and erosional in nature.

Interpretation

Within this facies, mud clasts are developed as a result of scouring of mud from the underlying unconsolidated mud bed. Scouring of mud needs a high energy current/wave action and subsequent deposition without significant transportation. Presence of mud clasts indicates intraformational type deposit under high current strength. Presence of mud clast conglomerate with sharp base indicates probably remnants of fluid mud beds eroded further upstream, not much transportation have along channel bases because very little erosion and fluid mudstone beds are observed (Eide et al., 2016).

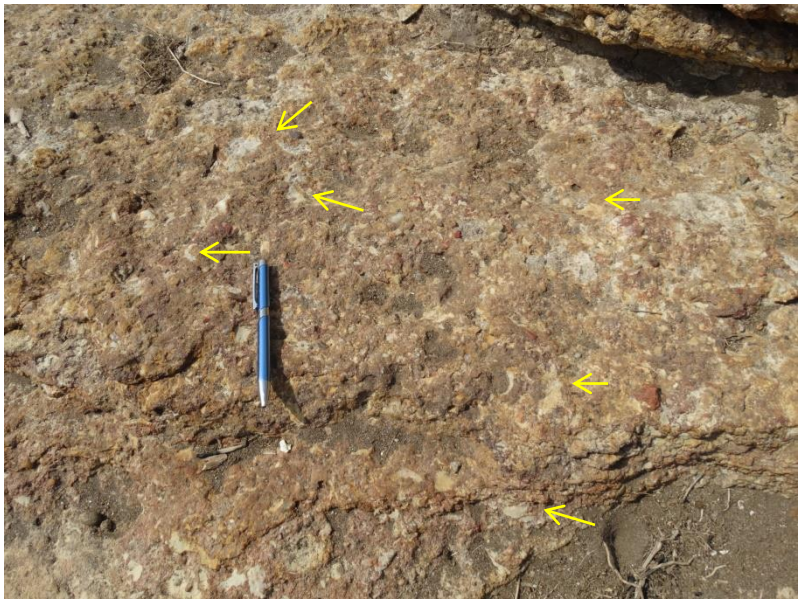

Figure: 3.23. Field photograph of mud clast conglomerate facies (4B) showing angular mud clasts (arrows). Length of the pen is 14.5 cm.

3.6.3. Facies 4C: Plane laminated sandstone facies

This facies comprises of sandstone layers with intermittent very thin mudstone layer. Overall mud contain is very less. The sandstone is fine grained with bed thickness varying from 2-25 cm. Soft-sedimentary deformation structures such as convolute laminae; load and flame structures are well preserved. This facies is mainly associated with sandstone-mudstone heterolithic facies (4A) but the mud contains and absence of frequent sandstone-mudstone beds makes it distinct from facies 4A.

Interpretation

Suspension deposit during the slack phase causes the formation of plane laminated fine-grained sandstone (Reineck and Singh, 1980). Presence of SSDS indicates density contrast between the two different lithounits during the time of deposition.

Figure: 3.24. Field photograph of plane laminated sandstone facies (4C). Length of the pen is 14.5 cm.

3.6.4. Facies 4D: Bioturbated sandstone facies

This facies is characterized by medium to coarse grain sandstone. Grains are moderately sorted, subangular in nature. The thickness of this facies varies from 40 cm to 2.5 m. Facies thickness is gradually increased from eastern part to western part of the study area. Very crude laminations are developed. In many areas, primary laminations are destroyed due to the intense

bioturbation (Figure 3.25A). Both the bioturbation intensity and the diversity increase towards the western part of the studied area. Microscopic studies of this sandstone show the enrichment of various fossil fragments along with microscale bivalve shell (Figure 3.25B, C). Mineralogically, this sandstone comprises of quartz, microcline feldspar, and muscovite. Grains are well sorted and rounded in nature.

Both vertical and horizontal burrows are preserved within this facies. U shaped, Y shaped, J shaped burrows of *Thalassinoid* and *Ophiomorpha* are most common types of burrows. Other important trace fossils are *Planolites, Skolithos, Palaeophycus, Arenicolites,* and *Rosselia.* A detailed description of these trace fossils is given in chapter-5

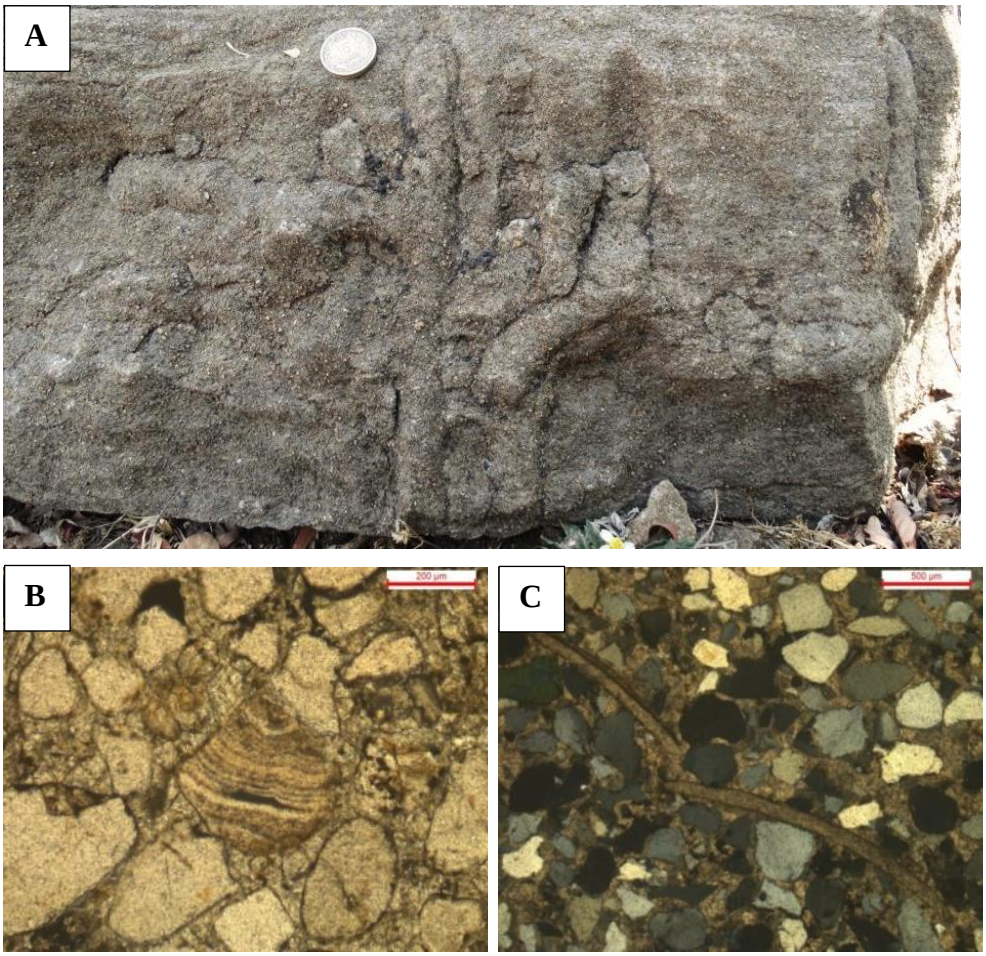

Figure: 3.25. A. Field photograph of bioturbated sandstone facies (4D). The diameter of the coin is 2.5 cm. **B.** Photomicrograph of bioturbated sandstone facies showing micro-scale bivalve shell along with well-rounded quartz grain. **C**. Photomicrograph of elongated fossil fragments within the bioturbated sandstone facies.

Interpretation

Intense bioturbation indicates nutrients rich, oxygenated environment present during deposition. Preservation of the burrows and very crude lamination indicates relatively slow rate of sedimentation. Destruction of the primary lamination by burrows indicates sedimentation and the burrowing process are simultaneous or just after deposition. Organism created passageways for feeding, air, and water movement thereby disturbing the parent material. *Thalassinoides-Ophiomorpha* bearing Glossifungites ichnofacies indicates a nearshore depositional setting (Buatois and Mangano, 2011).

3.6.5. Facies 4E: Green sandstone facies

This facies is characterized by coarse-grained, well sorted and rounded green colored sandstone. In the western part of the studied area, this facies type is predominant. Overall it is massive in nature (Figure 3.26A) but near Phata section presence of small trough cross-stratification is observed. The thickness of the facies varies from 40 cm to 2m. In some section (Phata) pebbles concentrations are observed locally. Petrographic studies reveal the presence of glauconite (Figure 3.26B) as an authigenic mineral within this facies.

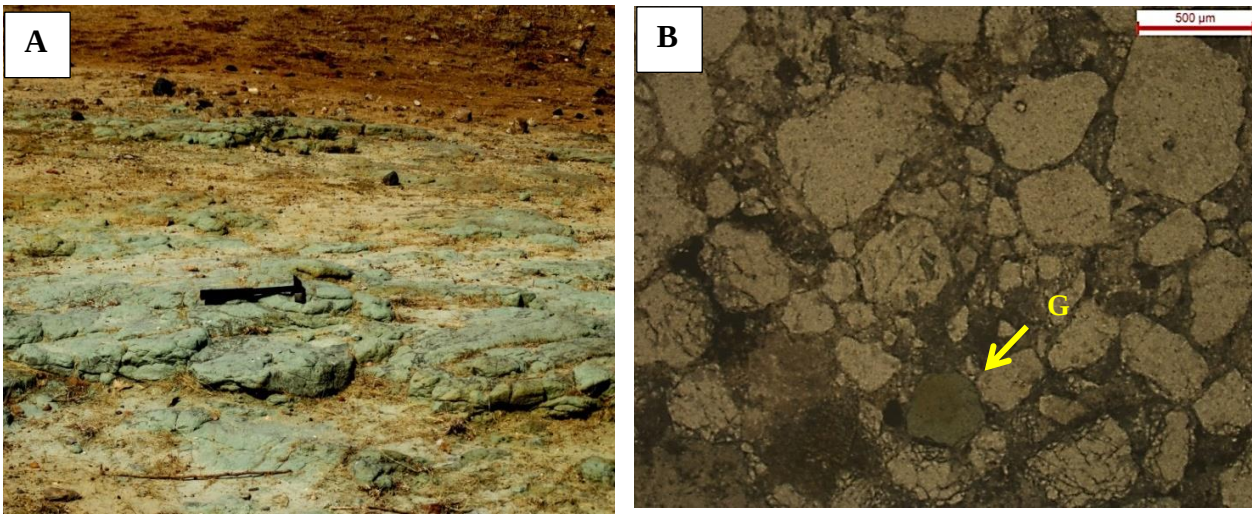

Figure: 3.26. A. Field photograph of green sandstone facies (4E). Length of the hammer is 30 cm. **B.** Photomicrophotograph of green sandstone facies shows the presence of glauconite (G).

Interpretation

Coarse-grained, well sorted, rounded nature of grains indicates the textural maturity of this rock unit. Presence of trough cross-strata specifies migration of ripple under current/wave action. Occurrences of glauconite indicate a shallow marine depositional condition which is also supported by the high textural maturity of the rock unit. Under wave action due to continuous to and fro action sand grains are reworked and become rounded and well sorted in nature.

3.6.6. Interpretation of Facies association 4

Laterally accreted foresets with mud drapes and lateral variation in foreset thickness within ripple cross-stratified sandstone subfacies indicate fluctuations in depositional condition, alternate high and low energy conditions. Bipolar cross-strata with development of herringbone cross-strata, sigmoidal cross-strata helps to interpret mutually opposite current activities. A gradual change from lenticular to wavy bedding indicates changes in current strength and supply of mud to sands, which is typical of a tidal flat regime. Reactivation surfaces with bi-directional cross-strata and lenticular/wavy bedding, mud clast conglomerate are the major sedimentary structures developed in a tidal environment (Kreisa and Moiola, 1986; Raaf and Boersma, 2007; Bhattacharya and Jha, 2014). Presence of these structures in the study area indicates that the facies association 4 is a product of tidal flat depositional setting. Sigmoidal cross-strata indicates the change in tidal flow velocities from slack phase to maximum velocity and then back to slack water phase (Kreisa and Moiola, 1986). Cyclic variation in the thickness and internal structures among tidal bundles is related to tidal strength which is controlled by periodicity of the lunar month (Kreisa and Moiola, 1986; Bhattacharya and Jha, 2014). More towards the western part the wave reworked tidal structures increases along with higher content of sandstone. In some part of the (Bagh section) Nimar Sandstone succession dominance of mudstone over sandstone with the development of wavy/lenticular bedding suggests deposition under lower intertidal setting. Presence of the bi-directional cross-strata, reactivation surface with mud drapes, wavy bedding indicates an overall upper subtidal to lower intertidal set-up where the supply of sand is more than mud. Presence of symmetrical ripple marks indicates interference of wave along with tidal activities. Towards the upsection of the FA-4 dominance of more sand within bioturbated sandstone facies (4D) and green sandstone facies (4E) along with glauconite indicates depositional condition was gradually changed from intertidal to subtidal setting under the influence of marine water.

3.7. Facies Association 5- Shore facies association

This facies association is comprised of four facies types namely- fossils bearing sandstone facies (5A), *Thalassinoides-Ophiomorpha* bearing thinly laminated sandstone-mudstone facies (5B), wave ripples bearing sandstone facies (5C) and massive mudstone facies (5D).

3.7.1. Facies 5A: Fossils bearing sandstone facies

This facies is characterized by fine to medium grain sandstone with the local occurrence of pebbles. The base of this facies is rich in gastropod body fossils. Towards the upsection, dominance body fossil of bivalve increases. Turreted gastropod shells (*Turritella*) are most abundant in this facies; they are associated with *Cardium (pelecypod)* (Figure 3.27A). Gastropod shells are characterized by tightly coiled and highly spired in nature. The spired portion of the shell is larger than the body whorle portion. Turreted gastropod shells often show opposite orientation with each other on the sandstone bedding surface. Symmetrical low amplitude long wavelength ripples, ladder back ripples and flat-topped ripples with bifurcated crest lines are also observed in this facies (Figure 3.27B). More towards the upper part of this facies presence of numerous *Ostrea* (Oyster) shells, a cemented variety of bivalve are found. In this facies, Oyster shells are lying with their left valve on the substrate, where they are firmly attached (Figure 3.27C). The height of the *Oyster* shell varies from 10 cm to 4cm.

Interpretation

Association of a turreted variety of gastropods (*Turritella*) and *Cardium* shells indicates a shallow marine depositional condition. The abundance of *Turritella* indicates shallow depth of the water with well-oxygenated, high nutrient and warm water condition (Malarkodi et al., 2009). *Ostrea* (*oysters*) are mainly lives in bays and estuaries settings. Their habitats must have water depths of 0–71 meters, ranging in temperatures of 6-20º Celsius; with salinity above 25 ppt. Presence of small scale symmetrical wave ripples indicates wave activity in very shallow water conditions (Bhattacharya and Jha, 2014).

It is generally believe that rounded crest and flat top of ripples are the results of the reworking of ripples during the process of emergence and also the ladder-back ripples are the result of the late stage wave action during the emergence (Collinson and Thompson, 1982). Low amplitude of the ripples indicates the shallow depth of water. Khosla and Sahani (2000) stated that, the presence of *Ostrea* indicates a near-shore sub-tidal environment.

Figure: 3.27. Field photographs of Fossils bearing sandstone facies (5A) showing **A.** gastropod (G) and bivalve shells (B) on the sandstone bedding surface. **B.** symmetrical flat-topped wave ripples with small scale ladder back ripples. **C.** body fossil of Ostrea, yellow arrow showing height of the shell. **D.** bi-polar orientations of gastropod shells (orientation of apex is marked by arrow heads). Length of the pen in A, B and C is 14.5cm and the diameter of the Coin is 2.5 cm.

3.7.2. Facies 5B: Thalassinoides-Ophiomorpha bearing thinly laminated sandstone-mudstone facies

Red colored, fragile, thinly laminated alternate sandstone-mudstone bed is characteristic of this facies (Figure 3.28). Under microscope also the alternate sand rich mud rich layer is prominent (Figure 3.29A). In the framework component of the rock quartz grain is dominant (Figure 3.29B). Alternate bioturbated and nonbioturbated zone is common within fine-grained sandstone-mudstone sequence. Burrows of *Thalassinoides* and *Ophiomorpha* are the main distinguishing feature of this facies, 30 to 40 cm long and 10 cm thick vertical "Y" shaped *Thalassinoides* tubes are observed. Due to intense bioturbation, primary bedding was extremely

disturbed and shows a fragile look. Mudstone layers which are not affected by bioturbation show development of thin laminae. At place, small-scale symmetrical ripple marks are observed within the sandstone bed.

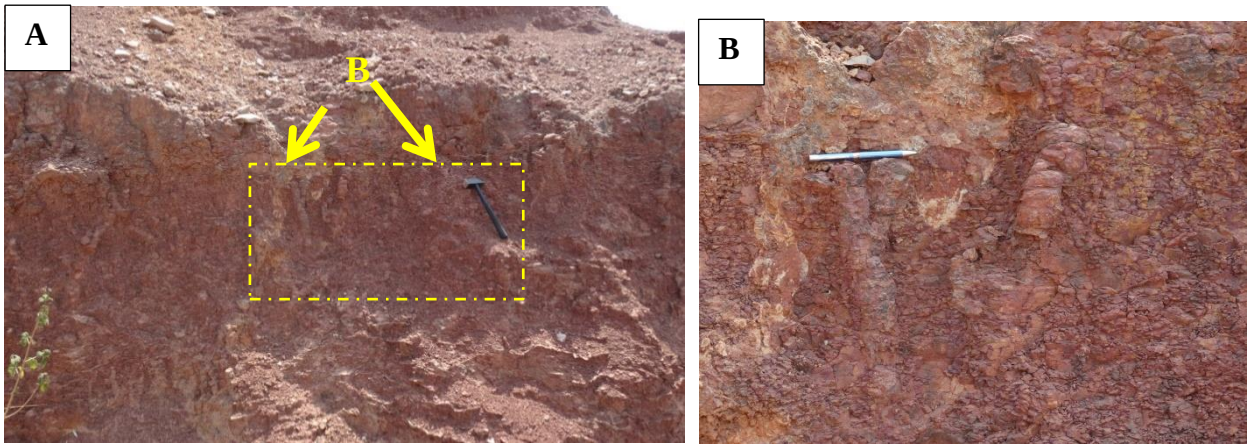

Figure: 3.28. A. Field photograph of *Thalassinoides-Ophiomorpha* bearing thinly laminated sandstone-mudstone facies (5B), showing well preserved vertical burrows (B).The part within the box is zoomed in B. Length of the hammer is 30 cm. **B.** Large scale vertical burrows of *Thalassinoides.* Length of the pen is 14.5 cm.

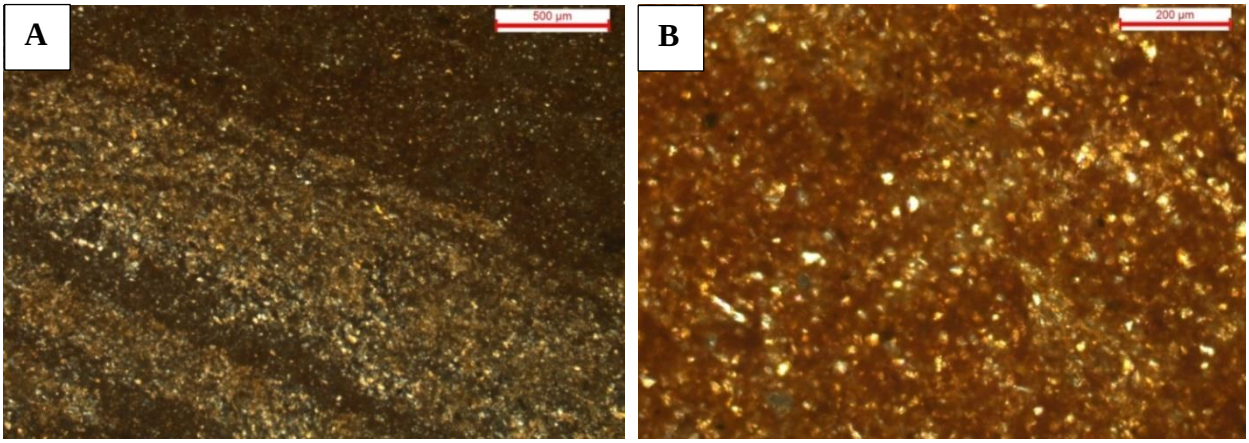

Figure: 3.29. Photomicrographs of *Thalassinoides–Ophiomorpha* bearing thinly laminated sandstone-mudstone facies showing **A.** alternate sand dominated and mud dominated layers. **B.** dominance of quartz grains within the framework component.

Interpretation

Thick mudstone is mainly a product of suspension fall out under low energy condition (Reineck and Singh, 1980). In this facies thick mudstone layers alternating with fine-grained sandstone indicates low energy depositional condition. The high intensity of bioturbation indicates oxygenated, nutrients-rich environment. Singh and Srivastava (1981) stated that *Thalassinoides* and *Ophiomorpha* are mainly associated with the shallow marine environment. Presence of small scale symmetrical wave ripples indicates shallow water condition with wave actions.

3.7.3. Facies 5C: Wave ripples bearing sandstone facies

This facies is characterized by coarse-grained, moderately sorted, subrounded grains of sand. Mineralogically, the sandstone is comprised of quartz grains along with siliceous cementation. Quartz grains show straight extinction dominantly but undulose extinction is also observed (Figure 3.30A). Line contact is the dominant grain to grain contact. The thickness of the individual bed varies from 10 cm to 15 cm. At the top of this facies symmetrical ripple with flat-top are observed. Crest lines are continuous with bifurcation (Figure 3.30B). They have spacing of more than 10 cm, smaller ladder back ripples occur in the troughs of the main ripple. Low amplitude long wavelength is the characteristic of this wave ripples. Internally the arrangement of the laminae gives chevron up building with the irregular bottom set (Figure 3.31).

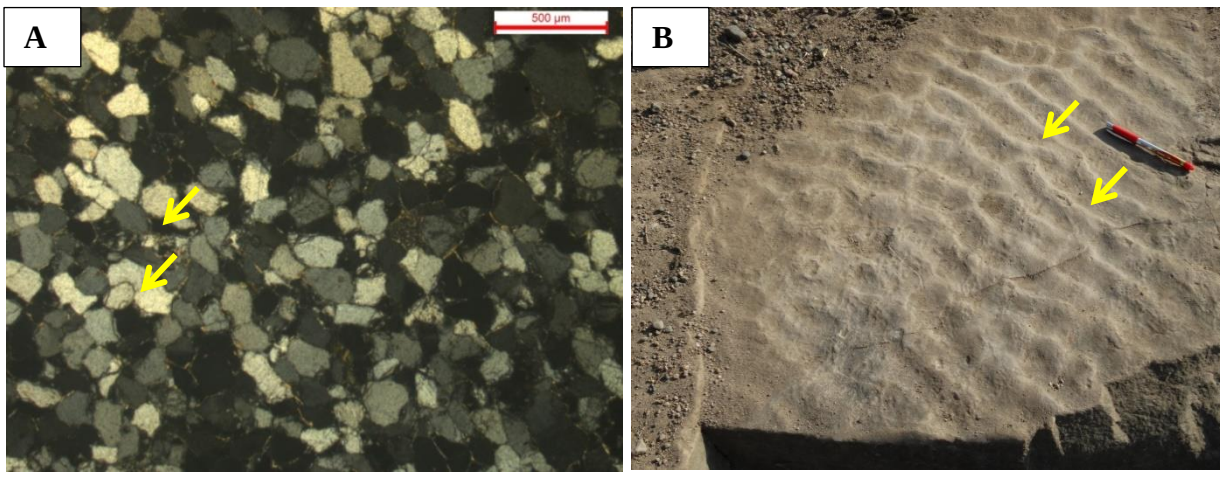

Figure: 3.30. A. Photomicrograph of wave ripples bearing sandstone facies (5C) shows well-sorted quartz grains along with siliceous cement (arrow indicates siliceous cement). **B.** Field photograph of symmetrical wave ripples with bifurcation of the crest lines (marked with arrows). Length of the pen is 14.5 cm.

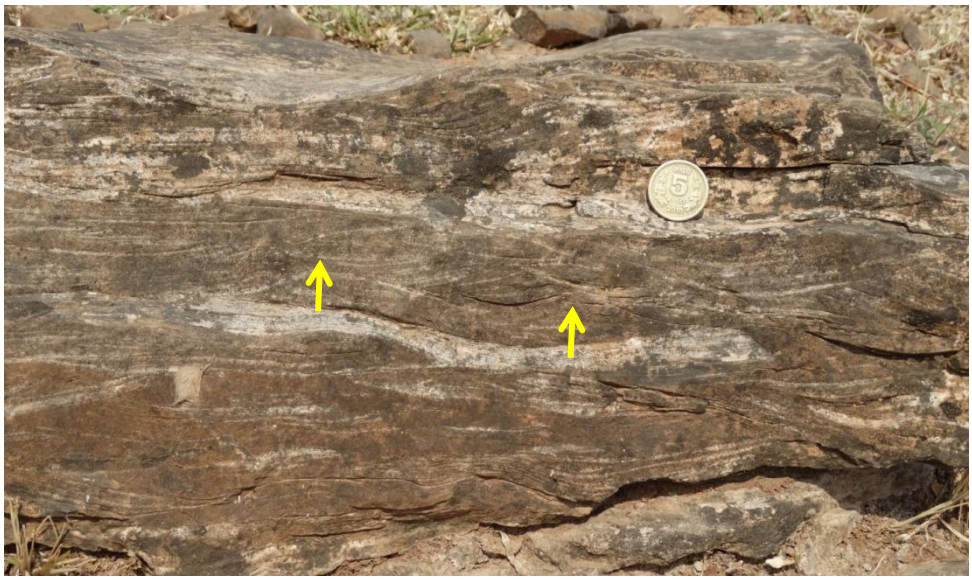

Figure: 3.31. Field photograph of wave ripples bearing sandstone facies (5C) showing chevron up building of the foresets (arrows). Diameter of the coin is 2.3 cm.

Interpretation

The grain size of this sandstone unit and the presence of symmetrical ripple indicate moderate energy condition under the influence of wave action. Due to interaction of oscillatory flow produced by wave and sediment substrate symmetrical wave ripples are formed (Harms et al., 1975). Low amplitude long wavelength of ripples indicates shallow depth of water. Presence of chevron up building suggests sufficient supply of sediment during the time of deposition.

3.7.4. Facies 5D: Massive Mudstone

This facies is characterized by red colored thick mudstone which is devoid of any sedimentary structures. Facies thickness varies from 6-120 cm. It is very friable in nature. The microscopic study of the mudstone indicates that mineralogically it is rich in quartz, opaque minerals, micaceous mineral, with some feldspar grains (Figure 3.32A). Feldspar grains are either partially or fully altered. The opaque minerals appeared as dark in color. The rock shows very faint layering by aggregated grains, one is dominated by quartz grains and the other one with dominant micaceous minerals. The modal concentration of quartz grain in the quartz-rich layer is about 55%. This facies is well developed in the eastern part of the basin (Near, Sitapuri area). Bioturbation is not observed within this facies. This facies shows a sharp contact with the upper Nodular Limestone Formation (Figure 3.32B).

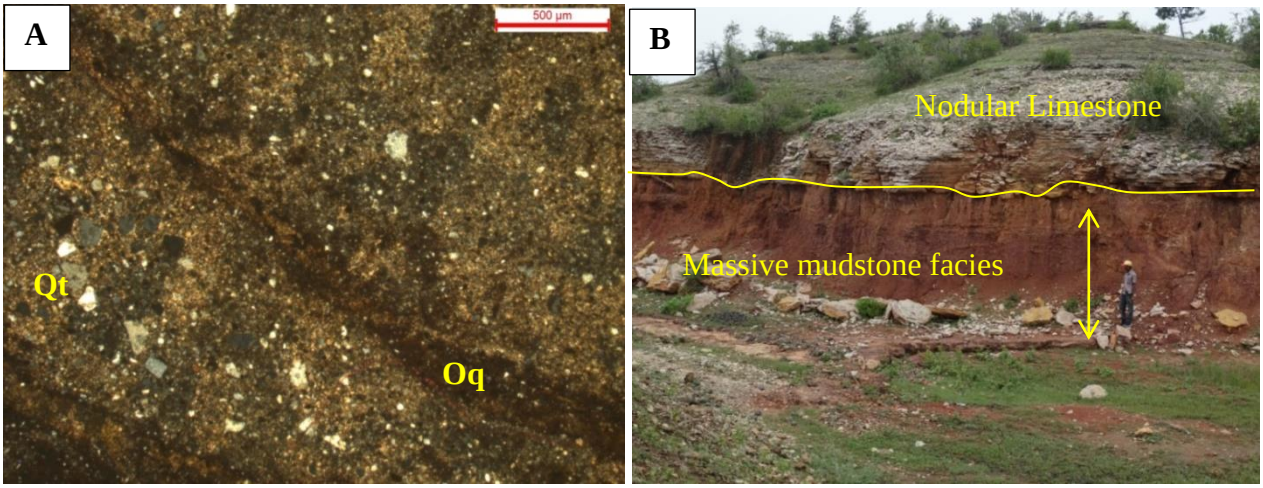

Figure: 3.32 A. Photomicrograph of massive mudstone facies (5D) showing quartz-rich (Qt) and opaque (Oq) rich layers**. B.** Field photograph of massive mudstone facies overlain by white colored Nodular Limestone Formation. Man in the picture is for scale.

Interpretation

Deposition of very fine sediments under very low energy conditions leads to this kind of thick massive mudstone. It is a suspension fallout deposit. Absence of bioturbation indicates an anoxic condition with increasing water level.

3.7.5. Interpretation of Facies Association 5

This facies association shows abundance of marine trace fossils and body fossils along with symmetrical wave ripples which indicates a shallow marine nearshore depositional setting. Presence of rounded /flat top ripples along with ladder back ripples suggests intermittent subaerial exposure of the ripples in a beach setting. The gradual increase of mud content and decreasing bioturbation intensity towards the upsection of this facies association indicates increasing water depth along with more suspension deposition.

3.8. Depositional environment of the Nimar Sandstone

Based on detailed facies analysis, three distinct depositional systems are identified within the Nimar Sandstone – (i) basal fluvial depositional system without significant effect of marine tide/wave reworkings, (ii) middle tide-influenced fluvio-tidal interactive system and (iii) the upper tide-wave reworked onshore setting (Figure 3.33). Significant mixing of fluvial and tide-wave processes from bottom to top of succession suggests an overall fluvio-marine interactive

depositional system was prevalent during Nimar sedimentation. Detailed account of all facies types in five facies associations of the Nimar Sandstone and their description and interpretation are summarized in Table 3.1.

The channel-fill facies association (FA-1) is laterally discontinuous, lenticular shaped, predominant in the basal part of the succession and consists of clast supported conglomerate facies (1A), matrix supported conglomerate facies (1B), pebbly sandstone facies (1C) and trough cross-stratified sandstone facies (1D). The finning upward successions of dominantly cross-stratified sandstones with concave-up base and abundant immature sediments indicate deposition from rapid high-energy currents, which confined in channels. The lenticular conglomerate occurring at the bottom of the Nimar Sandstone demarcates channel lag deposits.

Overbank facies association (FA-2), closely associated with the channel-fill facies association (FA-1), is dominated by - (i) sandstone-mudstone interbedded facies (2A) with vertical burrows (e.g., *Skolithos)*, and (ii) plane bedded sandstone facies (2B). The overall finer grain size of this association with ample mud indicates that this facies deposited in the floodplains of the channels. In the lower part of the succession, alternate deposition of FA-1 and FA-2 indicates their deposition in fluvial-dominated settings. FA-1 and FA-2 are well developed in the eastern and central part of the study area, which signify fluvial sedimentation in Nimar Sandstone was confined mainly in the eastern and the central parts of the basin.

Juxtaposition of this facies association with fluvial-dominated fluvio-tidal facies association (FA-3) in the middle part of the succession indicates that the depositional condition shifted from an overbank to inter-distributary bay setting due to frequent inundation by tidal flooding. However, fluvial sediment supply was much higher than tidal sedimentation. Sediments were affected by tidal current and formed poorly developed bi-directional cross-strata and reactivation surfaces, within large scale trough cross-stratified sandstone facies (3A) and planar cross-stratified sandstone facies (3B). In the central part, mainly in the Bagh and the Rampura sections, FA-3 is well developed. Intimate association of sediments of FA-3 with channel-fill fluvial sediments (FA-1) and the overbank deposits (FA-2) and overall progradational character of the succession indicate deposition within a bay-head delta zone within a fluvial-tidal interactive depositional system.

The tide dominated fluvio-tidal facies association (FA-4) is distributed throughout the study area. Within the FA-4, sandstone-mudstone heterolithic facies (4A) and plane-laminated sandstone facies (4C) are abundant and well developed in Bagh and Man river section. The mud clast bearing conglomerate facies (4B) is restricted locally in those sections. Within the

sandstone-mudstone heterolithic facies (4A) evidences of tides are well preserved in the form of tidal bundles, tidal rhythmites, reactivation surfaces with double mud drapes and bi-directional cross-strata. Predominance of tidalites in the middle part of Bagh and Man section indicates a well-developed intertidal flat environment. Bioturbated sandstone facies (4D) and green sandstone facies (4E) are dominantly sandstone-rich and are well developed more towards the western part of the basin (e.g., Akhara and Phata sections). The dominance of sandstone over mudstone within these two facies indicates relatively higher energy conditions. The intensity of bioturbation also increases towards the western part. At the top part of the FA-4, presence of wave reworked tidal features, interference ripples and increasing sand content indicates a shift from inter-tidal to sub tidal depositional condition. Overall, the intertidal to subtidal flat within a fluvio-tidal mixed setting with less wave activities indicates a sheltered tide-dominated wave-influenced estuary setting for central part of the study area, where the influence of wave is less.

More towards the up section wave influence gradually increases within the shore facies association (FA-5). Vertical stacking of FA-5 over FA-4 indicates a change in depositional pattern from tide-dominated to more wave-dominated. Presence of *Ostrea* and *Turritella* shells in the fossil-bearing sandstone facies (5A) indicates relatively stable ground with a shallow open marine condition, which is also supported by the presence of ladder-back ripples, low amplitude flat-topped wave ripples within it and the associated *Thalassinoides-Ophiomorpha* bearing thinly laminated sandstone-mudstone facies (5B). In wave ripples bearing sandstone facies (5C) abundant flat-topped wave ripples, ripples with bi-furcated crest line, ladder-back ripples, and combined-flow ripples bear signatures of shallow wave reworking and intermittent exposures, suggesting a shore depositional setting with dominant wave action. In this facies association, mud content gradually increases towards the up section. The thick massive mudstone facies (5D) of FA-5 appeared as a sheet over the total Nimar Sandstone succession. Continuous, thick and massive nature of the mudstone indicates a prolonged suspension deposit under high water level condition.

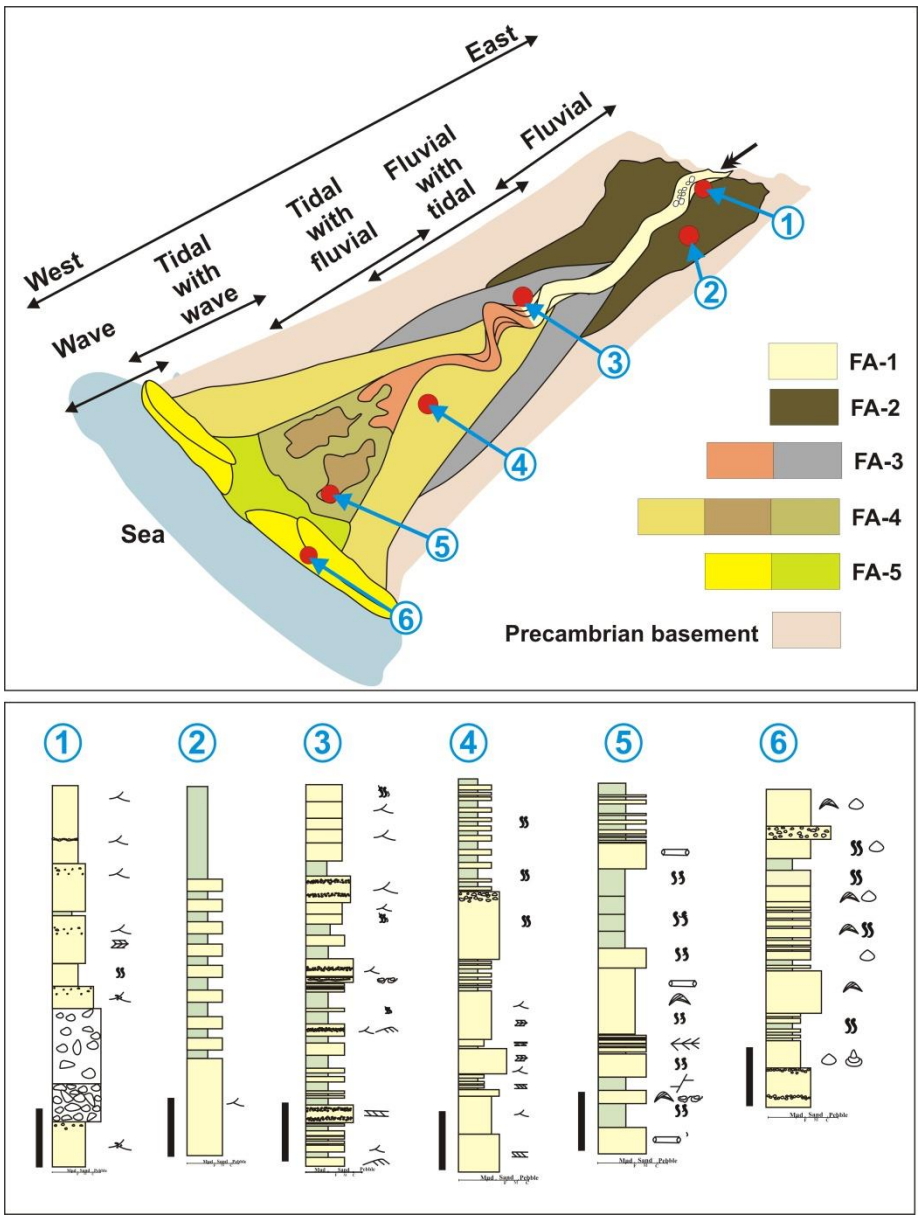

Figure: 3.33. Conceptual depositional model for Nimar Sandstone showing distribution of various facies types in the study area. Representative vertical lithologs (1-6) for different parts of the proposed model is also shown.

Overall facies succession manifests - (i) increase in the mud content and (ii) predominance of marine trace fossils and body fossils towards the upsection and spatially from east to west, which indicates gradually increasing water depth and west to eastward encroachment of more open coastal conditions. Thus, the overall facies architecture reveals an onlapping of the shore facies association on the underlying sediments. This facies association constitutes the top part of the Nimar Sandstone succession and is conformably overlain by bivalve- and echinoid-bearing limestone of the Nodular Limestone Formation, indicating the development of more open marine conditions in the study area. Gradual increase in marine conditions towards

upsection is an evidence of a prolonged, sustained marine transgressive condition in the Narmada valley during the late Cretaceous.

3.9. Summary

Systematic interpretation of facies from Nimar Sandstone reveal total seventeen facies types from the study area. All these facies are grouped under five facies association based on their genetic appearances –

- Basal portion of the successions occupied by the channel-fill facies association (FA-1) and overbank facies association (FA-2), which appeared as a blanket over FA-1. Middle portion of the succession contain mixed fluvio-tidal sediments of fluvial dominated fluvio-tidal facies association (FA-3), and tide dominated fluvio-tidal facies association (FA-4). Upper part is dominated by wave reworked tidal sediments of shore facies association (FA-5).
- Distribution pattern of these facies association and their forming processes signify overall deposition was took place in a fluvio-marine interactive estuary setting, where sedimentation was started under fluvial process followed by a mixed fluvio-tidal process and then more marine influence towards the upsection. The overall depositional setting are classified into three major sub-environment-
    - A river dominated (FA-1) inner estuary with an overbank setting (FA-2). Along with Sand dominated channel bars in a bay-head delta zone which influenced by tidal current (FA-3).
    - Tidal flat environment dominantly inter-tidal to sub-tidal setting in the middle part of the succession (FA-4).
    - An outer estuary zone where wave-reworked sub-tidal flat environment prevailed with gradually increases of water level in the upsection (FA-5).
- Overall depositional environment and the distribution pattern of the facies indicate an eastward encroachment of marine water with gradual increase of water level during the deposition of Nimar Sandstone in the study area.

CHAPTER-4

Tide and wave generated structures

4.1. Introduction

Evidences of tidal activities are preserved both in modern and ancient sedimentary succession. Vertically accreted planar deposits (tidal rhythmites) and laterally accreted foreset bedforms (tidal bundles) within sandstone-mudstone heterolithic units are known as tidalites. Tidalites preserved the ancient record of tidal cyclicities. The thickness of the individual laminae within tidalites is directly proportional to the strength of the tidal current which in turn is directly and positively related to the magnitude of the daily rise and fall of the tide (tidal range). Over periods of days, months, or years, changes in tidal current strength related to various lunar/solar cycles are reflected in the change in thicknesses of vertically stacked laminae (Mazumder, 2004; Kvale, 2012). Tidalites are the tool for tracing the evolutionary history of the Earth-Moon system (Williams, 1989; Kvale et al., 1999). From the late Cretaceous Nimar Sandstone Bhattacharya and Jha (2014) first time documented tidalites and by measuring variation in foreset thicknesses of tidal bundles they calculated lunar tidal periodicities and Earth-Moon orbital distance of the late Cretaceous time. Several tide generated structures are reported from sandstone-mudstone heterolithic facies (4A) of the Nimar Sandstone (Bhattacharya and Jha, 2014), like bundled sediment couplets (one sand foreset followed by a mud drape) with lateral thickness variation, bipolar strata bundles with development of herringbone cross strata, frequent reactivation surfaces, lenticular/wavy bedding and pinstripe heterolithic strata. In addition, various wave-generated features like wave ripples and wave modified ripples are commonly associated with the tidalites. In this chapter detailed documentation of each tide generated, as well as wave reworked tidal structures are presented and interpreted in terms of prevalent palaeodepositional condition.

4.2. Tide generated sedimentary structure

Tide-dominated fluvio-tidal facies association (FA-4) mainly bears the evidences of palaeo tidal activities from the study area. FA-3 and FA-5 have very crude evidence of tide i.e., poorly developed bi-directional cross-strata, reactivation surfaces and mud drapes; FA-5 is mainly enriched with tidal trace fossils (e.g. *Balanoglossites* isp., *Asterosoma* isp., *Rosselia* isp.). The sandstone-mudstone heterolithic facies (4A) is enriched with tide generated primary sedimentary structures, which is abundantly present in the middle part of the succession. Major

tide generated primary structures are- i) laterally-accreted strata bundle with reactivation surface, ii) bi-directional cross strata set with the development of herringbone cross-strata, iii) vertically-accreted strata bundle with wavy and lenticular bedding and iv) sigmoidal strata. In the sandstone-mudstone heterolithic facies (4A) individual sandstone beds are characterized by abundant ripple cross-laminae with development of bundled foresets. The change from sand to mud is commonly gradational, although the contact between mud and overlying sand is sharp and abrupt. Foreset geometry often changes laterally from straight, truncating, concave up with asymptotic toe, to sigmoidal. Detail descriptions and interpretation of different tide generated features are given below.

4.2.1. *Laterally accreted strata bundle with reactivation surface*

Rippled cross-stratified sandstone subfacies (4A1) is the host for these structures. The laterally accreted bundles are more prominent in the Bagh section. At the base of this structure, cm thick set of planar lamination was observed. Thicknesses of cross-strata set varies from 6 to 15 mm. A systematic down current change in grain-size across the bundles within individual set is observed (Figure 4.1). Reactivation surfaces or sigmoidal shaped laminae of fine grained sandstone separate the bundles from one another. Each laterally accreted foreset is bounded by a thin (~ 2-3 mm) laminated horizontal mud layer. Towards the down current direction mud is more abundant. The thickness of sandstone foresets varies from 2 to 4 mm. whereas the thickness of mudstone drapes are ranged from 0.5-1.2 mm. Individual small ripple bedforms are also preserved. Different foresets are accreted laterally against prominent reactivation surfaces. At places, bi-directional cross-strata were crudely developed (Figure 4.2A).

Interpretation:

Boersma (1969) stated that migration of ripples during a major tide is producing such type of bundles. Presence of reactivation surfaces between the laterally accreted bundles indicate frequent changes in tidal current and intensity during or between tides (Klein, 1977). Truncated sigmoidal mudstone drape or horizontal mudstone layers on each bundle indicate a pause or stagnant phase during the tidal activity (Kreisa and Moiola, 1986). Downcurrent change in thickness and grain size throughout the bundles represent systematic variation in the strength of successive tides (Bhattacharya et al., 2012).

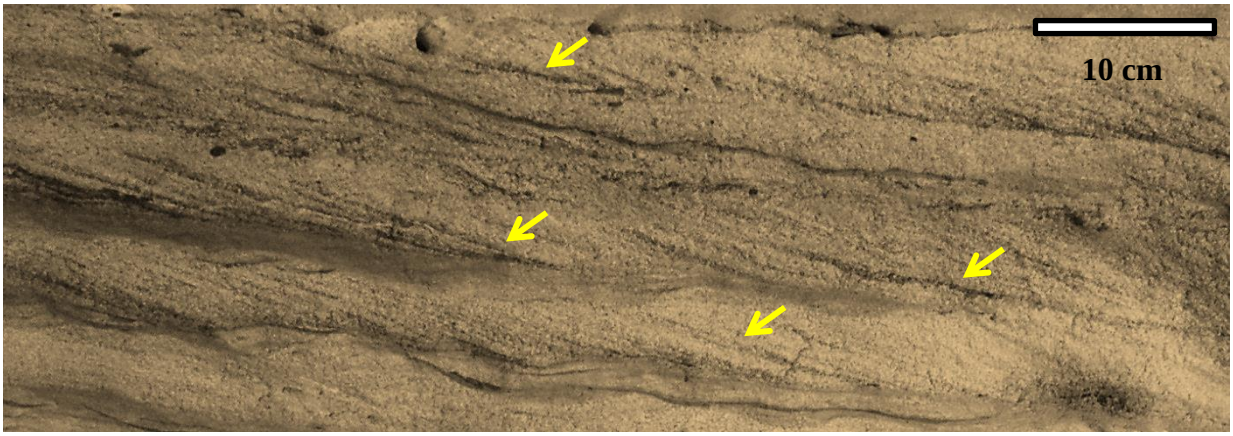

Figure: 4.1. Field photograph of lateral accretions of strata bundles against reactivation surfaces. Arrow marks show several reactivation surfaces along with mud drapes.

4.2.2 Bi-directional cross strata set with the development of herringbone cross-strata

Bi-directional cross-strata sets occur within thick (~1m thick) coarse-grained sandstone bed of sandstone-mudstone heterolithic facies. In each of the set sandstone foreset and toeset are draped by thin mudstone layer, forming tidal bundled (Figure 4.2A). The shift from sand laminae to mud laminae is commonly gradational, whereas the contact between mud laminae and next sand laminae is abrupt. Foreset thickness and inclination vary laterally in cyclic pattern within one strata set. Foreset geometry often changes laterally from straight, truncating, to concave up with asymptotic toe to sigmoidal. Different foresets are accreted laterally against prominent reactivation surfaces. Climbing ripples are abundant within the individual strata bundles (Figure 4.2B). Thickness of the foreset varies both laterally and vertically. At the bottom part of the set boundaries successive mud drapes on the sand foresets become flat and merge together producing thin mud veneers. At places top of the small ripples are draped by thin mud. Locally, preservation of individual ripple with mutually opposite flow direction has led to development of herringbone cross-strata (Figure 4.2B).

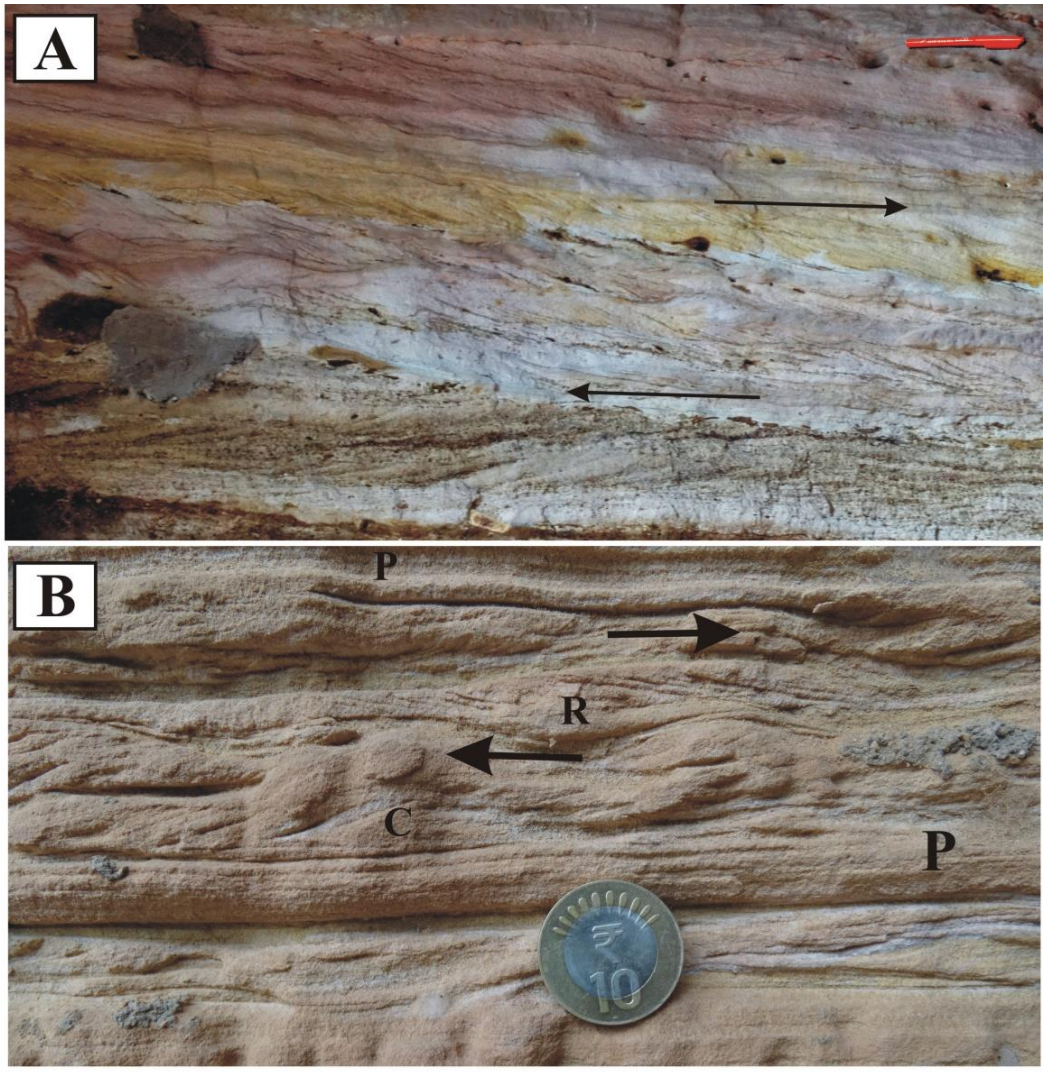

Figure: 4.2. A. Field photograph of ripple cross-stratified sandstone subfacies (4A1) showing mutually opposite foreset orientations in adjacent strata sets. Length of the pen is 14.5 cm. **B**. Field photograph of bi-directional strata bundles with the development of small climbing ripples (C) and reactivation surfaces (R) ripples show rounded, symmetrical crests plane lamination (P). Diameter of the coin is 2.5 cm.

Interpretation

Formation of mutually opposed cross-strata bundles with local development of herringbone cross-strata suggests current reversals under ebb-flood tidal fluctuations (Bhattacharya and Bhattacharya, 2006, 2010, Bhattacharya and Jha, 2014). Due to changes in velocity of the tidal current during or between the tidal phases reactivation surfaces are developed (Klein, 1977). Presence of thick mud drapes along the sandstone forsets signifies alternate slack phases in between dominant tidal currents. Thick-thin alternate foreset of sandstone-mudstone indicates a diurnal inequality in tidal current (Kvale 2006, 2012). The abundance of sandstone beds over

mudstone and abundance of mutually opposite cross-strata sets suggest deposition in subtidal condition (Bhattacharya and Jha, 2014).

4.2.3. *Vertically accreted strata bundles*

Vertically accreted strata bundles are represented by alternating sets of ripple cross-laminae and horizontal planar laminae (Figure 4.3A). Characteristically, the alternation is on a scale of a few centimeters. Ripple forset followed by planar laminated thin sand-mud veneer on their top is the main characteristic of these strata bundles. There is a tendency of the ripples to climb near the upper part of the cosets. Amplitudes of the ripples vary from 5cm to 7cm. Overall there is an upward decrease in grain size and foreset thickness (0.7 cm to 1 cm) of the ripple cross-laminated units. The apparent reverse orientation of vertically adjacent cross-sets has given rise to herringbone structure locally (Figure 4.2A). Discontinuous, flat, isolated cross-laminated sand lenses (Lenticular bedding) and wavy bedding are interbedded within thick mud layers (Figure 3.21), where mudstone is dominant over the sandstone. Wavy mudstone alternate with discontinuous ripple bedded sandstone. The thicknesses of the layers vary from 5 to 20 cm. In lenticular bedding, sand lenses are 2-4 cm in thickness and asymmetrical and discontinuous in nature. Gradually in up section sand lenses become interconnected and symmetrical in nature.

Interpretation

Greb and Archer (1995) stated that alternating sets of thick-thin sandstone-mudstone laminae indicate fluctuation in energy condition, where thicker sandstone lamina are deposited under traction current and alternating thin mudstone are the product of suspension fallout during the slack phase. Presence of interbedded ripple cross-laminae with thin planar-lamination within sandstone indicates a change in depositional energy condition. Round crested ripples with systematic drapes of mudstone on each ripple indicate alternate shallow water wave action with tidal current. Presence of lenticular and wavy bedding suggests an increase in mud supply over the sand. Increase in mud supply at a certain phase prohibits the migration of bedforms and leading to the formation of lenticular bedding (Reineck and Singh, 1980). Continuous sand lenses in wavy bedding indicate the deposition and preservation of both the sand and muds (Reineck and Singh, 1980). Due to the minimal supply of sand isolated, flat sand lenses are developed. Towards the up section gradation from lenticular to wavy bedding indicates continuous supply of sand and mud; where from the base to top supply of sand gradually increases. Climbing ripples represent rapid accumulation of sediments over the migration of the

bedforms. Vertically accreted tidal bundles with mud interbed indicate an upper intertidal-flat domain for the deposition of the sediments (Kreisa and Moiola, 1986).

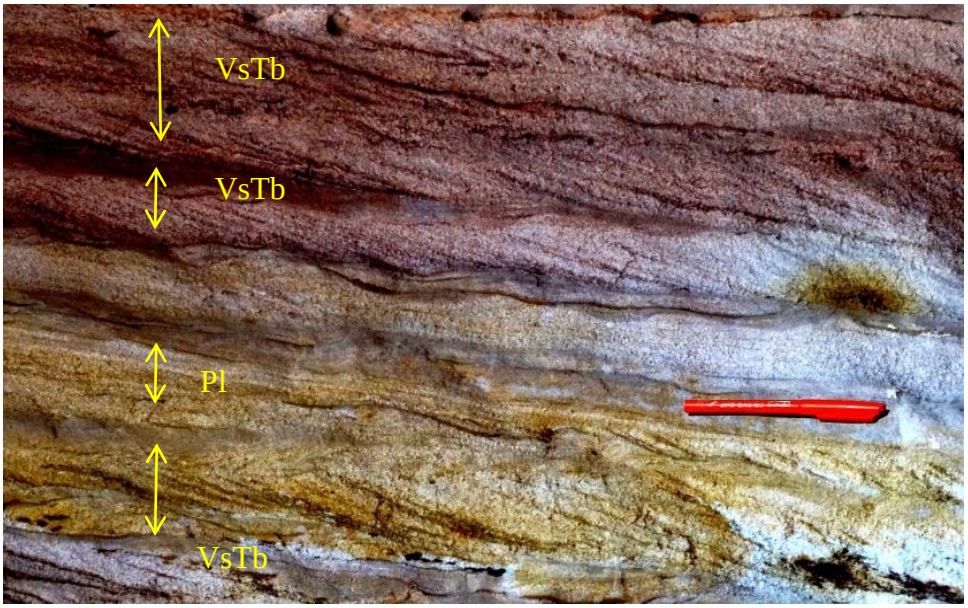

Figure: 4.3. Field photograph of vertically stacked tidal bundles (VsTb) showing alternate thick–thin cycles along with planar lamination (Pl). Length of the pen is 14.5 cm.

4.2.4. Sigmoidal strata

The sandstone beds of the sandstone-mudstone heterolithic facies are characterized by low dipping topsets (5˚-8˚) with moderately dipping (20˚) sigmoidal foresets (Figure 4.4). Down current termination of the foreset near the bottom set boundary is also prominent. Each of the foreset is draped by thin mud veneer. The low angle topset laminae tie a gap between crest of the bedform and the brink point from where the laminae become steeper. In few places thickness of the mud drapes increases. Sigmoidal cross lamine bundles generally develop from laterally accreted planar-tabular cross-laminae. Reactivation surface is prominent within these strata bundles. Both the upper and lower bounding surface of the strata sets are covered by thinly laminated mud layers.

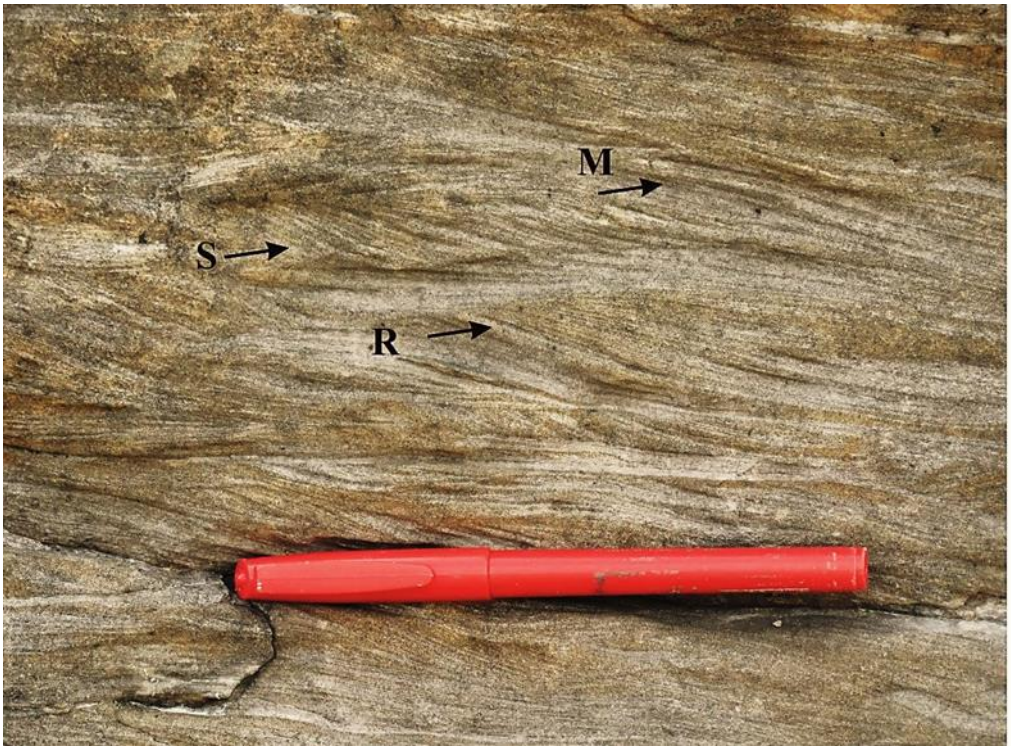

Figure: 4.4. Field photograph of sigmoidal cross strata bundles (S), reactivation surfaces (R) and mud drapes (M). Length of the pen is 14.5 cm.

Interpretation

Mainly migration of linguoid ripples under high energy condition formed sigmoidal cross-strata (Bass and De Koning, 1995). In the study area dominance of low angel top sets of these cross-strata indicate migration of humpback ripples which are considered responsible for the formation of this sigmoidal strata bundle (Sunderson and Lockett, 1983). In Low-angle topset the area between the crest point and the brink point represents a zone of non-flow separation, and flow separation occurs near the brink point (Bhattacharya and Jha, 2014). Mud draping on these bundles represents pause phase in between successive tidal currents (Bhattacharya and Bhattacharya, 2006). Formation of sigmoidal bundles needs higher tidal flow velocity condition.

4.2.5. Cyclical Tidal Rhythmites

Inter-laminated, near horizontal beds of mudstone and fine sandstone are the characteristic of this tidal rhythmites (Mazumder and Arima, 2013) (Figure 4.5). The thickness of the sandstone laminae ranges between 1-8 mm and mudstone laminae thickness vary between 0.5-2 mm. Sandstone-mudstone heterolithic facies of FA-4 is the host of the tidal rhythmic structures, often alternated with laterally accreceated cross strata bundles in vertical succession. Rhythmites are characterized by alternate thick-thin pairs of the sandstone-mudstone layer forming alternate sand-dominated and mud-dominated zones.

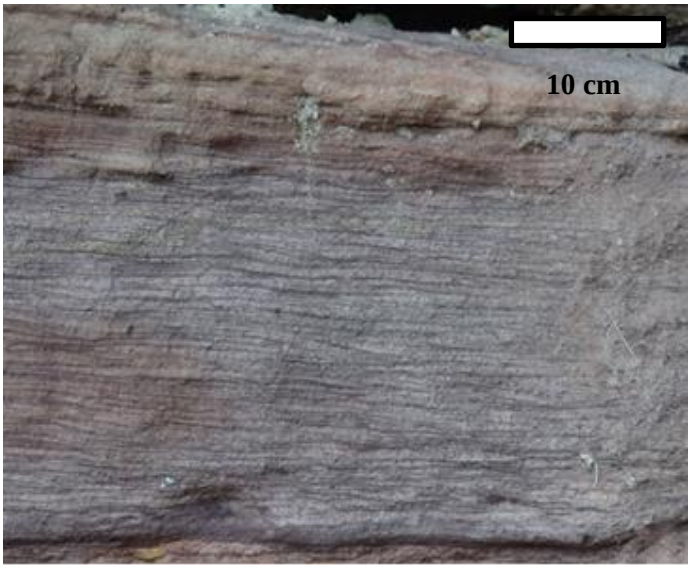

Figure: 4.5. Field photograph of tidal rhythmites in thick-thin alternate layers of a sandstone-mudstone unit of sandstone-mudstone heterolithic facies (4A).

Interpretation

Cyclical tidal rhythmites point to sheltered intertidal flats typically at the inner part of macro-tidal estuaries (Fan, 2013). Mm thick sandstone-mudstone inter-laminae indicate a deposition from suspension fallout in a relatively calm water condition (Greb and Martino, 2005). The variation of lamina thickness is due to the rhythmic fluctuations in the rate of suspension settlement of sediments.

4.3. Significance of tidal Structures in the study area

In the study area tidalites are mainly associated with the tide dominated fluvio-tidal facies association (FA-4). Presence of laterally accreted tidal bundles, herringbone cross-strata and sigmoidal cross-strata, within the ripple cross-stratified sandstone subfacies (4A1) indicates a subtidal depositional setting. Similarly, alternate thick-thin cyclical tidal rhythmites, vertically accreceated cross-strata, wavy and lenticular bedding are considered as a product of inter-tidal flat (Fan, 2013). The overall depositional condition for FA-4 is mainly tide-dominated. Within the tidal rhythmites alternate sandstone-mudstone couplets indicate dominant tidal current followed by a slack phase between two successive tides (Allen, 1981). Presence of abundant reactivation surfaces within sandstone-mudstone heterolithic facies (4A) is an indication of frequent changes in tidal current intensity and direction. Systematic variations in tidal strength during the sedimentation are recorded in terms of down current variation of foreset thickness and grains size across the laterally accreted strata bundles. Abundance of sigmoidal cross-strata

bundles over laterally accreted bundles towards the up section indicates increasingly higher tidal flow velocity (Bhattacharya and Bhattacharya, 2006). In vertically accreted tidal bundles thinly laminated sandstone-mudstone layer indicates periodic flow fluctuations, where sand deposited from traction current and mud deposited from suspension during quiescent phases. Alternate sand-dominant and mud-dominant units with variation in thicknesses of sandstone foresets and mudstone drapes suggest alternate spring–neap-spring tidal cycles (Greb and Archer, 1995). Mazumdar and Arima (2005) stated that, cyclical interlamination of sandstone-mudstone layers is the product of intertidal flat setting. Bi-directional cross-strata sets with predominance of sandstone indicate mutually opposite and higher tidal current strength under ebb-flood tidal fluctuations (Bhattacharya and Bhattacharya, 2006, 2010).

The middle portion of the Nimar Sandstone succession is mainly occupied by the tide-dominated fluvio-tidal facies association (FA-4) and distributed throughout the study area. Central and eastern part of the study area is mainly dominated by muddy, fine-grained sediments along with tidal rhythmites, lenticular/wavy beddings and inclined heterolithic strata. Sand content within FA-4 increases up section, particularly more towards the western part of the study area. Facies 4D and 5B is mainly enriched with tidal trace fossils (discussed in chapter 5) with more sand. Dominance of this two facies types is mainly observed in the western part of the study area. The predominance of sandstone over mudstone more towards the western part along with bi-directional cross-strata indicates a subtidal flat setting. So it can be concluded from the tidal structures that central and eastern part of the study area is mainly controlled by an inter-tidal setting whereas the western part is under sub-tidal setting. Based on the tidal features overall an intertidal to the subtidal flat depositional condition is inferred for the middle portion of the Nimar Sandstone succession.

4.4. Wave generated structures

Wave reworked tidal structures, as well as wave dominated bedforms, are well preserved in the study area. Symmetrical wave ripples, interference ripples, ladder back ripples, flat-topped ripples and combined flow ripples are documented from the tide dominated fluvio-tidal facies association (FA-4) and shore facies association (FA-5). In ripple cross-stratified sandstone subfacies (4A1) of FA-4 wave reworked tidal structures are dominant. In the vertical section wave ripples are preserved as bundled up-building of cross-strata with sharp lower and upper boundary (Figure 4.6A). In general, wave ripple beds are underlain and overlain by planar laminated thick sandstone beds and they are in common capped by a wavy draping surface with

poorly developed bi-directional cross-strata (Figures 4.6B, 4.7). At places wave ripple shows tuning fork like bi-furcation of crest lines along with ladder back ripples (Figures 3.27B, 3.30B, 4.8). Ripples with rounded crests and symmetrical profiles with sand/mud drapes on top indicate reworking of tidal sediments by shallow water waves. Within the wave reworked tidal bundles foresets are dipping in opposite direction (Figure 4.7). Wave reworking of the tidal bundles is often very prominent towards the western part, producing varied combined flow ripples and wave-generated tidal bundles (Figure 4.6A). In shoreface facies association (FA-5) symmetrical sinuous crested ripple marks are abundant towards the western part of the study area.

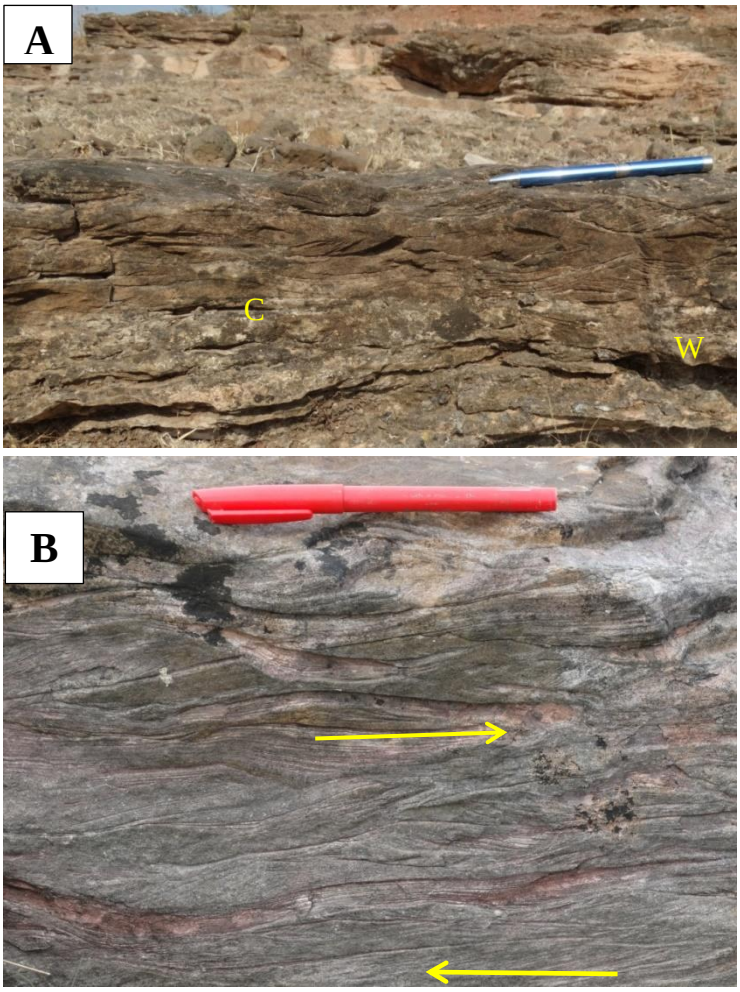

Figure: 4.6. A. Field photograph of wave ripples (W) with bundled-up building of laminae and combined flow ripples (C). **B.** Field photograph of wave reworked tidal bundles with poorly developed bi-directional cross strata within the sandstone-mudstone heterolithic facies. Length of the pen is 14.5 cm.

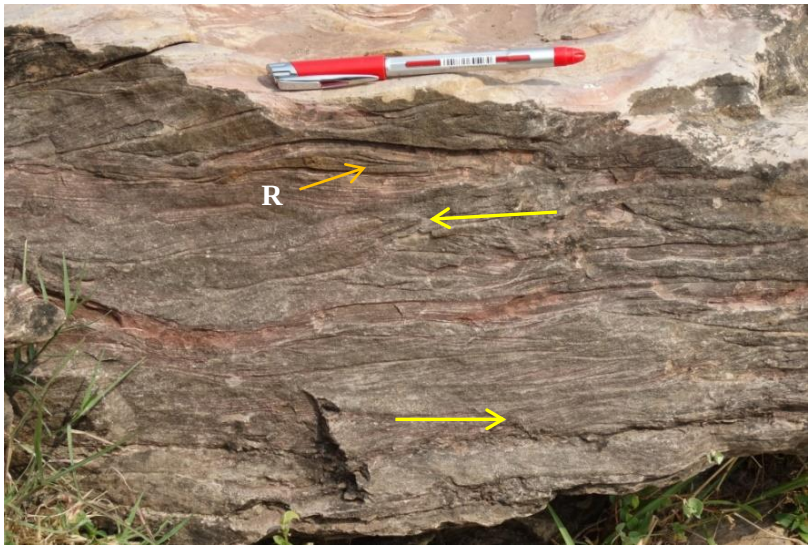

Figure: 4.7. Field photograph of wave reworked tidal bundles along with bi-directional cross-strata and reactivation surface (R). Length of the pen is 14.5 cm.

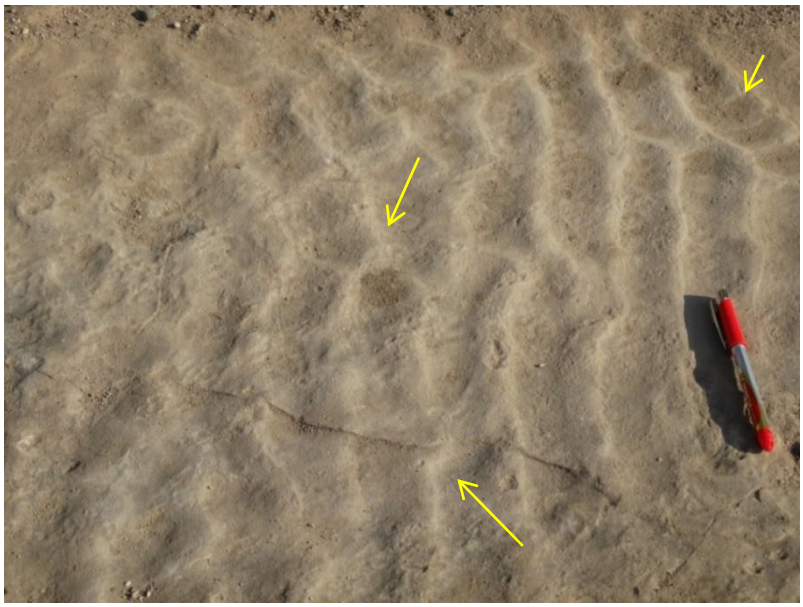

Figure: 4.8. Field photograph of wave ripples with sinuous and bi-furcated (arrows) crest lines. Length of the pen is 14.5 cm.

4.5. Significance of wave-generated sedimentary structures in the study area

Presence of symmetrical ripples with tuning fork-like bifurcations of crest lines and development of bundled cross-laminations are characteristic of wave generated bedforms (Boggs, 2012). Wave generated tidal bundles along with bi-directional cross-strata, and reactivation surface signify an interaction between tide-wave energies. Wave reworked tidal structures are dominant mainly towards eastern and central part of the study area. Symmetrical

ripple marks with some sinuosity in their crest lines indicates migration of bedforms under the influence of tidal current drag during settling time. Small scale symmetrical wave ripples with flat-top within the Nimar sandstone indicate a very shallow water conditions and deposition above wave-base (Bhattacharya and Jha, 2014). Presence of wavy lamination within cross-stratified sandstone indicates fluctuation from unidirectional current to oscillatory flow during their deposition (Bhattacharya and Bhattacharya, 2006, 2010). Draping of wavy lamination on a cross-stratified bed is a product of a shallow protected coastal area; an estuarine condition (Yang et al., 2008). However, the intensity of wave-generated bedforms (symmetrical ripples, ladder back ripples, flat-topped ripples, chevron up building structures) increases towards the western part of the study area, which indicates the prevalence of more wave-dominated open marine conditions.

4.6. Discussion

Tidalites, tidal rhythmites, and associated wave-reworked tidal features are dominated within FA-4 and FA-5 in the middle-upper part of the succession. The lower part of the tide dominated fluvio-tidal facies association (FA-4) is the product of an intertidal flat setting whereas the upper part of FA-4 (bioturbated sandstone facies, green sandstone facies) and shore facies association (FA-5) interpreted as deposited in lower intertidal to the subtidal condition. In the various studied successions of Nimar Sandstone repetition of such facies types (sand dominated and mud dominated) indicates rapid fluctuation between subtidal-intertidal-subtidal settings. The dominance of tidal structures in the middle part of the succession followed by wave generated bedforms towards the up section suggests gradually increases in wave energy over the tide. In the middle part, well preservation of tidal structures also suggests that deposition was going to a protected area (sheltered estuary condition) where wave influence was low. Laterally accreted tidal bundles, bi-directional cross-strata, vertically accreted cross-strata, sigmoidal cross-strata, inclined heterolithic cross-strata are the major tidal features in the Nimar Sandstone along with wave reworked tidal bundles, symmetrical ripples. Preservation of both tidal and wave features in the study area is gradational both in spatio-temporal direction. From the eastern to western part of the study area dominance of wave generated structures increases. Well preservation of tide-generated structure in the eastern and central part of the study area indicates restricted/sheltered marine condition whereas in the western part deposition was going on open marine condition. Sequential gradation of tide to wave generated structures towards the up section bears the evidence of a shift in depositional condition from intertidal to subtidal to open marine setting.

4.7. Summary

- All the tide and wave generated primary structures are mainly confined within the FA-4 and lower part of the FA-5.
- Tide generated structures like lenticular bedding, wavy bedding, inclined heterolithic structures are the product of inter-tidal flat setting.
- Ripple laminated bi-directional cross-strata and sigmoidal cross-strata indicates a sub-tidal setting.
- Preservation of the more tidal structures along with wave reworking more towards the eastern and central portion of the study area indicates deposition took place in a sheltered estuary condition where tidal structures are protected from wave energy.
- The dominance of wave generated structure more towards the up section of successions and western part of the study area indicates an open marine coastal condition.
- Both the tide and wave generated primary structures along with the fluvial deposit at the lower portion with finning up a succession of the Nimar Sandstone signifies, a fluvial-to marine transitional sedimentation for the studied area under an estuary setting.

CHAPTER- 5

Ichnology

5.1. Introduction

Ichnology has been used to interpret palaeoenvironments, palaeodepositional settings and palaeoclimatic condition. Palaeodepositional interpretations are generally based on the diversity, intensity, distribution of ichnoforms and their assemblages in a sedimentary deposit. For example, the Skolithos ichnofacies (Pemberton et al., 1992) interbedded with hummocky cross-stratified sandstone shows an extremely close association with proximal offshore depositional environments (Frey and Pemberton, 1984; Howard and Frey, 1984; Frey, 1990; MacEachern and Pemberton, 1992; Pemberton and MacEachern, 1997; Bromley and Uchman, 2003; Bann et al., 2004). Similarly, planar-laminated structure in association with local bioturbation of Nereites ichnofacies along with sporadic occurrences of the Cruziana ichnofacies (Pemberton et al., 1992) indicates influence of turbidity current in the depositional setting (Crimes et al., 1974). As stated by Seilacher (1953) an ichnofacies is a "recurring association of trace fossils through the Phanerozoic on a global scale and it is meant for sedimentary facies and the interpreted depositional environment". Along with the term ichnofacies, "ichnofabric" is also associated commonly in ichnology. Ichnofabric was first described by Ekdale and Bromley (1983) as "that aspect of sediments texture and internal structure that arises from bioturbation and bioerosion at all scales related to the level of biological input". Several factors can control the pattern of ichnofabric like the rate of bioturbation, sedimentation rate and the composition of the substrate. Gingras et al. (2012) pointed that, ichnological data can provide more reliable interpretation when used with other sedimentological data for a particular depositional setting, as certain ichnofacies point to a particular set of depositional condition. So an ichnofacies study is a combination of the study of ichnotypes, ichnofabric and ichnoassemblages and the palaeoenviromental history.

This chapter includes, detailed description of various ichnoforms, ichnoassemblage and interpretation of the dominant controlling factors in terms of the palaeoecology and palaeodepositional environment of the Nimar Sandstone. Tide-dominated fluvio-tidal facies association (FA-4) and shore facies association (FA-5) are the main hosts for ichnoforms

within the Nimar Sandstone. Within the FA-4 and FA-5 sandstone-mudstone heterolithic facies (4A) plane laminated sandstone facies (4C), bioturbated sandstone facies (4D) and *Thalassinoides –Ophiomorpha* bearing thinly laminated sandstone-mudstone facies (5B) are the major facies types enriched with various ichnoforms. Overall bioturbation diversity in the study area is low and the intensity of the bioturbation is more in the western part with respect to the central and eastern part of the study area.

5.2. Methodology and Material

Field based systematic ichnological data were acquired from fifteen outcrop locations of which four outcrops show abundant trace fossils in the study area. The major four outcrops are distributed in Chikapoti, Rampura, Akhara and Sitapuri, area respectively (location 2, 6,5 and 15in figure 2.4). Detailed study of the trace fossils in terms of ichnodiversity, bioturbation intensity; ichnoassemblages and palaeodepositional conditions are described from the Nimar Sandstone. The ichnoassemblages of the various trace fossils was defined based on variations in substrate type, the taxonomic affinity of trace fossils and palaeoenviromental controls. Field observations and field photographs are used to describe the ichnofossils and the ichnoassemblages from the study area, accompanied by polished slabs for detailed study of the internal morphology of various ichnoforms. Identification of the ichnoforms is made up to the genus level.

5.3. Ichnoforms

Total fourteen ichnoforms (Table 5.1) are identified from the study area namely, *Arenicolites* isp., *Asterosoma* isp., *Balanoglossites* isp., *Laevicyclus* isp., *Monocraterion* isp., *Ophiomorpha* isp., *Palaeophycus* isp., *Planolites* isp., *Rosselia* isp., *Scalarituba* isp., *Skolithos* isp., *Spongeliomorpha* isp., *Taenidium* isp. and *Thalassinoides* isp. Systematic descriptions of different ichnogenus are given below (in alphabetical order).

5.3.1. *Arenicolites* isp. (Figure 5.1)

Description: *Arenicolites* is represented by a pair of circular aperture on the sandstone bedding surface. In vertical section, this ichnofossil is represented by two closely placed limbs of a continuous J-shaped or U-shaped tube. Burrows are endichnial, full relieved, vertical in nature.

Size: The diameter of the burrows aperture varies from 0.3 to 0.6 cm and the average gap is ~1cm.

Substrate: Medium to fine-grained sandstone of the bioturbated Sandstone facies (4D) and sandstone-mudstone heterolithic facies (4A).

Associations: *Skolithos* isp., *Spongeliomorpha* isp., *Ophimorpha* isp., and *Thalassinoides* isp.

Remarks: *Arenicolites* isp. is considered as dwelling trace of suspension feeding organism (Bromley,1996). *Arenicolites salter* is interpreted as both dwelling and feeding burrow of suspension feeding annelids (Hakes, 1976) or small crustaceans (Goldring, 1962). *Arenicolites* can occur in different environments like eolian, marine, freshwater lacustrine and fluvial (Eagar et al., 1985). According to Crimes (1977), *Arenicolites* are typical of a shallow marine setting where sufficient oxygen circulation is present.

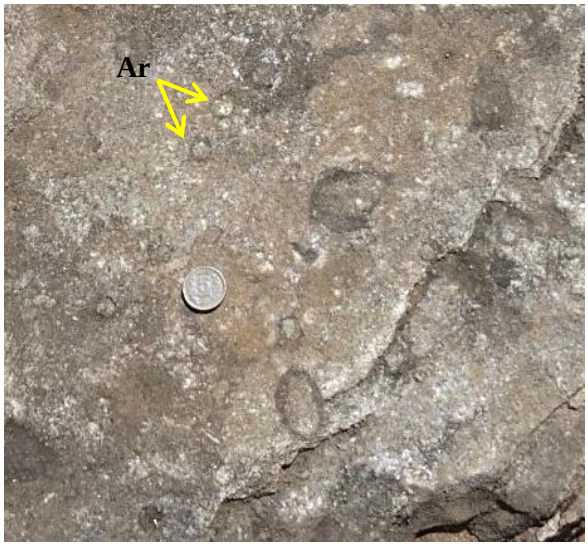

Figure: 5.1. Field photograph of *Arenicolites* isp. (Ar) on the bedding surface of sandstone-mudstone heterolithic facies (4A).The diameter of the coin is 2.3 cm.

5.3.2. Asterosoma isp. (Figure 5.2)

Description: Horizontal and sub-horizontal bulbs arranged radially or in a fan-like manner. The filling of the bulbs comprises concentrically laminated sediments enclosing a central to subcentral tube. The concentric structures are composed of mud and very fine-grained sand. The intersection of bulbs is commonly observed in cross-section.

Size: Average bulb diameter is 5.84 cm and the maximum length of the bulb is ~10.32 cm.

Substrate: Preserved as full relief on sandstone bed of the bioturbated sandstone facies (4D).

Association: *Rosselia* isp., *Spongeliomorpha* isp., *Ophiomorpha isp*., and *Thalassinoides* isp.

Remarks: Lower Palaeozoic *Astresoma* has occurred in several different environments (Seilacher and Meischner, 1964) but it is most common in shallow marine setting **(**Bromley and Uchman, 2003). It is an opportunistic trace fossil in a shallow marine setting especially in tidal flat environments (Chamberlain, 1978). It has been described as constituents of several ichnofabric. Howell et al. (1996) distinguished Jurassic *Asterosoma* ichnofabric, dominated by *Asterosoma* and *Teichichnus* typical of a restricted environment like sheltered estuary or lagoonal setting.

Figure: 5.2. Field photograph of *Asterosoma* isp. (As) on the sandstone bedding surface in the bioturbated sandstone facies (4D).The diameter of the coin is 2.3 cm.

5.3.3. Balanoglossites isp. (Figure 5.3)

Description: This ichnoform is charaterzied by bedding-plane parallel burrows, burrow wall is absent, and have same general morphology with ichnogenus *Thalassinoides.* They are most abundant in the Bagh cave section.They are straight to slightly sinuous, burrows fill material is similar to the host rock. Burrows are irregular, simple or branched with constrictions and rare narrower blind branches. Burrows are unlined with sharp margins. They were found mainly on the lower bedding surfaces of the sandstone-mudstone heterolithic facies (4A) and preserved as natural casts or infills.

Size: This ichnoform has a maximum width of 10-15mm and length varies from 1-1.2 cm.

Substrate: Fine grain sandstone, mudstone of sandstone-mudstone heterolithic facies (4A).

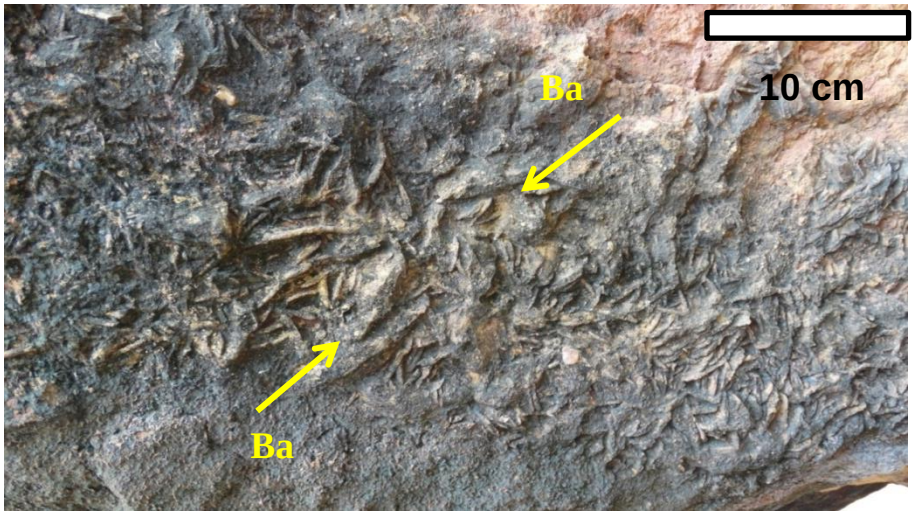

Figure: 5.3. Field photograph of *Balanoglossites* isp (Ba), preserved on sandstone sole surface of the sandstone-mudstone heterolithic facies (4A).

Associations: *Skolithos* isp. *Ophimorpha* isp., and *Thalassinoides* isp.

Remarks: The ichnogenus *Balanoglossites* is a relatively complex trace fossil. It comprises of U- or Y-shaped tunnels connected by shafts that record both burrowing and boring trace-maker action (Knaust, 2008). The unlined, sharp boundaries of the burrows indicates that they were made in firm sediment (probably microbially stabilized). Kaźmierczak & Pszczółkowski (1969) stated that, *Balanoglossites* was produced by annelids and enteropneusts. Patel & Desai

(2009) reported grouped funnel burrows similar to *Balanoglossites* which indicates the intertidal zone of a lagoonal or estuary setting.

5.3.4. Laevicyclus isp. (Figure 5.4)

Description: This ichnoforms is characterized by a central vertical stuff surrounded by concentric scrapping circles. The outer ring is thick and prominent and encloses the inner tube. The outer ring sediments are coarser than the inner shaft fill, which appers distinct. Ichnoforms are mainly preserved as positive epirelief to hyporelief. The diameter of the burrow is constant throughout and infill material is different from the surrounding.

Size: The diameter of the vertical stuff is 1.67 cm and the total diameter including the scrapping circles is up to 2.67 cm.

Substrate: This burrow is present on the sandstone bedding surface of fine to medium grained sandstone of the ripple cross-stratified sandstone subfacies (4A1).

Association: *Planolites* isp.

Figure: 5.4. Field photograph of *Laevicyclus* isp. (La) and *Planolites* isp. (Pl), preserved on sandstone bedding surface in the ripple cross-stratified sandstone subfacies (4A1). The diameter of the coin is 2.5 cm.

Remarks: Present specimen resembles well with *L. mongraensis* reported by Tiwari et al. (2011) from the Bhuban Formation of Mizoram. This species was originally described from Bagh bed, Gujarat (Chiplonkar and Badve, 1970). Subsequently, Badve and Ghare (1980) and Kundal and Sanganwar (1998) reported this ichnoforms from other exposures of Bagh Group and Patel et al. (2008) described these from the Jurassic of the Habo dome, Gujarat. *Laevicyclus* is comparable with feeding burrow of recent annelid Scolecolepis (Seilacher, 1953).

5.3.5. *Monocraterion* isp. (Figure 5.5)

Description: Vertical funnel structure (simple or multiple) penetrated by a central straight or slightly curved (unbranched), plugged tube. Vertical shaft is surrounded by concentric rings, which are filled by different material from the host rock.

Size: The diameter of the stuff is 1.66 cm and the total diameter of the burrow is 3 cm.

Substrate: Wave ripples bearing sandstone facies (5C).

Associations: *Skolithos* isp.

Remarks: Frey and Howard (1985) suggested that *Monocraterion* should be viewed as an ichnospecies of Skolithos; however, multiple authors (e.g., Alpert, 1974; Fillion and Pickerill, 1990; Jensen, 1997) considered the funnel-shaped morphology as distinct and characteristic of a separate ichnogenus. Eroded specimens of *Monocraterion* may be diagnosed as specimens of *Skolithos*, while from upper bedding plane views, specimens may be diagnosed as *Rosselia* and/or *Laevicyclus* (Fillion and Pickerill, 1990; Jensen, 1997). It is a dwelling burrow formed by marine worms or worms, like organisms in shallow marine setting.

.

Figure: 5.5. Field photograph of *Monocraterion isp*. (Mn), preserve on the sandstone bedding surface of fine-grained sandstone of the wave ripples bearing sandstone facies (5C). The diameter of the coin is 2.5 cm.

5.3.6. *Ophiomorpha* isp. (Figure 5.6)

Description: This ichnogenus is represented by straight burrows. The lower portion of burrow is curved with distinct nodular lining. They can be either perpendicular or oblique to the bedding plane. The burrows are filled up with the same material as that of the substrate and have a circular cross-section on the bedding plane.

Size: The length of the burrow is ~2-3 cm and the diameter is 0.5 cm. On the bedding plane diameter of the circular part varies from ~1-1.3 cm.

Substrate: Medium-grained sandstone of the bioturbated Sandstone facies (4D).

Associations: *Spongeliomorpha* isp. and *Thalassinoides* isp.

Remarks: *Ophiomorpha* isp. burrows are interpreted as shaft morphologically and domichnia ethologically (Rotnicka, 2005; Tiwari et al., 2011; Mude et al., 2012). *Ophiomorpha* is probably formed by shrimp-like crustaceans maintaining a deep tier. The burrows are formed in fairly turbulent water condition (Seilacher, 2007).

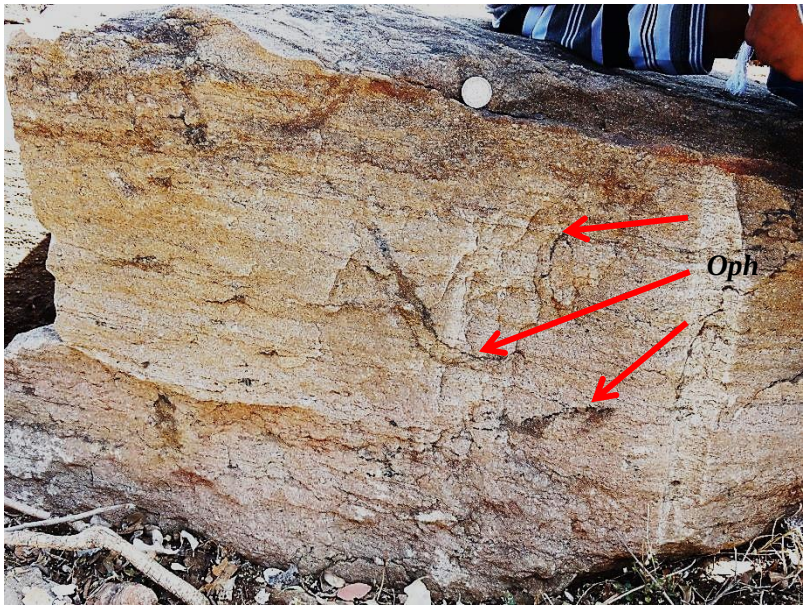

Figure: 5.6. Field photograph of *Ophiomorpha isp.* (Oph), preserved in the vertical section of the bioturbated sandstone facies (4D). The diameter of the coin is 2.3 cm.

5.3.7. *Palaeophycus* isp. (Figure 5.7)

Description: These are endichnial burrows with thick lining; smooth walls with structureless burrow fill similar to the host material. Certain burrows are present in full relief with thin lining. They are often unlined with ring-like structures arranged serially on the tubes (Tewari et al., 2011).

Size: The length of the burrow ranges from ~7.5-8 cm and the diameter varies from ~0.5-0.7cm.

Substrate: Medium grained sandstone of bioturbated sandstone facies (4D).

Association: *Ophiomorpha isp.* and *Thalassinoid isp.*

Remarks: *Palaeophycus* is a eury-benthic facies-crossing form produced probably by polychaetes or annelids (Pemberton & Frey 1982). Tunnels of *Palaeophycus* represents dwelling burrows of presumed predators and suspension feeders.

Figure:5.7 Field photograph of *Palaeophycus* isp. (Py), preserved on a section oblique to the bedding plane in bioturbated sandstone facies (4D) in the study area. The length of the pen is 14.5 cm.

5.3.8. Planolites isp. (Figure 5.4)

Description: Relatively large, smooth, straight to gently curve or undulose cylindrical burrows. Hyporelief, predominantly cylindrical, smooth walled, unlined, unbranched to rarely branched, near parallel to oblique to the bedding plane.

Size: Dimension varies from different burrow populations; length of burrow varies from 10 to 18 cm and diameter from 0.8 to 1.3 cm.

Substrate: Fine to medium-grained sandstone of ripple-cross laminated sandstone subfaceis (4A1).

Association: *Laevicyclus* isp.

Remarks: *Planolites* is generally regarded as belonging to fodinichnia/pascichnia ethological group and has been considered as a product of vermiform deposit feeder actively back-filling the burrow (Uchman, 1998). These occur in wide range of environment and are abundantly

found in middle shoreface to offshore siliciclastic deposits (Frey and Howard, 1985; Vossler and Pemberton, 1989).

5.3.9. Rosselia isp. (Figure 5.8)

Description: This ichnogenus is represented by a vertical or oblique orientation of burrows with bedding plane and made up of irregularly spaced alternations of dark and light concentric laminae (Figure 5.8A). Lamina is conical to irregularly bulbous concentric in nature. Vertical sections show elongated cone-shaped burrows. At places full cylindrical form of the burrow is preserved. The horizontal section presents as ovate or circular shape (Figure 5.8B) with a narrow mud or sand-filled central shaft.

Size: Average diameter of burrows varies from 2.47 cm to 5.5 cm, ranging maximum up to 16.6 cm. The average diameter of the central shaft with the concentric laminae is ~5.06 cm.

Figure: 5.8. A. Field photograph of *Rosselia isp.* (Ro), preserved on a section oblique to the bedding plane in the bioturbated sandstone facies (4D). **B.** Field photograph of *Rosselia isp. (*Ro) preserved on the bedding surface of the bioturbated Sandstone facies (4D). The diameter of the coin is 2.3 cm.

Substrate: Medium-grained sandstone of bioturbated sandstone facies (4D).

Association: *Astresoma isp.*

Remarks: Well-developed specimens of *Rosselia* are spindle-shaped, with conical forms resulted from erosional truncation. The ichnogenus *Rosselia* has been typically reported from shallow-marine deposits (Uchman and Krenmayr, 1995). Specimens of *Rosselia* are isolated or form crowded clusters. The isolated specimens show a vertical orientation in the fine-grained deposits of the lower shoreface, whereas an inclined orientation is typical in sandier tidal channel deposits (Howard and Frey, 1984).

5.2.10. Scalarituba isp. (Figure 5.9)

Description: These are subcylindrical, sinuous or straight burrows showing scalariform ridges. These are parallel or oblique to bedding and are often preserved as hypichnial, epichnial or semi-relief traces.

Size: Burrow diameter varies from 4-7 mm and length 4-8 cm.

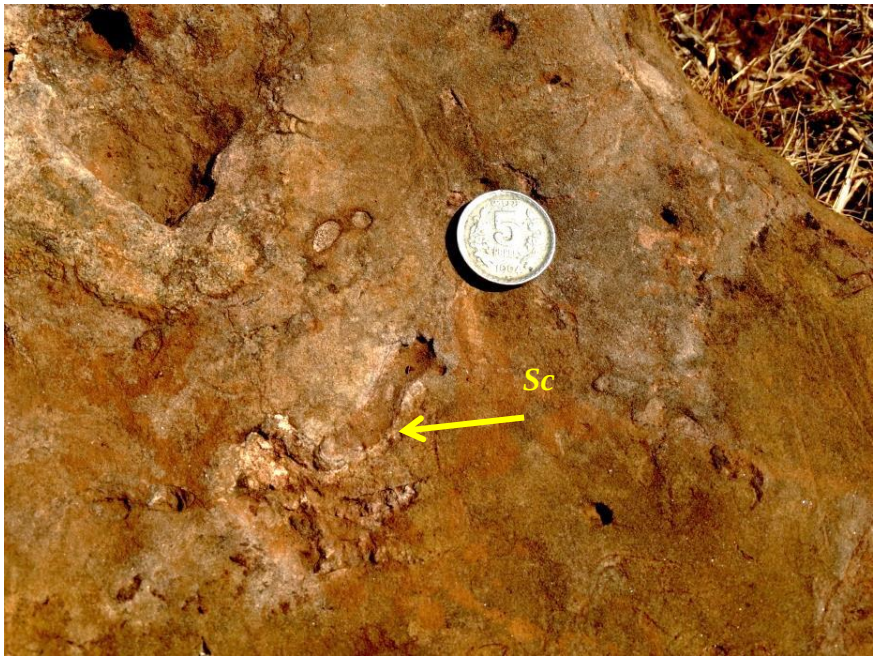

Figure: 5.9. Field photographs of *Scalarituba isp*. (Sc) on the sandstone bedding surface of wave ripples bearing sandstone facies (5C). The diameter of the coin is 2.3 cm.

Substrate: Fine to medium grained sandstone of wave ripples bearing sandstone facies (5C).

Associations: *Taenidium* isp., *Palaeophycus* isp.

Remarks: Scalarituba isp. is regarded as shallow-marine facies–transgressive ichnotaxa. These are interpreted as internal trails of sediment-eating worm or worm-like organisms (Henbest, 1960; Conkin and Conkin, 1968; Häntzschel, 1975)

5.3.11. Spongeliomorpha isp. (Figure 5.10)

Description: Burrow preserved as a full relief, cylindrical to subcylindrical and consisting of scratch-mark in the form of ridges and grooves; irregularly branched. Burrows are usually circular or oval in cross-section.

Size: Dimensions vary from different burrow populations; maximum length of the burrow is observed up to 24 cm and diameter varies from 2.3 cm to 3 cm.

Substrate: Coarse to medium grain sandstone of bioturbated sandstone facies (4D).

Association: *Ophiomorpha* isp. and *Thalassinoides* isp.

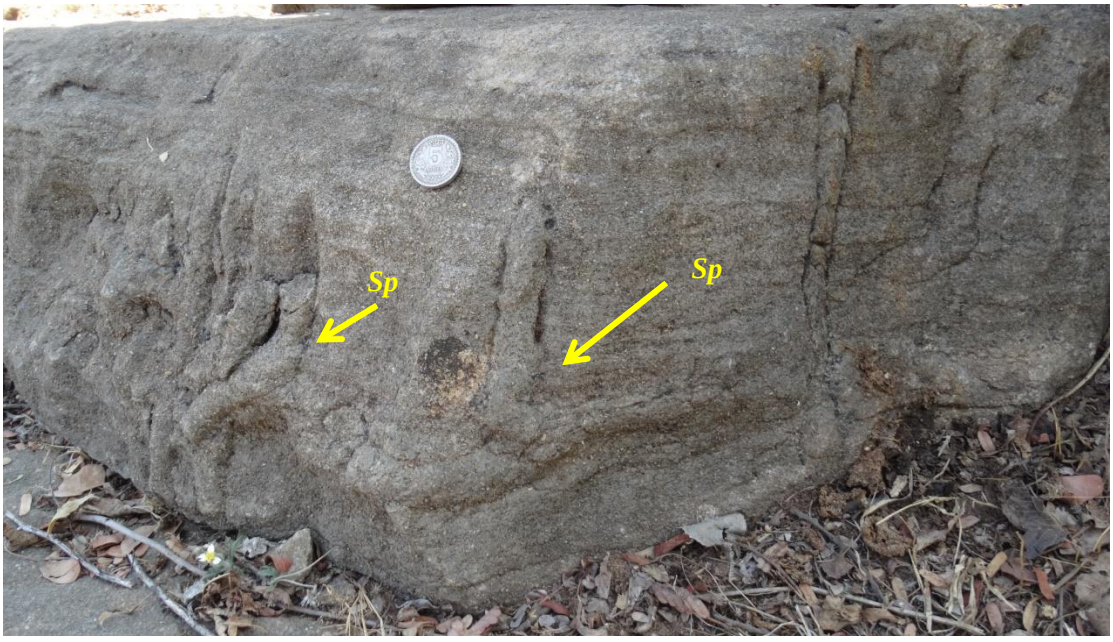

Figure: 5.10. Field photograph of *Spongeliomorpha* isp. (Sp) making 3-d network within vertical section of the bioturbated sandstone facies (4D). The diameter of the coin is 2.3 cm.

Remarks: They formed a 3D network within the coarse grain sandstone. It is considered as dwelling burrows of suspension feeding arthropods (Kennedy, 1967; Fürsich, 1973), and possibly polychaetes (Fürsich et al., 1981).

5.*3.12. Skolithos* isp. (Figure 5.11)

Description: Endichnial, full relief. Cylindrical to subcylindrical, unbranched vertical burrows with distinct or indistinct walls, circular in cross-section; closely crowded or isolated in nature. The burrow fill differs from the host sediment but is commonly filled with sand.

Size: The diameter of the burrows varies from 5mm to 18 mm and length varies from ~1.5- 4 cm.

Substrate: Mainly dominated within the coarse grain green sandstone facies (4E), medium to coarse-grained bioturbated sandstone facies (4D), also observed within the sandstone-mudstone interbedded facies (2A).

Association: *Thalassinoides* isp. and *Ophiomorpha* isp.

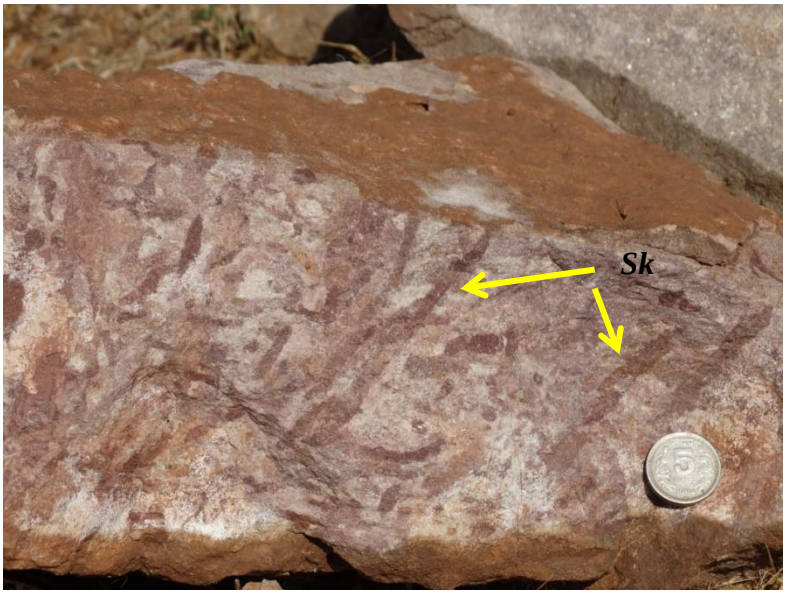

Figure: 5.11. Field photograph of *Skolithos isp*. (Sk) preserved in the vertical section of bioturbated sandstone facies (4D). The diameter of the coin is 2.3 cm.

Remarks: *Skolithos* is widely recognized in shallow intertidal deposits (Seilacher, 1967) and in various shallow marine environments (Alpert, 1974; Fillion and Pickerill, 1990). These are thought to be probably produced by annelids or phoronids (Alpert, 1974).

5.3.13. *Taenidium* isp. (Figure 5.12)

Description: Epichnial, concave epirelief; unbranched, cylindrical, horizontal, straight to gently curve with variable meandering, meniscate burrows. The burrow contains thick segmented fills articulated as well spaced symmetrical menisci; the distance between menisci is less than the burrow width. The burrow fill is identical to the host material.

Size: Lengths of the burrows are variable but diameters of the burrows are constant, and ranging between 3-5 mm.

Substrate: Sandstone of Bioturbated sandstone facies (4D).

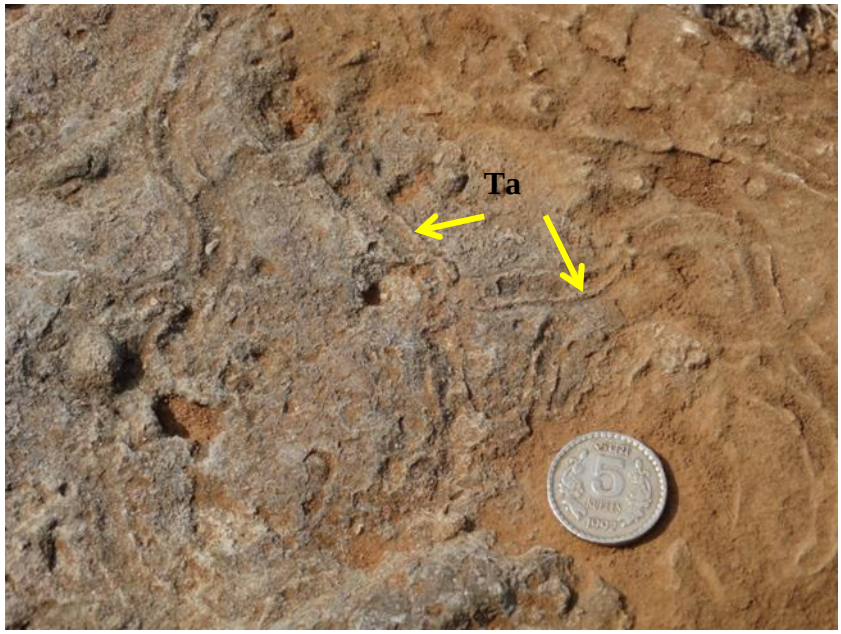

Figure: 5.12. Field photograph of *Taenidium* isp. (Ta), preserved on sandstone bedding surface of the bioturbated sandstone facies (4D). The diameter of the coin is 2.3 cm.

Association: *Thalassinoides* isp, and *Skolithos* isp.

Remarks: *Taenidium* has been reported from the flysch deposits (Heer, 1877), fluvial deposits (Fernandes and Carvalho, 2006).The cylindrical burrow exhibits typical periodic filling of the tunnel in the backward direction. They are mainly produced by annelid worms.

5.3.14. *Thalassinoides* isp. (Figure 5.13)

Description*:* Various forms of *Thalassinoides* are observed in the study area. Simple, vertical to inclined, branched burrows which normally show a swelling tendency at the point of bifurcation. In cross-sections, it is circular to subcircular in shape. The outer surface is smooth to granular. The filling material is fine-grained, reddish brown sandstone, similar to the host rock (Figure 5.13A). In some burrows, bifurcations are commonly T-shaped and also shows swelling at the junction (Figure 5.13B). At some places fillng material of burrows different from the host rock.

Size:. Length of branch varies from 11 to 15 cm and diameter varies from 3 to 4 cm.

Substrate: Sandstone-mudstone unit of *Thalassinoides-Ophiomorpha* bearing thinly laminated sandstone-mudstone facies (5B), bioturbated Sandstone facies (4D).

Association: *Thalassinoides* is the most abundant ichnoforms in the study area, commonly associated with *Skolithos* isp., *Ophiomorpha* isp., *Scalarituba* isp. and *Spongeliomorpha* isp.

Remarks: *Thalassinoides* is widely reported from the shallow to deep marine environments (Bromley and Frey, 1974; Demircan, 2008); however, nonmarine occurrences are also reported (Pollard 1988; Buatois and Mángano 2004). This ichnogenus is generally classified as a combination of dwelling and feeding structures, usually attributed to infaunal crustacean decapods probably Callianassids or similar arthropods (Frey et al., 1984; Bromley 1996; Ekdale and Bromley, 2003). *Thalassinoides* differs from *Ophiomorpha* by the lack of pellets on its walls. However, intergradations between the two genera are known to occur (Frey et al., 1978), and they constitute a typical example of compound traces (Bertling et al., 2006). *Thalassinoides* is a facies-crossing form most typical of the shallow marine environment (Frey et al., 1984).

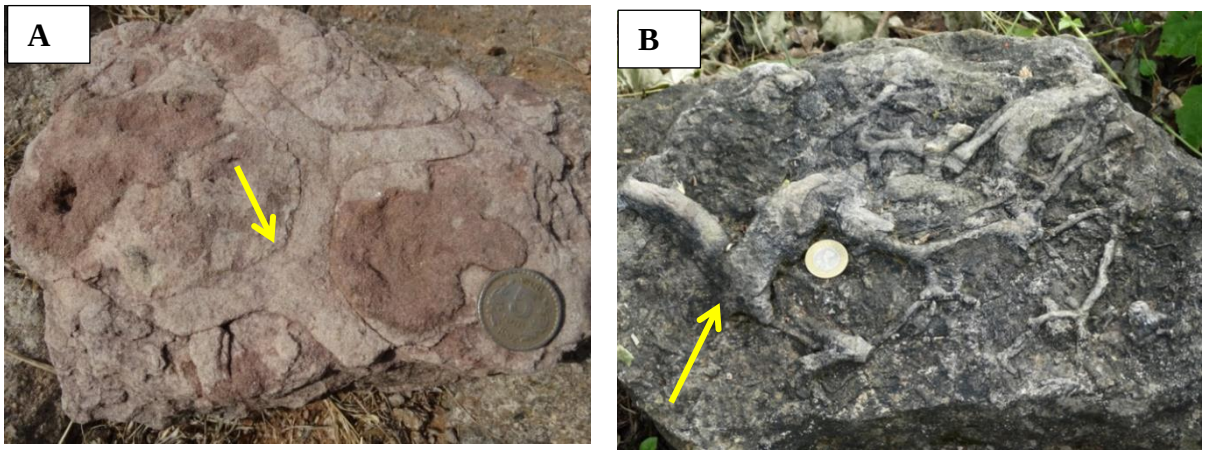

Figure: 5.13. A. Field photograph of *Thalassinoides* showing Y shaped bifurcations (arrow). **B.** Field photograph of *Thalassinoides* showing T shaped bifurcation (arrow). The diameter of the coin is 2.3 cm.

5.4. Ichnoassemblages

Ichnological interpretation of palaeodepositional environment mainly depends on the diversity, size, bioturbation intensity and distribution of the associated ichnofossil assemblages within the sediments (Gingras et al., 2011). Successions in the study area like Chikapoti, Rampura, Akhara and Sitapuri are mainly enriched with trace fossils (Figures 5.14, 5.15, 5.16, and 5.17). Based on the distribution and assemblages of different ichnoforms in distinct horizons of the studied successions, the ichnofossils are grouped under four ichnofacies – (i) mixed Skolithos-Glossifungites ichnofacies, (ii) mixed Cruziana-Glossifungites ichnofacies, (iii) Glossifungites ichnofacies and (iv) mixed Cruziana-Skolithos ichnofacies. The lower portion of the Nimar sandstone succession dominated by facies association: FA-1, which is barren in terms of trace fossils. Very few isolated *Skolithos* isp. are found within the FA-2 near Baria section. Sediments within the Tide-dominated fluvio-tidal facies association (FA-4) and the shore facies association (FA-5) is the main repository of ichnofossils.

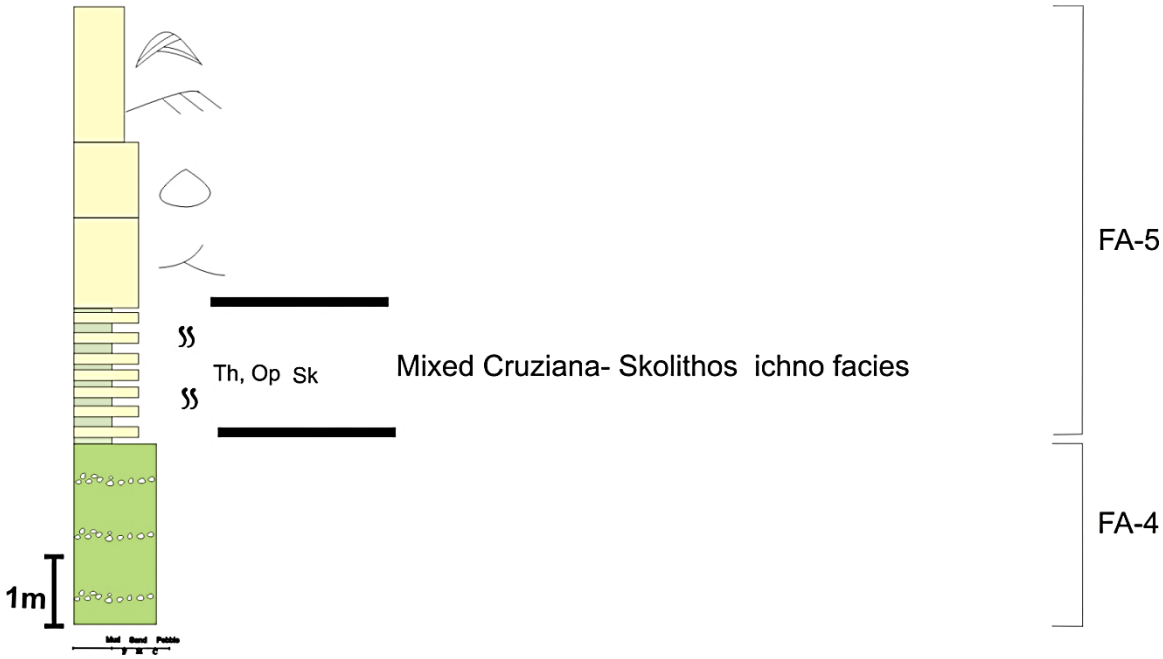

Figure: 5.14. Distribution of different trace fossils and ichnofacies type in the Chikapoti area.

Abbreviations (for Figures 5.14- 5.17)

Ar- *Arenicolites* isp., As- *Asterosoma* isp., Mo- *Monocraterion* isp., Op- *Ophiomorpha* isp.,Pl- *Planolites* isp., Py- *Palaeophycus* isp., Ro- *Rosselia* isp., Sc- *Scalarituba* isp., Sp- *Spongeliomorpha* isp., Sk- *Skolithos* isp., Th- *Thalassinoides* isp., Ta- *Taenidium* isp.

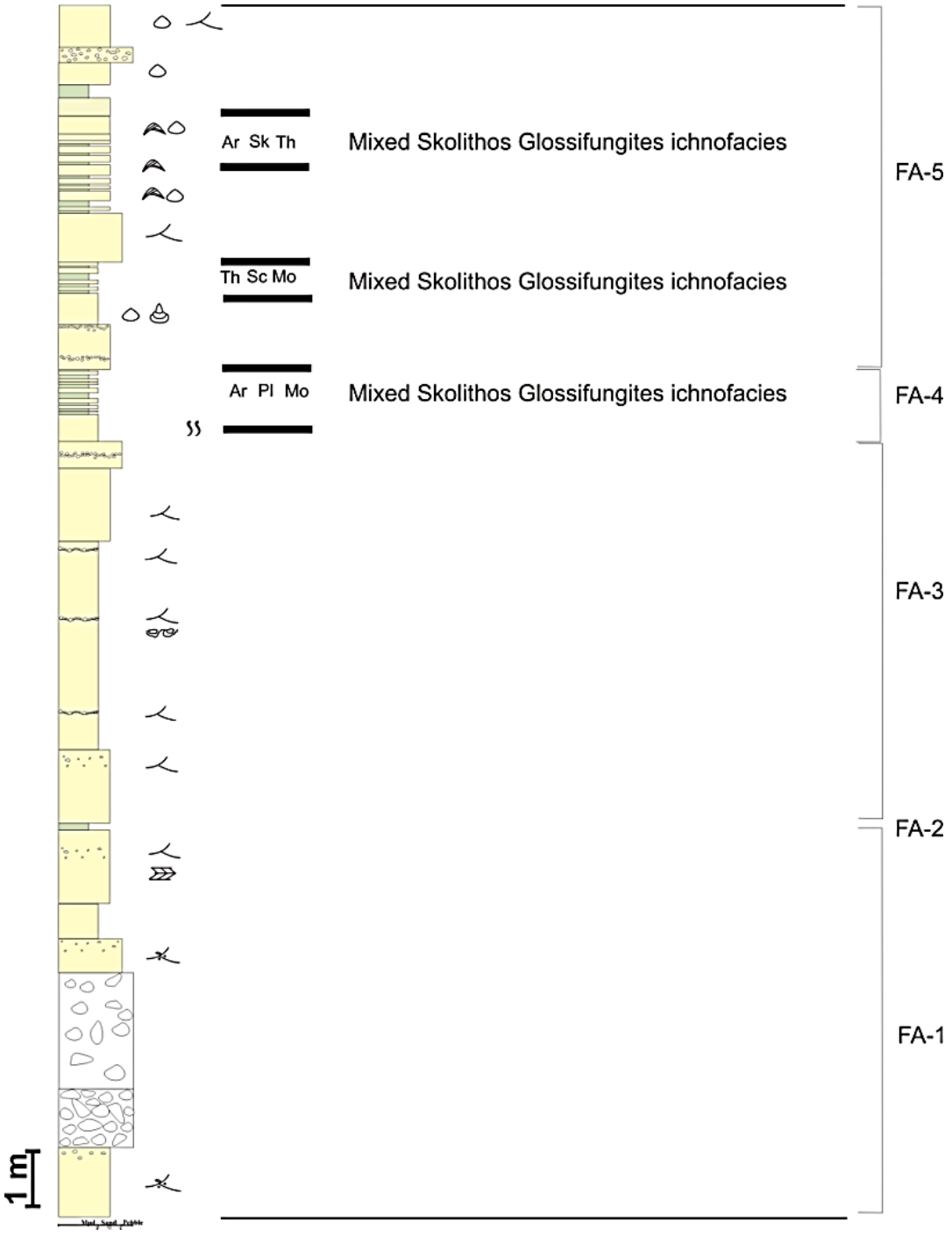

Figure: 5.15. Distribution of different trace fossils and ichnofacies types in the Rampura section.

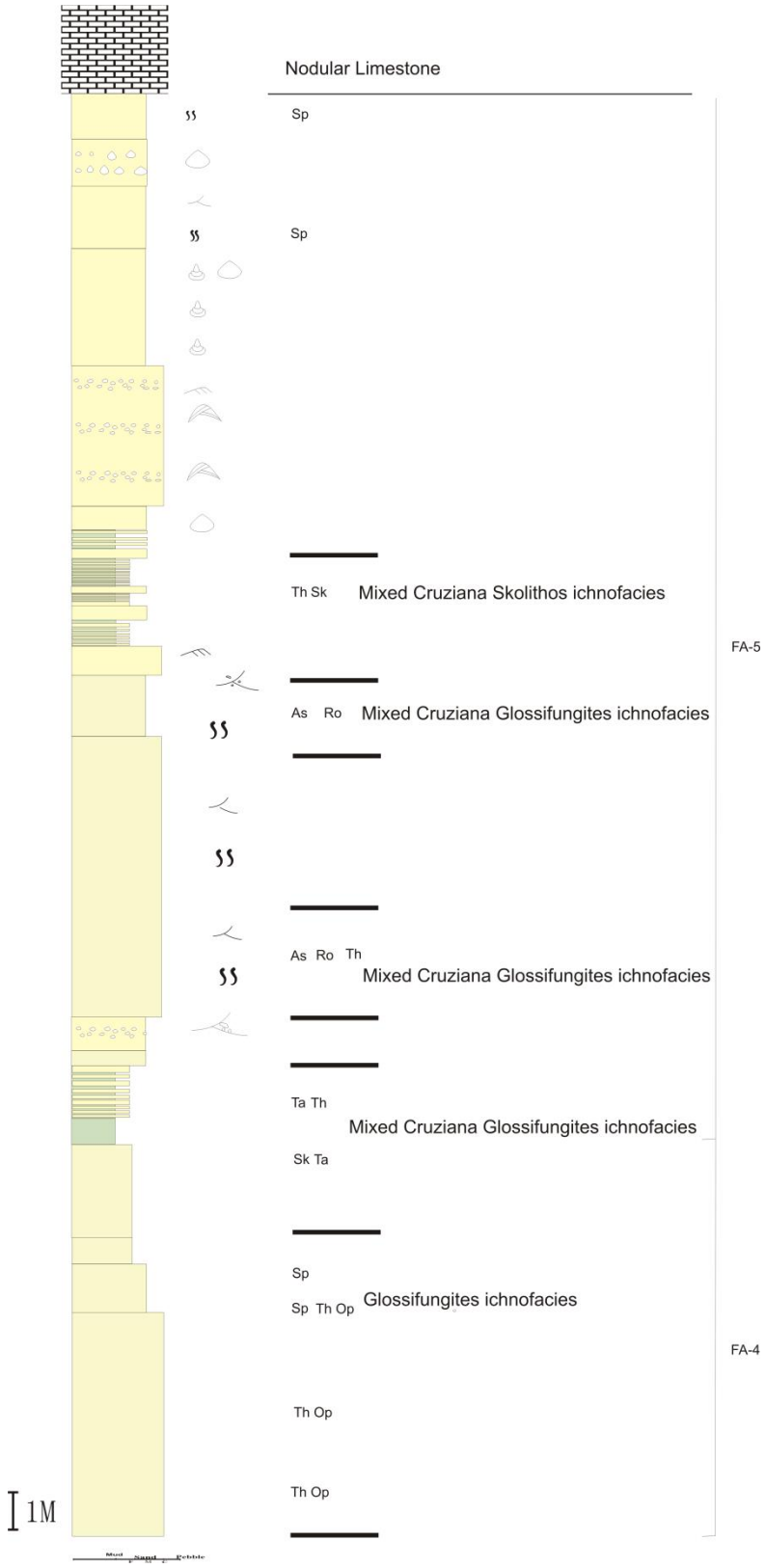

Figure: 5.16. Distribution of different trace fossils and ichnofacies types in the Akhara section.

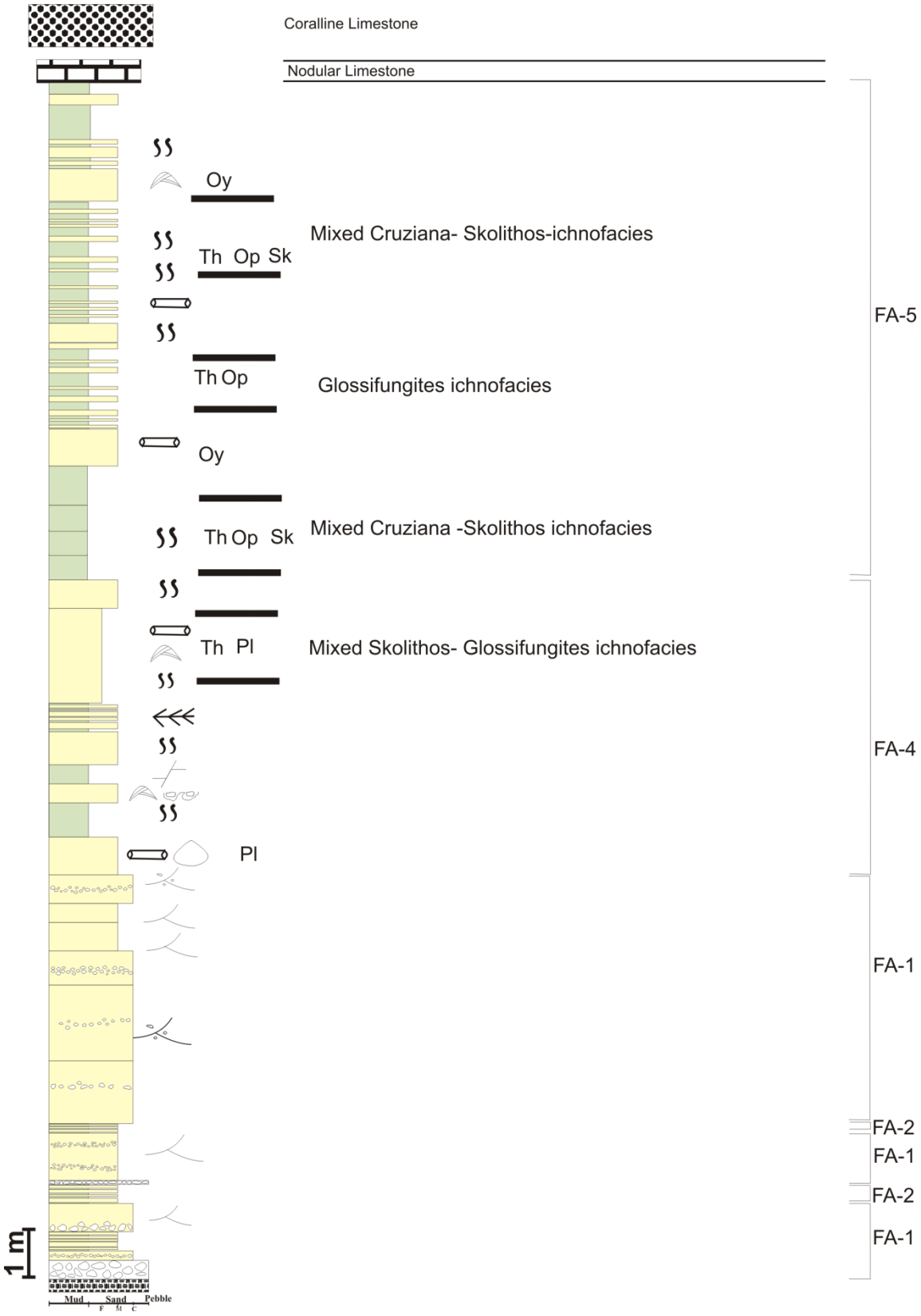

Figure: 5.17. Distribution of different trace fossils and ichnofacies types in the Sitapuri area.

Towards the up section bioturbated sandstone facies (4D) is the host for deposit feeding burrows along with few suspension feeders. The dominant trace fossils are *Rosselia* isp. and *Asterosoma* isp. , *Scalarituba* isp. and *Thalassinoides isp., Scalarituba isp*. and *Taenidium isp.*, along with some sporadic occurrences of *Planolites isp.*, and *Palaeophycus isp.* Bioturbation intensity of these assemblages is moderate which increases more towards the western part of the basin. Bioturbation intensity of *Rosselia-Asterosoma* assemblage is high and also diversified. Maximum bioturbation intensity observed near the Akhara area. All these assemblages correspond to mixed Cruziana-Glossifungites ichnofacies. Both the horizontal and vertical burrows are common in the study area. The central part of the basin shows dominance of horizontal burrow over vertical burrows. In the western part of the study area (Akhara, Jobat area) vertical burrows are more abundant.

Near Akhara, top part of the bioturbated sandstone facies (4D) comprises of 3D networks of *Spongeliomorpha* with *Ophiomorpha* and *Thalassinoides* assemblages. This assemblage has low diversity but high bioturbation intensity and is characterized by vertical branching burrows of suspension feeders. This trace fossil assemblage is characteristics of the Glossifungites ichnofacies.

Topmost part of the Nimar Sandstone succession, comprising of thick mudstone bed in alternation with thin sandstone bed, which is domicile for *Thalassinoides-Skolithos* assemblage. These trace fossil assemblage is characterized by large-scale vertical burrows of *Thalassinoides, Skolithos,* and *Ophiomorpha,* mainly observed in the Sitapuri section. This assemblage has high bioturbation intensity which destroyed the primary bedding. Association of deposit feeding burrows along with vertical domiciles of suspension feeders indicates a mixed Cruziana-Skolithos ichnofacies.

Table: 5.1. List of ichnofossil with trophic groups found in the different localities.

Ichnogenus	Trophic Group	Area/Localities
Arenicolites	Suspension feeder	Rampura, Akhara
Asterosoma	Deposit feeder	Akhara
Balanoglosite	Deposit feeder	Bagh
Laevicyclus	Suspension feeder	Rampura
Monocraterion	Suspension feeder	Rampura
Planolites	Deposit feeder	Rampura
Palaeophycus	Deposit feeder	Akhara
Ophiomorpha	Suspension feeder	Sitapuri, Bagh, Akhara
Rosselia	Deposit feeder	Akhara
Scalarituba	Deposit feeder	Rampura
Spongeliomorpha	Suspension feeder	Akhara
Skolithos	Suspension feeder	Sitapuri, Akhara, Chikapoti
Taenidium	Deposit feeder	Akhara
Thalassinoides	Deposit feeder	Sitapuri, Bagh, Rampura, Akhara

5.5. Discussion

Seilacher (1967) suggested that suspension feeders are mainly found at nearshore condition whereas deposit feeders in offshore based on the food availability. The suspension feeding organism may also be excluded from deeper waters due to decreasing concentration of dissolved oxygen, whereas deposit feeding organisms are better adapted than the suspension feeders for exploiting reducing aqueous or sedimentary environment (Theede et al., 1969; Sarkar et al., 2009). So, both deposit feeders and suspension feeders can live in shallow as well as deeper water setting. Trace fossils of Nimar sandstone, as described in this chapter, belongs to both suspension feeder and deposit feeder types. Presence of both mixed Skolithos and Cruziana ichnofacies along with Glossifungites in the study area indicates a typical brackish

water estuarine condition (Pemberton and Wightman, 1992; MacEachern and Pemberton, 1994; Buatois and Mangano, 2002, 2004, Nagendra et al., 2010). Ichnofacies association of the studied area indicates strong influence of shallow marine depositional condition, predominantly under tidal activities.

Basal part of the Nimar Sandstone is dominated by the channel fill facies association (FA-1), which is devoid of any trace fossils. Absence of ichnoforms in the basal portion of the study area indicates high fluvial discharge. The overbank facies association (FA-2) which is a product of fluvial sedimentation (discussed in Chapter 3) comprises of *Skolithos* isp. Bioturbation intensity and diversity in this facies association are low, organism have low tolerance limit under fresh water condition (Sarkar and Chowdhury, 1992; Dashtgard et al., 2008). Towards the up section within tide-dominated fluvio-tidal facies association, increasing bioturbation intensity and diversity indicates fluctuation in depositional conditions in terms of energy, salinity, oxygen supply, and food supply. Presence of *Arenicolites* isp., *Balanoglosite* isp., *Monocraterion* isp., *Skolithos i*sp., *Thalassinoides* isp., *Laevicyclus i*sp., in association with various tidalites (discussed in Chapter 4) designates a change in salinity condition due to incursion of marine water. Abundance of more horizontal burrows in the middle portion of the succession near the central part of the studied area (Bagh, Rampura area) indicates a slow rate of sedimentation under intertidal flat setting. Near Akhara area presence of the ichnogenus, *Rosselia* isp., *Asterosoma* isp., *and Thalassinoides* isp. typically indicates shallow-marine depositional setting (Uchman and Krenmayr, 1995). According to Cotter (1973), an association of *Rosselia* isp., with *Asterosoma* isp., and *Thalassinoides* isp. indicates a lower foreshore to upper shoreface condition. So, probably the western part of the study area (Akhara, Jobat) is product of lower foreshore to upper shoreface depositional setting. The dominance of green sandstone facies (4E), wave ripples bearing sandstone facies (5C) in the western part also supported the ichnological interpretation of nearshore depositional setting. Presences of thick mudstone along with thin sandstone beds in the upper part of the Nimar Sandstone indicate gradually subsiding energy condition. *Thalassinoides-Ophiomorpha* bearing thinly laminated sandstone/mudstone facies (5B) over the wave ripples bearing sandstone facies (5C) with intense bioturbation indicates slow rate of suspension fall out under relatively low energy condition (below fair weather wave base).

Table: 5.2. Facies wise distribution of ichnofossils,ichnoassemblages and ichnofacies and their implication on depositional environment.

Facies Name and association	Ichnofossils	Ichno assemblages	Ichnofacies	Spatial Significance	Interpretation
Sandstone-mudstone interbedded facies (2A) FA-2	*Skolithos*	–	–	Very few vertical burrows are found mainly at Baghini Temple section and Dhursal section	Overbank deposit.
Sandstone-mudstone heterolithic facies (4A) FA-4	*Monocraterion, Planolites Arenicolites*	*Monocraterion – Planolites,*	Mixed Skolithos-Glossifungites	This ichnofacies is mainly observed in a central and western part of the studied area. Major localities are Rampura Akhara	Tidal setting intertidal to subtidal condition.
	Skolithos, Thalassinoides, Balanoglossites	*Skolithos - Thalassinoides*			
Bioturbated sandstone facies (4D) FA-4	*Rosselia, Asterosoma*	*Rosselia-Asterosoma*	Mixed Cruziana-Glossifungites	Akhara section	Intertidal to subtidal flat, dominantly subtidal
	Scalarituba, Thalassinoides	*Scalarituba-Thalassinoides*		Akhara section	Subtidal flat near shore condition of an estuary
	Scalarituba Teichichnus, Planolites	*Scalarituba-Teichichnus*			
	Spongeliomorpha, Ophiomorpha, Thalassinoides	*Spongeliomorpha-Thalassinoides*	Glossifungites ichnofacies		
Thalassinoides-Ophiomorpha bearing sandstone-mudstone heterolithic facies (5B) FA5	*Thalassinoides, Ophiomorpha, Skolithos*	*Thalassinoides - Skolithos*	Mixed – Cruziana-Skolithos ichnofacies	This facies appeared almost all the area at the topmost of the succession, dominantly near Sitapuri area (Eastern most part), and Akhara area	More marginal marine setting

Mixed Skolithos-Glossifungites ichnofacies, mixed Cruziana-Glossifungites ichnofacies, Glossifungites ichnofacies and mixed Cruziana-Skolithos ichnofacies in Nimar Sandstone succession indicates increasing marine influence with fluctuating energy condition. Overall low-diversity trace fossil suite in the Nimar Sandstone results from a low salinity condition, as well as fluctuating currents and sedimentation rates (Weimer et al. 1982). Presence of mixed ichnofacies, low ichno diversity, abundance of marine ichnoforms and dominance of infaunal organisms over epifaunal organisms along with bivalve and gastropod body fossils suggest an estuary setting for the study area. The detailed environmental setting of the study area based on the ichnological studies is given in the Table 5.2

5.6. Summary

- ✓ The late Cretaceous Nimar sandstone successions have low bioturbation diversity and low to medium bioturbation intensity, which gradually increase from eastern to the western part of the basin.
- ✓ Dominant ichnogeneus are *Arenicolites* isp., *Asterosoma* isp., *Balanoglossites* isp., *Laevicyclus* isp., *Monocraterion* isp., *Ophiomorpha* isp., *Palaeophycus* isp., *Planolites* isp., *Rosselia* isp., *Scalarituba* isp, *Skolithos* isp., *Spongeliomorpha* isp., *Taenidium* isp., *Thalassinoides* isp., producing both horizontal and vertical burrows.
- ✓ Presence of both suspension feeders and deposit feeders indicated a mixed ichnofacies types. Four ichnofacies are identified based on the ichno assemblages- mixed Skolithos-Glossifungites ichnofacies, mixed Cruziana-Glossifungites ichnofacies, Glossifungites ichnofacies and mixed Cruziana-Skolithos ichnofacies,.
- ✓ The lower fluvial facies succession (dominantly FA-1) is devoid of any ichno fossils. The overbank deposits (FA-2) contain sporadic vertical burrows of *Skolithos* isp.
- ✓ The middle portion of the succession, dominant with both mixed Cruziana-Glossifungites ichnofacies and Glossifungites ichnofacies, signifies a middle estuarine setting under the tidal influence with fluctuating salinity.
- ✓ Intense bioturbation with both suspension and deposit feeding burrows within the sandstone-mudstone unit of facies 5B of FA-5 indicates a slow rate of suspension fall-out.

- ✓ Based on the ichno forms it is concluded that overall Nimar sedimentation took place in a fluvio-marine transitional condition under the influence of tide in an estuary setting.

CHAPTER-6

Soft sediment deformation structures

6.1. Introduction

Soft-sediment deformation occurs in unconsolidated sediment, prior to lithification during or shortly after deposition and close to the surface. The structures formed due to such deformation are known as soft-sediment deformation structures (SSDS). These are also identified as penecontemporaneous deformation, synsedimentary deformation, early-diagenetic deformation, pre-lithification deformation or contorted bedding by several authors (Maltman, 1984, 1994; Van Loon, 2009; Kundu et al., 2015; Roy and Banerjee, 2016). They are common in sand and sandstones that are loosely packed and rapidly deposited (Lowe, 1975; Maltman, 1994) and are formed due to liquefaction, fluidization or a combination of these processes (Lowe, 1975).

Fluidization is a process where upward-directed shear of fluid flowing through a porous medium counter acts the grain weight, and reducing the material strength (Lowe, 1976; Allen, 1982; Nichols et al., 1994; Frey et al., 2009). Liquefaction takes place when grain weight is temporarily transferred to the pore fluid through either the collapse of a loose grain packing or an increase in pore-fluid pressure (Lowe, 1976; Seed, 1979; Allen, 1982). The triggering factors, which control the deformation of soft or partly-consolidated sediment, can be ascribed to slope instability, to the loading of sediments and escape of water or to shaking of sediment due to seismic activity (Shanmngam, 2016, 2017). These different factors can often produce similar structures, but some characteristics can be extremely useful to understand the origin of sediment deformation (Moretti and Sabato, 2007). For the formation of a soft-sediment deformation structure, three criteria are needed simultaneous-

i. a driving force to deform primary sedimentary features,
ii. a deformation mechanism to enable the sediment to deform, and
iii. the trigger mechanism initiated by the action of some natural agent.

To identify the trigger of liquefaction two methodologies are followed: first, to demonstrate that liquefaction was the deformation mechanism; and, second, to determine the agent that triggered liquefaction. The SSDS can be formed due to various external forces like sudden

mass movement, unequal loading in adjacent layers of the sediment due to density difference, slump activity and gravity-driven density current and shaking of the earth surface by passing seismic waves during the earthquake and biological and chemical agents (Owen et al., 2011).

The beds or deposits bearing signatures of seismic activities are known as seismites (Seilacher, 1969, 1984). The term 'seismites' is used to describe association of soft-sediment deformation structures (SSDS) having varied geometry and following common diagnostic characters (Hilbert- Wolf et al., 2009) - (a) a strong association with faults as a potential trigger, (b) the observed deformation must be consistent with those having a known seismic origin, (c) a wide spread lateral continuity, (d) a gradual increase in intensity and frequency towards epicenter, (e) absence of any other trigger mechanisms, (f) vertical repetition of deformational layers and (g) the deformed layer bounded above and below by two undeformed beds (Seilacher, 1984; Seth et al., 1990; Cojan and Thiry, 1992; Owen, 1995; Sarkar et al., 1995; Obermeier, 1996; Mazumder et al., 2006; Van Loon, 2009; Owen et al., 2011; Moretti and Van Loon, 2014; Sarkar et al., 2014 and many others). Presence of seismites gives valuables ideas about basin dynamics, palaeoseismic activities, magnitude and intensity of the seismic activities (Obermeier, 1996; Rodríguez-Pascua et al., 2000).

In the study area various SSDS are recorded (Jha et al., 2017) from Nimar Sandstone. Sedimentation of the Nimar Sandstone was taken places within an ENE–WSW-trending Son-Narmada rift valley setting (Biswas, 1987). The major components of the Son-Narmada rift valley are two dominant east–west-trending–deep-seated faults, the Son-Narmada North Fault and the Son-Narmada South Fault (Figure. 1.1 B) (Biswas, 1987; Tewari et al., 2001) and several major lineaments. Three phases of reactivation of Son-Narmada rift setting were recorded at the different time period of the earth history (Tewari et al., 2001). Detailed tectonic set up of the study area is already discussed in chapter 2. In this chapter, we studied the various SSDS from Nimar Sandstone and described them with an attempt to identify and interpret the driving forces and the trigger mechanism.

6.2. SSDS in Nimar Sandstone

The major SSDS from Nimar Sandstone includes convolute laminae, load and flame structures, pseudonodules, slump structures, contorted beds, syn-sedimentary faults and sand dykes. They

are commonly concentrated within sandstone–mudstone heterolithic facies (4A) and large scale trough cross-stratified sandstone facies (3A). These SSDS-bearing beds recur in vertical intervals and are overlain and underlain by undeformed sedimentary beds. A detailed description of those SSDS and the trigger mechanisms are given below.

6.2.1. Convolute Laminations

Convolute laminations are characterized by sharp crests and board troughs, developed within sandstone beds of the sandstone-mudstone heterolithic facies (4A). Large scale convolutes (Figure 6.1) are preserved within the large scale trough cross-stratified sandstone facies (3A). Locally the crests are broad and partially truncated by overlying undeformed sandstone bed. Both the simple and complex type convolutes are preserved. Simple convolutes are regular and symmetrical (Figure 6.2A), with well-preserved internal laminae, whereas in the complex convolute laminae are wrinkled in nature (Figure 6.2B). Circular, semi-circular or crescent-shaped troughs of various sizes are common. The cores of larger troughs show complex deformation. Overlapping of the convolute with each other has made them more complex. Lamination within these convolutes are more compressed and thinner near the crest area than in the trough. The crest areas have been frequently penetrated by sand rich fluid injected from bottom, causing lateral truncation of the crests. The fluidal sand is carried upward along the escape channels and deposited at the top of the erosional plane. At places, small scale faults are also observed. Convolute laminae are displaced by these small scale faults. Faults die out both in upward and down directions. They are more common within the complex convolutes.

Figure: 6.1. Field photograph of simple convolute laminae (CL) within large scale trough cross-stratified sandstone facies (3A) along the Bagh River section. The length of the hammer is 30 cm.

Figure: 6.2. A. Field photograph of simple convolute laminae with truncated top preserved within sandstone-mudstone heterolithic facies (4A). **B.** Field photograph of the multi-lobed complex convolute structure in association with pseudonodules within the sandstone- mudstone heterolithic facies (4A). The Length of the pen is 14.5cm.

Interpretation

Development of the studied convolutes within restricted lithounit indicates the liquefaction process was restricted to a certain time. Such large scale convolutes with water escape structures indicate a release of enormous amount of pore fluid and reduction of shear strength of the sand unit due to sudden tremor. In the sandstone-mudstone heterolithic facies (4A) multiple lobed complex convolutes bears the signatures of multiple phases of deformation in short time span (Bhattacharya and Bandyopadhyay, 1998). Due to the truncation of the crest, internal laminae are inclined in nature. Presence of micro faults/ growth faults within the convolute laminae indicate a more intense deformation of brittle-ductile nature, possibly due to the presence of sufficient pore water within the sediment during deformation. Episodic

occurrence of convolute laminae, and bounded by undeformed beds indicate that the trigger mechanism was related to seismic activities (Cojan and Thiry, 1992).

6.2.2. Load and Flame Structure

Load and flame structures are characterized by tongue-shaped flames of mud or silty layer with loads of sand. Height and length of the flames vary from 6- 28 cm and 11 -31 cm, respectively. Tongue-shaped flames show abrupt truncation with overlying sandstone beds. Flames are commonly thick and broad at their apex but in some places, they are thin and sharp in nature (Figure 6.3). The sand load and associated flame structures appear as isolated features in certain beds. They are mostly developed within the sandstone-mudstone heterolithic facies (4A), with few present within the large scale trough cross-stratified sandstone facies (3A).

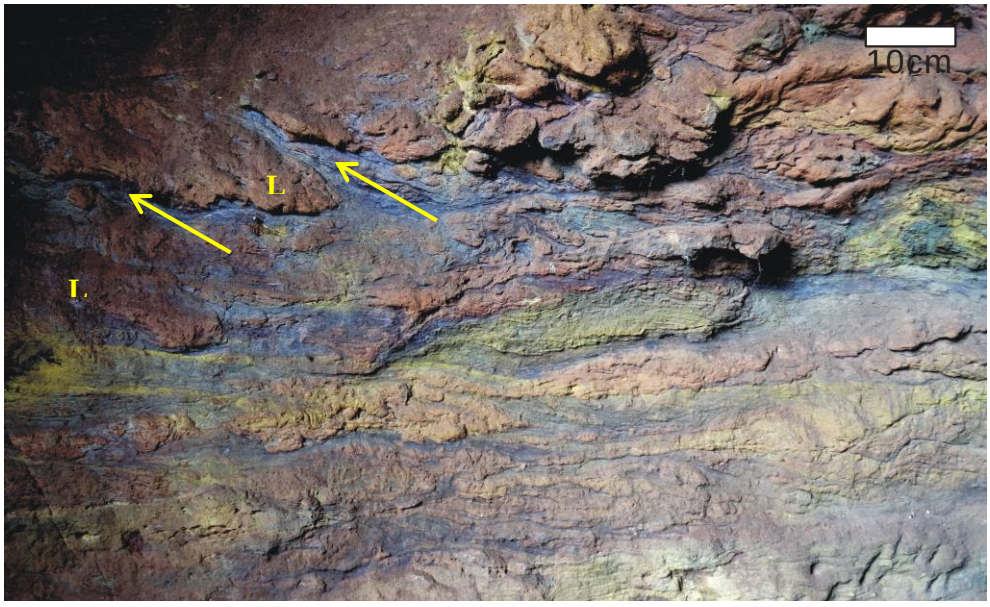

Figure: 6.3. Field photograph of load and flame structures showing loaded sand (L) within the mud and flames (marked by arrow).

Interpretation

Gravitational instability due to the density differences of liquefied unconsolidated sediment layers causes the formation of load and flame structure (Owen, 2003). Anketelle et al. (1970) stated that, when a higher density material (coarse to medium grained sandstone) overlies a lower density material (fine grained sandstone, siltstone/mudstone), a density contrast formed.

In such system due to liquefaction shear strength of the material is reduced and a gravitational readjustment occurs. Due to drastic reduction in shear strength of the liquefied sediment higher density beds collapse and relatively lower denser material starts to flow upward depending on relative dynamic viscosity contrast to produce load and flame structures (Alfaro et al., 1997). With increasing liquefaction at places continuity of the bed from the source strata breaks and detached and formed load of sandstone within mudstone in the study area. Such liquefaction process can be triggered by any mechanism such as loading, storm activity, mass movement or seismic shocks.

6.2.3. Slump Structure

A thick (~ 58cm) chaotic mixture of sandstone and mudstone layer was observed in the Bagh section within the sandstone-mudstone heterolithic facies (4A). This chaotic layer was bounded by two undeformed beds. Top part of this slump show intense loading of sandstone within mudstone (Figure 6.4). Small scales folding are present within slump structure. In some restricted portion of the slump convolute laminae is developed.

Interpretation

Such complex structure with high asymmetricity were generally developed under a hydroplastic condition of a quasi-liquid state (Chivelet et al., 2011). Restiction of the slump structure in between two undefromed beds indicates a certain time limit for the intense liquefaction. In the middle portion intensely deformed primary bedding indicates massive reduction of shear strenght due to high relase of pore fluid under liquefaction event. At the top part of the slump presence of load and flame stuctures indicates relatively lesser intensity of deformation. From bottom to top part intensity of the deformation was gradually decreasing. Downslope movement of semi-consolidated sediment over relatively more plastic layer under the influence of gravity is responsible for the formation of slump structures (Owen, 1987; Bose et al., 1997). Presence of small-scale folding and convolute lamination within the slump indicates a complex compressional setting.

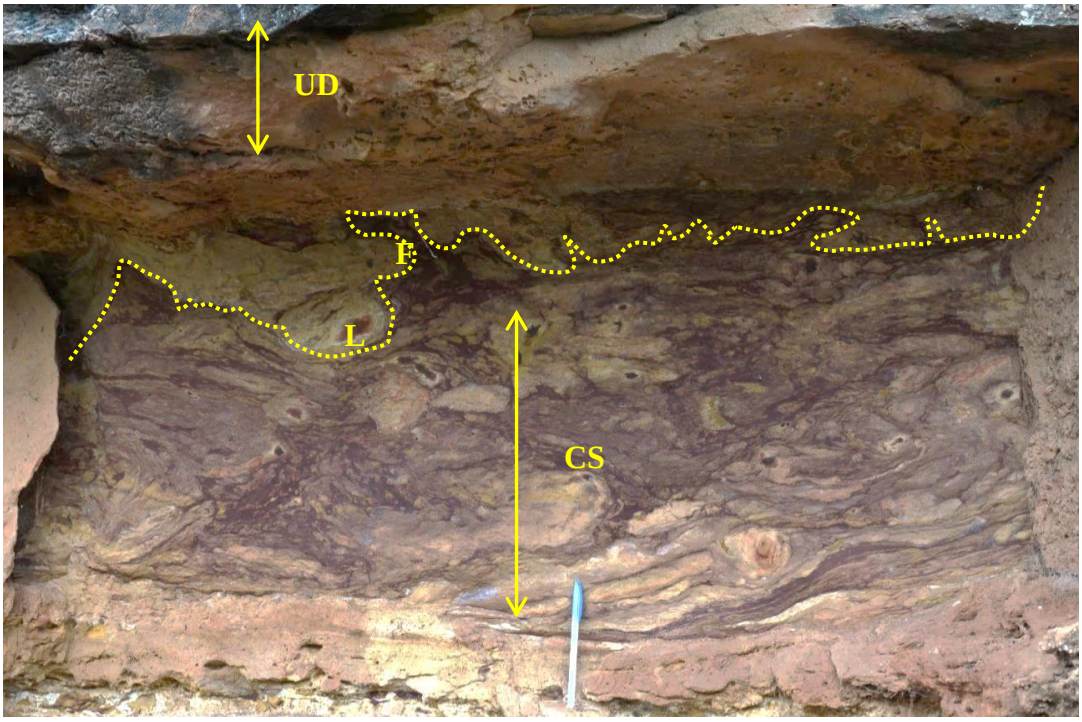

Figure: 6.4. Field photograph of complex clump structure (CS) within the heterolithic facies bounded by two undeformed beds (UD). At the top part load (L) and flame (F) structure developed. The length of the pen is 14.5 cm.

6.2.4. Contorted Bedding

This structure is represented by small scale contortions within the sandstone foresets of the large scale trough cross-stratified sandstone facies (3A). The maximum thickness of the individual bed is 19 cm and bounded by two undeformed beds. Contortions in each sandstone foresets are restricted in a particular part of the foresets (Figure 6.5).

Interpretation

Upward movement of liquefied unconsolidated sediment is responsible for the formation of such deposits. Due to sudden shock pore fluid pressure was released and the material started to move upward and formed interfacial cups between each foresets (Owen, 1995). Formation of the contorted bedding within the sandstone foresets in a particular direction indicates upward movement of fluidized sediment followed a specific pathway.

.Brenchley and Newall (1977) stated that, contorted beddings are generally related with a high rate of sedimentation, possibly associated with storm activity. However, he also stated that seismic activity related to fault movement of the underlying basement was equally important for the formation of contorted bedding. In the study area, no such evidences of storm activity were observed. Mazumder et al. (2006) stated that seismic shocks may also responsible for such upward movement of unconsolidated sediments.

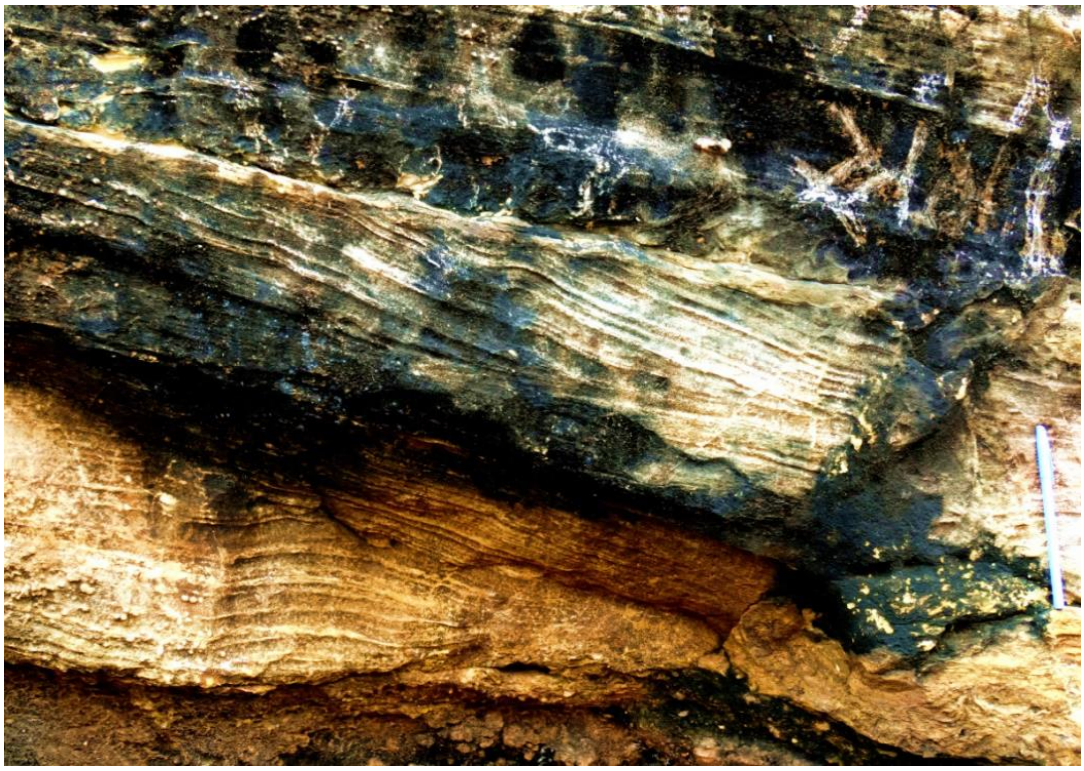

Figure: 6.5. Field photograph of contorted bedding developed within the large scale trough cross-stratified sandstone facies (3A). The length of the pen is 14.5 cm.

6.2.5. Synsedimentary fault

A few centimeters to meters long upward propagating syn-sedimentary faults constitute another important and abundant SSDS in the study area. They are mainly associated with the sandstone-mudstone laminae and show the displacements of the laminae (Figure 6.6A). The faults die out both in upward and downward directions. Locally, these faults show fault-propagating folds within the convolute (Figure 6.6B). In few places, injection of fluid along the fault plane formed sand dykes. Conjugate pair of such faults led to the formation of

downsagging graben-like structures (Figure 6.6C). The throw along these faults reaches maximum near the base and decreases upwards. They are generally small scale normal faults with 23-66 cm in length. These structures are mainly observed within the sandstone-mudstone heterolithic facies (4A), commonly bounded by undeformed beds. At places, these syn-sedimentary faults displaced the convolute laminae and made them more deformed in nature.

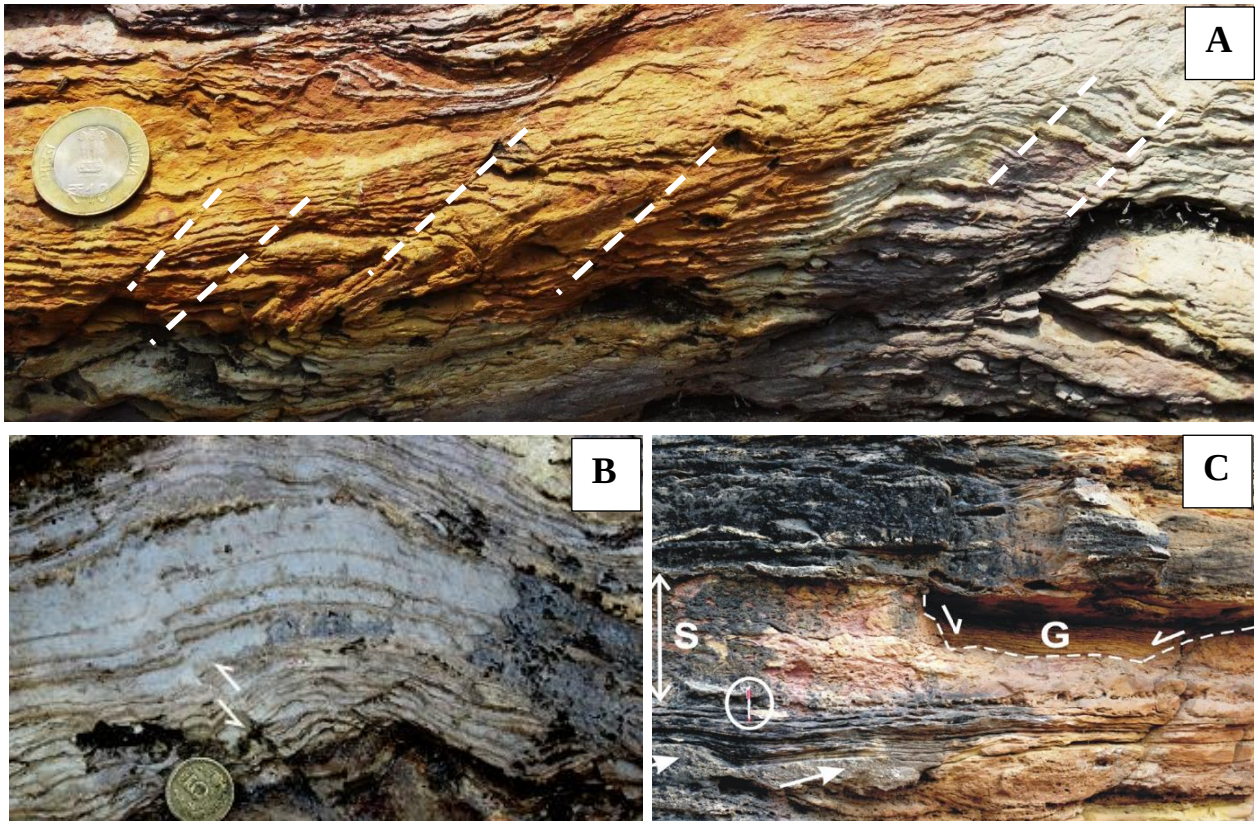

Figure: 6.6. A. Field photograph of multiple sets of syn-sedimentary faults (marked by dashed line) within sandstone-mudstone heterolithic facies. The diameter of the coin is 2.5 cm. **B.** Syn sedimentary faults developed within sandstone-mudstone heterolithic facies (4A). The diameter of the coin is 2.3 cm. **C**. Field photograph of fault-bounded graben-like downsagging structure (G) along with thick slump structure (S). The arrow shows presence of undeformed ripple bedforms below. Length of the pen (encircled) is 14.5 cm.

Interpretation

Both upward and downward truncation with an upward change in a throw indicates a growth fault of syn-sedimentary origin (Seliacher, 1969). Horizontal extension due to the repeated

loading of liquefied sediment by any vibratory motion is responsible for such graben-like downsagging (Ghosh, 1993). A gradual decrease in throw along the faults bounding the grabens indicates gradual waning of earthquake aftershock (Bhattacharya and Bandhopadhayay, 1998). Liquefaction along with fluidization is liable for the repetitive reactivation of the faults with sediment injection along the fault planes with an upward decrease of net throw (Bhattacharya and Bhattacharya, 2010). The truncation and displacement of the convolute laminae (discussed in section 6.2.1) by syn sedimentary faults bears the evidence of the relative time lag between formation of the faults and other deformed beds (convolute laminae).

6.2.6. Pseudonodules

Pseudonodules are represented by isolated elliptical, conical, spherical or elongated sandstone balls within the mudstone layers of the sandstone-mudstone heterolithic facies. Sandstone balls are massive in nature and laminae of the mudstone rotated against the boundary of these sand balls. Size of sandstone pseudonodules varies from 5–25cm. Larger pseudonodules often shows 'L'-shape (Figure 6.7) with form discordant internal laminae and parallel orientation of the long, basal axes with the lower boundary of the host mudstone bed.

Interpretation

Formation of pseudonodules is attributed to density contrast, due to repetitive liquefaction, loading and sagging during the deposition of sandstone over the mudstone bed (Kuenen, 1958). In such condition, more dense sandstone bed sank within the mudstone and created balls of different shapes and sizes. Development of pseudonodules within the mudstone bed indicates the quasi-liquid state of the mudstone bed after shaking (Elliot, 1965). The load induced deformation may be due to the fast rate of sediment accumulation (Ricci Lucchi, 1995). Formation of pseudonodules by the seismic origin has also been suggested by workers like Cojan and Thiry (1992), Rodríguez-Pascua et al. (2000).

Figure: 6.7. Field photograph of Pseudonodules, arrow indicates 'L' shape of the pseudonodules.

6.2.7. Sand dyke

Sand dykes are characterized by sand filling linear feature, which shows a discordant relationship with the bedding planes of the sandstone- mudstone heterolithic facies (4A) in the study area. They are straight in nature but in few places, they show a sinuous pattern. Length of the sand dyke varies from 5-11cm. Wrinkling of the laminae along the dykes is common (Figure 6.8).

Interpretation

Liquefied unconsolidated sediment injected across the sandstone- mudstone bed formed this type of structure. Intrusion of materials derived from some underlying source and its emplacement upwards under abnormal pressure along some fractures or cracks formed sand dykes (Montenat et al., 2007). In the study area liquefied sediment flow along the fault line and created a prominent displacement of the adjacent sand-mud layers. Presence of complex deformation structure like wrinkles of laminae near such discordant body indicates activation of the syn-sedimentary fault during the deposition of the sand dyke.

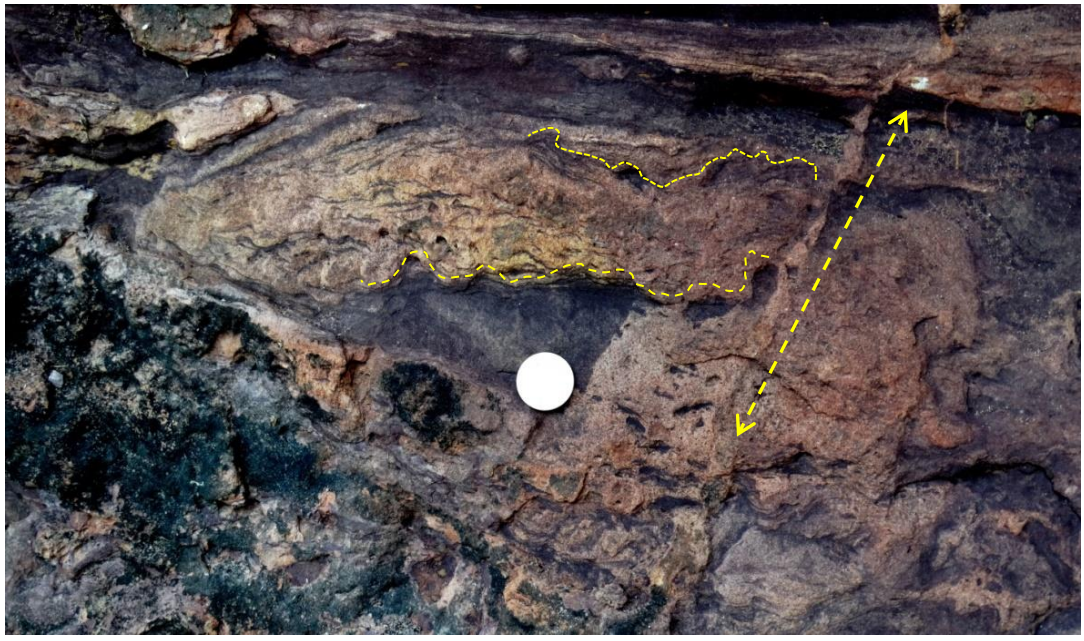

Figure: 6.8. Field photograph of injected sand dyke (marked with dashed arrow) within the heterolithic facies. Yellow dotted lines show the deformed laminae along with vertical dyke. The diameter of the coin is 2.5 cm.

6.3. Distribution of the SSDS in the study area

In the study area based on the occurrence of various SSDS at the different stratigraphic level, they are categorized into three associations (Jha et al., 2017) -

- Convolutes with pseudonodules and complex slump folds in successive sandstone-mudstone beds (Figures 6.2B, 6.9A, 6.10). This association mainly occurs in the Bagh area.
- Connotation of convolutes with thick water-escape columns cross-cutting these convolutes (Figures 6.9B, C) and is separated by undeformed beds of the sandstone–mudstone heterolithic facies.
- Multiple lobed complex convolutes in association with syn sedimentary faults (Figure 6.10) within thin sandstone–mudstone interbeds in both the Man river section and the Bagh area.

All these three associations occur at particular stratigraphic horizons, laterally persistent and are bounded by undeformed beds (Figures 6.9 A, B).

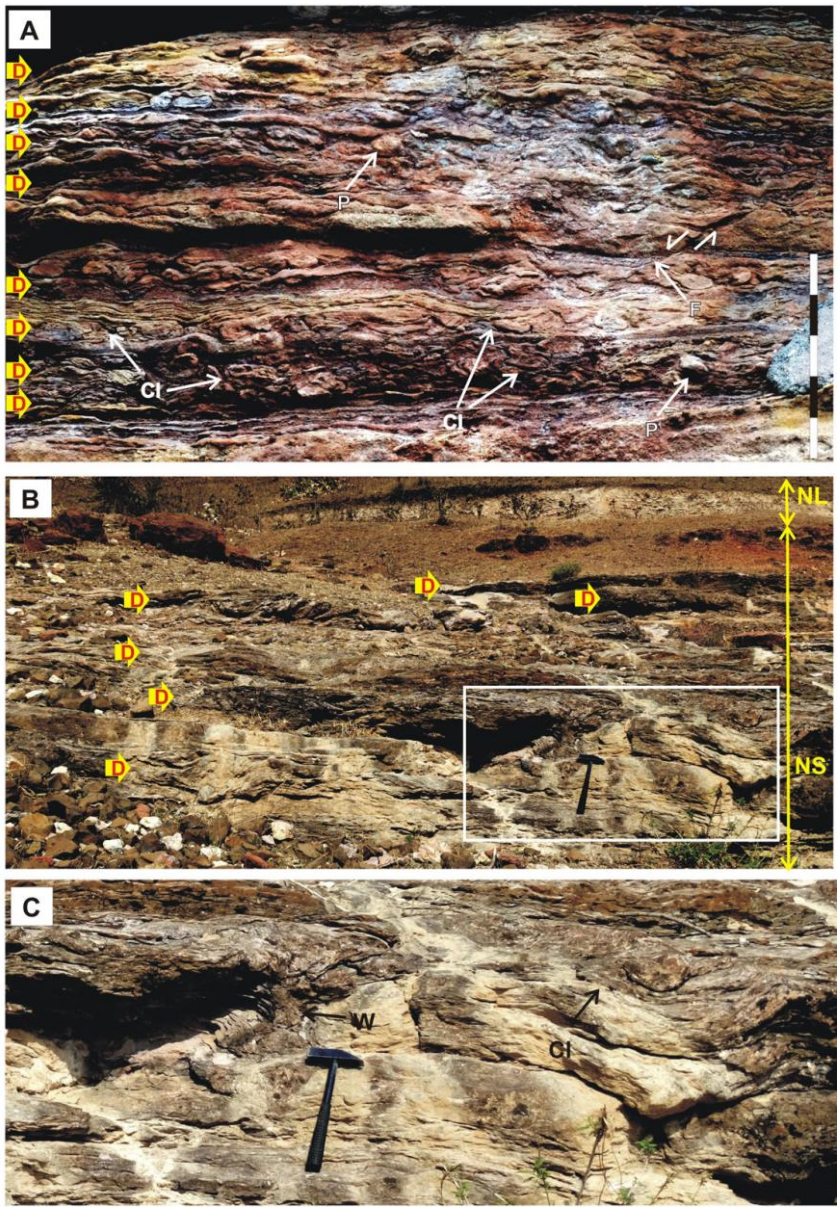

Figure: 6.9. Field photographs of association of various SSDS in beds of Nimar Sandstone. **A.** Multiple deformed layers (D) alternating with undeformed layers, within sandstone–mudstone heterolithic facies (4A), exposed near Bagh section. Complex, multi-lobed convolutes (Cl) are associated with flames and pseudonodules (P) and are affected by small fault (F). Nature of displacements of the convoluted beds by the fault indicates syn- to post-depositional deformation. The vertical scale bar is of 1 meter in length. **B.** Persistent deformed beds (D) separated by undeformed beds within Nimar Sandstone (NS) succession in the Man (Awaldaman) River section. Hammer length is 30 cm. The part within white box is zoomed in

C. showing complex convolutes (Cl) with vertical water-escape channels (W). NL-Nodular Limestone.

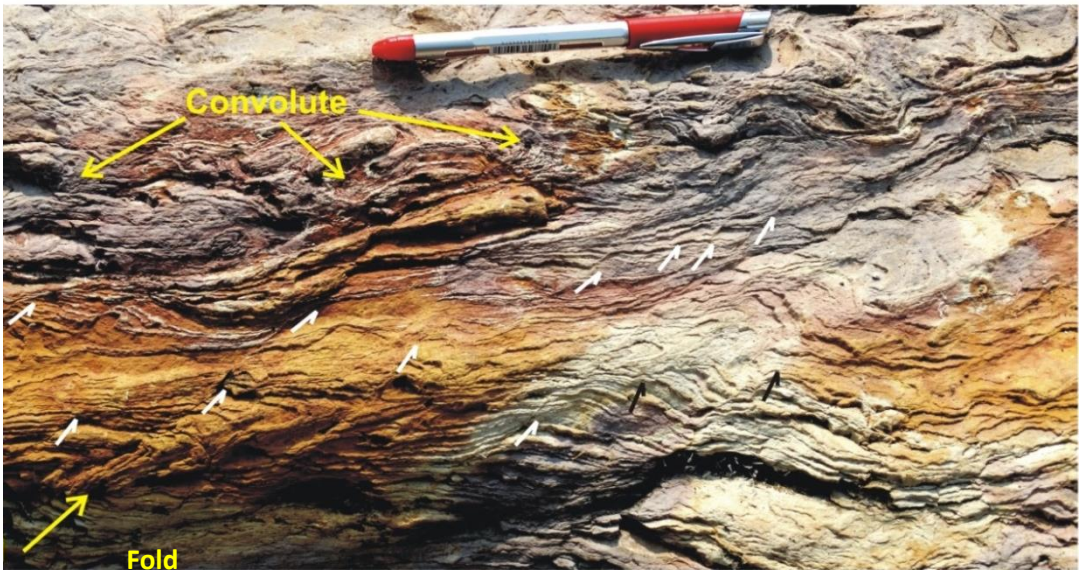

Figure: 6.10. Field photograph of SSDS bearing beds, exposed in the Man (Awaldaman) river section, showing association of recumbently folded thin sand–mud heterolithic beds, associated with centimeter-scale en echelon faults (marked with black and white arrows) overlain by complex, multi-lobed convolutes. Length of the pen in photograph is 14.5 cm.

6.4. Trigger mechanism of the studied SSDS

Abundance of different soft sediment deformation structures like convolute lamination, load and flame structure, contorted bedding, pseudonodules, slump structure, syn-sedimentary fault with graben-like downsagging structure and sand dyke confined within the sandstone-mudstone heterolithic facies (4A) and large scale trough cross-stratified sandstone facies (3A) (Figure 6.11) indicates liquefaction and fluidization of unconsolidated sediments. Sudden shock by pounding storm waves, overloading of sediments, mass movement or seismic shock may cause such deformation within the unconsolidated sediment. The increase in pore fluid pressure of unconsolidated sediments with a sudden reduction of shear strength initiated this type of deformation.

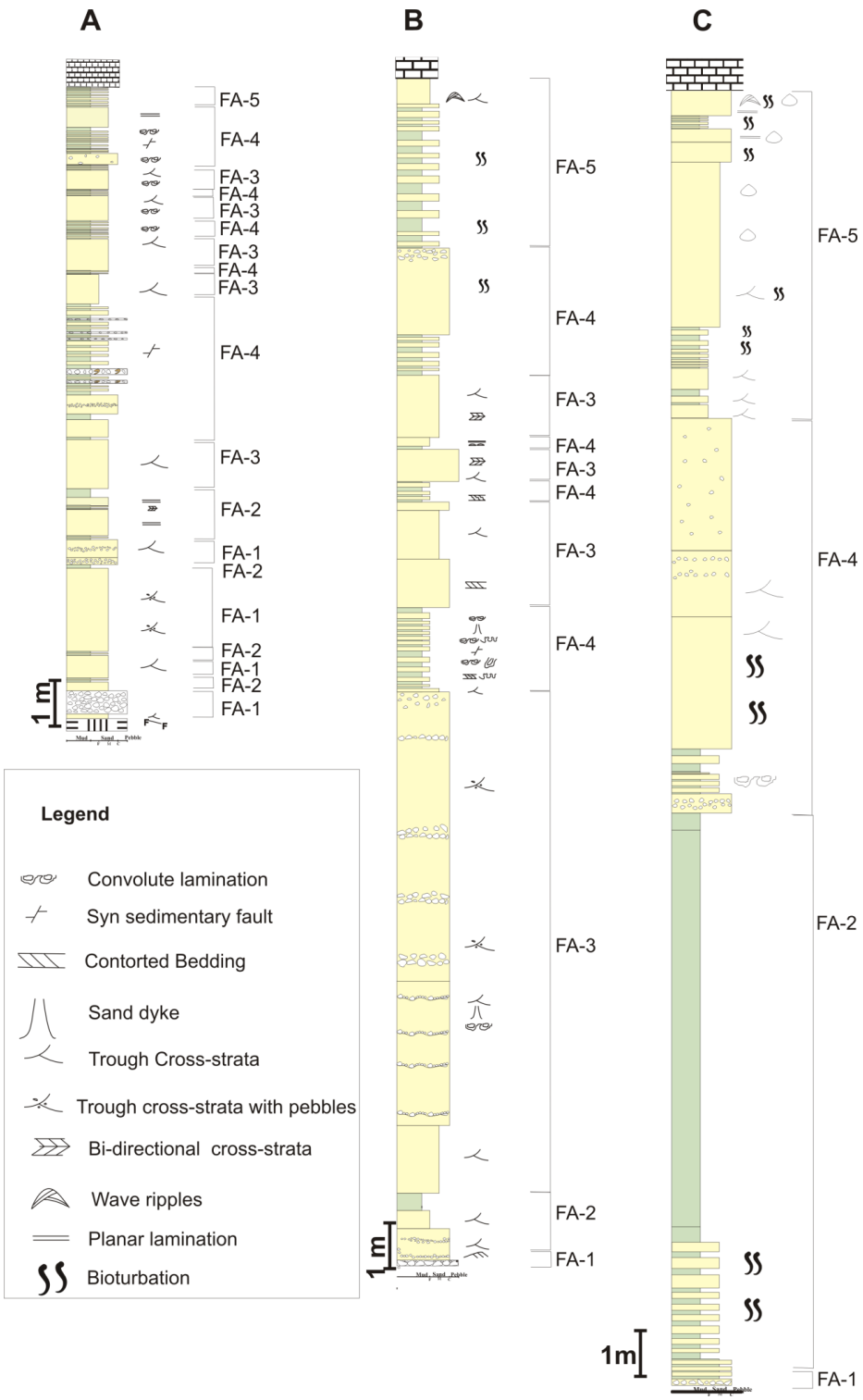

Figure: 6.11. Vertical sedimentary lithologs showing distribution of various SSDS **A.** Man (Awaldaman) river section, eastern part of the study area. **B.** Bagh section, central part of the study area. **C.** Dhursal section, western part of the study area.

Loosely packed siltstones to fine-grained sandstones are competent for formation of SSDS (Moretti, 1999). The sudden impact of the storm waves within the depositional system produces an intense bottom current which may exceed the shear velocity and may initiate liquefaction of sediments (Owen, 1987). In the study area well preservation of tidal, wave features and absence of large scale hummocky cross-strata or any storm-generated sedimentary features indicates that no such storm activity occurred during the time of Nimar sedimentations. So, storm waves are not responsible to trigger the studied SSDS. Sudden overloading within unconsolidated sediment may initiate dewatering of the sediment and reduces the shear strength. The prevailing density contrast and grain size variation within the SSDS horizon in Nimar Sandstone is not enough for formation of such large scale, laterally extended SSDS. In fact, no such large scale load structure, completely deformed laminae are observed within the sandstone-mudstone heterolithic facies and large scale trough cross stratified sandstone facies as evidence of overloading or mass movement of the sediment. So, the effects of the overloading are ruled out. Rapid sedimentation is a very common trigger mechanism for liquefaction in the sand-on-sand system and in the sand-in-clay system. Moretti et al. (2001) recorded that the rapid deposition of sand could prompt liquefaction at a great depth below the water-sediment interface and that excess pore water pressure can remain very high in the underlying sediments for many hours. In the study area presence of moderately sorted, subrounded to rounded grains, well developed bedding plane, cross-stratification, alternate sandstone-mudstone bedding, preservation of ripple forms ruled out the process of rapid sedimentation for Nimar Sandstone. Then, rapid sedimentation is not the trigger mechanism for the studied SSDS. Sometimes due to intense bioturbation laminae can be deformed but in Nimar Sandstone SSDS bearing beds are not associated with such intense organic trace activities (like plant roots or mammals foot print). Unequal loading in a glacial setting causes fluidization (Van Loon and Brodzikowski, 1987; Obermeier, 1996; Dionne, 1998; Le Heron et al., 2005) in a glaciogenic environment but Nimar sedimentation has no evidence of glaciation. Lateral extension with repetition of the soft sediment deformation structures in an irregular interval, with close association of syn- sedimentary fault, graben-like structure and sand dyke indicates recurrent, non-periodic, short term, high energy shock activities in the basin. Seismic shock is the main trigger mechanism for this type deformation. Within the studied SSDS deformation structures have repetitive nature with a gradual increase in complexity indicates a repetition of shocks in different phases. As stated by Moretti and Sabato (2007), formation of

slump structure generally need a steep slope but in the study area general slope is near horizontal. According to Well et al. (1980) seismically induced slump may formed in very gentle slope (0.4º-0.25º). Bhattacharya and Bandhopadhyay (1998) interpreted formation of slump in a flat environment is an evidence of palaeoseismicity. So, the Seismic shock is proposed as trigger mechanism for the studied SSDS. Seismic shock as triggered mechanism for SSDS is already proposed by many researchers from different localities (Seilacher, 1969, 1984; Lowe, 1975; Well et al., 1980; Field et al., 1982; Allen, 1982, 1985; Altermann, 1986; Brodzikowski et al., 1987; Brodzikowski and Haluszczak, 1987; Seth et al., 1990; Owen, 1995; Rossetti and Santos, 2003; Mazumder et al., 2006; Moretti and Sabato, 2007; Schnellmann et al., 2005).

According to Moretti and Van Loon (2014) and Van Loon (2014), tectonically induced beds or layers bearing SSDS with repetitive occurrences, large lateral extension, bounded by undeformed beds, increasing complexity near to active fault system is termed as Seismites. In the study area different beds of the sandstone-mudstone heterolithic facies are showing similar characteristic, and accordingly they are identified as Seismites (Jha et al., 2017).

6.5. Implication of the Seismites

Implications of the seismites to estimate the palaeo magnitude and epicentral distance have been incited in various literatures (Sims, 1975; Hempton and Dewey, 1983; Allen, 1986; Audemard and De Santis, 1991; Cojan and Thiry, 1992; Guiraud and Plaziat, 1993; Obermaier et al., 1993; Marco and Agnon, 1996; Bhat et al., 2013). According to Atkinson (1984), M5 is the lowest earthquake magnitude which can initiate the liquefaction in sediments because earthquakes of magnitude less than 5 are not of sufficient duration to trigger the liquefaction process. For the formation of various SSDS different magnitudes are required, Kuenen (1958) stated that, formation of pseudonodules required shock of a magnitude exceeding 6.5. Sand dikes have been interpreted as related to the earthquake of magnitude ranging from 5 to 8 (Audemard and De Santis, 1991; Obermaier et al., 1993). According to Galli (2000), 90% of the liquefaction sites are located within 40 km range from the epicenter. Rest 10 % of the liquefaction sites situated within a maximum distance of 100 km, which are affected by a very high magnitude earthquake (M>9). In the studied seismites presence of pseudonodules and sand dyke indicates earthquake of 6-8 palaeomagnitude with epicenter distance within 40 km

(Jha et al., 2017). The major deep seated faults which lie within 40 km radius from study area are viz., the Son-Narmada South Fault and the Son-Narmada North Fault (Tewari et al. 2001). Some minor faults/lineaments viz., the Barwani-Sukta Fault, the Dhar Lineament, the Rakhabdev Lineament and the Jaoalaier Lineament lie beyond 40 km radius from the study area (Figure 1.1). According to Acharya and Roy (2000), the Son-Narmada South fault was reactivated during the late Cretaceous time. There are no record of evidences regarding reactivation process of the other faults and lineaments. Reactivation time of the Son-Narmada South Fault is slightly postdated with the Nimar sedimentation time, so another new phase of reactivation of the Son-Narmada South Fault was interpreted by Jha et al. (2017) based on the presence of seismites within the Nimar Sandstone.

Formation of each seismites bed within the Nimar Sandstone indicates a tectonic disturbance, in the nearby vicinity. The Nimar Sandstone records sedimentation history in a fault-bounded Son-Narmada rift setting. Seismites are dominant within the middle-upper part of succession mainly associated with fluvio-tidal mixed facies association of FA-4. Presence of repetitive seismites bed within the FA-4 indicates tectonic disturbances during the sedimentation. Alternate deformed and undeformed bed with preservation of tidal features indicates marine sedimentation and tectonic disturbance within the Nimar Sandstone were contemporaneous process. Jha et al. (2017) stated that, incursion of marine water during Nimar sedimentation and seismites has a strong correlation; reactivation of Son-Narmada South Fault during the Cenomanian caused sequential subsidence of the land part within the Indian Plate, which invited subsequent incursion of the sea water from the west. Preservation of seismites with marine sediments bears the evidence (Figure 6.12) of such subsidence and marine incursion.

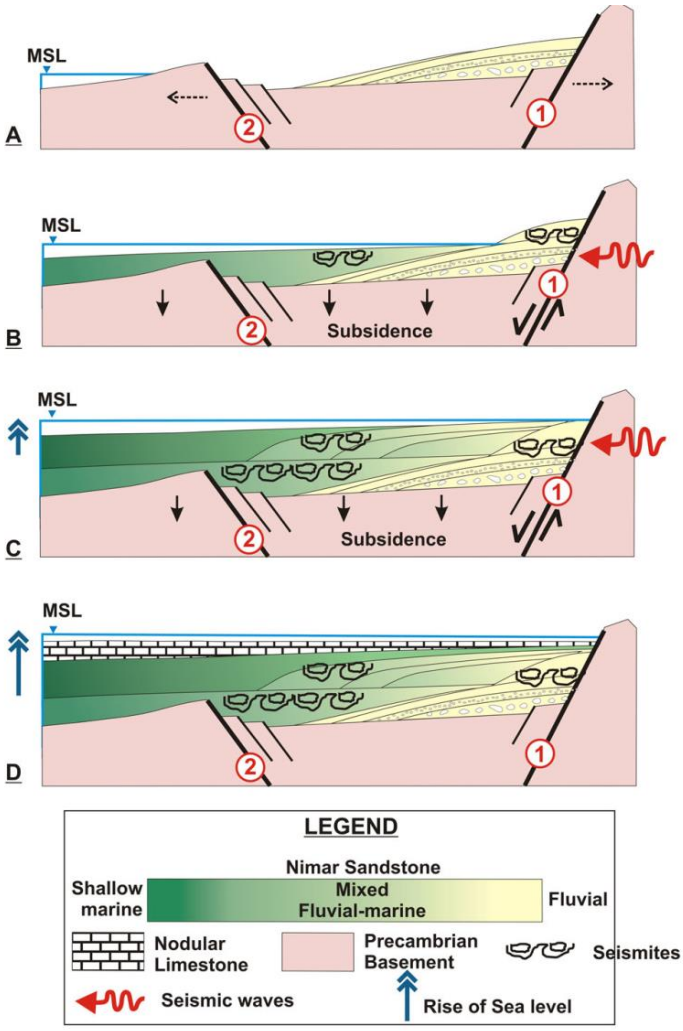

Figure: 6.12. Schematic diagram showing the relation of seismites and dominant tectono-sedimentary events during deposition of the Nimar Sandstone in the Son-Narmada rift valley (Jha et al., 2017). **A.** Deposition of fluvial sediments within the continental riftogenic basin. Fault 1 was active in the Early Cretaceous, whilst Fault 2 was not active. **B.** Reactivation of Fault 1 caused basinal subsidence, which led to marine encroachment into land and deposition of mixed fluvio-marine sediments. Propagation of seismic shocks produced seismites within FA-4 and FA-5. **C.** Further subsidence led to onlap of shallow marine sediments and development of seismites. **D.** Significant sea level rise in the relatively stable basin and deposition of Nodular Limestone. Events A, B and C took place during the Cenomanian time and event D during the Turonian.

6.6. Summary

In the study area SSDS are mainly confined within the FA-4 and FA-5. A detailed SSDS study from the Nimar Sandstone helps to conclude that-

- Convolute lamination, slump structure, contorted bedding, pseudonodules, sand dikes, load and flame structures and syn-sedimentary faults are the dominant SSDS in the study area.
- The trigger mechanism of these SSDS is seismic shock and the SSDS bearing beds are interpreted as seismites.
- The studied Seismites indicate a palaeo earthquake of magnitude 6-8.
- Reactivation of Son-Narmada South Fault triggered seismic shocks during Nimar Sandstone sedimentation.
- Activation of the fault caused basinal subsidence, which shifted the depositional condition of Nimar Sandstone from fluvial to fluvio-marine setting due to significant marine incursion.

CHAPTER 7

Geochemistry of Nimar Sandstone

7.1. Introduction

The geochemical composition of terrigenous sedimentary rocks is an important tool to understand the palaeodepositional setting of any sedimentary terrain. It is a function of the complex interplay of various factors such as provenance, weathering, transportation and diagenetic pattern (Bhatia, 1983). Apart from these factors tectonism has a primary control on the rock composition (Pettijohn et al., 1972). Before the use of geochemical composition, petrographic studies were widely used for provenance study, but its usage is limited within sandstone only. Blatt et al. (1985) stated that interbedded argillite-mudrock members of sedimentary sequences have not been widely used for determination of provenance and tectonic setting because of grain size. This restriction does not apply to bulk chemical data. Based on the degree and pattern of weathering, mobile or unstable elements are removed from the rock, leaving the immobile elements. Hence, the ratio of various mobile and immobile elements within a sedimentary rock depicts the provenance types and degree of weathering (Roser and Korsch, 1986; Armstrong-Altrin et al., 2004; Kumar et al., 2017). The ratio of immobile to mobile elements changes in different tectonic settings. It increases towards the passive margin to the relative tectonic stability setting (Armstrong-Altrin et al., 2004). Bhatia (1983) stated that a decreasing trend in (Fe_2O_3 + MgO), TiO_2, (Al_2O_3/SiO_2) and increasing trend in (K_2O/Na_2O) and Al_2O_3/ (CaO+Na_2O) in sandstone suites from oceanic island arc to continental arc to active continental margin to passive margins was developed. This trend implies that, as sandstones become more mature, there are an increase in quartzose content and a decrease in the unstable detrital grains (Bhatia, 1983)

Geochemistry of sandstone and shale has been widely used to obtain the information regarding the provenance, depositional setting, tectonic setting and degree of weathering (Crook, 1974; Bhatia, 1983; Taylor and McLennan, 1985; Bhatia and Crook, 1986; Condie et al., 1992; McLennan et al., 1993; Kumar et al., 2017). In the study area, facies architectural pattern, various primary sedimentary structures, presence of tidal features and ichnofabric indicates a mixed fluvio-marine depositional setting for the Nimar sedimentation. This chapter deals with

the evaluation of sandstone, sandstone-mudstone heterolith and mudstones/shale of the Nimar sandstone in respect to its ambient palaeoweathering conditions, provenance and source rock characteristics, by using major oxide geochemistry.

7.2. Material and Methods

For geochemical analysis, fresh samples were collected from the outcrops of the study sections. The samples were washed thoroughly with distilled water to remove any contamination. A total 17 nos. of samples were collected for major element (oxides) geochemistry among which 12 are sandstone samples, 3 mudstone samples and 2 samples of heteroliths (see Table 7.1). Powders of all these 17 samples were analyzed for major elements (oxides) geochemistry using X-Ray Fluorescence (XRF) (Model BRUKER S8 TIGER Sequential Spectrometer). These analyses were carried out by skilled professionals at the Petrology and Geochemistry Division, Wadia Institute of Himalayan Geology (WIHG), Dehradun, India. Detailed geochemical data are presented in Table 7.2.

Table: 7.1. Details of the samples collected for major element geochemistry from Nimar Sandstone.

Sl No.	Sample No. for XRF	Facies type	Litho type	Field Location
1	N2	Trough cross-stratified sandstone facies (1D)	Sandstone	Man River Section
2	N3	Large scale trough cross-stratified sandstone facies (3A)	Sandstone	Man River Section
3	N4	Plane laminated sandstone facies (4C)	Sandstone	Man River Section
4	N20	Large scale trough cross-stratified sandstone facies (3A)	Sandstone	Ghoda Section
5	N7	Sandstone-mudstone heterolithic facies (4A)	Sandstone	Rampura Section
6	N8	Trough cross-stratified sandstone facies (1D)	Sandstone	Baghini Temple Section
7	N12	Green sandstone facies (4E)	Sandstone	Chikapoti Section
8	N13	Bioturbated sandstone facies (4D)	Sandstone	Chikapoti Section
9	N15	Green sandstone facies (4E)	Sandstone	Ghoda Section
10	N18	Sandstone-mudstone interbedded facies (2A)	Sandstone	Baghini Temple Section
11	N21	Green sandstone facies (4E)	Sandstone	Phata Section
12	N16	Sandstone-mudstone interbedded facies (2A)	Sandstone with mud chips	Baghini Temple Section
13	N6	Sandstone-mudstone interbedded facies (2A)	Mudstone	Raisinghpura Section
14	N14	Sandstone-mudstone heterolithic facies (4A)	Mudstone	Ghoda Section
15	N17	*Thalassinoides-Ophiomorpha* bearing thinly laminated sandstone-mudstone facies (5B)	Mudstone	Baghini Temple Section
16	N5	Sandstone-mudstone heterolithic facies (4A)	Heteroliths	Raisinghpura Section
17	N9	Sandstone-mudstone interbedded facies (2A)	Heteroliths	Dhursal Section

7.3. Geochemical Results

The major elements (wt. %) concentrations of the Nimar Sandstone are reported in Tables 7.2, and their ratios in Table 7.3. The data are compared to the average compositions of the Post-Archean Australian Shale (PAAS), which are considered as representative of the upper continental crust (UCC), from Taylor and McLennan (1985), and the Cody Shale (SCO), USGS (the standards used during the analysis at WIHG). The sandstones consist of 94.19 to 45.06 wt.% SiO_2; 16.10 to 1.21 wt.% Al_2O_3; 0.11 to 0.97 wt.% TiO_2; 0.32 to 5.97 wt.% Fe_2O_3; 0.01 to 0.2 wt.% MnO; 0.18 to 19.91 wt.% CaO; 0.01 to 7.99 wt.% MgO; 0.07 to 7.99 wt.% Na_2O; 0.86 to 4.69 wt.% K_2O and 0.01 to 0.11 wt.% P_2O_5. Total iron is expressed as Fe_2O_3. Index of Compositional Variation (ICV) of Cox et al. (1995) in which ICV = (Fe_2O_3 + K_2O + Na_2O + CaO + MgO + MnO + TiO_2) / TiO_2 commonly used to represent relative abundance of clay minerals vs. rock forming minerals. Values of ICV more than 1 indicate the presence of fewer clay minerals and more rock-forming minerals such as plagioclase, K-feldspar, amphiboles, pyroxenes and lithic (Cox et al., 1995). ICV values of the studied samples vary from 0.7 to 17.93 (average= 2.64) (Table 7.2), which indicates the presence of both rock-forming mineral (dominantly feldspar) and clay minerals. It is known that the values of (K_2O/Al_2O_3) of clays are less than 0.3 and the values of the same ratio of feldspars range from 0.3 to 0.9 (Table 7.3).

The values of (K_2O/Al_2O_3) ratio of the studied samples range from 0.14 to 0.7 (average= 0.30). Ratio of (K_2O/Na_2O) indicates the presence or absence of K-bearing minerals such as K-feldspar, muscovite, biotite. In the studied area (K_2O/Na_2O) ratio is high (average= 12.48) (Table 7.3). The positive correlation of Na_2O with SiO_2 and MgO (Table 7.4) indicates the presence of smectite clay minerals within the studied samples. According to McKinley et al. (2009) smectites in sandstones are not always co-deposited with sand grade sediment but can be incorporated into the sand by bioturbation, soft-sediment deformation, and mechanical infiltration. CaO exhibits strong negative correlation with SiO_2 (r = -0.94) (Table 7.4) suggesting that the carbonates are primary rather than secondary (Feng and Kerrich, 1990). The (SiO_2/Al_2O_3) ratio indicates maturity of a sedimentary rock, in studied sedimentary rocks this ratio is relatively high (50.40-4.29, average=16.15). The (SiO_2/Al_2O_3)ratio of $\geq$5 represents a chemically mature sedimentary rock (Roser et al., 1996).

Table: 7.2. Major element concentrations (in wt. %) of 17 sedimentary rock samples collected from the Nimar Sandstone. The data are compared to the average compositions of the Post-Archean Australian Shale (PAAS), which are considered as representative of the upper continental crust (UCC), from Taylor and McLennan (1985), and the Cody Shale (SCO), USGS (the standard used during the analysis and provided by WIHG)

Sample	SiO_2 (wt %)	Al_2O_3(wt %)	TiO_2(wt %)	Fe_2O_3(wt %)	MnO(wt %)	CaO (wt %)	MgO (wt %	Na_2O (wt %	K_2O (wt %)	P_2O_5 (wt %)	LOI	TOTAL	PIA	CIA	CIW	ICV	CMI
N2	94.19	2.20	0.17	0.52	0.18	0.38	0.01	0.09	0.32	0.11	1.84	100.01	80.00	73.58	82.40	0.76	42.81
N3	56.75	6.34	0.78	2.21	0.20	10.86	5.78	0.11	1.26	0.05	16.42	100.76	31.65	34.14	36.63	3.34	8.95
N4	45.06	4.38	0.52	3.88	0.16	15.43	7.99	0.10	0.92	0.03	21.80	100.27	18.22	21.03	22.00	6.62	10.29
N5	69.03	16.10	0.73	4.20	0.01	0.18	0.52	0.46	2.19	0.04	4.96	98.42	95.60	85.05	96.18	0.51	4.29
N6	79.53	12.10	0.34	1.02	0.01	0.43	0.30	0.14	1.48	0.02	3.31	98.68	94.91	85.51	95.50	0.31	6.57
N7	56.85	7.84	0.44	1.06	0.19	18.36	0.00	0.07	0.86	0.12	12.53	98.32	27.47	28.90	29.84	2.68	7.25
N8	68.17	5.00	0.38	0.36	0.06	13.17	0.01	0.08	1.03	0.05	12.72	101.03	23.05	25.93	27.40	3.02	13.63
N9	89.99	3.29	0.29	1.49	0.06	1.36	0.02	0.11	0.97	0.05	2.32	99.95	61.21	57.42	69.12	1.31	27.35
N12	87.07	5.44	0.13	1.18	0.01	0.31	0.38	0.14	3.17	0.02	1.76	99.61	83.46	60.04	92.36	0.98	16.01
N13	89.32	4.59	0.33	0.33	0.03	0.36	0.01	0.14	3.07	0.05	1.56	99.79	75.25	56.25	90.18	0.93	19.46
N14	78.44	8.63	0.51	2.37	0.01	0.34	0.81	0.14	4.69	0.02	2.41	98.37	89.14	62.54	94.73	1.03	9.09
N15	60.98	1.21	0.11	0.43	0.20	19.91	0.12	0.07	0.86	0.09	16.84	100.82	1.72	5.49	5.71	17.93	50.40
N16	84.65	7.17	0.54	0.65	0.04	0.69	0.26	0.14	1.72	0.06	3.01	98.93	86.78	73.77	89.63	0.56	11.81
N17	70.57	11.66	0.74	5.97	0.02	0.16	1.20	0.64	2.65	0.04	4.84	98.49	91.85	77.17	93.58	0.98	6.05
N18	61.64	10.94	0.97	4.11	0.05	7.58	0.79	0.10	0.63	0.05	11.69	98.55	57.31	56.83	58.75	1.30	5.63
N20	72.44	6.37	0.33	0.71	0.02	9.23	0.01	0.10	1.20	0.02	8.79	99.22	35.66	37.69	40.57	1.82	11.37
N21	89.56	3.79	0.16	0.32	0.00	0.57	0.21	0.13	1.77	0.01	3.38	99.90	74.26	60.54	84.41	0.83	23.63
Avarage	73.78	6.89	0.44	1.81	0.07	5.84	1.08	0.16	1.69	0.05	7.66	99.48	60.44	53.05	65.23	2.64	16.15
UCC value	66.00	15.20	0.60	5.00	0.10	4.20	2.20	3.90	3.40	0.2	NA	NA	NA	61.50	NA	NA	NA
PAAS	62.80	18.90	1.00	7.10	0.10	3.70	2.20	1.20	3.70	0.20	NA	NA	NA	75.30	NA	NA	NA
SCO	62.80	13.70	0.60	5.10	0.10	2.80	2.70	0.90	2.80	0.20	NA	NA	NA	68.50	NA	NA	NA

Table: 7.3. Ratios of major oxides concentration of 17 sedimentary rock samples collected from the Nimar Sandstone.

Sample	N2	N3	N4	N5	N6	N7	N8	N9	N12	N13	N14	N15	N16	N17	N18	N20	N21	Avarage
Al_2O_3/K_2O	6.88	5.03	4.76	7.35	8.18	9.12	4.85	3.39	1.72	1.50	1.84	1.41	4.17	4.40	17.37	5.31	2.14	5.26
K_2O/Al_2O_3	0.15	0.20	0.21	0.14	0.12	0.11	0.21	0.29	0.58	0.67	0.54	0.71	0.24	0.23	0.06	0.19	0.47	0.30
Fe_2O_3/K_2O	1.63	1.75	4.22	1.92	0.69	1.23	0.35	1.54	0.37	0.11	0.51	0.50	0.38	2.25	6.52	0.59	0.18	1.45
K_2O/Na_2O	3.56	11.45	9.20	4.76	10.57	12.29	12.88	8.82	22.64	21.93	33.50	12.29	12.29	4.14	6.30	12.00	13.62	12.48
Al_2O_3/TiO_2	12.94	8.13	8.42	22.05	35.59	17.82	13.16	11.34	41.85	13.91	16.92	11.00	13.28	15.76	11.28	19.30	23.69	17.44
MgO/Al_2O_3	0.00	0.91	1.82	0.03	0.02	0.00	0.00	0.01	0.07	0.00	0.09	0.10	0.04	0.10	0.07	0.00	0.06	0.20
SiO_2/Al_2O_3	42.81	8.95	10.29	4.29	6.57	7.25	13.63	27.35	16.01	19.46	9.09	50.40	11.81	6.05	5.63	11.37	23.63	16.15
Fe_2O_3/MgO	52.00	0.38	0.49	8.08	3.40	17.82	36.00	74.50	3.11	33.00	2.93	3.58	2.50	4.98	5.20	71.00	1.52	18.85
Fe_2O_3+MgO	0.53	7.99	11.87	4.72	1.32	1.06	0.37	1.51	1.56	0.34	3.18	0.55	0.91	7.17	4.90	0.72	0.53	2.90
Al_2O_3/SiO_2	0.02	0.11	0.10	0.23	0.15	0.14	0.07	0.04	0.06	0.05	0.11	0.02	0.08	0.17	0.18	0.09	0.04	0.10
$Log(SiO_2/Al_2O_3)$	1.63	0.95	1.01	0.63	0.82	0.86	1.13	1.44	1.20	1.29	0.96	1.70	1.07	0.78	0.75	1.06	1.37	1.10
$Log(K_2O/Na_2O)$	0.55	1.06	0.96	0.68	1.02	1.09	1.11	0.95	1.35	1.34	1.53	1.09	1.09	0.62	0.80	1.08	1.13	1.03
$Log(Fe_2O_3/MgO)$	0.11	-0.42	-0.31	0.91	0.53	-0.86	1.56	1.87	0.49	1.52	0.47	0.55	0.40	0.70	0.72	1.85	0.18	0.70
$Log(Na_2O/K_2O)$	-0.55	-1.06	-0.96	-0.68	-1.02	-1.09	-1.11	-0.95	-1.35	-1.34	-1.53	-1.09	-1.09	-0.62	-0.80	-1.08	-1.13	-1.03
$Log(MgO/Al_2O_3)$	-2.34	-0.04	0.26	-1.49	-1.61	0.86	-2.70	-2.22	-1.16	-2.66	-1.03	-1.00	-1.44	-0.99	-1.14	-2.80	-1.26	-1.48
$Log(K_2O/Al_2O_3)$	-0.84	-0.70	-0.68	-0.87	-0.91	-0.96	-0.69	-0.53	-0.23	-0.17	-0.26	-0.15	-0.62	-0.64	-1.24	-0.72	-0.33	-0.62

Table: 7.4. Values of Pearson's coefficient correlation of major oxides of the analyzed samples from Nimar Sandstone.

Oxides	SiO_2	Al_2O_3	TiO_2	Fe_2O_3	MnO	CaO	MgO	Na_2O	K_2O	P_2O_5
SiO_2	1									
Al_2O_3	0.272715	1								
TiO_2	0.116264	0.756206	1							
Fe_2O_3	-0.02224	0.664315	0.773992	1						
MnO	-0.60974	-0.18874	-0.00327	-0.04558	1					
CaO	-0.9481	-0.50914	-0.37713	-0.25176	0.539794	1				
MgO	-0.16386	0.02594	0.397185	0.442861	0.056077	-0.00874	1			
Na_2O	0.314652	0.682799	0.494076	0.735353	-0.28923	-0.48947	0.02827	1		
K_2O	0.541936	0.418771	0.211147	0.243721	-0.39811	-0.61788	-0.03611	0.466514	1	
P_2O_5	-0.5239	-0.14585	-0.06275	-0.08543	0.884076	0.468622	-0.10926	-0.22746	-0.33974	1

7.4. Discussion

7.4.1. Geochemical classification

Clastic sedimentary rocks are classified in different categories based on their chemical composition (Crook, 1974; Pettijohn, 1975; Blatt et al., 1980; Herron, 1988). Sandstones of the present study were classified according to the scheme proposed by Herron (1988). In the bivariate diagram of Log (Fe_2O_3/K_2O) vs. Log (SiO_2/Al_2O_3) (after Herron, 1988) the studied sandstones are classified as litharenite, sublithic arenite, arkose and subarkose (Figure 7.1A). Crook (1974) classified sandstone into 3 types (quartz-rich, quartz-intermediate and quartz-poor) based on their Na_2O and K_2O contents. In the K_2O wt. % vs. Na_2O wt. % bivariate diagram (after Crook, 1974) the studied sandstones are plot essentially in the quartz-rich field (Figure 7.1B).

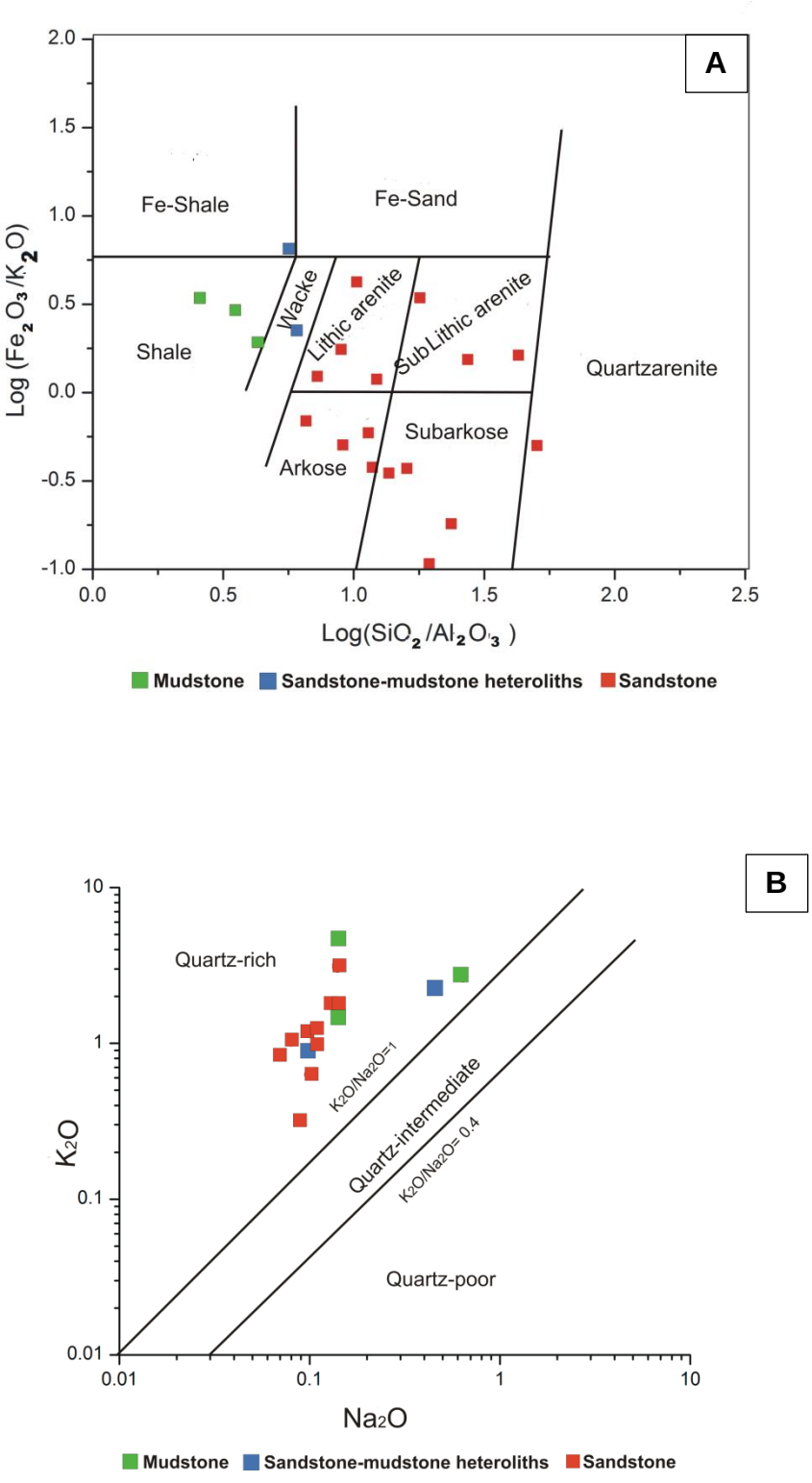

Figure: 7.1. Geochemical classification of clastic sedimentary rock. **A.** Log (Fe_2O_3/K_2O) vs. Log (SiO_2/Al_2O_3) bivariate diagram. **B.** K_2O wt. % versus Na_2O wt. % bivariate diagram.

7.4.2. Provenance

To recognize the provenance of siliciclastic sedimentary rock several discrimination diagrams are proposed by various authors (Taylor and McLennan, 1985; Floyd and Leveridge, 1987; Roser and Korsch, 1988; Floyd et al., 1989; McLennan et al., 1993; Condie, 1993). The major element discrimination diagram of Roser and Korsch (1988) has been used to decipher the provenance of Nimar Sandstones (Figure 7.2A), which indicates quartz rich sedimentary provenance and some components of mafic igneous provenance. In Roser and Korsch (1988) diagram the quartz rich sedimentary provenance was drawn based on the chemical composition of sandstones and argillites of Ordovician Greenland Group and provenance of these terrains was a highly weather granitic-gneissic terrain (Laird, 1982). In the studied samples abundance of feldspar (ICV value = 2.64) indicates a source near to depositional site. The (K_2O/Na_2O) ratio (average 12.48) (Table 7.3) also suggests abundance of K-bearing minerals (McLennan et al., 1983; Nath et al., 2000; Osae et al., 2006). Aluminum concentration is mainly measured for detrital flux, and positive correlation of Al_2O_3 with K_2O, Na_2O and TiO_2 indicate that these elements are associated entirely with detrital phase (Nagarajan et al., 2007). (Al_2O_3/K_2O) ratio (average = 5.26) indicate that K-bearing minerals have a significant influence on Al distributions and bulk of the Al and K primarily are contributed by clay minerals (Mc Lennan et al., 1983). The abundant quartz and K-bearing minerals in the study area originated from granite-gneiss and quartz rich sedimentary or meta-sedimentary provenance. The (SiO_2/Al_2O_3) ratio (average 16.15) suggests that there were chemically mature sedimentary rocks involved in the source area.

The Al_2O_3 and TiO_2 contents of the siliciclastic sedimentary rocks are also significant in provenance identification. Since Al and Ti are immobile elements, during weathering of source rocks they remain as residue due to the low solubility of their oxides and hydroxides (Stumm and Morgan, 1981; Sugitani et al., 1996). Therefore, the values of (Al/Ti) ratios of any sedimentary rock can be considered to be very close to those of their parent rocks. McLennan et al. (1980) recognizing the significance of Al and Ti in the provenance studies, and proposed Al_2O_3 wt. % vs. TiO_2 wt. % bivariate discrimination diagram to decipher provenance of siliciclastic rocks. On this plot studied samples show dominantly Granodiorite to Granite trend line along with mixed “3 Granite+1Basalt” (McLennan et al., 1980) (Figure 7.2B).

Hence considering all these factors it can be concluded that Nimar Sandstone sediments were may derive from the basement rock of mixed granitic gneiss, basalt and quartzite of Bijawar (Table 2.1).

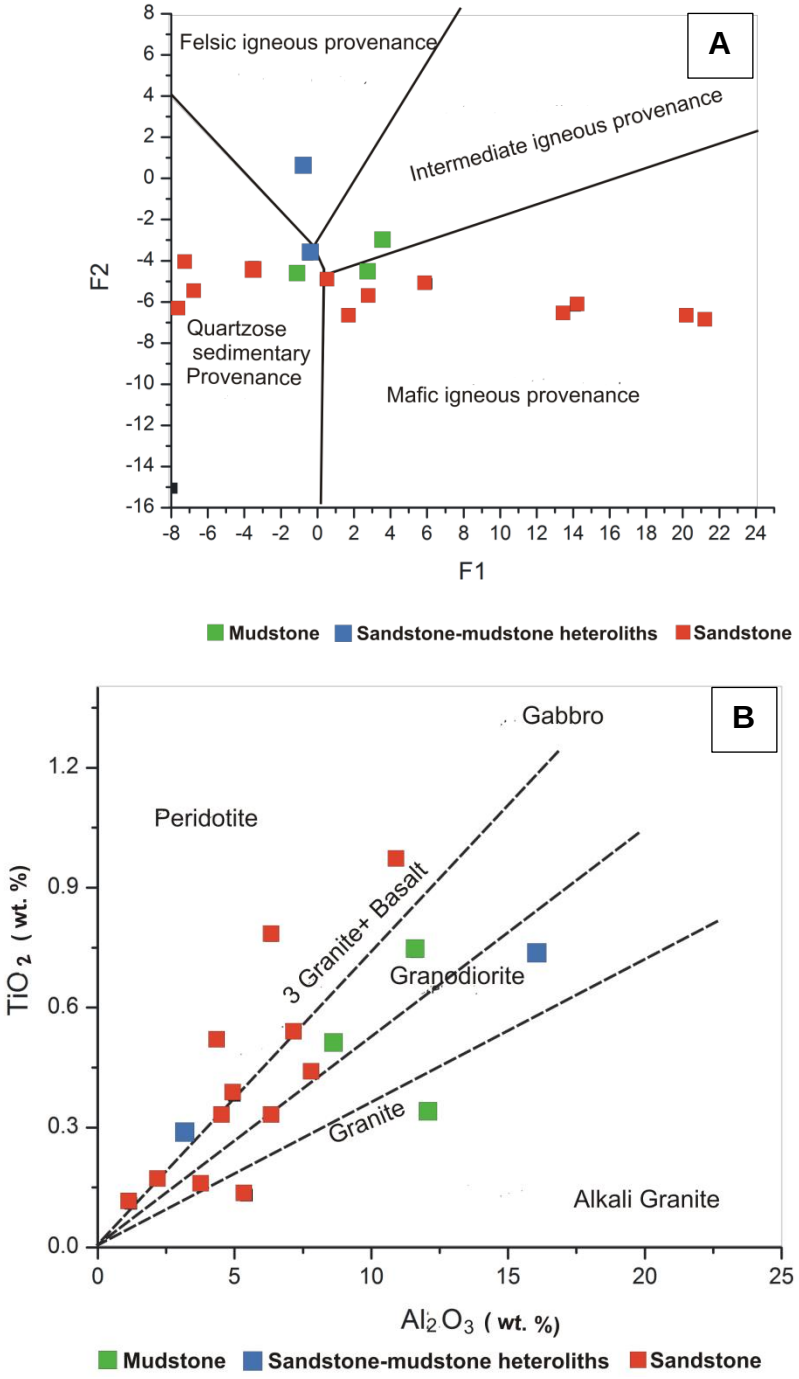

Figure: 7.2. A. Provenance discrimination diagram for sandstones (after Roser and Korsch, 1988). Discriminant Function 1 = (-1.773×TiO_2%) + (0.607×Al_2O_3%) + (0.76×Fe_2O_3T %) + (1.5×MgO %) + (0.616×CaO %) + (0.509×Na_2O %) + (-1.22×K_2O %) + (-9.09). Discriminant Function 2 = (0.445×TiO_2%) + (0.07×Al_2O_3%) + (-0.25×$Fe_2O_3^T$ %) + (- 1.142×MgO %) +

(0.432×Na_2O %) + (1.426×K_2O %) + (-6.861). **B.** Provenance discrimination diagram TiO_2 wt. % versus Al_2O_3 wt. % bivariate plot (after McLennan et al., 1980). The "granite line" and "3 granite + 1 basalt line" are after Schieber (1992).

7.4.3. *Palaeotectonic setting*

The chemical compositions of siliciclastic sedimentary rocks are significantly controlled by tectonic settings of the depositional basins. Therefore, the siliciclastic rocks from different tectonic settings have terrain-specific geochemical signatures, like (Fe_2O_3 + MgO) have high abundance in oceanic island arc setting, continental island arc type sandstone has lower value of (Fe_2O_3 + MgO), whereas the passive margin setting sandstones are enriched with SiO_2 (Bhatia, 1983; Bhatia and crook, 1986; Roser and Korsch, 1986). Various major element based discrimination diagrams have been proposed to infer tectonic setting of provenance of ancient siliciclastic sedimentary rocks by several researchers (Maynard et al., 1982; Bhatia, 1983; Bhatia and Crook, 1986; Roser and Korsch, 1986; McLennan et al., 1990; McLennan and Taylor, 1991, Floyd et al., 1991). The most discriminating parameters are (Fe_2O_3 (Total) +MgO), TiO_2 and SiO_2, (K_2O+Na_2O) (Bhatia and Crook, 1986; McLennan et al., 1990). Due to the low mobility and low residential time in seawater Fe and Ti are most important tools to decipher palaeotectonic setting (McLennan et al., 1990). However Mg has high residential time in sea-water but it remains unchanged in nature in several tectonic setting (Blat et al., 1980). In the present study analyzed samples mainly show a passive margin setting both in (Fe_2O_3+MgO) vs. TiO_2 tectonic discrimination diagram (Figure 7.3A) (Bhatia, 1983) and SiO_2 vs. (K_2O/Na_2O) discrimination diagram (Figure 7.3B) (Roser and Korsch, 1988). Few samples are not laid within the passive margin fields in the (Fe_2O_3+MgO) vs. TiO_2 diagrams. According to Bhatia (1983), clastic sedimentary rocks of passive margin setting show large variation in their composition, which sometimes may overlay with the characteristic of active margin sandstones. But lower ratio of (Fe_2O_3 (Total) +MgO), (Al_2O_3/SiO_2) and a higher ratio of (K_2O/Na_2O) helps to distinguished them from active margin setting sandstone. The studied rock samples show higher ratios of (K_2O/Na_2O) value (Table 7.3).

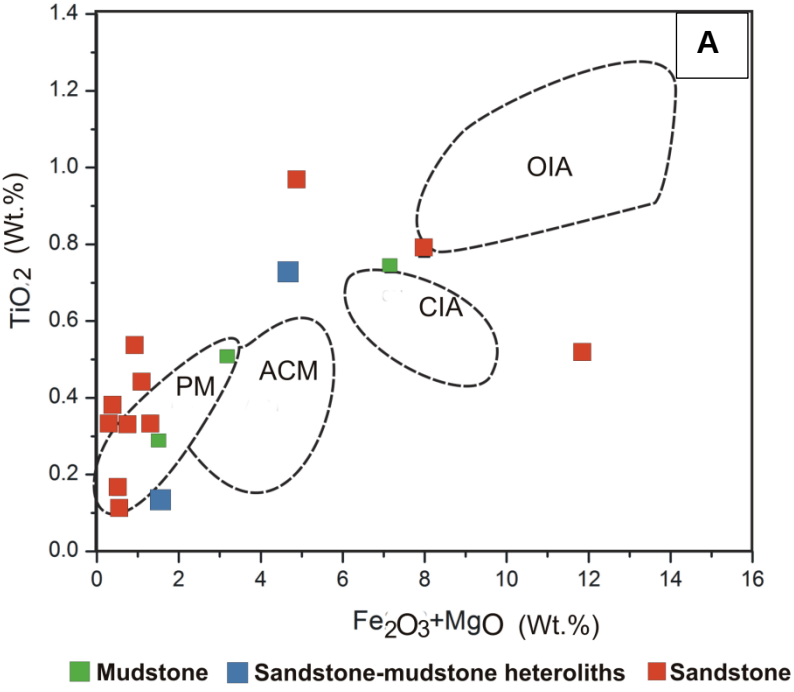

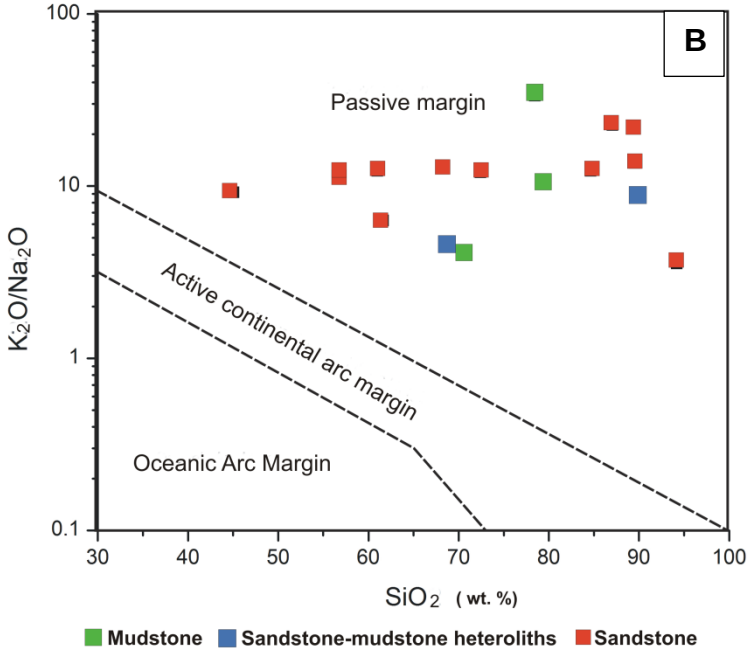

Figure: 7.3. Tectonic setting discrimination diagrams based on major element composition of clastic sedimentary rock. **A**. (Fe_2O_3 (Total) + MgO) wt. % versus TiO_2 wt. % diagram (Bhatia, 1983). PM: Passive Margin, ACM: Active Continental Margin, CIA: Continental Island Arc, OIA=Oceanic Island Arc. **B.** SiO_2 wt. % versus (K_2O/Na_2O) diagram (Roser and Korsch, 1986).

7.4.4. Palaeoweathering

Weathering is an important phenomenon, which significantly influence the geochemical properties of any sedimentary rocks (McLennan et al., 2003). During intense chemical weathering Ca, Na and K are mainly removed from source rocks. If the siliciclastic sedimentary rocks are free from alkali metasomatism, then their alkali contents ($K_2O + Na_2O$) and (K_2O/Na_2O) ratios are considered as reliable indicators of the intensity of weathering of source material (Lindsey, 1999). Various indices are proposed by researchers for interpretation of degree of palaeoweathering. Among the recognized indices of weathering/alteration, the Chemical Index of Alteration (CIA; Nesbitt and Young, 1982, equation i) is a conventional method of quantifying the degree of source weathering. Source weathering and elemental redistribution during digenesis also can be calculated by using Plagioclase Index of Alteration (PIA; Fedo et al., 1995, equation ii) and Chemical Index of Weathering (CIW; Harnois, 1988, equation iii). The equations of the above indices are given below:

$$CIA = \{Al_2O_3 / (Al_2O_3 + CaO + Na_2O + K_2O)\} \times 100 \ldots\ldots\ldots \text{(i)}$$

$$PIA = \{(Al_2O_3 - K_2O) / ((Al_2O_3 - K_2O) + CaO + Na_2O)\} \times 100 \ldots\ldots \text{(ii)}$$

$$CIW = \{Al_2O_3 / (Al_2O_3 + CaO + Na_2O)\} \times 100 \ldots\ldots\ldots\ldots\ldots \text{(iii)}$$

Average CIW and PIA values (65.23%; 60.44%) (Table 7.2) of the studied area indicates a moderate degree of source weathering. Average CIA value (51.77%) indicates intermediate chemical weathering for the Nimar Sandstone. CMI (chemical maturity Index) ratio of (SiO_2/Al_2O_3) is also used to measured degree of chemical weathering. During transportation and recycling along with weathering quartz or Si-rich phases are increases at the expanse of phyllosilicates or Al-rich phases in a sedimentary rock. Therefore, the ratio of (SiO_2/Al_2O_3) provides an estimation of the compositional maturity of sediment during or after chemical weathering. In the studied samples average (SiO_2/Al_2O_3) ratio (Table 7.3) is 16.15, which indicate compositionally mature sediments.

7.4.5. Palaeoclimatic condition and Sediment maturity

Recycling of siliciclastic rock affects mostly the (SiO_2/Al_2O_3) ratio, which basically indicates the maturity of a sedimentary rock (Roser and Korsch, 1986; Roser et al., 1996). Value of (SiO_2/Al_2O_3) ratio > 5.0 in sandstone indicates of progressive maturity (Roser et al., 1996). The (SiO_2/Al_2O_3) ratios of the studied sample are high (average= 16.15) and the (K_2O/Na_2O) ratio is also high (average = 12.48). High values of (SiO_2/Al_2O_3) and (K_2O/Na_2O) ratio together indicate more matured and recycled nature of the sediments. Suttner and Dutta (1986) proposed a binary SiO_2 wt. % versus (Al_2O_3+K_2O+Na_2O) wt. % diagram to constrain the climatic condition during sedimentation of siliciclastic sedimentary rocks. The studied samples plot essentially in the field of semi-arid to a humid climatic condition and the ratio of (SiO_2/Al_2O_3) suggest increasing chemical maturity (ratio of >5 indicates progressive chemical maturity) (Figure 7.4).

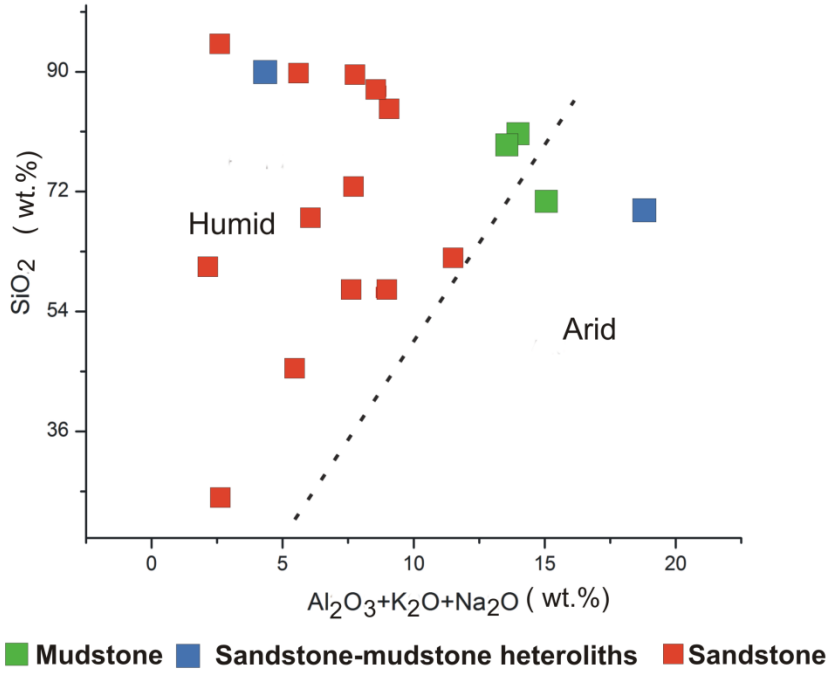

Figure: 7.4. SiO_2 wt. % versus (Al_2O_3+K_2O+Na_2O) wt. % variation diagram showing palaeoclimatic conditions during Nimar sedimentation (after Suttner and Dutta, 1986).

7.4.6. Palaeodepositional condition

MgO and Al_2O_3 are the major oxides which helps to distinguish between the marine and nonmarine setting for any sedimentary rock. Mg is rich in marine water whereas Al comes from continental weathering debris formed due to the chemical breakdown of feldspar.

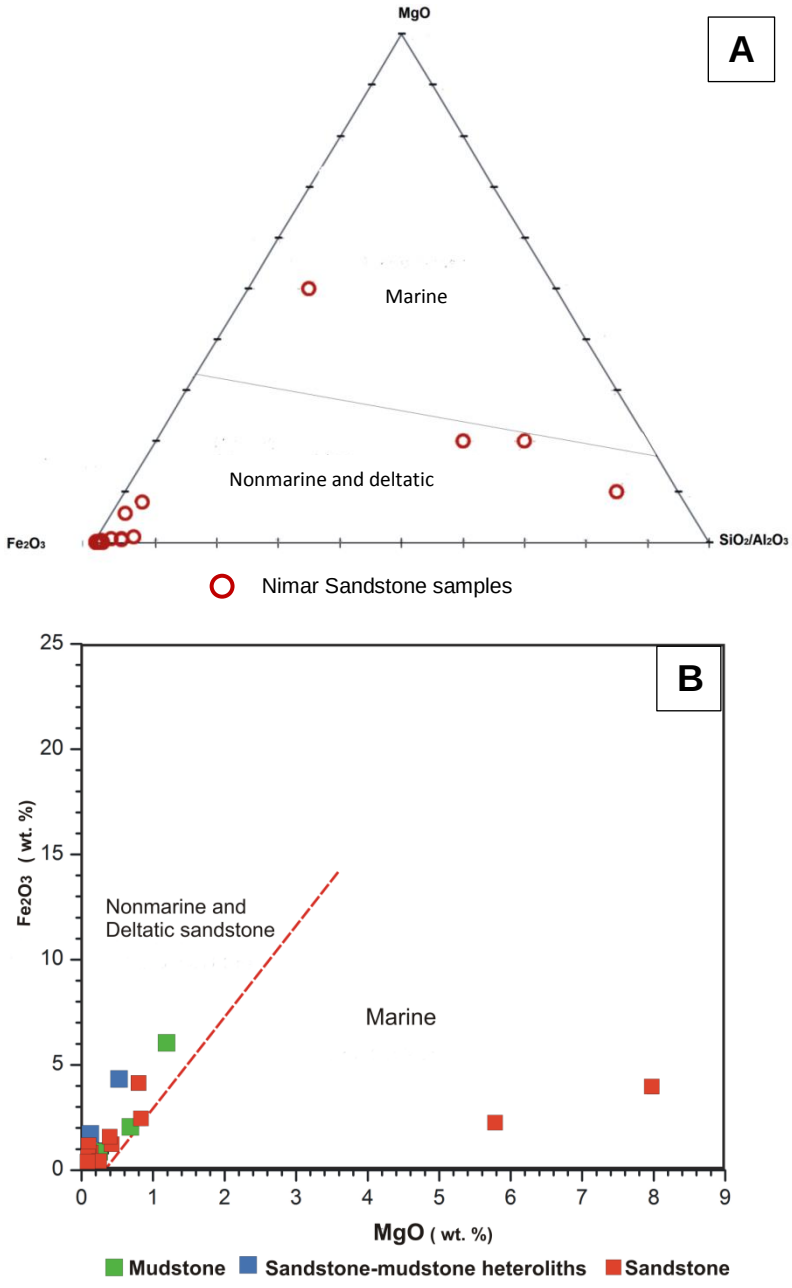

Figure:7.5. A. Binary and **B.** ternary diagrams showing characterization and differentiation of marine from non-marine sandstones (after Ratcliffe et al., 2007). Nimar sediments spread over both the fields indicating a mixed transitional environment.

The calculated ratio of (MgO/Al_2O_3) for the studied sample ranges from 0.02 to 1.8 (avarage 0.20) (Table 7.3) which indicates a marine to nonmarine transitional condition. Fe_2O_3 and MgO concentration also varied with the change from marine to the nonmarine setting. Plotting of Fe_2O_3 vs. MgO data in separate binary and ternary diagrams (following Ratcliffe et al.,2007), confirm that the studied samples show a transitional environment since the sediments plotted both in the non-marine to deltaic as well as marine sandstone fields (Figures 7.5A, 7.5B).So, the geochemical composition of the Nimar Sandstone also validated the graduall changes from freshwater to shallow marine condition from lower to upper part of the succession during the depostion of Nimar Sandstone.

7.5. Summary

Significant observations of the geochemical study of Nimar Sandstone is given below:

- ✓ Geochemical classification based on Log(Fe_2O_3/K_2O) vs. Log(SiO_2/Al_2O_3) values show that the rocks are lithic arenite, sublithic arenite, subarkose and arkose in nature.
- ✓ K_2O (wt. %) vs. Na_2O (wt. %) values demonstrate that Nimar Sandstone is quartz-rich in nature.
- ✓ ICV value indicates sediments are dominated by both K-bearing rock-forming and clay minerals.
- ✓ SiO_2 (wt. %) vs. ($Al_2O_3+K_2O+Na_2O$) (wt. %) variation diagram indicates rocks are minerologically mature in nature and deposited under humid palaeoclimatic condition.
- ✓ Discrimination diagram (following Roser and Korsch, 1988) for provenance decipher mixed quartzos-mafic igneous rocks in the source area. Similar granite-granodioritic-basaltic mixed source composition is obtained from TiO_2 (wt. %) vs. Al_2O_3 (wt. %) plot.
- ✓ (Fe_2O_3+MgO) vs. TiO_2 and SiO_2 vs (K_2O+Na_2O) tectonic discrimation diagrams shows Nimar Sedimentation was going on a passive margin setting with moderate weathering condition.
- ✓ Binary diagram of Fe_2O_3 vs. MgO and ternary diagram of Fe_2O_3-MgO-(SiO_2/Al_2O_3) indicate palaeodepositional setting of the studied area was transitional nonmarine-shallow marine condition.

.

CHAPTER-8

Discussion

8.1. Introduction

In this chapter, we discussed the main facets and findings of the present research work from Nimar Sandstone. During the present research work sedimentary facies analysis, study of primary sedimentary structures, geochemical analysis, and the ichnological study were carried out. The final outcomes are compiled to reconstruct the palaeogeography of the Nimar Sandstone and to construct a comprehensive sedimentary basin model in the light of sequence stratigraphic architecture. The model deciphers predominant transgressive-regressive (T-R) cycles in the fluvio-marine Nimar Sandstone succession in response to the influence of late Cretaceous marine incursion in the Indian plate.

8.2. Reconstruction of the Nimar Sandstone depositional environment

8.2.1. Implications of sedimentary facies analysis and its outcome

The fluvio-marine sediments of the Nimar Sandstone unconformably overlies the Proterozoic Bijawara gneiss (Singh and Srivastava, 1981). During the late Cretaceous time, fluvial sedimentation of Bagh Group was started within the Son-Narmada rift setting. The lower portion of the Nimar Sandstone succession was comprised of immature fluvial sediments of FA-1and FA-2. The present research work showed the certain evidenced of tide reworking of the channel-fill sediments (FA-3, FA-4) in the middle part of the succession and wave reworking of the tidal sediments in the upper part (FA-4 and FA-5) of the succession. Tide-wave led sediments of the Nimar Sandstone indicate a transition from fluvial sediments of FA-1 and FA-2 to tidally influenced fluvial sediment of FA-3, tide-dominated sediments FA-4 and wave reworked tidal sediments of FA-5.

Thus, the predominant facies associations and their architecture in the Nimar Sandstone signifies deposition in three major sub-environments within the fluvio-marine interactive estuary setting –

- a fluvial-dominated zone initially , with transition from fluvial channels (FA-1) to floodplains (FA-2), with few tide-affected fluvial deposits (FA-3) in the basal part of the succession, mainly dominated in the eastern and central part of the studied area.

- a mixed energy central estuary zone in the middle-upper part of the succession, which consists of transitional fluvio-tidal channels (FA-3), tidal flats, associated with tidal channels and bars (FA-4) mainly dominated in the central part of the studied area.
- a wave-dominated shore environment in the outer estuary zone (top part of FA-4 with FA-5) present in the upper part of the succession.

8.2.2. Tidalites and their implications on palaeoenviromental

The Nimar Sandstone preserves thick packages of tidally-influenced sediments in the middle part of the succession. These tidally-influenced sediment packages are commonly stacked under thick-thin sandstone-mudstone heterolithic unit along with some wave reworked features. Preservation of these sediment packages indicates a low energy depositional condition where waves are present but they do not have enough energy to rework the tidal sediments. Preservation of mud drapes indicates the slack phase of water. Alternate sand dominated and mud dominated heterolith indicates fluctuations in energy condition. Alternate fluvial (FA-1, FA-2), fluvial-dominated tidally influenced sediments (FA-3) followed by tide-dominated wave reworked sediments (FA-4, FA-5) portrayed distinct depositional cycles from a fluvio-marine mixed depositional setting. In the middle-upper part of the Nimar Sandstone succession, the wave-dominated sediments of FA-5 overlies the tidally influenced sediments of FA-4, which is repetitive in nature. These distinct cycles indicate repeated changes in water-depth over short intervals under a tide-wave interactive system as a product of periodic marine inundation and intercalations. Such repetitive cycles with a fining-up sequence indicates inundation of fluvio-tidal channel by marine water under a typical estuarine setting (Nichols, 2009). In the study area overall dominance of tidal features over wave features indicates a tide-dominated wave-influenced estuary.

8.2.3. Implications of trace fossils and sediment-organism interaction pattern

Ichnology is an important tool used in understanding certain parameters of a sedimentary environment, such as rate of sedimentation, salinity conditions, substrate types and oxygen and nutrient supply (Ekdale et al., 1984; Bromley, 1996; Pemberton et al., 1992; Taylor et al., 2003; McIlroy, 2004; Gingras et al., 2011; Bromley and Uchman, 2003 and many others). Any changes in these parameters have direct and or indirect impact on the association, abundance and diversity of trace fossils (Bromley, 1996; Gibert and Ekdale, 1999; Gingras et al., 2002; Chakraborty and Bhattacharya, 2005). So, to interpret palaeoenvironmental and palaeoecological conditions of any sedimentary succession, study of ichnofabric analysis is the

best method. In the study area, vertical and horizontal traces of suspension feeders, as well as deposit feeders produced by worm-like organisms, crustaceans, and few mollusks, are dominant. The studied trace fossils are grouped into four ichnofacies types, mixed Skolithos-Glossifungites ichnofacies, mixed Cruziana-Glossifungites ichnofacies, Glossifungites ichnofacies and mixed Cruziana- Skolithos ichnofacies. The lower part of the Nimar Sandstone succession was mainly devoid of any trace fossils. In the middle and upper part of the successions intensity and diversity of trace fossils increases. Fluctuation in energy condition, the transition of fluvial to marine depositional setting affected the ecological condition of the study area. Availability of food, salinity condition, and supply of bottom-oxygen were controlled by various depositional processes that indirectly or directly influenced the habitat and the activities of the organisms. Depending on this ecological factor ichnofabric pattern was gradually changed from basal to the top part of the succession.

8.2.4. Implications of seismites

At different stratigraphic levels of the Nimar Sandstone succession, various SSDS are first time reported by Jha et al. (2017). Those SSDS bearing sediment units are interpreted as Seismites. Common SSDS described are convolute laminae, pseudonodules, load and flame structures, syn-sedimentary faults, slumps and sand dykes. In Nimar Sandstone SSDS are mainly present in the middle part of the succession, which phases of a substantial shift in the depositional conditions from fluvial-dominated to a transgressive tide-wave-influenced estuarine system with basinal subsidence. Presence of pseudonodules and sand dykes within this formation indicates a palaeo-earthquake of magnitude of 6-8. The occurrences of seismites signify a new phase of reactivation of the Son-Narmada South Fault in the basinal area and resulted in concomitant marine transgressions (Jha et al., 2017) during the Late Cretaceous time.

8.2.5. Implications of geochemical analysis

The geochemical analyses also bear evidence of marine sedimentation in Central India during the time of Nimar sedimentation. Major oxide ratios and variant diagrams also signify a passive margin setting for the deposition of Nimar Sandstone and the provenance is acidic in nature, quatzosedimentary to granodioritic in composition. The palaeoclimatic condition was semi-arid to humid in nature during the Cenomanian time. The major element oxides ratios also clearly attest the existence of a marine-influenced transitional estuarine depositional system. So, the geochemical analysis supports the inferred fluvio-marine depositional model of the Nimar Sandstone.

8.3. T-R cycles and depositional sequences

Vertical and spatial distribution of lithounits of the five facies associations in Nimar sandstone depict an overall fining-upward retrogradational succession, as evident from the vertical sedimentary logs of all the sections. Overall transgressive nature of the depositional systems is also evident from the gradual changeover from dominant fluvial systems near the lower part, followed by fluvial-tidal mixed systems in the middle part and the mixed tide-wave open marine systems in the upper part of the succession. Keeping in view the west to eastward encroachment of the sea (as discussed in section 3.7), correlations were made in three sections across the dip profile – (i) a section in the westernmost part of the basin, in the Akhara-Phata area, incorporating log data of locations 1-5, (Figure 8.1) (ii) a section in the central part of the basin, in the Bagh area, incorporating logs of locations 6-11 (Figure 8.2), and (iii) a section in the easternmost part of the study area, in the Awaldaman-Ratitalai area, including the logs of locations 12-15 (Figure 8.3). Another correlation across all the strike parallel sections the dip profile section (Figure 8.4) is also prepared incorporating logs of Sitapuri, Raisinghpura, Bagh, Akhara and Chikapoti from east to west. These correlations provide clear evidences of stratal stacking patterns along the length (E-W) and width (N-S) of the basin and reflects the nature and effect of marine incursions at different areas in response to changing base level and resultant accommodation.

Within the overall fining-up trend, two distinct fining-up successions are clearly visible in almost all the logs, depicting two successive stacked transgressive cycles within the Nimar succession (Figures 8.1- 8.4), namely - (i) lower transgressive cycle (TL), incorporating fluvial sediments of FA-1 and FA-2 mostly, with some fluvio-tidal sediments of FA-3, occupying the lower part of the logs, and (ii) upper transgressive cycle (TU), which includes fluvio-tidal and shore sediments of FA-3, FA-4 and FA-5. Several coarsening-up (regressive) and fining-up (transgressive) cycles of lower rank are recorded within these two dominant transgressive cycles.

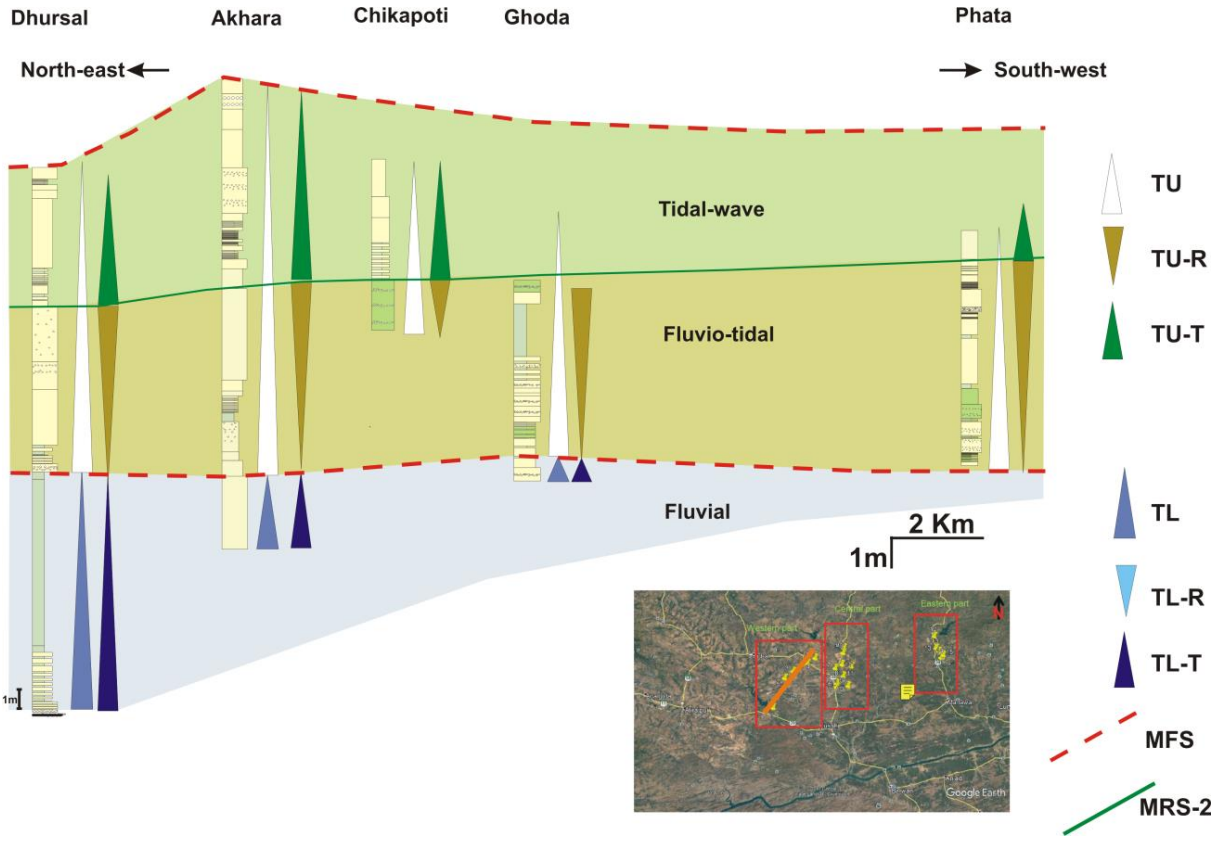

Figure: 8.1. Correlation of the lithologs in the western part of the study area, showing transgressive- regressive cycles of different order. The actual locations covered in this section is marked by orange line in the inset map (Figure 2.4). Abbreviations are TL-R- Lower transgressive coarsening up sequences, TL-T Lower transgressive finning up sequence, TU-R Upper transgressive coarsening up sequence TU-T Upper transgressive finning up sequence, MFS- Maximum flooding surface, MRS- Maximum regressive surface.

Correlations of these lower rank T-R cycles across different sections in the basin manifest mutual balance between sedimentation, base level conditions and its effect on net accommodation creation, which varies from area to area based on its actual position in the basin during deposition.

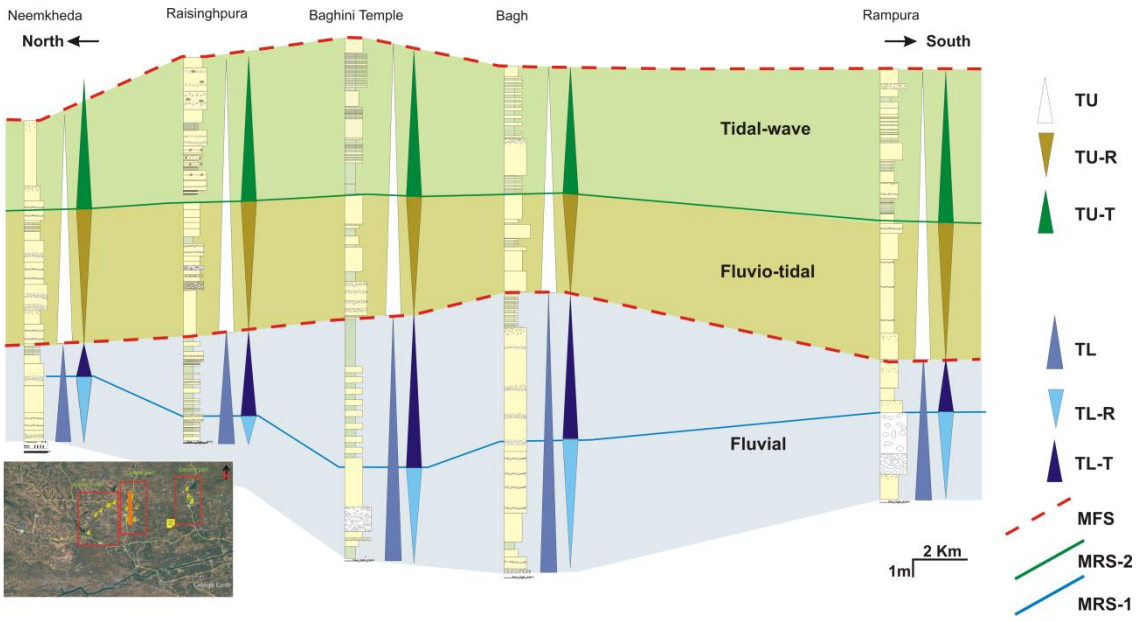

Figure: 8.2. Correlation of the lithologs in the central part of the study area, showing different transgressive- regressive cycles. The actual locations covered in this section is marked by orange line in the inset map (Figure 2.4). Abbreviations used are same as used in figure 8.1.

The lower transgressive cycle (TL) depicts a lower rank coarsening-up (regressive) (TL-R) succession, followed by a fining-up (transgressive) (TL-T) succession in most of the areas. In the central and the eastern sections (Figure 8.2 8.3), the fluvial succession is represented by initial coarsening-up to fining-up stacking pattern, indicating initial progradational (regressive) to a retrogradational (transgressive) pattern. The changeover from coarsening-up to fining-up succession is marked by a maximum regressive surface (MRS-1). Such coarsening-up progradational packages in fluvial systems indicates lowstand conditions, where base level rise was overpaced by sediment supply. As the rate of base level rise increased, more accommodation and raised graded river profile caused flooding and deposition of finer overbank deposits over the earlier sand-depositing areas.

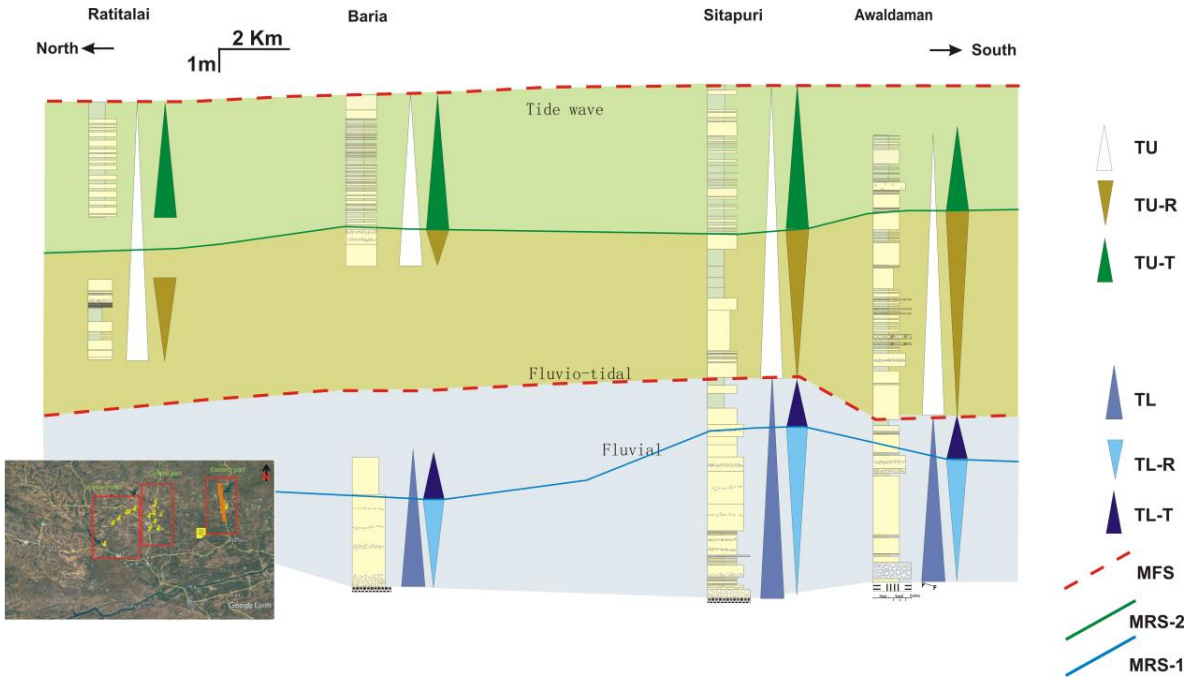

Figure: 8.3. Correlation of the lithologs in the eastern part of the study area showing different transgressive- regressive cycles. The actual locations covered in this section is marked by orange line in the inset map (Figure 2.4). Abbreviations used are same as used in figure 8.1.

This led to fining-up retrogradational succession (FA-2 over FA-1) in most of the areas, indicating a fluvial transgressive phase. Predominance of mud-rich floodplain deposits manifest rising base level conditions, leading to – (i) raising of river profile, (ii) more deposition than incision, and (iii) backstepping associated with aggradation of sediments. However, in some areas (e.g., Bagh, Rampura etc., Figures 8.2, 8.4), particularly in places where the fluvial channel was strongly affected by incoming tidal currents during this marine encroachment, tidally-reworked coarser clastics were deposited over FA-1 resulting in stacked, thick channel-fill sandstone beds (of FA-3). In the western section, (Figure 8.1) the fluvial system is not well preserved except in the Dhursal area. The fluvial succession shows a gradual fining-up stratal stacking pattern with abundance of fine-grained overbank deposits, indicating a low energy flooding condition under the dominant transgressive phase. The Lower transgressive cycle (TL) is directly overlain by the upper transgressive (TU) cycle (Figures 8.1-8.4). The separating surface is a flooding surface, represented by fine grained overbank deposit (of FA-2) in most of the areas. Sustained rise led to local stagnations, leading to fine-grained aggradational packages (local highstand conditions). In many cases, the surface is demarcated as the start of change from finning-up to coarsening-up. However, in many areas, the layers depicting transition from

TL to TU is associated with soft-sediment deformations (both above and below), which Jha et al. (2017) interpreted as seismites related to reactivation of faults and basinal sagging. Since base level rise was associated with basinal sagging, the falling stage conditions were not truly effective or completely absent in the basin, which explains the missing signatures of an intermittent falling stage in between two successive transgressive cycles within the Nimar Sandstone succession.

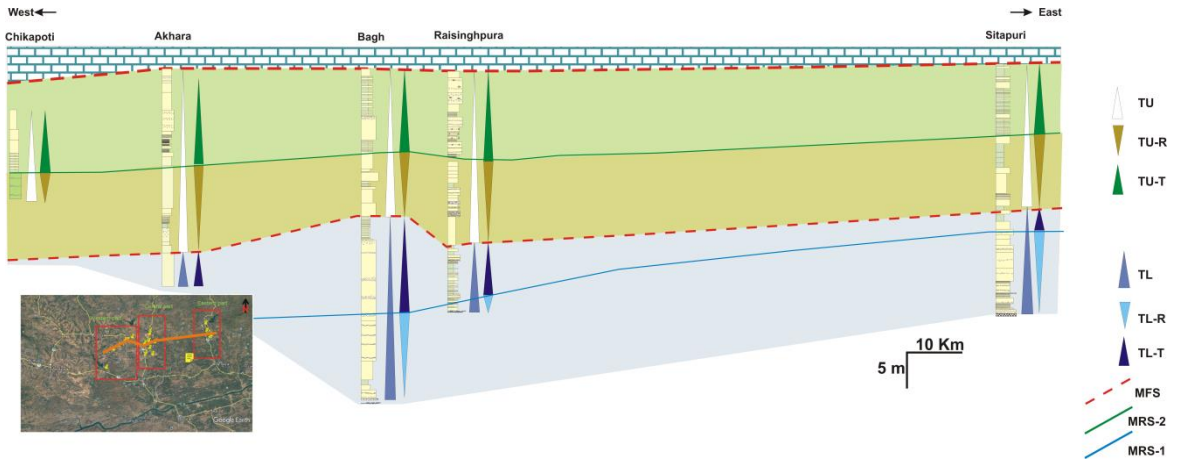

Figure: 8.4. Strike parallel correlation of lithologs along dip section from east to west of the study area, showing different transgressive- regressive cycles. The actual locations covered in this section is marked by orange line in the inset map (Figure 2.4). Abbreviations used are same as used in figure 8.1.

The upper transgressive cycle (TU) consists of two predominant lower-order cycles, (i) initial progradational regressive cycle (TU-R), followed upward by (ii) final retrogradational transgressive cycle (TU-T) (Figures 8.1-8.4). The transition from progradational to the retrogradational cycle is demarcated by a maximum regressive surface (MRS-2). Stacked retrogradational successions manifest sustained onlap of the marine tide- and wave-led systems over the underlying fluvial successions. Coarsening-up succession in TU-R is dominated by signatures of tidal sedimentation (FA-4), with minor records of fluvial inputs (FA-3). Such progradation indicate another lowstand condition, where significant amount of sediments supplied by river was reworked by encroaching tidal currents to deposit as bay head delta and tidal bars in front of the river mouth. Several lower rank coarsening-up and fining-up stratal packages (smaller parasequences) are present within the TU-R, indicating frequent change in base level and accommodation conditions in response to tidal-fluvial interactions and sediment supply.

Such lowstand stratal package is overlain by a transgressive package (TU-T), which consists of tide and wave-led sediments (of FA-4 and FA-5) (Figures 8.1- 8.4). The stratal stacking pattern is fining-up in nature in most of the areas, whereas it changes to sand-rich coarsening-up succession locally (Figures 8.1, 8.2). Such variation is caused due to differential energy conditions imparted in different part of the basin during the marine flooding event, which led to varied depositions from – (i) wave-reworked shoreface sands with marine bivalves and gastropods and trace fossils in the western part (more open marine), to (ii) relatively finer-clastic rich with abundant *Ostrea* and firm ground trace fossils, characteristic of brackish water condition in the eastern part (landward, sheltered estuary like). Thickness of the sediment package in TU-T also varies significantly with maximum thickness and sand-rich in the western part, and gradually thickness diminishing and changing to mud-rich towards the east. The TU-T indicates the early phase of transgression and is succeeded by a late phase of transgression manifested by the deposition of the overlying Nodular Limestone unit throughout the basin. The Nodular Limestone marks the further transgression (flooding), during which the entire basin was transformed to near open marine carbonate depositing setting. So, for Nimar Sandstone succession, the contact with the overlying limestone unit (Figure 8.5) is considered as the peak transgression, and is marked by another maximum flooding surface (MFS).

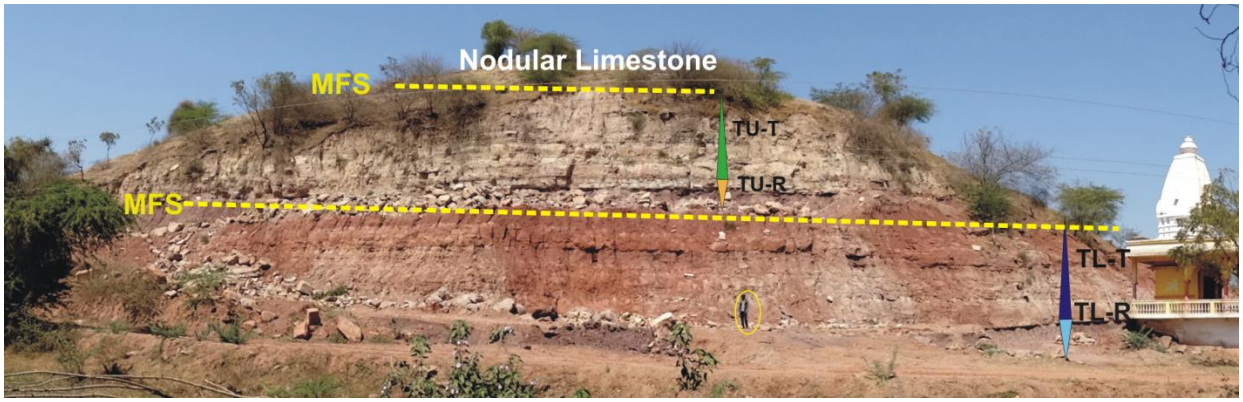

Figure: 8.5. Exposed section beside the Baghini Mandir, showing multiple transgressive-regressive cycles (marked by TL-R, TL-T, TU-R, TU-T). Note the occurrence of two maximum flooding surfaces (MFSs). The person (encircled) is for scale. Abbreviations used are same as used in figures 8.1-8.4.

8.4. Sequence stratigraphic architecture

The repetitive arrangement of facies and their associated stratal geometry present in successions of sediments and sedimentary rocks are analyzed in the study of sequence stratigraphic. These studies include patterns of stacking of the strata and the changes that do occur in them within a certain time frame. The definite patterns of the stratal stacking help to determine the order in which they were deposited to explain the geometric relationships and the architecture of sedimentary strata. Each stacking pattern of the strata represents a particular genetic type of deposit with a unique sedimentation pattern resulting from the interplay of accommodation space and the rate and amount of sedimentation within the basin (Eriksson et al., 2012, 2013). Common genetic types of deposits are low stand regressive, high stand regressive and transgressive. These units, referred to as low stand system tract, high stand system tract and transgressive system tract respectively, are the building blocks of the sequence stratigraphic surfaces. These surfaces help to illustrate the patterns of facies shift. The recurrence of the same types of surface through geologic time (or through vertical section) defines cyclicities of changes in accommodation space and/or sediment supply, which directly correspond to the rock record (Catuneanu, 2006; Catuneanu et al., 2012; Eriksson et al., 2012, 2013; Wagreich et al., 2014).

Considering the depositional age of the Nimar Sandstone (Cenomanian, ~100.5-93.5 MY), bounded by unconformity at the bottom and the Nodular Limestone (of Turonian age) at top, the overall transgressive retrogradational succession represent part of a 2^{nd} order transgressive systems tract (TST) within the overall late Cretaceous base level cycle (encompassing the entire Bagh Group and overlying sediments). Such 2^{nd} order base level fluctuations are commonly related to global tectono-eustatic changes. In Nimar Sandstone, the 2^{nd} order TST is further subdivided into two stacked transgressive cycles (TL and TU), which are identified as the 3^{rd} order transgressive systems tracts (3^{rd} order TSTs). Each TST is further divided into regressive-transgressive cycles (T-R cycles), and are identified as the system tracts of 4^{th} order. Details of stratal stacking pattern in system tracts of different order, the bounding surface and inferred sea level curves are shown in figure 8.6. Following is the description of the different systems tracts, parasequences and the nature of the confining boundaries in Nimar Sandstone.

8.4.1. 2^{nd} order System Tract

The entire Nimar sedimentary succession constitutes part of a 2^{nd} order transgressive systems tract (TST). The TST is fining-upward, retrogradational in nature and depicts gradual

changeover from fluvial, to fluvio-marine to marine-dominated depositional conditions from bottom to top. However, the TST is overlain by the Nodular Limestone, which marks the maximum extent of the transgression, and the contact demarcates the maximum flooding surface (MFS). The bottom boundary of the TST is an unconformity, which basically marks the contact with the underlying Proterozoic basements (Figure 8.6). As the sedimentation started with creation of positive accommodation in this basin, we do not get any traditional lower boundary (e.g., maximum regressive surface) for the 2nd order TST.

8.4.2. 3rd order Systems Tracts

Successively stacked transgressive cycles (TL and TU) within the 2nd order TST are identified as 3rd order transgressive systems tracts (3rd order TSTs) (Figure 8.6). The lower TST is characterized by the fining up, retrogradational successions of fluvial onlapping systems, indicating the initial phases of the major transgression. Lower boundary of this is same as the 2nd order TST, while the upper boundary is demarcated by flooding surfaces of 3rd order. Such flooding surfaces are represented by thick over bank deposits, sharply overlain by thick sandstones of the overlying transgressive cycle. Soft-sediment deformation structures are often associated with/near to this surface. The upper TST is characterized by another fining-up, retrogradational succession of fluvio-tidal to tide-wave led coastal onlapping system, pointing to the second transgression phase within the major transgression. This TST directly overlies flooding surface of the underlying TST, and is often associated with soft-sediment deformation structures near the basal part. The top surface of this TST is demarcated by the start of Nodular limestone, and is marked by maximum flooding event under this transgression (Figure 8.5).

8.4.4. The 4th order System Tracts

The coarsening- and fining-up successions of relatively shorter lengths (TL-R, TL-T, TU-R, TU-T, etc.) within the 3rd order TSTs are identified as the systems tracts of 4th order (Figure 8.6). Two low stand systems tracts (LST) in the form of coarsening-up successions (TL-R and TU-R). Each lowstand condition is succeeded by a transgressive systems tract (TST) of 4th order, manifested by fining-up facies successions (TL-T and TU-T) (Figure 8.6). The systems tracts of 4th order essentially demarcate stratal stacking patterns during a particular phase of base level change of relatively higher frequency.

The LSTs indicate normal regressive lowstand conditions formed by more sedimentation over-pacing the slow rate of base level rise. This led to a fluvial progradational succession near the

lower part, characterized by stacked channel fill deposits of FA-1 separated by overbank deposits (FA-2). Increasing overbank deposits near the upper part of this succession indicate more accommodation is created due to relatively higher rate of base level rise. The upper lowstand condition manifests interactions of fluvial and tidal depositional systems with progradation of the fluvial systems into the encroaching tidal system. The lower LST is bounded by the unconformity at the base (the contact with underlying Proterozoic basement rocks) and a maximum regressive surface (MRS-1) at the top marked by the change over from coarsening up to fining up stratal architecture observed in field exposures as well as in the log sections (Figures 8.1-8.5). The upper LST is demarcated by the maximum flooding surface (of the underlying TST) at the bottom and another maximum regressive surface (MRS-2) at the top (Figures 8.6).

The lower transgressive systems tract, represented by the fining-up succession of TL-T, is characterized by thick overbank deposits with isolated channels formed by creation of more accommodation due to higher rate of base level rise than the rate of sediment supply. The lower TST is predominantly a fluvial TST, with meager influences of the tidal encroachments (forming FA-3) leading to backstepping stratal packages towards the west (Figure 8.6). The upper TST is represented by another retrogradational fining-up succession (TU-T) that overlies the upper LST. The upper TST is characterized by backstepping tidal and wave-reworked sediments (of FA-4 and FA-5, respectively), indicative of coastal onlap due to significant base level rise resulting in creation of net accommodation. Both the TSTs are demarcated by the maximum regressive surfaces (MRS-1 for lower TST and MRS-2 for upper TST) at the bottom (Figure 8.6). In the top, the TSTs are commonly bounded by the flooding surfaces of 4^{th} order, which are represented by finer-clastics of relatively smaller thickness and shorter lateral extents. The bounding surfaces are frequently replaced by different facies assemblages in response to short-term base level fluctuations and its varied effect in different parts of the basins.

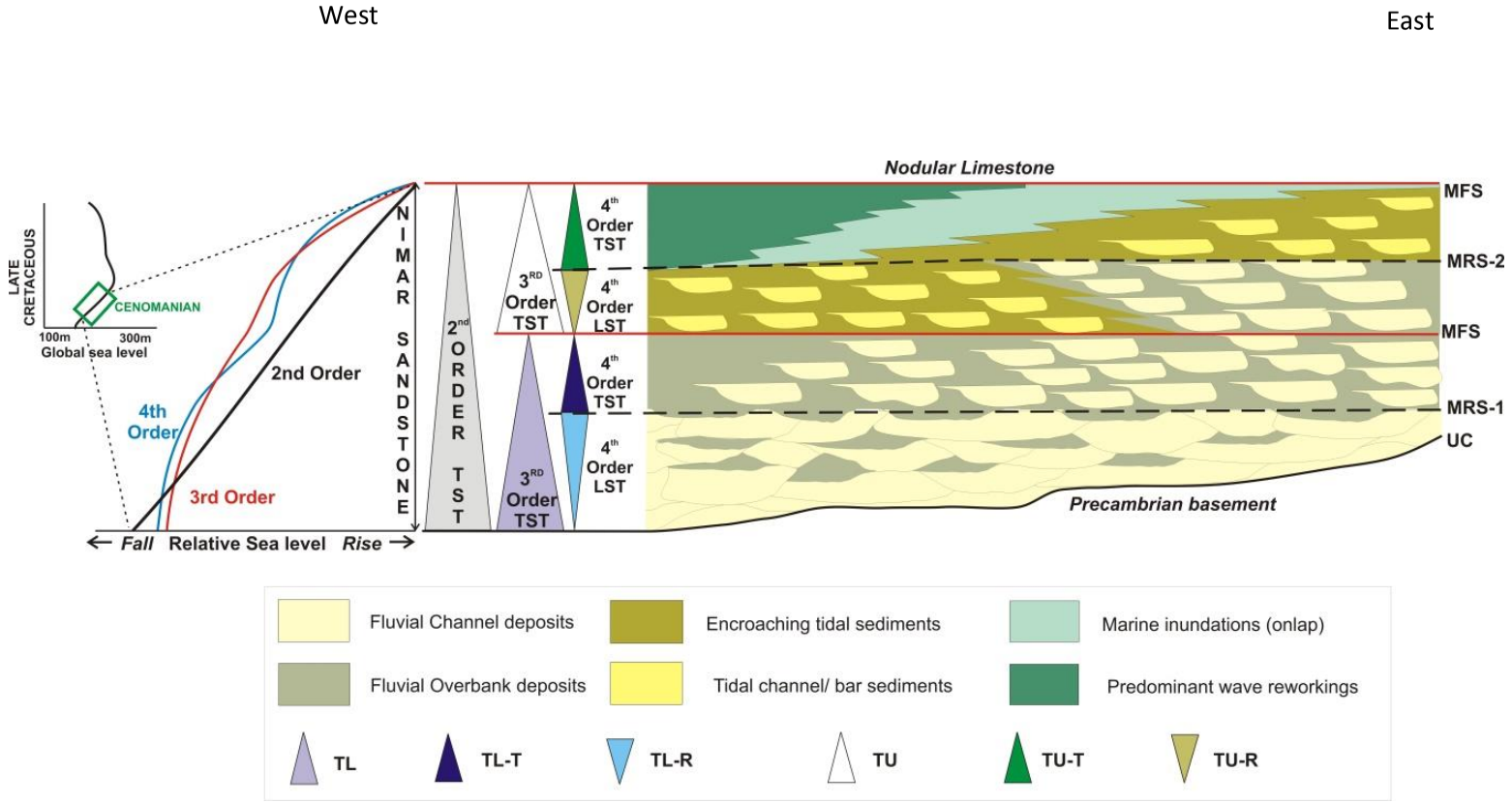

Figure: 8.6. Conceptual sequence diagram showing, stratal stacking patterns and the sequence boundaries defining several system tracts within the Nimar Sandstone succession along East-West line in the study area. The inferred sea level curves (Black- 2nd order, Red- 3rd order, and Blue- 4th order) during the Cenomanian time forms a part of major sea level rise during late Cretaceous. The global sea level curve during late Cretaceous is given in the inset diagram (modified after Haq, 2014). Abbreviations are same used in Figure 8.1.

8.5. Discussion on palaeogeography

The Cretaceous global sea level rise led to significant marine transgressions that affected part of the western and central India (Acharya and Lahiri 1991; Singh and Mishra, 2000; Desai et al., 2013). As a result of that event, large part of Central Indian land part was inundated under sea water, resulting in shift in depositional conditions from pure continental to marine/marginal marine. One such example of marine transgressions and change in depositional conditions is well recorded in the late Cretaceous Bagh Group of Rocks, preserved within the Narmada rift valley in Central India. The Nimar Sandstone (Cenomanian age), occurring as the lowermost unit within the Bagh Group, bears such excellent signatures of marine transgressions with change in depositional environment from fluvial, fluvio-marine to marine in a predominant siliciclastic depositional system. Effect of transgression is evident till deposition of the overlying Nodular Limestone (Turonian age), which demarcate the maximum extent of the transgressive event.

Analysis of the Nimar Sandstone succession in the light of transgressive-regressive cycles reveals two stacked transgressive events (of 3^{rd} order) within an overall large 2^{nd} order transgressive cycle (2^{nd} order TST, as discussed in the previous section). Flooding during the first transgressive event affected the initial fluvial system as rising base level led to increasing accommodation along with raised fluvial graded profile. This caused thick accumulation of the channel-fill and overbank deposits in the lower part of the Nimar Sandstone. An east-west flowing river system is deciphered, with distribution of coarser-dominant to finer-dominant sediments from east to west. In the western part of the basin, the fluvial system is affected by tidal intermixing, indicating significant marine encroachment and fluvial-tidal interference (Figure 8.7). The effect of tidal influence is more pronounced in the upper transgressive cycle, which records prevalent drowning of the underlying fluvial system. The effect of this drowning is more dominant in the western part and relatively less in the eastern part, indicating the marine encroachment took place from west to east with development of tide-influenced estuarine system in the west changing to more fluvial-dominated bay head delta systems in the east. Overall facies architecture indicates development of a tide-influenced estuarine system (Figure 8.7), where three distinct depositional zones can be deciphered, namely,

(i) a fluvial-tidal interactive inner estuary zone, developed in the eastern part of the basin, characterized by tide-reworked thick channel-fill and overbank deposits,

(ii) tide-dominated central estuary zone, developed in the central part of the basin, characterized by development of tidal sand bars and sand and mud flats based on extent

of inundations, mutual strength of tidal and fluvial systems and type of net accommodation created, and

(iii) tide-wave dominated outer estuary part, developed in the western part of the basin, characterized by more open marine tide and wave reworked sediments of shore environments.

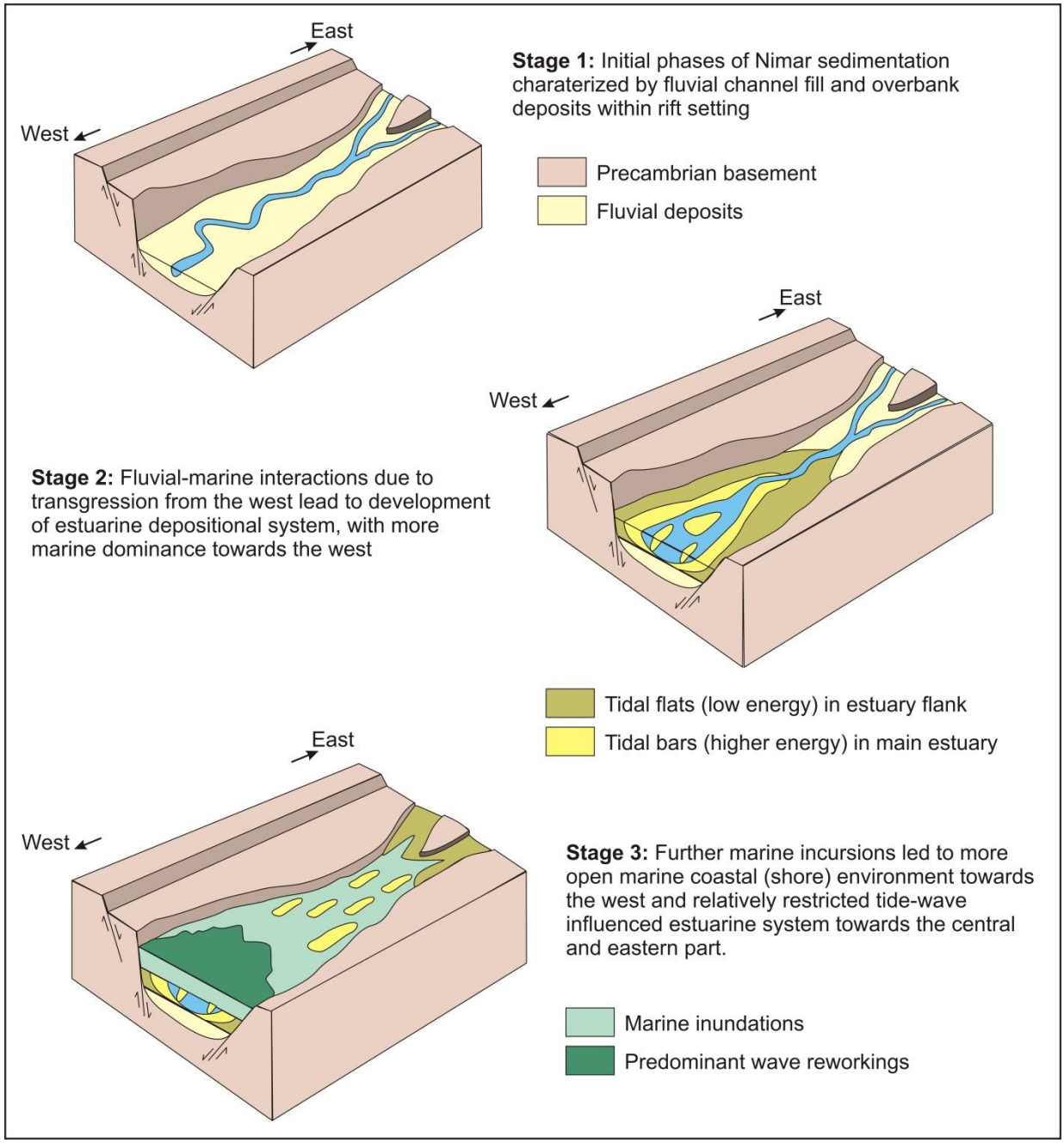

Figure: 8.7. Schematic 3D palaeogeographic model during the deposition of Nimar Sandstone.

Successive stacking of such transgressive cycles was caused by constant rise in base level in response to rising sea level along with basinal subsidence caused by reactivation of basin

marginal faults in the Narmada rift basin (Jha et al., 2017). During late stage of the transgression, this outer estuarine open marine condition encroached further landward inundating the entire basin, which led to a shallow, low energy condition with deposition of the Nodular Limestone as an apron over the underlying Nimar Sandstone. Thus, the shift in the depositional conditions from fluvial-dominated to a transgressive tide-wave influenced estuarine system attests to significant tectono-sedimentary changes accompanied by prolonged events of marine transgressions in the Narmada rift basin during the late Cretaceous time.

8.6. Conclusion

The present research work can be summarized as –

I. A detailed sedimentological study in terms of facies analysis, ichnology, geochemistry and sequence stratigraphy of the Nimar Sandstone helps to sort out the long standing confusion about the depositional condition of the Bagh Group.

II. Detailed facies analysis reveals total seventeen facies types and they are clubbed under five facies associations - Channel-fill facies association (FA-1), Overbank facies association (FA-2), Fluvial-dominated fluvio-tidal facies association (FA-3), Tide-dominated fluvio-tidal facies association (FA-4) and Shore facies association (FA-5).

III. This research work evidently shows that Nimar sedimentation was going under three depositional setting - a fluvial-dominated inner estuary zone, with transition from fluvial channels (FA-1) to floodplains (FA-2) to tide-affected fluvial deposits (FA-3), a transitional central estuary zone consisting of transitional fluvio-tidal channels (FA-3), tidal flats, associated with tidal channels and bars (FA-4) and a wave-dominated shallow marine outer estuary zone (top part of FA-4 with FA-5) with gradual increasing water depth in the upper part of the succession.

IV. Detailed ichnological study shows sediment-organism interaction pattern is directly controlled by the depositional setting, which indicates changing palaeoecological factors in the fluvio-marine interactive system.

V. Geochemical analysis shows during sedimentation a warm humid climatic condition was prevailed in a passive margin setting. Major oxide ratios along with sedimentological and ichnological interpretation support the fluvio-marine depositional model.

VI. Association of SSDS in the fluvio-marine sedimentary unit indicates formation of SSDS and incursion of marine water in the basin are two inter-related event and studied SSDS are identified as seismites.

VII. Reactivation of Son-Narmada South Fault during the Cenomanian caused sequential subsidence of the land part within the Indian Plate, which invited subsequent incursion of the sea water in the basin.

VIII. Overall fining up succession of the Nimar Sandstone constitutes part of a 2^{nd} order transgressive system tract (TST) within the Bagh Group of rocks.

IX. Presence of alternated coarsening up finning up succession signifies systematic variation in net supply of sediment, accommodation space and base level fluctuations during Nimar sedimentation.

X. Based on the stratal stacking pattern, several system tracts, and bounding surfaces three major sea level curves of 2^{nd} order, 3^{rd} order and 4^{th} order are established from Nimar Sandstone.

XI. In Nimar Sandstone transgressive retrogradational-regressive progradational cycles are controlled by both the tectono-eustatic factors and late Cretaceous global sea level rise.

The proposed tectono-sedimentary model based on integrated sedimentological-ichnological-sequence stratigraphic study helps to reconstruct the palaeogeography in Central India during the late Cretaceous time. Such palaeogeographic model can be applied in similar transgressive fluvio-marine sedimentary successions formed in passive margin riftogenic basinal settings, where transgression is controlled by both eustatic changes and tectonic subsidences.

References

1. Abdul Azeez, K.K., Unsworth, M.J., Patro, P.K., Harinarayana, T., Sastry, R.S., 2013. Resistivity structure of the Central Indian tectonic zone (CITZ) from multiple Magnetotelluric (MT) profiles and tectonic implications. Pure and Applied Geophysics 170, 2231-2256.
2. Acharya, S.K., Lahiri, T.C., 1991. Cretaceous palaeogeography of Indian subcontinent: A review. Cretaceous Research 12, 3-12.
3. Acharya, S.K., Roy, A., 2000. Tectono thermal history of the Central Indian tectonic zone and reactivation of the major faults/shear zones. Journal of Geological Society of India 55(3), 239-256.
4. Akhtar, K., Majtaba Khan, M., Ahmad, A.H.M., 1994. Petrofacies, provenance and tectonic setting of Nimar Sandstone (Lower Cretaceous), Rajpipla-Jobat area. Journal of Geological Society of India 44, 533-539.
5. Akhtar, K., Khan, D.A., 1997. A tidal island model for carbonate sedimentation: Karondia Limestone of Cretaceous Narmada basin. Journal of Geological Society of India 50, 481-490.
6. Alfaro, P., Morett, M., Soria, J.M., 1997. Soft-sediment deformation structures induced by earthquakes (seismites) in Pliocene lacustrine deposits (Guadix–Baza Basin, Central Betic Cordillera). Eclogae Geol. Helv. 90, 531-540.
7. Allen, J.R.L., 1970. Physical processes of Sedimentation. An Introduction. London: G.Allen & Unwin. pp 248.
8. Allen, J.R.L., 1981. Lower Cretaceous Tides revealed by cross-bedding with mud drapes. Nature 289, 579-581.
9. Allen, J.R.L., 1982. Sedimentary Structures, Their Characters and Physical Basis, Vol. I. Elsevier: Amsterdam pp 459-463.
10. Allen, J.R.L., 1985. Principles of Physical Sedimentology, Allen & Unwin, London, pp 272.
11. Allen, J.R.L., 1986. Earthquake magnitude-frequency, epicentral distance, and soft-sediment deformation in sedimentary basins. Sedimentary Geology 46, 67-75.
12. Alpert, S.P., 1974. Systematic review of the genus Skolithos. Journal of Paleontology 48(4), 661-669.

13. Altermann, W., 1986. The Upper Paleozoic pebbly mudstone facies of Peninsular Thailand and Western Malaysia continental margin deposits of Paleoeurasia. Geologische Rundschau International Journal of Earth Sciences 75(2), 79-89.

14. Andreton, R., 1985. Clastic facies model and facies analysis. In: Brenchley , P.J., Williams, P.J .(Eds),Sedimentology : Recent developments and Applied Aspects, Published for the Geological Society by Blackwell Scientific publications, Oxford, pp 31-47.

15. Ankketell, J.M., Cegia, J., Dzulynski, S., 1970. On the deformational structures in systems with reversed density gradients. Rocznik Polskiego Towarzystwa Geologicznego (Yearbook of the Polish Geological Society / Annales Societatis Geologorum Poloniae) 40, 3-30.

16. Armstrong-Altrin, J.S., Lee, Y.I., Verma, S.P., Ramasamy, S., 2004. Geochemistry of sandstones from the upper Miocene Kudankulam Formation, southern India: Implications for provenance, weathering, and tectonic setting. Journal Sedimentary Research 74, 285-297.

17. Atkinson, G., 1984. Simple computation of liquefaction probability for seismic hazard applications. Earthquake Spectra 1, 107-123.

18. Audemard, F.A., De Santis, F., 1991. Survey of liquefactions structures induced by recent moderate earthquakes. Bulletin: International Associations of Engineering Geology 44, 5-16.

19. Auden, J.B., 1949. Dyke in Western India- A discussion of their relationship with the Deccan Trap. Trans Nat Inst Sci India 3, 123-157.

20. Baas, J.H., De Koning, H., 1995. Washed-out-ripples: their equilibrium dimensions, migration rate and relation to suspended-sediment concentration in very fine sand. Journal of Sedimentary Research A65, 431-435.

21. Badve, R.M., Ghare, M.A., 1978. Palaeontological aspect of Bagh Beds, India. Recent Researches Geology (Hindustan Publishing Group Delhi) 4, 388-402.

22. Badve, R.M., Ghare, M.A., 1980. Ichnofauna of the Bagh Beds from Deva river valley, south of Narmada. Biovigyanam 6, 121-130.

23. Bann, K.L., Fielding, C.R., MacEachern, J.A., Tye, S.C., 2004. Differentiation of estuarineand offshore marine deposits using integrated ichnology and sedimentology:Permian Pebbley Beach Formation, Sydney Basin, Australia. In: McIlroy, D. (Ed.), Theapplication of ichnology to palaeoenvironmental and stratigraphic analysis.Geological Society, London, Special Publication, pp. 179–211.

24. Bansal, U., Pande, K., Banerjee, S., Nagendra, R., Jagadeesan, K.C., 2018. The timing of oceanic anoxic events in the Cretaceous succession of Cauvery Basin: Constraints from 40Ar/39Ar ages of glauconite in the Karai Shale Formation. Geological Journal, 1-8. https://doi.org/ 10.1002/gj.3177.

25. Bardhan. S., Gangopadhyay. T.K., Mondal. U., 2002. How far did India drift during the late Cretaceous? *Placenticeras kaffrarium* Etheridge, 1904 (Ammonoidea) used as a measuring tape. Sedimentary Geology 147, 193-217.

26. Barr, F.T., 1972. Cretaceous biostratigraphy and planktonic foraminifera of Libya. Micropaleontology 18, 1-46.

27. Barron, E.J., 1987. Global Cretaceous Palaeogeography- International Geologic Correlation Program project- 191. Palaeogeography Palaeoclimatology Palaeoecology 59, 207-214.

28. Bertling, M., Braddy, S.J., Bromley, R.G., 2006. Names for trace fossils: a uniform approach. Lethaia 39, 265-286.

29. Best, J.L., Kostaschuk, R.A., 2002. An experimental study of turbulent flow over a low angle dune. Journal of Geophysical Research 107(C9), 3135.

30. Bhat, G.M., Pandita, S.K., Singh, Y., Sharma, S., 2013. Estimation of Source Parameters of Local Earthquakes in Jammu and Kashmir, India. International Journal of Scientific and Research Publications 3(2), 1-5.

31. Bhatia, M.R., 1983. Plate Tectonics and Geochemical Composition of Sandstones. The Journal of Geology 91(6), 611-627.

32. Bhatia, M.R., Crook, K.A.W., 1986. Trace element characteristics of graywackes and tectonic setting discrimination of sedimentary basins. Contri Mineral Petrology 92,181-193.

33. Bhattacharya, B., Bandyopadhyay, S., Mahapatra, S., Banerjee, S., 2012. Record of tide wave influence on coal bearing Permian Barakar Formation, Raniganj Basin, India. Sedimentary Geology 268, 25-35.

34. Bhattacharya, B., Jha, S., 2014. Late Cretaceous diurnal tidal system: a study from Nimar Sandstone, Bagh Group, Narmada Valley, Central India. Current Science 107(6), 1032-1037.

35. Bhattacharya, H.N., Bandyopadhyay, S., 1998. Seismites in a Proterozoic tidal succession, Singhbhum, Bihar, India. Sedimentary Geology 119, 239-252.

36. Bhattacharya, H.N., Bhattacharya, B., 2006. A Permo-Carboniferous tide-storm interactive system: Talchir Formation, Raniganj Basin, India. Journal of Asian Earth Sciences 27, 303-311.

37. Bhattacharya, H.N., Bhattacharya, B., 2010. Soft-sediment deformation structures from an ice-marginal storm-tide interactive system, Permo-Carboniferous Talchir Formation, Talchir Coal basin, India. Sedimentary Geology 223, 380-389.

38. Bhattacharya, S.K., Jain, R.A., Tripathi, S.C., Lahiri, T.C., 1997. Carbon and Oxygen isotopic compositions of Infratrappen limestones from Central and western India and their depositional environment. Journal of Geological Society of India 50, 289-296.

39. Biswas, S.K., 1987. Regional tectonic framework structure and evolution of western marginal basins of India. Tectonophysics 135, 307-327.

40. Blanford, W.T., 1869. Geology of Western Sind. Mem. Geologial Survey of India . XVII(1).

41. Blatt, H., Caprara, J.R., 1985. Feldspar dispersal patterns in shales of the Vanoss Formation (Pennsylvanian), south-central Oklahoma. Journal of Sedimentary Petrology 55, 548-552.

42. Blatt, H.G., Middleton, G.V., Murray, R.C., 1980. Origin of Sedimentary Rocks. 2nd ed., Prentice-Hall, New Jersey, pp 634.

43. Boersma, J.R., 1969. Internal structure of some tidal mega-ripples on shoal in the Westerschelde estuary, the Netherlands: report of a preliminary investigation. Geologie en Mijnbouw 48, 409-414.

44. Boersma, J.R., Terwindt, J.H.J., 1981. Neap-spring sequences in intertidal shoal deposits in a mesotidal estuary. Sedimentology 28, 151-170.

45. Boggs Jr, S., 2012. Principles of Sedimentology and Stratigraphy, 5th edition. Pearson Prentice Hall, New Jersey, USA, 287-289.

46. Bose, P.K., Banerjee, S., Sarkar, S., 1997. Slope-controlled seismic deformation and tectonic framework of deposition of Koldaha Shale, India. Tectonophysics 269, 151-169.

47. Bose, P.K., Das, N.G., 1986. A transgressive storm and fair weather wave dominated shelf sequence: Cretaceous- Nimar Formation, Chakrud. M.P., India. Sedimentary Geology 46, 147-167.

48. Bose, P.N., 1884. Geology of the Lower Narmada valley between Nimawar and Kawant. Mem. Geological Survey of India 21(1), 72.

49. Brenchley, P.J., Newall, G., 1977. The significance of contorted bedding in Upper Ordovician sediments of the Oslo region, Norway. Journal of Sedimentary Research 47(2), 819-823.

50. Brodzikowski, K., Haluszczak, A., 1987. Flame structures and associated deformations in Quaternary glacio lacustrine and glaciodeltaic deposits: examples from central Poland. In: Jones, M.E., Preston, R.M.F. (Eds.), Deformation of sediments and sedimentary rocks: Geological Society Special Publication 29, 279-286.

51. Bromley, R.G., Frey, R.W., 1974. Redescription of trace fossil *Gryolithes* and taxonomic evalution of *Thalassinoides, Ophiomorpha* and *Spongeliomorpha.* Bulletin of the Geological Society of Denmark 23, 311-335.

52. Bromley, R.G., 1996. Trace Fossils, Second edition. London, Glasgow, Weinheim, New York, Tokyo, Melbourne, Madras: Chapman & Hall, pp 1-361. ISBN 0 412 61480 4.

53. Bromley, R. G., Uchman, A., 2003. Trace fossils from the Lower and Middle Jurassic marginal marine deposits of the Sorthat Formation, Bornholm, Denmark. Bulletin of the Geological Society of Denmark 52, 185-208.

54. Buatois, L.A., Mángano, M.G., 2002. Trace fossils from Carboniferous floodplain deposits in western Argentina: implications for ichnofacies models of continental environments. Palaeogeography Palaeoclimatology Palaeoecology 183, 71-86.

55. Buatois, L.A., Mángano, M.G., 2004. Animal substrate interactions in freshwater environments: applications of ichnology in facies and sequence stratigraphic analysis of fluvio-lacustrine successions. In: McIlroy , D (ed.) The Applications of Ichonology to Palaeoenvironmental and Stratigraphic analysis. Geological Socitey London , Special publications 228, 311-333.

56. Buatosis, L., Mangano, M.G., 2011. Ichnology: Organism-Substrate Interactions in Space and Time. Geological Magazine 149(4), 750.

57. Cande, S.C., Stegman, D.R., 2011. Indian and African plate motions driven by the push force of the Reunion plume head. Nature 475, 47-52.

58. Carmona, N.B., Buatois, L.A., Mángano, M.G., Bromley, R.G., 2008. Ichnology of the lower Miocene Chenque Formation, Patagonia, Argentina: Animal-substrate interactions and the Modern evolutionary fauna. Ameghiniana 45, 93-122.

59. Catuneanu, O., 2006. Principles of Sequence Stratigraphy. Elsevier, Amsterdam, pp, 375.

60. Catuneanu, O., Martins-Neto, M.A., Eriksson, P.G., 2012. Sequence stratigraphic framework and application to the Precambrian. Marine and Petroleum Geology, 33(1), 26-33.

61. Chakraborty, A., Bhattacharya, H.N., 2005. Ichnology of a Late Palaeozoic (Permo-Carboniferous) Glaciomarine Deltaic Environment, Talchir Formation, Saharjuri Basin, India. Ichnos 12, 31-45.

62. Chamberlain, C.K., 1978. Recognition of trace fossils in core. SEPM Short Course 5, 119-166.

63. Chiplonkar, G.W., 1939. Lamellibranchs from the Bagh Beds. Proc. Ind. Acad. Sci. Ser. B 10(4), 255-274.

64. Chiplonkar, G.W., Badve, R.M., 1969. Trace fossils from the Bagh Beds. Journal of Palaeontological Society of India 15, 1-5.

65. Chiplonkar, G.W., Badve, R.M., 1970. Trace fossils from the Bagh Beds. Journal of Palaeontological Society of India14, 1-10.

66. Chiplonkar, G.W., Badve, R.M., 1972. Newer observations on the stratigraphy of the Bagh Beds. Journal of Geological Society of India 13(1), 92-95.

67. Chiplonkar, G.W., Badve, R.M., 1973. Palaeontology of the Bagh Beds- I Bivalvia (excluding Inoceramidae and Ostracea). Journal of Palaeontological Society of India 17, 67-114.

68. Chiplonkar, G.W., Ghare, M.A., 1975. Some additional trace fossils from the Bagh Beds. Bull. Ind. Geol. Assoc. 8(1), 71-84.

69. Chiveleta, J.M., Palmab, R.M., Gómeza, J.L., Kietzmann, D.A., 2011. Earthquake-induced soft-sediment deformation structures in Upper Jurassic open-marine microbialites (Neuquén Basin, Argentina. Sedimentary Geology 235, 210-221.

70. Choi, K.S., 2010. Rhythmic climbing-ripple cross-lamination in inclined heterolithic stratification (IHS) of a microtidal estuarine channel, Gomso Bay, West Coast of Korea. Journal of Sedimentary Research 80, 550-561.

71. Choi, K.S., Dalrymple, R.W., Chun, S.S., Kim, S.P., 2004. Sedimentology of modern inclined heterolithic stratification (IHS) in the macrotidal Han River delta, Korea. Journal of Sedimentary Research 74, 677-689.

72. Cojan, I., Thiry, M., 1992. Seismically induced deformation structures in Oligocene shallow-marine and aeolian coastal sands (Paris Basin). Tectonophysics 206, 79-89.

73. Collinson, J.D., Thompson, D.B., 1982. Sedimentary Structures. Allen and Unwin, London, 194.

74. Condie, K.C., 1993. Chemical composition and evolution of the upper continental crust: Contrasting results from surface samples and shales. Chem. Geol. 104, 1-37.

75. Condie, K.C., Boryta, M.D., Liu, J., Quian, X., 1992. The origin of khondalites: geochemical evidence from the Archaean to Early Proterozoic granulitic belt in the North China Craton. Precambrian Research 59, 207-223.

76. Conkin, J.E., Conkin, B.M., 1968. Scalarituba missouriensis and its stratigraphic distribution. Univ. Kansas Paleont. Contr 31, 1-7.

77. Cotter, E., 1973. Large *Rosselia* in the Upper Cretaceous Ferron Sandstone Utah. Journal of Paleontology 47, 975-978.

78. Cox, R., Low, D.R., Cullers, R.L., 1995. The influence of sediment recycling and basement composition on evolution of mudrock chemistry in the southwestern United States. Geochim. Cosmochim. Acta. 59(14), 2919-2940.

79. Crawford, A.R., 1978. Narmada-Son Lineament of India traced into Madagascar. Journal of Geological Society of India 19(4), 144-153.

80. Crimes, T.P., Marcos, A., Perezestaun, A., 1974. Upper ordovician turbidites in western Asturias: A facies analysis with particular reference to vertical and lateral variations. Palaeogeography Palaeoclimatology Palaeoecology 15(3), 169-184.

81. Crimes, T.P., Harper, J.C., 1977. Trace fossils 2. Geological Journal, Special issue 9, 91-138.

82. Crook, K.A.W., 1974. Lithogenesis and geotectonics : the significance of compositional variations in flysh arenites (graywackes). In: Dott RH and Shaver RH (Eds), Modern and Ancient geosynclinal sedimentation. SEPM Special Publication 19, 304-310.

83. Dangerfield, F., 1818. Some accounts of caves near Bagh called Panch Pandoo. Trans. Lit. Soc., Bombay 2, 194-204.

84. Dashtgard, S.E., Gingras, M.K., Pemberton, S.G., 2008. Grain-size controls on the occurrence of bioturbation. Palaeogeography Palaeoclimatology Palaeoecology 257(1), 224-243.

85. Deconto, R.M., Pollard, D., 2003. Rapid Cenozoic glaciation of Antarctica induced by declining atmospheric CO_2. Nature 421, 245-249.

86. Demrican, H., 2008. Trace fossil associations and palaeoenvironmental interpretation of the late Eocene units (SW-Thrace). Bulletin of the Mineral Research and Exploration 136, 29-47.

87. Desai, B.G., 2013. Ichnological analysis of transgressive marine tongue in prograding deltaic system: Evidences from Ukra Hill Member, Western Kachchh, India. Journal of Geological Society of India 82(2), 143-152.

88. Dionne, J.C., 1998. Sedimentary structures made by shore ice in muddy tidal-flat deposits, St. Lawrence estuary, Québec. Sedimentary Geology 116, 261-274.

89. Duncun, P.M., 1987. Note on the echinoidea of the Cretaceous series of the Lower Narbada region (with remarks upon their geological age). Records of the Geological Survey of India 20(2), 81-92.

90. Eagar, R.M.C., Baines, J.G., Collinson, J.D., Hardy, P.G., Okolo, S.A., Pollard, J.E., 1985. Trace fossil assemblages and their occurrence in Silesian (mid-Carboniferous) deltaic sediments of the Central Pennine Basin, England. In: H.A. Curran (ed.), Biogenic structures, their use in interpreting depositional environments, - Society of Economic Paleontologists and Mineralogists, Special Publication 35, 99-149.

91. Eide, C.H., Howell, J.A., Buckley, S.J., Martinius, A.W., Oftedal, B.T., Henstra, G.A., 2016. Facies model for a coarse-grained, tide-influenced delta: Gule Horn Formation (Early Jurassic), Jameson Land, Greenland. Sedimentology 63(6), 1474-1506.

92. Ekdale, A.A., Bromley, R.G., 1983. Trace fossils and ichnofabric in the Kjølby Gaard Marl, upper-most Cretaceous, Denmark Bulletin Geological Society of Denmark 31, 107-119.

93. Ekdale, A.A., Bromley, R.G., Pemberton, S.G., 1984. Ichnology: The Use of Trace Fossils in Sedimentology and Stratigraphy. SEPM Short Course 15, 317.

94. Ekdale, A.A., Bromley, R.G., 2003. Paleoethologic interpretation of complex Thalassinoides in shallow-marine limestones, Lower Ordovician, Southern Sweden. Palaeogeography Palaeoclimatology Palaeoecology 192(1).

95. Elliott, R.E., 1965. A classification of subaqueous sedimentary structures based on rheological and kinematical parameters. Sedimentology 5, 193-209.

96. Elliott, T., 1986. Siliciclastic shorelines, in Reading, H.G., ed., Sedimentary environments and facies (2nd ed.): Oxford, Blackwell Scientific Publications, 155-188.

97. Eriksson, P.G., Catuneanu, O., Bumbu, A., 2012. First- and second-order global sequence stratigraphic correlations and accommodation charts for the Kaapvaal, Karelian, Sao Francisco (-Congo) and Slave cratons: An introduction. Marine and Petroleum Geology 33(1), 1-7.

98. Eriksson, P.G., Banerjee, S., Catuneanu, O., Corcoran, P.L., Eriksson, K.A., Hiatt, E.E., Laflamme, M., Lenhardt, N., Long, D.G.F., Miall, A.D., Mints, M.V., Pufahl, P.K.,

Sarkar, S., Simpson, E.L., Williams, G.E., 2013. Secular changes in sedimentation systems and sequence stratigraphy. Gondwana Research 24(2), 468-489.

99. Fagherazzi, S., Howard, A.D., Wiberg, P.L., 2004. Modeling fluvial erosion and deposition on continental shelves during sea level cycles. Journal of Geophysical Research 109, 148-227.

100. Fan, D.D., 2013. Classifications, sedimentary features and facies associations of tidal flats. Journal of Palaeogeography 2(1), 66-80.

101. Fedo C.M., Nesbitt H.W., and Young G.M., 1995. Unraveling the effects of potassium metasomatism in sedimentary rock sand paleosols, with implications for paleoweathering conditions and provenance. Journal of Geology. 23, 921-924.

102. Feng, R., Kerrich, R., 1990. Geochemistry of fine-grained clastic sediments in the Archean Abitibi greenstones belt, Canada: implications for provenance and tectonic setting. Geochim. Cosmochim. Acta. 54, 1061-1081.

103. Fernandes, A.C.S., Carvalho, I.S., 2006. Invertebrate ichnofossils from the Adamantina Formation (Bauru Basin, Late Cretaceous), Brazil. Revista Brasileira de Paleontologia, 9, 211-220.

104. Field, M.E., Gardner, J.V., Jennings, A.E., Edwards, B.D., 1982. Earthquake induced sediment failures on a slope, Klamath River Delta, California. Geology 10, 542-546.

105. Fillion, D., Pickerill, R.K., 1990. Ichnology of the Upper Cambrian? To Lower Ordovician Bell Island and Wabana groups of Eastern Newfoundland, Canada, Palaeontographica Canadiana 7, 1-83.

106. Floyd, P.A, Leveridge, B., 1987. Tectonic environment of the Devonian Gramscatho basin, south Cornwall: framework mode and geochemical evidence from turbiditic sandstones. Journal of the Geological Society 144, 531-542

107. Floyd, P.A., Winchester, J.A., Park, R.G., 1989, Geochemistry and tectonic setting of Lewisian clastic metasediments from the Early Proterozoic Loch Maree Group of Gairloch, N.W. Scotland. Precambrian Research 45(1-3), 203-214.

108. Forster, R., Meyer, R., Risch, H., 1983. Ammoniten and planktonische Foraminiferen aus den Eibrunner Mergeln (Regensburger Kreide, Nordostbayern). Zitteliana 10, 123-141.

109. Fourteau, R., 1918. Les Echinides des Bagh Beds. Rec. Geological Survey of India 49(1), 34-53.

110. Frey, R.W., Howard, J.D., Pryor, W.A., 1978. Ophiomorpha: its morphological, taxonomic, and environmental significance. Palaeogeography Palaeoclimatology Palaeoecology 23, 199-229.

111. Frey, R.W., Curran, H.A., Pemberton, S.G., 1984. Tracemaking activities of crabs and their environmental significance: the ichnogenus Psilonichnus. Journal of Paleontology 58, 333-350.

112. Frey, R.W., Pemberton, S.G., 1984. Trace Fossil Facies Models. In: Walker, R.G., Ed., Facies Models, 2nd Edition, American Association of Petroleum Geologists, Tulsa, 189-207.

113. Frey, R.W., Howard, J.D., 1985. Trace fossils from the Panther Member, Star Point Formation (Upper Cretaceous), Coal Creek Canyon, Utah. Journal of Palaeontology 59, 370-404.

114. Frey, R.W., 1990. Trace fossils and hummocky cross-stratification, Upper Cretaceous of Utah. Palaios 5, 203-218.

115. Frey, S.E., Gingras, M.K., Dashtgard, S.E., 2009. Experimental studies of gas-escape and water-escape structures: mechanisms and morphologies. Journal of Sedimentary Research 79, 808-816.

116. Friedrich, O., Erbacher, J., Moriya, K., Wilson, P.A., Kuhnert, H., 2008. Warm saline intermediate waters in the Cretaceous tropical Atlantic Ocean. Nat. Geosci. 1, 453-457.

117. Friedrich, O., Norris, R.D., Erbacher, J., 2012. Evolution of middle to Late Cretaceous oceans — A 55 m.y. record of Earth's temperature and carbon cycle. Geology 40, 107-110.

118. Funnell, B.M., 1990. Global and European Cretaceous Shorelines, stage by stage. – In R.N. Ginsburg & B. Beaudoin (eds): Cretaceous resources, events and rhythms. Kulwer. The Netherlands, pp 221-235.

119. Fursich, F.T., 1973. Thalassinoides and the origin of nodular limestones in the Corallian Beds (Upper Jurassic) of southern England. Neues Jahrbuch für Geologie und Paläontologie, Abhandlungen 12, 719-735.

120. Fürsich, F.T., 1981. Invertebrate trace fossils from the Upper Jurassic of Portugal. Communicoes dos Servicos Geológicos de Portugal 67, 153-168.

121. Galli, P., 2000. New empirical relationships between magnitude and distance for liquefaction. Tectonophysics 324, 169-187.

122. Gangopadhyay, T.K., Halder. K., 1996. Significance of the first record of nautiloid from the Upper Cretaceous Bagh Group of rocks. Current Science 70(6).

123. Gangopadhyay, T.K., Bardhan, S., 1998. Apertural modifications and jaw structures of placenticeratid ammonites from the Upper Cretaceous Bagh Group, central India. NeuesJahr. Geol. Pal.-Monatshefte 4, 193-202.

124. Gangopadhyay, T.K., Bardhan, S., 2000. Dimorphism and a new record of *Barroisiceras* de Grossouvre (Ammonoidea) from the Coniacian of Bagh, central India. Canadian J. Earth Sci. 37, 1377-1387.

125. Ganguly, T., Bardhan, S., 1993. Dimorphism in Placenticeras mintoi from the Upper cretaceous Bagh Beds, Central India. Cretaceous Research 14, 757-756.

126. Ghosh, S.K., 1993. Structural Geology: Fundamentals and Modern Developments. Pergamon, Oxford, pp 598.

127. Gibert, J.M. de., Ekdale, A.A. 1999. Trace fossil assemblages reflecting stressed environments in the Middle Jurassic Carmel Seaway of central Utah. Journal of Paleontology 73, 711-720.

128. Gingras, M.K., Pickerill, R., Pemberton, G.S., 2002. Resin cast of modern burrows provides analogs for composite trace fossils. Palaios 17, 206-211.

129. Gingras, M., Maceachern, J.A., Dashtgard, S.E., 2011. Process ichnology and the elucidation of physico-chemical stress. Sedimentary Geology 237(3-4), 115-134.

130. Gingras, M., Maceachern, J.A., Dashtgrad, S.E., 2012. The potential of trace fossils as tidal indicators in bays and estuaries. Sedimentary Geology 279, 97-106.

131. Goldring, R., 1962. The trace fossils of the Baggy Beds (Upper Devonian) of North Devon, England, Palaont Zetischr 36, 232-257.

132. Govindan, A., 1993. Cretaceous anoxic events, sea level changes and microfauna in Cauvery Basin, India. In: Proceedings of Second Seminar on Petroliferous Basins of India, Indian Petroleum Publishers 1, 161-176.

133. Greb, S.F., Archer, A.W., 1995. Rhythmite sedimentation in a mixed tide and wave deposit. Hazel Patch Sandstone (Pennsylvanian) Eastern Kentucky Coalfield. Journal of Sedimentary Research B65, 96-106.

134. Greb, S.F., Martino, R.L., 2005. Fluvial–estuarine transitions in fluvial-dominated succession: examples from the Lower Pennsylvanian of the Central Appalachian Basin. Special Publication in International Association of Sedimentologist 35, 425-451.

135. Grosheny, D., Ferry, S., Lecuyer, C., Merran, Y., Mroueh, M., Granier.B., 2017. The Cenomanian-Turonian Boundary Event (CTBE) in northern Lebanon as compared to regional data – Another set of evidences supporting a short-lived tectonic pulse

coincidental with the event?. Palaeogeography, Palaeoclimatology, Palaeoecology 487, 447-461.

136. Guha, A.K., Ghosh, B.K., 1970. Palaeoecology and Palaeogeography of Bagh Beds Upper Cretaceous Proc. Indian Sci. Congres. 51st Session.

137. Guiraud, M., Plaziat, J.C., 1993. Seismites in the fluviatile Bina sandstones: identification of paleoseismes and discussions of their magnitudes in a Cretaceous synsedimentary strike-slips basin (Upper Bennue, Nigeria). Tectonophysics 225, 493-522.

138. Hakes, W.G., 1976. Trace fossils and de-positional environment of four clastic units, Upper Pennsylvanian megacyclo-thems, northeastern Kansas. University of Kansas Paleontological Con-tributions, Article 63, 46.

139. Hallam, A., 1992. Phanerozoic sea-level changes. Columbia University Press, New York, pp 266.

140. Hancock, J.M., Kauffman, E.G., 1979. The great transgressions of the Late Cretaceous. Journal of Geological Society of London 136, 175-186.

141. Häntzschel, W., 1975. Trace fossils and problematica. In K. Teichert (ed.): Treatise on invertebrate palaeontology. Part W. Boulder: Geological Society of America/ Kansas University Press.

142. Haq, B.U., 2014. Cretaceous eustasy revisited. Global and Planetary change 113, 44-58.

143. Haq, B.U., Hardenbol, J., Vail, P., 1988. Chronology of fluctuating sea levels since the Triassic. Science 235, 1156-1167.

144. Harms, J.C., Southard, J.B., Spearing, D.R., Walker, R.G., 1975. Depositional environments as interpreted from primary sedimentary structures and stratification sequences: Tulsa, Oklahoma, Society of Economic Paleontologists and Mineralogists Short Course No. 2, 161.

145. Harms, J.C., Southard, J.B., Walker, R.G., 1982. Structures and sequences in clastic rocks: Society of Economic Paleontologists and Mineralogists, Short Course No. 9.

146. Harnois, L., 1988. The CIW index: a new Chemical Index of Weathering. Sedimentary Geology 55, 319-322.

147. Heer, O., 1877. Flora Fossilis Helvatiae. Die vorweltliche Flora der Schweiz. Verlag J. Wurster and Co., Zürich, pp 182.

148. Hempton, M.R., Dewey, J.F., 1983. Earthquake-induced deformational structures in young lacustrine sediments, East Anatolian fault, Southeast Turkey. Tectonophysics 98, 7-14.

149. Henbest, L.G., 1960. Fossil spoor and their environmental significance in Morrow and Atoka series, Pennsylvanian, Washington Country, Arkansas US Geological Survey, Professional paper 4008, 383-385.

150. Herron, M.M., 1988. Geochemical classifications of terrigenous sands and shales from core or log data. Journal of Sedimentary Petrology 58, 820-829.

151. Hilbert- Wolf, H.A., Simson, E.L., Simson, W.S., Tindall, S.E., Wievich, M.C., 2009. Insight into Syn depositional fault movement in a foreland basin, trends in Seismites of Upper Creatceous Wahweap Formations, Kaiparowits Basin, Utha, U.S.A. Basin Research 21, 856-871.

152. Hilbrecht, H., Arthur, M.A., Schlanger, S.O., 1986. The Cenomanian Turonian boundary event: sedimentary, faunal and geochemical criteria developed from stratigraphic studies in NW-Germany. In: O. Walliser (Editor), Global Bio-Events. Lecture Notes Earth Science 8, 345-351.

153. Hilbrecht. H., Bralower, T.J., Frieg, C., Troger, K.A., Voigt, S., Voigt, T., 1996. Shallow water facies during the Cenomanian Turonian anoxic event: Bio-Events, isotopes and sea level in southern Germany. Cretaceous Research 17, 229-253.

154. Howard, J.D., Frey, R.W., 1984. Characteristic trace fossils in nearshore to foreshore sequences, Upper Cretaceous of East-Central Utah. Canadian Journal of Earth Sciences 21, 200-219.

155. Howell, J.A., Flint, S.S., Hunt, C. 1996. Sedimentological aspects of the Humber Group (Upper Jurassic) of the SouthCentral Graben, UK North Sea. Sedimentology 43, 89-114.

156. Huber, B.T., Hodell, D.A., Hamilton, C.P., 1995. Middle-Late Cretaceous climate of the southern high latitudes: stable isotopic evidence for minimal equator-to-pole thermal gradients. Geological Society of America Bulletin 107, 1164-1191.

157. Huene, F.,Von., Matley, A.A., 1933. The Cretaceous Saurischia and Ornithischia of the Central Provinces of India. Palaenontol. Indica. 21(1), 1-74.

158. Jafar, S.A., 1982. Nannoplankton evidence of Turonian transgression along Narmada valley, India and Turonian–Coniacian boundary problem. Journal of Paleontolgical Society of India 27.

159. Jain, S.C., Nair, K.K.K., Yedekar, D., 1995. Geology of the Son-Narmada-Tapti lineament zone in Central India. Geological Survey of India Special publication 10.

160. Jaitly, A.K., Ajane, R., 2013. Comments on Placenticeras mintoi (Vredenburg, 1906) from the Bagh Beds (Late Cretaceous), Central India with special reference to Turonian Nodular Limestone horizon. Journal of Geological Society of India 81, 565-574.

161. Jensen, S., 1997. Trace fossils from the Lower Cambrian Mickwitzia sandstone, south-central Sweden. Fossils & Strata 42, 111.

162. Jha, S., Bhattacharya, B., Nandwani, S., 2017. Significance of seismites in the Late Cretaceous transgressive Nimar Sandstone succession, Son-Narmada rift valley, central India. Geological Journal 52, 768-783.

163. Jopling, A.V., Walker, R.G., 1968. Morphology and Origin of ripple-drift cross lamination, with examples from the Plesitocene of Massachusetts. Journal of Sedimentary Petrology 38, 971-984.

164. Kauffman, E.G., Caldwell, W.G.E., 1993. The Western Interior Basin in space and time. In: Caldwell, W.G.E., Kauffmann, E.G. (Eds.), Evolution of the Western Interior Basin.Geol. Assoc. Canada Spec. Paper 39, 1-30.

165. Kazmierczak, J., Pszczolkowski, A., 1969. Burrows of enteropneusta in Muschelkalk (Middle Triassic) of the Holy Cross Mountains, Poland. Acta Palaeontologica Polonica 14, 299-317.

166. Keatinge, R.H., 1856. On Neocomian fossils from Bagh and its neighbourhood. J. Bomb. Br. Roy. Asiatic Soc. Ind. 5, 621-625.

167. Keatinage, R.H., Blackwell, 1857. Selections from Record Bombay Government, No. XLIV, 7.

168. Kellar, G., Berner, Z., Adatte, Stueben, D., 2004. Cenomanian–Turonian and d13C, and d18O, sea level andsalinity variations at Pueblo, Colorado. Palaeogeography, Palaeoclimatology, Palaeoecology 211, 19-43.

169. Kennedy, W.J., 1967. Burrows and surface traces from the Lower Chalk of southern England. Bull. Brit. Mus. (nat. Hist.), Geol. 15, 127-167.

170. Kennedy, W.J., Walaszczyk, I., Cobban, W.A., 2000. Pueblo Colorado, USA, candidate Global Boundary Stratotype Section and Point for the base of the Turonian Stage of the Cretaceous, and for the base of the Middle Turonian Substage, with a revision of the Inoceramidae (Bivalvia). Acata Geologica Polonica 50, 295-334.

171. Khosla, A., 2001. Diagenetic alterations of Late Cretaceous dinosaur eggshell fragments of India. Gaia 16, 45-49.

172. Khosla, A., Sahni, A., 1995. Parataxonomic classification of Late Cretaceous Dinosaur eggshells from India. Journal of Palaeontological Society of India 40, 87-102.

173. Khosla, A., Sahni, A., 2000. Late Cretaceous (Maastrichtian) Ostracodes from the Lameta Formation, Jabalpur Cantonment area, Madhya Pradesh, India. Journal of the Palaeontological Society of India 45, 57-78.

174. Khosla, A., Kapur, V.V., Sereno, C., Wilson, J.A., Wilson, G.P., Dutheil, D., Sahni, A., Singh, M.P., Kumar, S., Rana, R.S., 2003. First dinosaur remains from the Cenomanian–Turonian Nimar Sandstone (Bagh Beds), District Dhar, Madhya Pradesh, India. Journal Palaeontological Society of India 48, 115-127.

175. Klein, G.D., 1971. A sedimentary model for determining paleotidal range. Geological Society of America Bulletin 82, 2585-2592.

176. Klein, G.D., 1977. Clastic Tidal Facies. Continuing Education Publishing Company, Champaign Illinois, pp. 49.

177. Knaust, D., 2008. Balanoglossites Mägdefrau 1932 from the Middle Triassic of Germany: Part of a complex trace fossil probably produced by burrowing and boring polychaetes. Paläontologische Zeitschrift 82, 347-372.

178. Kreisa, R.D., Moiola, R.J., 1986. Sigmoidal tidal bundles and other tide-generated structures of the Curtis Formation, Utah. Bulletin of the Geological Society of America 97, 381-387.

179. Kuenen, P.H., 1958. Experiments in geology. Transaction Geological Society of Glasgow 23, 1-37.

180. Kumar, K., Tewari, R., Agnihotri, D., Sharmaa ,A., Pandita , S.K., Suresh S.K. Pillai, Singh, V., Bhat, G.D., 2017. Geochemistry of the Permian-Triassic sequences of the Guryul Ravine section, Jammu and Kashmir, India: Implications for oceanic redox conditions. GeoResJ 13, 114-125.

181. Kumar, S., 2014. Taxonomic revision of late Cretaceous (Turonian) Bivalves from Narmada Basin, Central India. Journal of Earth Science and Engineering 4, 500-515.

182. Kundal, P., Sanganwar, B.N., 1998. Stratigraphical, palaeogeographical and palaeoenvironmental significance of fossil calcareous algae from Nimar Sandstone Formation, Bagh Group (Cenomanian-Turonian) of Pipaldehla, Jhabua District, MP. Current Science 75(7), 702-703.

183. Kundal, P., Sanganwar, B.N., 1998. Stratigraphy and Palichnology of Nimar Sandstone, Bagh Beds of Jobat area, Jhabua district , M.P. Journal of Geological Society of India 51 (5), 619-634.

184. Kundu, A., Eriksson, P.G., Matin, A., 2015. Soft-sediment deformation structures in the sub-Himalayan Middle Siwalik Subgroup, Lish River section, India. Episodes, 38(3), 197-207.

185. Kvale, E.P., 2006. The origin of neap-spring tidal cycles. Marine Geology 235, 5-18.

186. Kvale, E.P., 2012. Tidal constituents of modern and ancient tidal rhythmites: criteria for recognition and analyses. In: Davis Jr., R.A., Dalrymple, R.W. (Eds.), Principles of Tidal Sedimentology. Springer, pp 1-16.

187. Kvale, E.P., Johnson, H.W., Sonett, C.P., Archer, A.W., Zawistoski, A., 1999. Calculating lunar retreat rates using tidal rhythmites. Journal of Sedimentary Research 69, 1154-1168.

188. Laird, M.G., 1987. Evolution of the Cambrian-Early Ordovician Bowers basin, northern Victoria Land, and its relationships with the adjacent Wilson and Robertson Bay terranes. Memorie Societu Geologicu Ituliunu, 33, 25-34.

189. Le Heron, D.P., Sutcliffe, O.E., Whittington, R.J., Craig, J., 2005. The origins of glacially related soft-sediment deformation structures in Upper Ordovician glaciogenic rocks: implication for ice-sheet dynamics. Palaeogeography Palaeoclimatology Palaeoecology 218, 75-103.

190. Leopold, L.B., Wolman, M.G., 1957. River Channel Patterns, Braided, Meandering and Straight. U.S. Geological Survey Paper 282-B.

191. Lindsey, D.A., 1999. An evaluation of alternative chemical classifications of sandstones. USGS Open File Report 99-34, pp 23.

192. Lowe, D.R., 1975. Water escape structures in coarse-grained sediments. Sedimentology 22, 157-204.

193. Lowe, D.R., 1976. Subaqueous liquefied and fluidized sediment flows and their deposits. Sedimentology 23, 285-308.

194. MacEachern, J.A., Raychaudhuri, I., Pemberton, S.G., 1992. Stratigraphic applications of the Glossifungites ichnofacies: delineating discontinuities in the rock record. In:Pemberton, S.G. (Ed.), Applications of Ichnology to Petroleum Exploration: A Core Workshop: SEPM Core Workshop No. 17, 169-198 (Tulsa, USA).

195. MacEachern, J.A., Pemberton, S.G., 1994. Ichnologic aspects ofincised-valley fill systems from the Viking Formation of the Western Canada Sedimentary Basin, Alberta, Canada. Society of EconomicPaleontologists and Mineralogists Special Publication 51, 129-157.

196. Malarkodi, N., Patel, S.J., Fayaudeen,, P.J., Mallikarjuna, U.B., 2009. Palaeoenviromental significance of trace fossils from the Paleocene sediments of the Pondicherry area, South India. Journal of Geological Society of India 74, 738.

197. Malaza, N., Liu, K., Zhao, B., 2013. Facies Analysis and Depositional Environments of the Late Palaeozoic Coal-Bearing Madzaringwe Formation in the Tshipise-Pafuri Basin, South Africa. ISRN Geology 11.

198. Mall, D.M., Singh, A.P., Sarkar, D., 2005. Structure and seismo tectonics of Satpura, Central India, Current Science 88, 1621-1627.

199. Maltman, A., 1984. On the term soft-sediment deformation. Journal of Structural Geology 6, 589-592.

200. Maltman, A., 1994. Deformation structures preserved in the rocks. In: Maltman, A. (Ed.), The Geological Deformation of Sediments. Chapman & Hall, London, pp 261-307.

201. Marco, S., Stein, M., Agnon, A., 1996. Long term earthquake clustering: A 50,000 year palaeoseismic record in Dead sea graben. Journal of Geophysical Research 101 B3, 6179-6191.

202. Maynard, J.B., Valloni, R., Yu, H.S., 1982. Composition of modern deep-sea sands from arc-related basins. In: Leggett JK (ed), Trench and Fore-arc sedimentation. Geological Society London Special Publication 10, 551-561.

203. Mazumder, R., 2004. Implications of lunar orbital periodicities from Chaibasa tidal rhythmite of late Paleoproterozoic age. Geology 32, 841-844.

204. Mazumder, R., Arima, M., 2005. Tidal rhythmites and their implications. Earth-Science Reviews 69(1), 79-95.

205. Mazumder, R., Van Loon, A.J., Arima, M., 2006. Soft-sediment deformation structures in the Earth's oldest seismites. Sedimentary Geology 186, 19-26.

206. Mazumder, R., Arima, M., 2013. Tidal rhythm in deep sea environment: an example from Miocene Misaki Formation, Miura Peninsula, Japan. Marine and Petroleum Geology 43, 320-325.

207. McGowen, J.H., Garner, L.E., 1970. Physiographic features and stratification types of coarse-grained point bars: Modern and ancient examples. Sedimentology 14, 77-111.

208. McIlroy, D., 2004. Ichnofabrics and sedimentary facies of a tide-dominated delta: Jurassic Ile Formation of Kristin Field, Haltenbanken, Offshore Mid-Norway. Geological Society London Special Publications 228(1), 237-272.

209. Mckee, E.D., 1965. Experiments on ripples lamination. In: Middleton.G.V., ed. Primary sedimentary structures and their hydrodynamic interpretation. Soc. Econ. Paleontologists Mineralogist Special Publication 12, 66-83.

210. McKinley, J., Ruffell, A., 2009. Smectite in sandstones: a reveiw of the controls on occurrence and behaviour during diagenesisclay mineral cements in sandstones. Worden r.h. and Morad s. eds pp 109-228.

211. Mclennan, S.M., Nance, W.B., Taylor, S.R., 1980. Rare earth element-Thorium correlation in sedimentary rocks, and the composition of the continental crust. Geochim. Cosmochim. Acta. 44, 1833-1839.

212. Mclennan, S.M., Taylor, S.R., Eriksson, K.A., 1983. Geochemistry of Archaean shales from the Pilbara Supergroup, Western Australia. Geochim. Cosmochim. Acta. 47, 1211-1222.

213. Mclennan, S.M., Taylor, S.R., Mcculloch, M.T., Maynard, J.B., 1990. Geochemical and Nd-Sr isotopic composition of deep sea turbidites: Crustal evolution and plate tectonic associations. Geochim. Cosmochim. Acta. 54, 2015-2050.

214. Mclennan, S.M., Taylor, S.R., 1991. Sedimentary rocks and crustal evolution: tectonic setting and Secular trends. Journal of Geology 99, 1-21.

215. McLennan, S.M., Hemming, S., McDaniel, D.K., Hanson, G.N., 1993. Geochemical approaches to sedimentation, provenance, and tectonics. Geological Society America Special publication 284.

216. Mclennan, S.M., Bock, B., Hemming, S.R., Hurowitz, J.A., Lev, S.M., McDaniel, D.K., 2003. The role of provenance and sedimentary process in the geochemistry of sedimentary rocks, in Lentz , D.R., (ed). Geochemistry of Sediments and Sedimentary Rocks: Evolutionary Considerations to Mineral Deposit- Forming Environments: Geological Associations of Canada. Geo Text 4, 7-38.

217. Miall, A.D., 1977. Lithofacies Types and Vertical Profile Models in Braided River Deposits: A Summary. In: Miall, A.D., Ed., Fluvial Sedimentology, Geological Survey of Canada, Calgary, 597-604.

218. Miall, A.D., 1982. Tertiary sedimentation and tectonics in the Judge Daly Basin, northeast Ellesmere Island Arctic Canada. Geological Survey of Canada paper 80, 17-30.

219. Miall, A.D., 2006. The Geology of Fluvial Deposists: Sedimentary Facies, Analysis and Petroleum Geology. Spring-Verlag, New York, 582.

220. Miller, K.G., Kominz, M.A., Browning, J.V., Wright, J.D., Mountain, G.S., Katz, M.E., Sugarman, P.J., Cramer, B.S., Christie-Blick, N., Pekar, S.F., 2005. The Phanerozoic record of global sea-level change. Science 310, 1293-1298.

221. Montenat, C., Barrier, P., Ott d'Estevou, P., Hibsch, C., 2007. Seismites: an attempt at critical analysis and classification. Sedimentary Geology 196, 5-30.

222. Moretti, M., Alfaro, P., Caselles, O., Canas, J.A., 1999. Modelling seismites with a digital shaking table. Tectonophysics 304, 369-383.

223. Moretti, M., Soria, J.M., Alfaro, P., Walsh, N., 2001. Asymmetrical softsediment deformation structures triggered by rapid sedimentation in turbiditic deposits (Late Miocene, Guadix Basin, southern Spain). Facies 44, 283-294.

224. Moretti, M., Sabato, L., 2007. Recognition of trigger mechanisms for soft-sediment deformation in the Pleistocenemlacustrine deposits of the Sant'Arcangelo Basin (Southern Italy): seismic shock vs. overloading. Sedimentary Geology 196, 31-45.

225. Moretti, M., Van Loon, A.J., 2014. Restrictions to the application of 'diagnostic' criteria for recognizing ancient seismites. Journal of Palaeogeography 3, 162-173.

226. Mude, S.N., Jagtap, S.A., Kundal, P., Sarkar, P.K., Kundal, M.P., 2012. Palaeonvironmental significance of ichnofossils from the Mesozoic Jaisalmer Basin, Rajasthan, North Western India, Proceedings of the International Academy of Ecology and Environmental Sciences 2, 150-167.

227. Müller, R.D., Sdrolias, M., Gaina, C., Steinberger, B., Heine, C., 2008. Long-Term Sea-Level Fluctuations Driven by Ocean Basin Dynamics. Science 319, 1357.

228. Murty, K.N., Dhokarikar, B.G., Verma, G.P., 1963. Plat fossils in Nimar Sandstone near Umrali, M.P. Current Science 32(1), 21-22.

229. Nagarajan, R., Madhavaraju, J., Nagendra, R., Armstrong-Altrin, J.S., Moutte, J., 2007. Geochemistry of Neoproterozoic shales of the Rabanpalli Formation, Bhima Basin, Northern Karnataka, southern India: implications for provenance and paleoredox conditions. Revista Mexicana de Ciencias Geologicas 24, 20-30.

230. Nagendra, R., Patel, S.J., Deepankar, R., Reddy, A.N., 2010. Bathymetric significance of the ichnofossil assemblages of the Kulakkalnattam sandstone, Ariyalur area, Cauvery Basin. Journal of the Geological Society of India 76(5), 525-532.

231. Nagendra, R., Kamalak Kannan, B.V., Sen, G., Gilbert, H., Bakkiaraj, D., Nallapa-Reddy, A., Jaiprakash, B.C., 2011. Sequence surfaces and paleobathymetric trends in Albian to Maastrichtian sediments of Ariyalur area, Cauvery Basin, India. Marine and Petroleum Geology 28, 895-905.

232. Nagendra, R., Sathiyamoorthya, P., Pattanayaka, S., Nallapa-Reddy, A., Jaiprakash, B.C., 2013. Stratigraphy and paleobathymetric interpretation of the Cretaceous Karai Shale Formation of Uttatur Group, Tamil Nadu, India. Stratigraphy and Geological Correlation 21, 675-688.

233. Nagendra, R., Reddy, A. N., 2017. Major geologic events of the Cauvery Basin, India and their correlation with global signatures, A review. Journal of Palaeogeography 6(1), 69-83.

234. Naidin, N.P., 1983. Late Cretaceous transgressions and regressions on the Russian platform. Zitteliana 10, 107-144.

235. Nath, B.N., Kunzendorf, H., Plüger, W.L., 2000. Influence of provenance, weathering, and sedimentary processes on the elemental ratios of the fine-grained fraction of the bedload sediments from the Vembanad lake and the adjoining continental shelf, southwest coast of India. Journal of Sedimentary Research 70, 1081-1094.

236. Nayak, K.K., 1987. Foraminifera from Nimar Sandstone of Bagh Beds, Jhabua District, Madhya Pradesh. Biovigyanam 13(1), 30-39.

237. Nesbitt, H.W., Young, G.M., 1982. Early Proterozoic climates and plate motions inferred from major element chemistry of lutites. Nature 299, 715-717.

238. Nichols, G., 2009. Sedimentology and Stratigraphy. Blackwell Science Ltd., London.

239. Nichols, R.J., Sparks, R.S.J., Wilson, C.J.N., 1994. Experimental studies of the fluidization of layered sediments and the formation of fluid escape structures. Sedimentology 41, 233-253.

240. Nicholson, K., 1992. Contrasting mineralogical-geochemical signatures of manganese oxides: guides to metallogenesis. Economic geology 87, 1253-1264.

241. Norris, R.D., Wilson, P.A., 1998. Low-latitude sea-surface temperatures for the mid-Cretaceous and the evolution of planktic foraminifera. Geology 26, 823-826.

242. Obermeier, S.F., Martin, J.R., Frankel, A.D., Youd, T.L., Munson, P.J., Munson, C.A., Pond, E.C., 1993. Liquefaction evidence for one or more strong Holocene earthquakes in the Wabash Valley of Southern Indiana and Illinois, with a preliminary estimate of magnitude. U. S. Geol. Surv. Prof. Paper 1536.

243. Obermeier, S.F., 1996. Use of liquefaction-induced features for paleoseismic analysis - an overview of how seismic liquefaction features can be distinguished from other features and how their regional distribution and properties of source sediment can be used to infer the location and strength of Holocene paleo-earthquakes. Engineering Geology 44, 1-76.

244. Oldham, T., 1858. On some additions to the knowledge of the Cretaceous rocks of India. Journal Asiatic Society Bengal 27(1), 112-128.

245. Osae, S., Asiedu, D.K., Yakubo, B., Koebrel, C., Dampare, S.B., 2006. Provenance and tectonic setting of Late Proterozoic Buem sandstones of southeastern Ghana: Evidence from geochemistry and detrital modes. Journal of African Earth Science 44, 85-96.

246. Owen, G., 1987. Deformation processes in unconsolidated sands. In: Jones, M.E., Preston, R.F.M. (Eds.), Deformation mechanisms in sediments and sedimentary rocks. Geological Society of London, Special Publication, 29, 11-24.

247. Owen, G., 1995. Soft-sediment deformation in Upper Proterozoic Torridonian sandstones (Applecross Formation) at Torridon, northwest Scotland. Journal of Sedimentary Research A65, 495-504.

248. Owen, G., 2003. Load structures: gravity-driven sediment mobilization in the shallow subsurface. In: Van Rensbergen, P., Hillis, R.R., Maltman, A.J., Morley, C.K. (Eds.), Subsurface Sediment Mobilization. Geological Society of London, Special Publication 216, 21-34.

249. Owen, G., Moretti, M., 2011. Identifying triggers for liquefaction induced soft-sediment deformation in sands. Sedimentary Geology 235, 141-147.

250. Pandita, S.K., Kotwal, S.S., Thakur, K.K., Bhat, G.M., Singh, Y., 2014. Lithofacies association and depositional history of Boulder Conglomerate Formation, Upper Siwalik Subgroup, Jammu Himalaya. Himalayan Geology 35(2), 135-145.

251. Paola, C., Wiele, S.M. , Reinhart, M.A., 1989. Upper-regime parallel lamination as the result of turbulent sediment transport and low-amplitude bed forms. Sedimentology 36, 47-59.

252. Pascoe, E.H., 1959. A Manual of the Geology of India and Burma. Journal of Geological Survey of India 2, 485-1343.

253. Patel, S.J., Desai, B.G., Vaidya, A.D., Shukla, R., 2008. Middle Jurassic trace fossils from Habo Dome, Mainland Kachchh, Western India. Journal of Geological Society of India 71, 345-362.

254. Patel, S.J., Desai, B.G., 2009. Animal–sediment relationship of the Crustaceans and Polychaetes in the intertidal zone around Mandvi Gulf of Kachchh, Western India; J. Geol. Soc. India 74, 233-259.

255. Pemberton, S.G., Frey, R.W., 1982. Trace fossil nomenclature and the Planolites-Palaeophycus dilemma. Journal of Palaeontology 56, 843-871.

256. Pemberton, S.G., MacEachern, J.A., Frey, R.W., 1992. Trace fossil facies models:Environmental and allostratigraphic significance. In R.G. Walker and N.P.Jones, eds., Facies models: Response to sea level change, Calgary. Canada: Geological Association of Canada. pp 47-72.

257. Pemberton, S.G., Wightman, D.M., 1992. Ichnologic characteristics of brackish water deposits. Society of Economic Palaeontologists and Mineralogists Core Workshop 17, 339-382.

258. Pemberton, S.G., MacEachern, J.A., 1997. The Ichnological Signatures of storm deposits: uses of trace fossils in event stratigraphy, in : Palaeontological Events Horizons Ecological and Evolutionary Implications (C.E. Brett. ed.) Columbia University Press. pp 73-109.

259. Pettijohn, F.J., 1957. Sedimentary rocks. New-York: Harper and Row, 718.

260. Pettijohn, F.J., 1975. Sedimentary Rocks. 3rd Edition, Harper and Row, Publishers, pp 628.

261. Pettijohn, F.J., Potter, P.E., Siever, R., 1972. Sand and Sandstone. New York, Springer-Verlag. pp 618.

262. Pollard, J.E., 1988. Trace fossils in coal-bearing sequences. Journal of Geological Socitey of London 145, 339-350.

263. Price, G.D., Hart, M.B., 2002. Isotopic evidence for early to mid-Cretaceous ocean temperature variability. Marine Micropaleontology 46, 45-58.

264. Raff, de. J.F.M., Boersma, J.R., 2007. Tidal deposits and their sedimentary structures (seven examples from Western Europe. Geologie en Mijnbouw 50.

265. Raiverman, V., 1975. Facies transition among Nimar, Bagh and Lameta beds. In Verma, et.al, Recent researches in geology. Hindustan Publishing Corporation, Delhi, 2, 123-139.

266. Rajshekhar, C., 1995. Foraminifera from the Bagh Group, Narmada Basin, India. Journal Geological Society of India 46, 413-428.

267. Rao, N.P., Tsukuda, T., Kosuga, M., Bhatia, S.C., Suresh, G., 2002. Deep lower crustal earthquakes in central India: inferences from analysis of regional broadband data of the 1997 May, 21, Jabalpur earthquake, Geophysical Journal International 148, 1-12.

268. Ratcliffe, K.T., Morton, A.C., Ritcey, D.H., Evenchick, C.A., 2007. Whole-rock geochemistry and heavy mineral analysis as petroleum exploration tools in the Bowser and Sustut basins, British Columbia, Canada. Bulletin of Canadian Petroleum Geology 55(4), 320-336.

269. Reading, H.G., 1986. In H. G. Reading (Ed.), Sedimentary environments and facies. Facies (2nd Ed), Oxford: Blackwell Scientific Publishing. pp 4-19.

270. Reddy, E.K., Rao, G.S., 2011. Mathematical methods. I.K. International Publishing House Pvt. Ltd, pp 688.

271. Reineck, H.E., Wunderlich, F., 1967a. Zeitmessungen an Gezeitenschichten. Nature Mus. 97, 193-197.

272. Reineck, H.E., Wunderlich, F., 1967b. A new method to measure rate of deposition of single lamina on tidal flats and shelf bottoms. 7th International Sedimentological Congress.

273. Reineck, H.E., Wundelich, F., 1968. Classifications and origin of flaser and lenticular bedding. Sedimentology 11, 99-104.

274. Reineck, H.E., Wunderlich, F., 1969. Die Entstehung von Schichten und Schichtbanken im Watt. Senckenbergiana Marit. 1, 85-106.

275. Reineck, H.E., Singh, I.B., 1973. Depositional Sedimentary Environments. Springer-Verlag, Berlin, 549.

276. Reineck, H.E., Singh, I.B., 1980. Depositional Sedimentary Environments. With reference to terrigenous clastics 2nd Rev. and updated edn, Springer-Verlag, Berlin, 549.

277. Ricci Lucchi, F., 1995. Sedimentological indicators of paleoseismicity. In: Serva, L., Slemmons, D.B. (Eds.). Perspectives in Paleoseismology, Association of Engineering Geologists Special Publication 6, 7-17.

278. Robinson, P.L., 1967. The Indian Gondwana Formations- A review. In IUGS 1st Symp. Gondwana Stratigraphy., Buenos Aires, 208-268.

279. Robson, J., Hodson, D., Hawkins, E., Sutton, R., 2014. Atlantic overturning in decline? National Geoscience 7, 2.

280. Rode, K.P., Chiplonkar, G.W., 1935. A contribution to stratigraphy of the Bagh beds. Current Science 4(5), 322-323.

281. Rodríguez-Pascua, M.A., Calvo, J.P., De Vicente, G., Gómez-Gras, D., 2000. Soft-sediment deformation structures interpreted as seismites in lacustrine sediments of the Prebetic Zone, SE Spain, and their potential use as indicators of earthquake magnitudes during the Late Miocene. Sedimentary Geology 135, 117-135.

282. Roper, M., Rothgaenger, M., 1995. Neue Fossilfunde aus der Regensburger Oberkreide. Teil 1: Eibrunner Mergel. Fossilien 3,180-184.

283. Roser, B.P., Korsch, R.J., 1986. Determination of tectonic setting of sandstone mudstone suites using SiO_2 content and K_2O/Na_2O ratio. Journal of Geology 94, 635-650.

284. Roser, B.P., Korsch, R.J., 1988. Provenance signatures of sandstone-mudstone suite determined using discrimination function analysis of major element data. Chemical Geology 67, 119-139.

285. Roser, B.P., Cooper, R.A., Nathan, S., Tulloch, A.J., 1996. Reconnaissance Sandstone geochemistry, provenance and tectonic setting of the lower Paleozoic terranes of the West coast and Nelson, New Zealand. New Zealand Journal of Geology and Geophysics 39, 1-16.

286. Rossetti, D.F., Santos Jr, A.E., 2003. Events of sediment deformation and mass failure in Upper Cretaceous estuarine deposits (Cametá Basin, northern Brazil) as evidence for seismic activity. Sedimentary Geology 161, 107-130.

287. Rotnicka, J., 2005. Ichnofabrics of the Upper Cretaceous Fine Grained Rocks from the Stolowe Mountains (Sudetes SW Poland). Geological Quarterly 49, 15-30.

288. Roy Chowdhury, M.K., Sastri, V.V., 1962. On the Revised classification of the Cretaceous and the associated rocks of the Man river section of the Narbada Valley. Rec. Geological Survey of India 91(2), 283-304.

289. Roy, A., Prasad, H.M., 2003. Tectonothermal events in Central Indian Tectonic Zone (CITZ) and its implication in Rhodinian crustal assembly. Journal of Asian Earth Sciences 22, 115-129.

290. Roy, S.K., Banerjee, S., 2016. Soft Sediment Deformation Structures in the Andaman Flysch Group, Andaman Basin: Evidence for Palaeogene Seismic Activity in the Island Arc. Berita Sedimentology 35, 55-74.

291. Sahni, M.R., Jain, S.P., 1966. Note on a revised classification of the Bagh Beds, Madhya Pradesh. Journal of Palaeontological Society of India 11, 24-25.

292. Sames, B., Wagreich, M., Wendler. J.E., Haq, B.U., Conra, C.P., Melinte-Dobrinescu, M.C., Hug. F., Wendler, I., Wolfgring, E., Yilmaz, I.Ö., Zorina, S.O., 2016. Review: Short-term sea-level changes in a greenhouse world — A view from the Cretaceous. Palaeogeography, Palaeoclimatology, Palaeoecology 441, 393-411.

293. Sanganwar, B.N., Kundal, P., 1997. Ichnofossils from Nimar Sandstone Formation, Bagh Group of Barwah area, Khargaon district, M.P. Gondwana Geology Magazine 12, 12-33.

294. Sarkar, S., Chaudhuri, A.K., 1992. Trace fossils in Middle Triassic fluvial redbeds, Pranhita-Godavari Valley, south India. Ichnos 2, 7-19.

295. Sarkar, S., Banerjee, S., Chakraborty, S., 1995. Synsedimentary seismic signatures in the Mesoproterozoic Koldaha Shale, Kheinjua Formation, central India. Indian Journal of Earth Sciences 22, 158-164.

296. Sarkar, S., Ghosh, S.K., Chakraborty, C., 2009. Ichnology of a Late Palaeozoic ice marginal shallow marine succession: Talchir Formation, Satpura Gondwana Basin, Central India. Plaeogeography, Palaeoclimatology, Plaeoecology 283, 28-45.

297. Sarkar, S., Choudhuri, A., Banerjee, S., Van Loon, A.J., Bose, P.K., 2014. Seismic and non-seismic soft-sediment deformation structures in the Proterozoic Bhander Limestone, Central India. Geologos 20, 89-103.

298. Sarkar, S.K., 1973. Sedimentology of the Nimar-Bagh-Lameta Complex around Awaldaman and Bagh areas, Dhar District, Central India. Unpublished Ph.D. thesis. Jadavpur University. pp 190.

299. Schieber, J., 1992. A combined petrographical-geochemical provenance study of the Newland Formation, Mid-Proterozoic of Montana. Geol. Mag., 129, 223-237.

300. Schnellmann, M., Anselmetti, F., Giardini, D., McKenzie, J., 2005. Mass movement-induced fold-and-thrust belt structures in unconsolidated sediments in Lake Lucerne (Switzerland). Sedimentology 52(2), 271-289.

301. Sebastian, L.N., Kai-Uwe, G. F., Bosence, D., Luciani, V., Craig, J., 2000. Discovery of marine Late Cretaceous carbonates and evaporites in the Kufra Basin (Libya) redefines the southern limit of the Late Cretaceous transgression. Cretaceous Research 21, 721-731.

302. Seed, H.B., 1979. Soil liquefaction and cyclic mobility evaluation for level ground during earthquakes. Proceedings of the American Society of Civil Engineers. Journal of the Geotechnical Engineering Division 105, 201-255.

303. Seilacher, A., 1953. Studien zur Palichnologie.I. Uber die Methoden der Palichnologie, Neues Jahrb. Geol. Palaeont. Abh. 96, 421-452.

304. Seilacher, A., 1967. Bathymetry of trace fossils. Marine Geology 5, 413-428.

305. Seilacher, A., 1969. Fault graded beds interpreted as seismites. Sedimentology 13, 155-159.

306. Seilacher, A., 1984. Sedimentary structures tentatively attributed to seismic events. Marine Geology 55, 1-12.

307. Seilacher, A., 2007. Trace fossil analysis. Springer Berlin Heidelberg New York.

308. Seilacher, A., Meischner, D., 1964. Fazies-analyse im Paliiozoikum des Oslo-gebietes. – Geologische Rundschau 54, 596-619.

309. Sellwood, B.W., Price, G.D., Valdes, P.J., 1994. Cooler estimates of Cretaceous temperatures. Nature 370, 453-455.

310. Seth, A., Sarkar, S., Bose, P.K., 1990. Synsedimentary seismic activity in an immature passive margin basin (Lower Member of the Katrol Formation, Upper Jurassic, Kutch, India). Sedimentary Geology 68, 279-291.

311. Shanley, K.W., McCabe, P.J., 1993. Alluvial architecture in a sequence stratigraphic framework: a case history from the Upper Cretaceous of southern Utah, U.S.A. *In Quantitative Modeling of Clastic Hydrocarbon Reservoirs and Outcrop Analogues* (S. Flint and I. Bryant, Eds.). International Association of Sedimentologists Special Publication **15,** pp 21-55.

312. Shanmugam, G., 2016. The seismite problem. Journal of Palaeogeorapghy 5(4), 318-362.

313. Shanmugam, G., 2017. Global case studies of soft-sediment deformation structures (SSDS): Definitions, classifications, advances, origins, and problems. Journal of Palaeogeography, 6(4), 251-320.

314. Shiraishi, F., Kano, A., 2004. Composition and spatial distribution of microencrusters and microbial crusts in upper Jurassic-lowermost Cretaceous reef limestone (Torinosu Limestone, Southwest Japan). Facies 50, 217-227.

315. Shiraishi, F., Yoshitomi, K., 2005. Sedimentary environments of upper Jurassic to Lower Cretaceous Reef limestones distributed in the western part of Yamaguchi Prefecture. Geological journal 111, 21-28.

316. Sims, J.D., 1975. Determining earthquake recurrence intervals from deformational structures in young lacustrine sediments. Tectonophysics 29, 141-152.

317. Singh, D., Mishra, U.K., 2000. Reconstruction of Cretaceous basins of Meghalaya, India. Journal of Indian Association of Sedimentologist 19(1), 59-68.

318. Singh, G., Ghose, R.N., 1977. Nimar Sandstone. In: lexicon of Gondwana Formation of India. Geol. Surv. Ind. Misc. Publ., no 36, 62-63.

319. Singh, I.B., Srivastava, H.K., 1981. Lithostratigraphy of Bagh beds and its correlation with Lameta Beds. Journal of Palaeontological Society of India 26, 77-85.

320. Skelton, P., 2003. The Cretaceous World. Cambridge University Press, Cambridge, pp 1-360.

321. Smith, A.B., 2010. The Cretaceous Bagh Formation, India: A Gondwana Window onto Turonian shallow water echinoid faunas. Cretaceous Research 31, 368-386.

322. Stewart, J., 1821. Geological notes on the strata between Malwa and Guzerat. Trans. Liter Soc. Bombay 3, 538-541.

323. Stoll, H.M., Schrag, D.P., 2000. High-resolution stable isotope records from the Upper Cretaceous rocks of Italy and Spain: Glacial episodes in a greenhouse planet? Geological Society of America Bull. 112, 309.

324. Stumm, W., Morgan, J.J., 1981. Aquatic Chemistry: An Prologue Emphasizing Chemical Equilibra in Natural Waters. John Wiley and Sons, New York, 780.

325. Sugitani, K., Horiuchi, Y., Adachi, M., 1996. Anomalously low Al_2O_3/TiO_2values for Archean cherts from the Pilbara block, westernAustralia – possible evidence for extensive chemical weathering on the early earth. Precambrian Research 80, 49-76.

326. Sundaram, R., Henderson, R.A., Ayyasami, K., Stilwell, J.D., 2001. A lithostratigraphic revision and palaeoenvironmental assessment of the Cretaceous system exposed in the onshore Cauvery Basin, Southern India. Cretaceous Research 22, 743-762.

327. Sunderson, H.C., Lockett, F.P.J., 1983. Flume experiments on bedforms and structures at the dune plane bed transition. In: Collinson, J.D., Lewin, I. (Eds.), Modern and Ancient Fluvial Systems: IAS Special Publication 6, 49-59.

328. Suttner, L.J., Dutta, P.K., 1986. Alluvial sandstone composition and palaeo-climate, 1. Framework mineralogy. Journal of Sedimentary Petrology 56(3), 32.

329. Tänavsuu-Milkeviciene, K., Plink-Björklund, P., 2009. Recognizing tide dominated versus tide influenced deltas: Middle Devonian strata of the Baltic Basin. Journal of Sedimentary Research 79(12), 887-905.

330. Taylor, S.R., McLennan, S.M., 1985. The continental crust: Its composition and evolution. Blackwell Sci. pp 312.

331. Tewari, H.C., Murty, A.S.N., Kumar, P., Sridhar, A.R., 2001. A tectonic model of Narmada region. Current Science 80, 873-878.

332. Theede, H., Ponant, A., Hiroki, K., Schlieffer, C., 1969. Studies on the resistance of marine bottom invertebrates to oxygen-deficiency and hydrogen content: Marine Biology 2, 325-337.

333. Thomas, R.G., Smith, D.G., Wood, J.M., Visser, J., Calverley-Range, E.A., Koster, E.H., 1987. Inclined heterolithic stratification-terminology, description, interpretation and significance: Sedimentary Geology 53, 123-179.

334. Tiwari, R.P., Rajkonwar, C., Lalchawimanwi., Paul, L.J.M., Ralte, V.Z., Patel, S.J., 2011. Trace fossils from Bhuban Formation Surma Group (Lower to Middle Miocene) of Mizoram, India and their palaeoenvironmental significance. J. Earth. Syst. Sci. 120, 1127-1143.

335. Tripathi, S.C., 2006. Geology and evolution of the Cretaceous Infratrappean Basins of Lower Narmada Valley, western India. Journal of Geological Society of India 67, 459-468**.**

336. Uchman, A., 1998. Taxonomy and ethology of flysch trace fossils: A revision of the Marian Ksiazkiewicz collection and studies of complementary material; Annales Societatis Geologorum Poloniae 68, 105-218.

337. Uchman, A., Krenmayr, H.G., 1995. Trace fossils from LowerMiocene (Ottnangian) molasse deposits of Upper Austria. – Paläontol Zeitschr 69 (3/4), 503-524.

338. Van Loon, A.J., 2009. Soft-sediment deformation structures in siliciclastic sediments: an overview. Geologos 15, 3-55.

339. Van Loon, A.J., 2014. The life cycle of seismite research. Geologos 20, 61-66.

340. Van Loon, A.J., Brodzikowski, K., 1987. Problems and progress in the research on soft-sediment deformations, Sedimentary Geology 50,167-193.

341. Vossler, S.M., Pemberton, S.G., 1989. Ichnology and Palaeoecology of ichnofabric. Earth Science Reviews 60, 227-259.

342. Vredenburg, H.W., 1907. The Ammonites of the Bagh Beds. Rec. Geological Survey of India, 36(2), 109-25.

343. Vredenburg, H.W., 1908. Additional note concerning a previous notice on "The Ammonites of the Bagh Beds". Rec. Geological Survey of India, 36(3), 239-240.

344. Wagreich, M., Lein, R., Sames, B., 2014. Eustasy, its controlling factors, and the limnoeustatic hypothesis—concepts inspired by Eduard Suess. Austrian Journal of Earth Sciences 107(1), 115-131.

345. Walker, R.G., 2006. Facies models revisited. In H. W. Posamentier & R. G. Walker (Eds.), Facies models revisited. Tulsa: SEPM (Society for Sedimentary Geology). Special Publication 84, 1-17.

346. Wang, C.S., 2013. Cretaceous paleogeography and paleoclimate and the setting of SKI borehole sites in Songliao Basin, northeast China. Palaeogeography Palaeoclimatology Palaeoecology 385, 17-30.

347. Wang, Y., Sames, B., Liao, H., Xi, D., Pan, Y., 2017. Late Cretaceous ostracod fauna from the Shenjiatun section (Songliao Basin, Northeast China). Biostratigraphic and palaeoecological implications. Cretaceous Research 78, 174-190.

348. Weimer, R.J., Howard, J.D., Lindsay, D.R., 1982. Tidal flats. American Association of Petroleum Geologists Memoir 31, 191-246.

349. Wells, J.T., Prior, D.B., Coleman, J.M., 1980. Flowslides in muds on extremely low angle tidal flats, northeastern South America. Geology 8, 272-275.

350. Williams, G.E., 1989. Late Precambrian tidal rhythmites in South Australia and the history of the Earth's rotation. Journal of the Geological Society of London 146, 97-111.

351. Xi, D.P., Cao, W.X., Huang, Q.H., Do Carmo, D.A., Li, S., Jing, X., Tu, Y.J., Jia, J.Z., Qu, H.Y., Zhao, J., Wan, X.Q., 2016. Late Cretaceous marine fossils and seawater incursion events in the Songliao Basin, NE China. Cretaceous Research 62, 172-182.

352. Yang, S.L., Li, H., Ysebaert, T., Bouma, T.J., Zhang, W.X., Wang, Y.Y., Li, P., Li, M., Ding, P.X., 2008. Spatial and temporal variations in sediment grain size in tidal wetlands, Yangtze Delta: On the role of physical and biotic controls. Estuarine, Coastal and Shelf Science, 77(4), 657-671.

353. Yedekar, D.B., Jain, S.C., Nair, K.K.K., Dutta, K., 1990. The Central Indian Collision Suture. Geological Survey of India Special Publication 28, 1-43.

354. Yoshida, M., Divi, R.S., Santosh, M., 2001. Precambrian Central India and its role in the Gondwanland-Rodinia context, Gondwana Research 4, 208-211.

355. Zakharov, Y.D., Shigeta, Y., Popov, A., Tatiana A. Velivetskaya, T.A., Afanasyeva, T.B., 2011. Cretaceous Climatic Oscillations in the Bering Area (Alaska and Koryak Upland): Isotopic and Palaeontological Evidence. Sedimentary Geology 235(1-2), 122-131.